

POLITECNICO DI TORINO

Corso di Laurea Magistrale in Ingegneria Energetica e Nucleare



TESI DI LAUREA MAGISTRALE

Industrial pollutants dispersion

Critical analysis of a French regulation for the determination of the minimum industrial chimney's height

Relatori

Andrea Carpignano

Mauro Montrucchio

Candidato

Giulia Grazioli

Anno Accademico 2018-2019

Abstract

Industrial pollutants dispersion: critical analysis of a French regulation for the determination of the minimum industrial chimney's height

Industrial emissions represent nowadays one of the most important contributions to the overall pollution of the atmosphere. In Europe, several efforts have been made in order to tackle the adverse effects derived from these sources on human health and environment. In such a contest, the aim of this study is to analyse in detail a specific regulation introduced in France for the determination of the minimum height of the stacks for power plants with nominal power lower than 50 MW, in order to assess its effectiveness in realistic applications. Three pollutant species are taken into account for the analysis: NO_2 , SO_2 and PM_{10} . The critical analysis is made through two types of evaluation. Firstly, the effects of several parameters involved in dispersion are quantified in order to establish whether the formula used for the assessment of the minimum height can take into account all the most important phenomena. After that, the peak of pollutant concentration at the ground obtained in many possible situations when the minimum height is set is compared to some threshold values defined in the regulation itself, in order to check the effectiveness of the formula. The estimation of the concentration is made through the software Fluidyn-PANACHE. The set of simulations to perform is chosen according to the Design of Experiments (DOE) methodology. It is demonstrated that the dispersion process is significantly influenced by the height of the stack as well as by the temperature of the pollutants emitted from the source, emphasising the importance of the effective stack height, understood as the sum of physical stack height and plume rise, on the dispersion process. The study also shows that the regulation ensures the respect of target values when dealing with SO_2 and PM_{10} ; in the case of NO_2 instead several exceedances occur, suggesting that the methodology for the determination of the minimum height should be improved. However, a deeper analysis of the terms involved in the calculation of the target ground concentration value reveals the presence of some inconsistencies in the regulation.

Key-words: industrial pollution, chimney, emission height, dispersion, CFD, Fluidyn-PANACHE, DOE, Fractional factorial design.

Acknowledgements

This master thesis is the result of a 5-months internship proposed by the Ceric laboratory and carried out at the LHEEA laboratory. I would like to thank the first one for giving me the opportunity to work on this project and the second one for hosting me during all the research period.

I wish I could express all my gratitude to my supervisor at the LHEEA laboratory, Boris Conan, for all the support and the precious advises he was always there to give me during all the period of my internship. Working with him I had the possibility to learn much more than I could ever expect.

I would also like to thank my supervisor at Ceric, François Coiffet, for all the advices and technical suggestions that helped me to have a better overview of the problem faced in this work.

Moreover, I would like to thank the professor Laurent Perret for his availability and his elucidations for the assessment of the problem for this project.

This research project was carried during my one-year Erasmus experience at the Ecole Centrale de Nantes. Coming back to my home institution, the Polytechnic of Turin, I had the possibility to further improve the quality of this master thesis thanks to the advices of my two additional supervisors, Andrea Carpignano and Mauro Montrucchio, to whom I would like to express my gratitude.

Finally, on a more personal level, I would like to thank the responsible of the Master *City and Urban Environments*, Isabelle Calmet, for the great help and support she always provided me during my stay in Nantes.

Contents

List of Figures	5
List of Tables	7
1 Reference regulations for industrial emissions	11
1.1 European Directive on air quality	11
1.2 French regulation on industrial chimneys height	12
2 Basics on industrial pollutants dispersion	14
2.1 Basics on atmospheric dispersion	15
2.1.1 Atmospheric boundary layer	15
2.1.2 Pollutants dispersion	16
2.2 Main factors influencing dispersion	17
2.2.1 Effective height of emission	17
2.2.2 Emitted species	18
2.2.3 Atmospheric conditions	18
2.2.4 Surface roughness	19
2.2.5 Presence of obstacles	21
2.3 Numerical modelling of dispersion	22
2.3.1 Eulerian methods	22
2.3.2 Lagrangian methods	23
2.3.3 Other methods	24
3 Design of the experiment	25
3.1 Assessment of the problem	25
3.1.1 Objectives of the analysis	25
3.1.2 Methodology for the resolution	26
3.2 Design of Experiments methodology	26
3.3 Choice of the parameters to analyze	28
3.4 Final simulation matrix	32
4 Numerical model assessment	35
4.1 Fluidyn-PANACHE	35
4.2 Setting of the model	35
4.2.1 Simulation mode	35
4.2.2 Domain	36
4.2.3 Setting of the source	36
4.2.4 Inlet conditions	37
4.2.5 Initial conditions	38

4.2.6	Boundary conditions	38
4.2.7	Physical models	39
4.2.8	Choice of the grid	40
4.2.9	Atmospheric stability assessment	42
4.2.10	Wind field development	43
4.2.11	Convergence criteria	44
4.2.12	Validation of the results	45
5	Results of the analysis	46
5.1	Analysis of simulations results	46
5.2	Parametric analysis	50
5.2.1	Main effects plot	50
5.2.2	Pareto chart	53
5.2.3	Interaction plot	54
5.3	Discussion of the regulation	57
5.3.1	Comparison with reference values	57
5.3.2	General regulation trends	61
6	Conclusions	63
A	Application of the regulation to real data	66
A.1	Comparison of the height obtained from the two different French regulations	66
A.2	Emission limits	69
B	Complements to the numerical model	70
B.1	Units conversion for source definition in Fluidyn-PANACHE	70
B.2	Turbulence modelling	71
C	Complements to the results	75
C.1	Summary of the results of simulations	75
C.2	Main parameters evaluated for each simulation	76
C.3	Evaluation of Case 1 with the Gaussian plume model	125
C.4	Main effect plots with lower concentration for Case 1	126
C.5	Interaction plots for the other species under evaluation	127
D	Maps of concentration	129
	Bibliography	136

List of Figures

1.1	Chimneys height prescribed by the French regulation [4]	12
2.1	Representation of the PBL [10]	15
2.2	Schematic representation of a plume [11]	16
2.3	Schematic representation of dispersion [14]	18
2.4	ABL structure at different hours of the day [18]	19
2.5	Example of the effect of atmospheric stability on wind profile [19]	20
2.6	Wind modification according to the value of z_0 (for neutral stability) [20]	20
2.7	Qualitative description of the flow close to an obstacle [6]	21
3.1	Pasquill stability classes [29]	30
3.2	Aerodynamic roughness length (z_0) related to the type of terrain (Wieringa, 1992)	31
3.3	Aiding table for the choice of the Fractional factorial design to use (highlight on the one used) [31]	32
3.4	Simulation matrix used for the analysis ($\frac{1}{4}$ factorial design with 2 levels)	34
3.5	Summary of the cases to perform	34
4.1	List of possible types of sources [35]	36
4.2	Grid independence results	41
4.3	Reference grid	41
4.4	Evaluation stability through potential temperature vertical profile	42
4.5	Dispersion profile on the XZ plane, where: (A) neutral case; (B) stable case; (C) unstable case	43
4.6	Example of developing wind profile	44
4.7	Evaluation of convergence through monitor point	45
5.1	Wind field for high z_0 cases (case 4)	46
5.2	Turbulent kinetic energy profile for a neutral case with high z_0 (case 4)	47
5.3	Example of ground concentration profile on Fluidyn-PANACHE (A) and evaluation of mean ground concentration (B) (case 9)	48
5.4	Summary of the results for mean ground concentration peak	49
5.5	Summary of the results for mean ground concentration peak	49
5.6	Main effects plot for all the pollutant species under evaluation	51
5.7	Main effects plot for the distance of the peak from the source	52
5.8	Pareto chart of the normalized effects	53
5.9	Interaction plot for NO_2	55
5.10	Pareto chart of main factors and interactions for NO_2	56

5.11	Comparison between peak of NO_2 at the ground and threshold value from regulation: (A) simulations in general locations; (B) simulations in PPA areas	58
5.12	Comparison between peak of SO_2 at the ground and threshold value from regulation: (A) simulations in general locations; (B) simulations in PPA areas	58
5.13	Comparison between peak of PM_{10} at the ground and threshold value from regulation: (A) simulations in general locations; (B) simulations in PPA areas	59
5.14	Trend of mean ground concentration and distance from the source according to the stack height	62
A.1	Power plants data	66
A.2	Table provided by the regulation for the determination of c_r	67
A.3	Table provided by the regulation for the determination of background pollution c_0	67
A.4	Concentration limits at the emission (Art. 10.II) [5]	69
B.1	Concentration units used on Fluidyn-PANACHE [32]	70
C.1	Summary of the results obtained with numerical simulations	75
C.2	Evaluation of NO_2 concentration at the ground (1 m) with Gaussian plume model (source at $x=0$ m)	125
C.3	Main effect plots for mean peak of ground concentration without the effect of case 1	126
C.4	Interaction plot for SO_2	127
C.5	Interaction plot for PM_{10}	128
C.6	Interaction plot for <i>Distance from the source</i>	128
D.1	NO_2 mean annual concentration in Nantes [42]	129
D.2	PM_{10} mean annual concentration in Nantes [42]	130
D.3	SO_2 mean annual concentration in Nantes [42]	130
D.4	NO_2 mean annual concentration in Paris [43]	131
D.5	PM_{10} mean annual concentration in Paris [43]	131
D.6	NO_2 mean annual concentration in Lyon [44]	132
D.7	PM_{10} mean annual concentration in Lyon [44]	132
D.8	NO_2 mean annual concentration in Pays de la Loire [42]	133
D.9	PM_{10} mean annual concentration in Pays de la Loire [42]	133
D.10	NO_2 mean annual concentration in Ile de France [43]	134
D.11	PM_{10} mean annual concentration in Ile de France [43]	134
D.12	NO_2 mean annual concentration in Rhone-Alpes [44]	135
D.13	PM_{10} mean annual concentration in Rhone-Alpes [44]	135

List of Tables

1.1	European limits for ground concentration (in parenthesis the maximum allowable number of exceedances per year) [3]	12
3.1	Summary of the parameters to evaluate and their levels	31
4.1	Initial ambient air conditions	38
4.2	List of physical models	39
4.3	Summary of physical models used in the analysis	40
5.1	Reference values used for the examination of the formula for chimneys height (from regulation)	57
5.2	Comparison between the value of c_0 given in the regulation and peak of concentration detected on maps of concentration	61

Introduction

Air pollution represents nowadays one of the most concerning problems for human health. The World Health Organization (WHO) estimates that it causes about 4.2 million of deaths every year [1], making it the biggest environmental risk to health [2]. It is a worldwide problem, even if some areas are more affected than others (i.e. Western Pacific and South East Asia), due for example to energetic policies. According to the WHO, 92% of the world's population lives in places where air quality levels exceed *WHO's Ambient Air quality guidelines* (considering annual mean of particulate matter with a diameter of less than 2.5 micrometres, $PM_{2.5}$). Such numbers confirm the gravity of this phenomenon, underlining the importance of the introduction of international and national policies in order to tackle air pollution and thus decrease the risks to human health. In the case of Europe, this is made with the emanation of the Directive 2008/50/EC (May 21, 2008), relative to Ambient Air Quality and a Cleaner Atmosphere for Europe [3]. In this document, both limits related to emission and ground concentration are established. Every European country must refer to this directive and adopt proper policies and regulations in order to respect the prescribed limits.

The premise for the introduction of efficient national or regional regulations is an exhaustive knowledge of the physical processes involved in pollutants dispersion and the capability to analyse and predict their effects in any possible situation. Different approaches are currently used to this end, any of them presenting some specific limitations given by the difficulty to represent accurately the complexity of this problem. The involvement of non-linear phenomena and a large number of factors with adverse effects should indeed be taken into account. Both external environmental conditions and more internal ones linked to the source characteristics are involved. A good regulation should be able to consider all the effects and establish proper criteria to prevent risks for human health as well as environmental issues.

In such a context, the aim of this project is to investigate in detail a specific regulation adopted in France aimed at preventing risks derived from pollutants produced by industrial sources, that represent one of the main contributions to low air quality. This regulation [4] prescribes the minimum height of a stack for power plants with nominal power lower than 50 MW. It will be attempted to establish whether the prescribed values properly take into account all the complexity of the dispersion problem, ensuring adequate pollutants concentration levels at the ground.

At this end, the performance of the regulation in terms of pollutants dispersion is evaluated considering many realistic situations. The test cases are found with the implementation of the *Design of Experiments* methodology. As support for the

evaluation, a parametric analysis is performed in order to understand and quantify the effects produced by different parameters on dispersion and to find configurations that can potentially produce high peaks of pollutants concentration at the ground. The analysis will be performed with the support of numerical simulations, implemented through the use of the software Fluidyn-PANACHE.

In the first part, the contents of the regulation will be examined in more detail. After that, the main principles on pollutants dispersion and the main parameters affecting the process, as well as a description of the current numerical modelling techniques, will be recalled. This information will be the starting point for the delineation of the assessment of the problem, that will be discussed and set up in the third chapter. Then, the numerical model used for the study will be described. Finally, the results obtained from simulations will be used to perform a critical analysis of the regulation.

Chapter 1

Reference regulations for industrial emissions

The aim of the present work being a critical analysis of the current French regulation on industrial chimneys height, the first objective is to present the contents of this document as well as its regulatory framework.

Reference should be made in particular to two main regulations:

- European directive on air quality (*Directive 2008/50/ec of the European parliament and of the council of 21 May 2008 on ambient air quality and cleaner air for Europe*)
- French directive on chimneys height (*Arrêté du 3 août 2018 relatif aux prescriptions générales applicables aux installations relevant du régime de l'enregistrement au titre de rubrique 2910 de la nomenclature des installations classées pour la protection de l'environnement*)

The relevant information for the aims of the analysis that is contained in these documents will be presented in the following.

1.1 European Directive on air quality

In 2008, the European Parliament emanated a regulation for the control of air quality aimed at protecting human health and environment [3], in which it is pointed out the importance of establishing objectives for ambient air quality to avoid, prevent or reduce harmful effects on human health and the environment. Target values, thresholds and limits for ground concentration are defined, as well as methodologies for the measurements techniques.

For the aim of the analysis, this Directive is especially relevant for the indication of the limits to ground concentration, that will be taken into account for the evaluation of the results (Annex XI.B). As it will be more fully explained later, in this study only three of the main industrial pollutants will be considered, namely NO_2 , SO_2 and PM_{10} . For these pollutants the regulation prescribes specific limits referred to different periods of time. These limits are summarised in Table 1.1.

Another relevant information for this study that can be extracted from this regulation concerns the height of measurement of the concentration at the ground.

Table 1.1: European limits for ground concentration (in parenthesis the maximum allowable number of exceedances per year) [3]

Reference period	$NO_2[\frac{\mu g}{m^3}]$	$SO_2[\frac{\mu g}{m^3}]$	$PM_{10}[\frac{\mu g}{m^3}]$
1 hour	200 (18 times/year)	350 (24 times/year)	-
1 day	-	125 (3 times/year)	50 (35 times/year)
1 year	40	-	40

Guidelines are indeed provided on the sampling methodology, specifying the following: *in general, the inlet sampling point shall be between 1,5 m (the breathing zone) and 4 m above the ground* (Annex III.C). This indication will be taken into account for the evaluation of the concentration at the ground.

1.2 French regulation on industrial chimneys height

The European regulation should be implemented by each European country through the introduction of national regulations. In the case of France, this is made with the *Code de l'Environnement*, a collection of regulations concerning the environment and its preservation that is periodically updated. As industrial sources represent one of the most important contributions to the overall pollution, the *Code* includes, among the others, a national regulation aimed at preventing risks from industrial pollutants [4], applied to power plants with a nominal power lower than 50 MW. For atmospheric emissions a minimum height of the stack is prescribed (Article 54.3). In addition, the limit values for pollutants emission (Article 58.2) and chimney exhausts velocity according to the volume flowrate (Article 55) are defined.

The determination of the height is not unique, being dependent on the specific application (turbines, motors, others). In the case of general power plants, this value is depending on two main parameters, namely the fuel type and the nominal power of the plant (Figure 1.1).

Type de combustible	1 MW et < 2 MW	2 MW et < 4 MW	4 MW et < 6 MW	6 MW et < 10 MW	10 MW et < 15 MW	15 MW et < 20 MW	20 MW et < 30 MW	30 MW et < 50 MW
Combustibles solides	10 m (15 m)	12 m (18 m)	14 m (21 m)	14 m (21 m)	15 m (22 m)	16 m (24 m)	19 m (28)	22 m (33 m)
Fioul domestique	5 m (7 m)	6 m (9 m)	8 m (12 m)		10 m (15 m)		11 m (17 m)	14 m (20 m)
Autres combustibles liquides	7 m (10 m)	8 m (12 m)	9 m (14 m)	11 m (17 m)	13 m (19 m)	14 m (21 m)	16 m (24 m)	19 m (29 m)
Gaz naturel, Biométhane	4 m (6 m)	5 m (7 m)	6 m (10 m)		8 m (12 m)		9 m (14 m)	10 m (17 m)
Autres combustibles gazeux	5 m (7 m)	6 m (9 m)	8 m (12 m)		10 m (15 m)		11 m (17 m)	14 m (20 m)

Figure 1.1: Chimneys height prescribed by the French regulation [4]

For each case two different values are indicated. The first one is referred to general situations; the height in brackets is instead referred to particular conditions of the power plant, located in areas referred to as PPA (Plan de Protection de l'Atmosphère, atmosphere protection plan).

A similar regulation is introduced for power plants in specific regulatory conditions (plants subjected to authorization) [5]. In this case although the height is evaluated by considering a specific formula (Article 23), given by:

$$h_p = \left(k \cdot \frac{q}{c_m}\right)^{\frac{1}{2}} \cdot (R \cdot \Delta T)^{-\frac{1}{6}} \quad (1.1)$$

where k is a constant provided by the regulation ($k = 340$ for gaseous pollutants, $k = 680$ for dust), q is the emission rate of pollutant (in $\frac{kg}{h}$), R is the volume flowrate (referred to the conditions of emission), ΔT is the difference between the exhausts temperature and the mean annual air one, c_m is the maximum contribution due to the plant to pollution at the ground (in $\frac{mg}{Nm^3}$), given by $c_m = c_r - c_o$ (c_r is a reference value for the considered pollutant provided by the regulation, c_o is the mean annual concentration at the considered location). The product $s = k \cdot \frac{q}{c_m}$ is evaluated for each different pollutant; it is then considered the maximum value obtained in order to estimate the height of the chimney.

Since the last two mentioned regulations are part of the same decree but they are applied to different power plants, in order to have a better comprehension it was attempted to find a possible relation between the two. It was demonstrated that the values for the height given by the table (Figure 1.1) are roughly obtained from Eq. 1.1 (Appendix A.1). For general power plants the value is obtained considering a medium annual background pollution, c_0 ; the terms in brackets are instead obtained by applying the formula considering a high value of c_0 .

Chapter 2

Basics on industrial pollutants dispersion

Considering the importance of the study of pollutants dispersion for air quality assessment, different methodologies have been developed in the last century in order to evaluate this phenomenon, whose main aim is to predict the pollutant concentration at some point distant from the source. The approaches used to study dispersion can be divided into four main categories: full-scale experiments, physical modelling, semi-empirical methods and CFD modelling [6]. Full-scale experiments consist in a direct measurement of the pollutant concentration under real atmospheric conditions. Such an approach presents many limits, not only because a limited number of points in space can be evaluated, but also because the same experiment cannot be repeated with the same atmospheric conditions. As an alternative, reduced-scale experiments (also referred to as wind-tunnel experiments) could be used. The main advantage is given by the possibility to control boundary conditions in order to simulate stationary flow conditions. Even in this case, one of the problems consists in the impossibility to extract the information about concentration in the space of the domain. Semi-empirical models are instead based on an analytical approach. In this case the plume of pollutants coming from the source is modelled using a Gaussian distribution; this procedure allows to evaluate the concentration at all the points of the domain of analysis. However, this methodology is based on different assumptions (constant meteorological conditions in space, pollutants with the same density of air, infinite domain, constant emission rate of pollutants) and it requires the use of empirical parameters. The application of this methodology is thus limited to simplified flow configurations and the evaluation of concentration is accurate only at distances larger than 100 m from the source [7]. In addition, they result in an overprediction of concentrations in low wind conditions [8].

Recently, Computational Fluid Dynamics (CFD) models have been increasingly used to study pollutants dispersion, due to the rapid development in computer hardware and numerical modelling. In this kind of methodology, the domain is divided into a certain number of points (cells) in order to convert the continuous problem into a discrete one. For all the cells partial differential equations are solved either by the use of finite difference methods or finite volume ones. In pollutants dispersion applications the conservation equations for wind field and concentration are solved. CFD models can provide good results in a relatively cheap computational cost, al-

lowing the evaluation of pollutants concentration in all the points of the domain. The application of this methodology is preferred especially for micro-scale problems [9]. The main disadvantage related to this approach for dispersion modelling is the difficulty to assess the quality of the results in terms of accuracy and reliability; the most common practice is to compare CFD results with wind tunnel experiments in discrete points in space.

The universality of the application of CFD methods, regardless of their limitations, makes this type of analysis the most appropriate for a parametric analysis as the one aimed at being performed in this study.

In the following, basic principles on pollutants dispersion as well as the methodologies for the numerical study of this phenomenon are described.

2.1 Basics on atmospheric dispersion

2.1.1 Atmospheric boundary layer

The modelling of dispersion mechanisms depends on the scale of the problem. As in this analysis industrial emissions are considered, the atmospheric boundary layer (ABL), also called planetary boundary layer (PBL), is involved. It represents the lower layer of the troposphere, influenced by the Earth's surface over a time period of one day (Figure 2.1). In this part of the atmosphere the interaction between air and surface occurs in two main forms: a mechanical contribution due to the shear stress generated by the motion of the wind that flows above the ground and a thermal contribution resulting in convective effects due to solar radiation. The combination of these two physical processes, that represents the turbulence of the system, determines a variable height of the ABL during the day; its height is in average about 1 km , but it can vary in a range from about 100 m to 2 km .

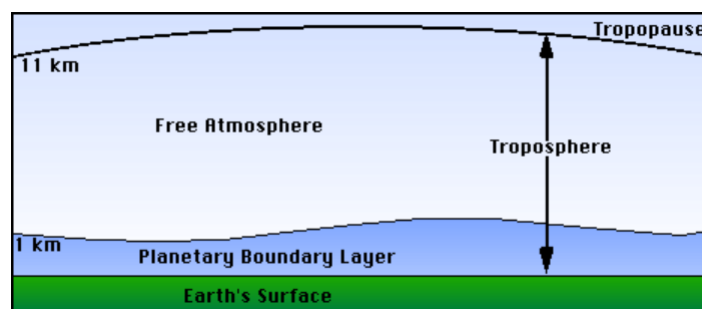


Figure 2.1: Representation of the PBL [10]

From a mathematical point of view, the modelling of this part of the atmosphere is made starting from Navier-Stokes formulations, that are based on conservation equations. In the ABL air is generally modelled as a constant density Newtonian fluid. According to this assumption, the description of the atmosphere can be expressed through conservation equations and thermodynamic equations (equation of state, continuity equation, momentum conservation, energy conservation, conservation of scalar quantities). These equations represent the starting point for all the

CFD approaches to modelling of pollutants dispersion. However, since in most of the cases the number of unknowns is larger than the number of equations, a closure problem that hinders the resolution of Navier-Stokes equations persists. To overcome this problem, different closure assumptions are generally used to model the atmosphere.

2.1.2 Pollutants dispersion

After the introduction of pollutants in the atmosphere a dispersion process occurs. Pollutants dispersion can be defined as the spread and movement of the particles emitted from a source into the atmosphere [11]. This phenomenon results from the combination of two main mechanisms: transport and diffusion. The first one is due to the action of wind, that according to its intensity and orientation allows the transportation of pollutants over long distances; as the mean wind velocity increases the dispersion increases as well. Diffusion is instead due to turbulence: the characteristic fluctuations in the flow allow the pollutant to spread in the air. An increase in turbulence determines a larger mixing. In general, pollutants dispersion is represented with a characteristic plume, resulting from the combination of the two effects (Figure 2.2).

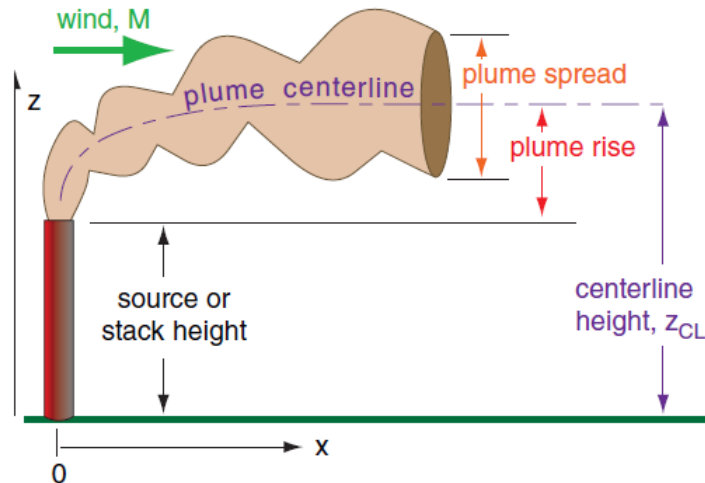


Figure 2.2: Schematic representation of a plume [11]

Moreover, when dealing with dispersion of pollutants other processes should be considered, namely chemical transformations and deposition on surfaces. Many compounds are indeed formed in the atmosphere by a series of complex, nonlinear chemical reactions, and sometimes they are even more harmful than their precursors. Deposition instead determines a sink term in dispersion, and it can occur both on dry surfaces (dry deposition) or humid ones (wet deposition).

2.2 Main factors influencing dispersion

Many factors can affect the measured concentration in a specific location and should be considered when dealing with pollutants dispersion. Generally speaking, it could be said that the phenomenon depends on three main factors: the conditions of emission (i.e. continuous or instantaneous release), the type of emitting source (diffuse, linear or isolated sources), external environmental conditions (such as meteorological conditions or topological features of the surrounding area). For industrial pollution the most common situation that can occur is a continuous emission from an isolated source.

The parameters are in general not independent from the others and a variation of one can determine a consequent change in the value of another. In the following a list of the main parameters that can affect industrial pollutants dispersion in the atmosphere and a brief description of their effects is attempted.

2.2.1 Effective height of emission

The height of emission strongly affects the measured concentration of pollutants at the ground. Considering the dispersion process, a higher location of the release point guarantees a larger dispersion of pollutants in the surrounding air, especially when the turbulence effect in the atmosphere is intense. Consequently, the mixing of pollutants in the air increases, determining a decrease in the measured peak concentration at the ground.

In the first place, the height of emission depends on the physical dimensions of the stack: a taller chimney guarantees a lower peak of ground concentration if all the other conditions do not change. According to this observation the increase of the stack height is thus a primary method to control air quality [12] and it is generally recommended in Good Engineering Practices (GEP) manuals [13].

When dealing with the modelling of dispersion though, the height of emission does not only depend on the stack height but also on another parameter named plume rise. It results from the combination of two effects: a buoyancy effect due to the difference of temperature between the particle and the surrounding air and a momentum effect related to the velocity of emission of the particle. In practice, the effective height of the stack H can be expressed as:

$$H = h_p + \Delta h \quad (2.1)$$

Where h_p is the real chimney height, Δh is the additional quantity due to the plume rise. In practice, the modelling considers a fictitious source located at H (Figure 2.3); the axis of the plume is considered at the effective height.

Different mathematical formulations have been developed in order to estimate the additional term due to the plume rise effect [15]. However, the most commonly adopted techniques are based on the formula of CONCAWE or Briggs formulas. Although all the methodologies are based on different hypothesis, they present a common feature, that is the dependence on the temperature of the source and the velocity of emission, that are related to thermal buoyancy and momentum effects respectively. In particular, an increase in the temperature of the source determines a larger temperature gradient with respect to air, resulting in a larger elevation of

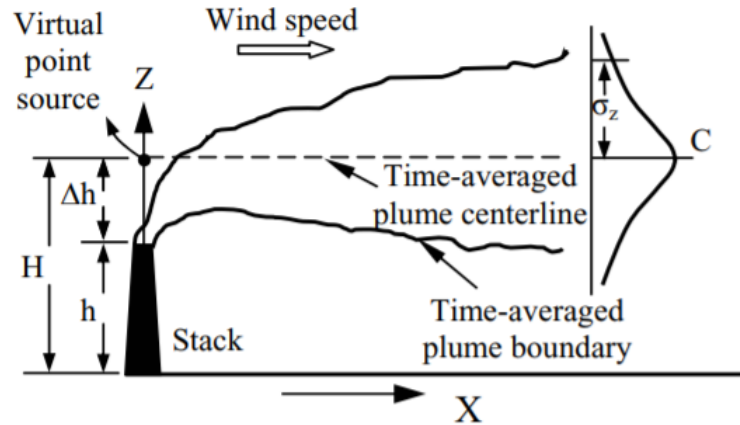


Figure 2.3: Schematic representation of dispersion [14]

the plume. A larger velocity of emission determines a higher plume rise too, due to a larger acceleration of the particle; in some cases, the increase of jet velocity can also have the same effect of an increase in the height of the stack [16].

2.2.2 Emitted species

Industrial sources can deal with different pollutants species. It is common to refer to two main types: gaseous phase pollutants and particles. The nature of the species determines different ground concentrations, due to several reasons. In the first place the density of each pollutant determines differences in the buoyancy effect. For example, light gases will have a different behaviour with respect to heavy ones and particulate matter. The difference in the behaviour is more significant in the case of complex terrains (as for example in urban environments) [7].

Moreover, chemical reactions could occur in the atmosphere. In this regard atmospheric pollutants can be divided into primary (when they do not undergo chemical reactions) and secondary (when they are a product of a transformation of primary pollutants that have participated to reactions). In the industrial field, the most concerning ones are SO_2 , particulate matter (primary pollutants) and NO_2 , that is a secondary pollutant generated from the reaction of NO with ambient air (producing O_3). Some studies showed that in particular conditions secondary pollutants behave differently from primary ones [17].

Finally, phase changes should be taken into account for specific emitted species (i.e. LNG , CO_2).

2.2.3 Atmospheric conditions

Atmospheric conditions can affect pollutants dispersion in different ways, that can be explained evaluating the structure of the ABL.

First of all, considering a flat and homogeneous terrain a diurnal cycle could be observed, regulated by the heating and cooling of the surface during the day (Figure 2.4). Starting from the sunset, a convective mixed layer arises, whose thickness increases with time. The formation of this layer, characterised by strong convection

effects, is due to thermal exchanges between the surface that is heated by solar radiation and surrounding air. As a consequence, during daylight hours a strong mixing occurs. During night instead, the surface cooling determines the formation of a stable boundary layer close to the ground that weakens vertical exchanges. Opposite buoyancy behaviour can thus be observed in these two situations.

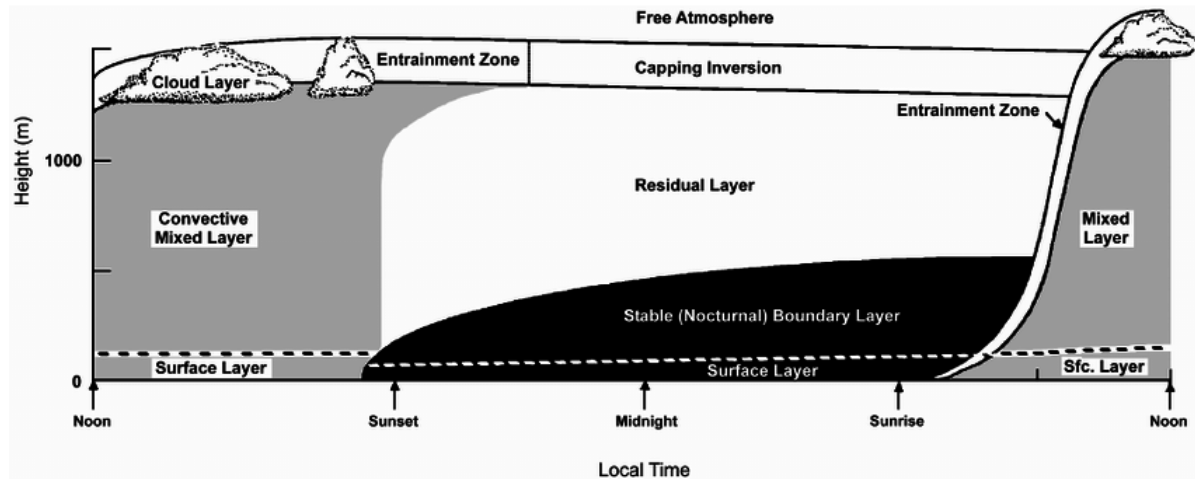


Figure 2.4: ABL structure at different hours of the day [18]

These physical processes determine the static stability of the atmosphere. When a convective mixing layer is developed an unstable stability, characterized by high turbulence, can be observed. During surface cooling instead a stable stability occurs, determining lower convective effects.

Buoyancy effects due to ABL structure strongly affect dispersion. For example, in some cases the variation of thickness of the mixing layer can account for more than 50% of the variation in near surface concentrations of pollutants; as the mixing layer increases the concentration decreases, especially when a high amount of pollutants is emitted. However, these effects depend on the type of pollutant: for primary ones an increase in the mixing layer reduces the mean and maximum values of concentration; for secondary pollutants (such as NO_2) this effect is weaker [17].

The dispersion is also affected by the presence of wind, who plays a major role in the transport. As wind intensity increases, thermal effects become less important and turbulence is mostly generated by the shear stress close to the ground. Such a situation occurs in the case of neutral atmospheric stability (like in the residual layer). However, atmospheric static stability and wind field are not separated effects, but a relation between the two exists. In particular, the atmospheric regime affects wind profile, determining different profiles especially close to the ground. An example is given in Figure 2.5.

2.2.4 Surface roughness

Surface roughness affects wind profile in the boundary layer due to the turbulence induced by the drag force close to the ground. In meteorology, to define the amount of mechanical mixing introduced by the surface roughness a specific parameter is used: the aerodynamic roughness length. Using this parameter, a surface is homogeneously described as composed by elements with the same average height. There are different methodologies to evaluate the value of z_0 , but in general, as a rule of

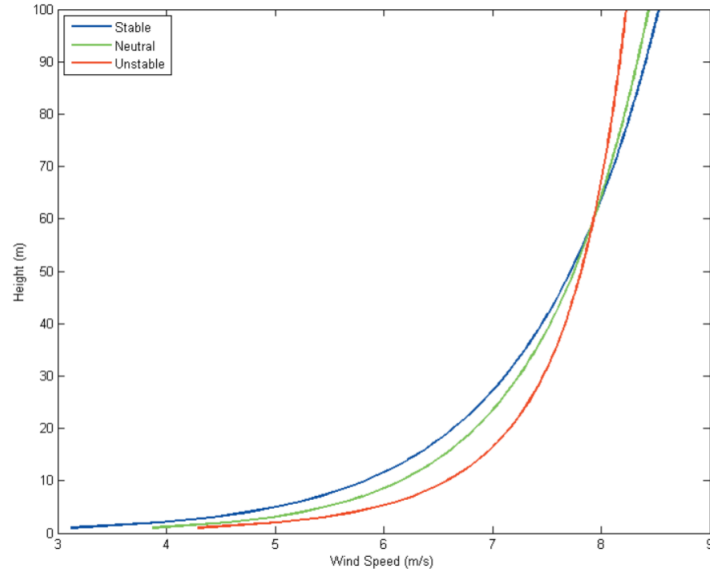


Figure 2.5: Example of the effect of atmospheric stability on wind profile [19]

thumb, it is considered equal to $\frac{1}{10}$ of the average height of the roughness elements that compose the surface [20]. By using this parameter, a relation can be established for the wind profile in neutral atmospheric conditions:

$$\frac{u(z)}{u^*} = \frac{1}{\kappa} \ln\left(\frac{z}{z_0}\right) \quad (2.2)$$

where u^* is the friction velocity, z_0 the aerodynamic roughness height, κ the Von Karman constant (about 0.41).

The effect of ground roughness on wind profile is shown in Figure 2.6 (in logarithmic scale). In this case it is considered a constant geostrophic wind speed at the top of the boundary layer (about 12m/s).

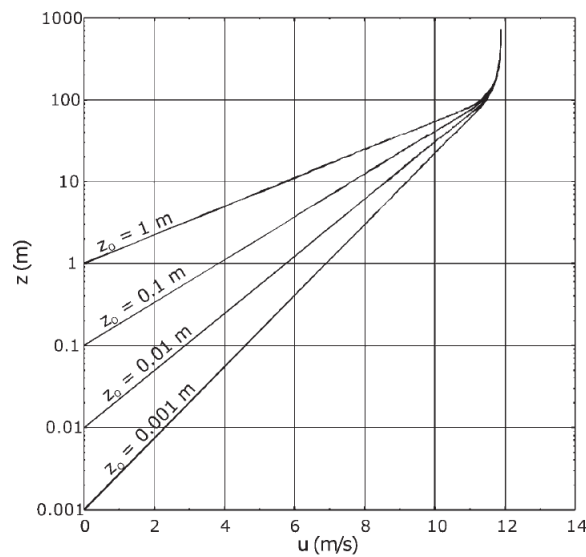


Figure 2.6: Wind modification according to the value of z_0 (for neutral stability) [20]

Homogeneous terrains are rarely encountered in reality, but this approach can be used as a basis to describe the flow in complex terrains.

2.2.5 Presence of obstacles

The presence of obstacles modifies the wind profile close to the element. For a given-shaped object, the characteristics of the flow depend very strongly on various parameters such as size, orientation, speed, and fluid properties. In general, different behaviours can be detected according to the type of flow, determined by its Reynolds Number, Re (that is the ratio between inertial and viscous effects). Especially for high Re (high inertial forces), that is the most common situation in reality, the presence of obstacles produces the formation of several effects such as flow separation (when the streamlines that represent the flow are not parallel anymore to the object profile), recirculation regions (changes in flow direction on the other side of the element), wakes, stagnation points [21]. Most of the studies are carried out considering standard shapes for the obstacles due to the high complexity of the problem. Figure 2.7 shows a qualitative description of the phenomena for a cubic obstacle.

Considering pollutants dispersion, given the difficulty to deal with obstacles, in

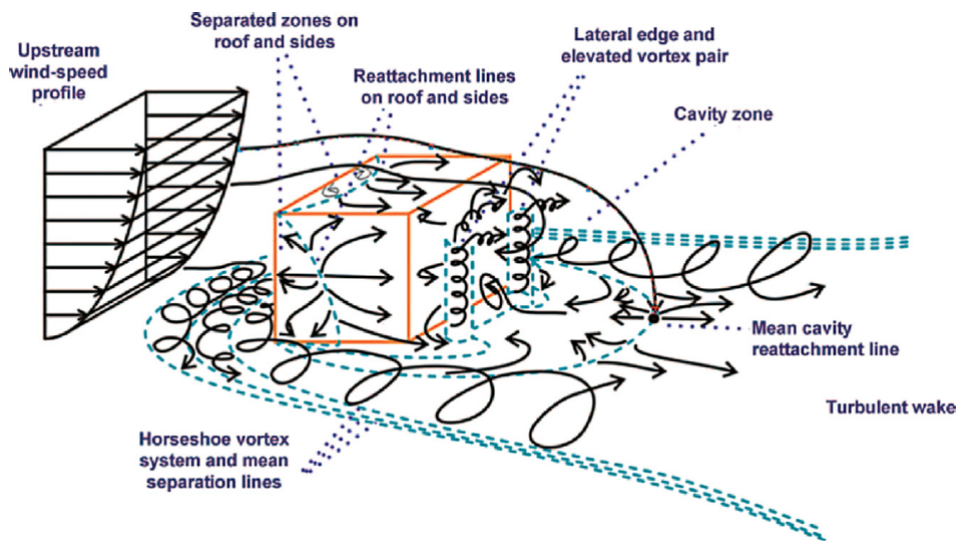


Figure 2.7: Qualitative description of the flow close to an obstacle [6]

most of the studies either the effect of thermal stratification or the presence of obstacles is neglected. The first term is neglected when assuming weak thermal buoyancy due to enhanced mixing by turbulence induced by the obstacle geometry [22]. The second hypothesis is made when dealing with far-field dispersion, because horizontal motion prevails on the vertical one [23]; the presence of obstacles is instead relevant especially for near-field releases (such as the ones that occur in cities). However, obstacles produce a large variability in pollutants ground concentration for the turbulence induced to the flow.

2.3 Numerical modelling of dispersion

There are different methodologies to numerical model pollutants dispersion in the atmosphere. The most common ones are based on the Eulerian or Lagrangian approach, even if other approaches are possible.

2.3.1 Eulerian methods

Eulerian methods are based on the solution of the advection-diffusion equation, solved in a fixed-coordinate frame. These numerical solutions are commonly used for pollutants dispersion in the ABL. Among them, the two most used modelling techniques to study dispersion with this approach are RANS and LES.

The first one is based on the resolution of Reynolds Average Navier-Stokes (RANS) equations. These are a formulation of Navier-Stokes equations obtained from a statistical approach, introduced by Reynolds to solve the high non-linearities and randomness that characterise turbulent flows. The method is based on the decomposition of the variables into a mean and a fluctuating part (the term representing turbulence). Applying Reynolds's average to solve concentration:

$$\frac{\partial \bar{C}}{\partial t} = -\bar{u}_i \frac{\partial \bar{C}}{\partial x_i} + \frac{\partial \bar{C}}{\partial x_i} \left(K_{ci} \frac{\partial \bar{C}}{\partial x_i} \right) + \bar{S} \quad (2.3)$$

Where \bar{C} is the average concentration evaluated in a discrete point, \bar{u}_i is the mean velocity in the i -th direction, $K_{ci} \frac{\partial \bar{C}}{\partial x_i}$ (with K_{ci} turbulent diffusivity) is used to model turbulent diffusion ($u_i \bar{c}$), \bar{S} is a term that accounts for concentration variances due to emission, deposition and chemical reactions.

Since also using RANS equations a closure problem persists, turbulence should be modelled. There can be different approaches to model turbulence; the most common ones are the $k-L$, the $k-\epsilon$, the $k-\omega$, chosen according to their applications and hypothesis for the formulation. The resolution of RANS equations for the flow field and concentration is made by means of either a finite difference or finite volume numerical scheme.

A particular solution of RANS equations, obtained with the use of different assumptions for the model (i.e. stationary meteorological conditions, pollutants with same density of air, constant turbulent diffusion coefficients), leads to the analytical formulation used by Gaussian models.

Another technique used to model dispersion is based on the use of filtered Navier-Stokes equations, namely the Large Eddies Simulation (LES) equations. According to this methodology, a filter is applied to define large and small scales for turbulent terms; large scales are directly resolved, while small ones are modelled. In this case the equation to solve for concentration \tilde{C} is:

$$\frac{\partial \tilde{C}}{\partial t} = -\tilde{u}_i \frac{\partial \tilde{C}}{\partial x_i} + \gamma_{sg} \frac{\partial \tilde{C}}{\partial x_i} + \tilde{S} \quad (2.4)$$

In which \tilde{u}_i is the velocity in the i -th direction resolved at large-scale, $\gamma_{sg} \frac{\partial \tilde{C}}{\partial x_i}$ is used to model subgrid-scale diffusion (γ_{sg} is the subgrid scalar diffusivity), \tilde{S} is the

a term that accounts for concentration variances due to emission, deposition and chemical reactions at large-scale.

Comparing the two approaches, LES modelling resolves large-scale unsteady motions and requires only small-scale modelling, while RANS one applies Reynolds average to the entire domain of application. These two approaches can result in significant differences. Several studies were carried out in order to evaluate the difference in pollutants dispersion between the two approaches. In general, experimental data is used as a reference to compare the results. The main differences between the two models are detectable when obstacles, and in particular when complex environments characterised by the presence of buildings, are involved (the difference is indeed larger for a street canyon than for a cubic obstacle [24]). In such a context indeed, the turbulence induced by the presence of obstacles determines large variations in the wind field, that affects dispersion as well. The way the two methods model fluctuation terms significantly affects the results.

The most significant difference is related to the fact that the high turbulence induced by buildings is primarily due to large-scale motions, which can be directly reproduced in LES [23]. Due to this, in most of the studies it is shown that LES results are in better agreement with experimental ones. Analysing the flow in more detail it was indeed shown that RANS underestimates turbulence diffusion in comparison with LES [24].

The better agreement of LES results with experimental ones suggests that this methodology should be preferred to RANS one. However, even if it not directly possible to compare computational costs of the two methodologies due to the different convergence criteria used by the two approaches, LES are generally 10 to 25 times more computationally expensive [23]. In addition, it should be considered that LES simulations were carried out in wind tunnels under well-controlled and near-ideal conditions, but when dealing with real situations the accuracy of the results could be the same order of RANS approach [25].

Considering the limitations of RANS models to reproduce unsteady fluctuations (due to the fact that the equations of the model consider steady conditions), a variation of this approach, namely the unsteady RANS (URANS) modelling, has been recently introduced. Better results can generally be obtained with this method when variability in wind is significant. However, since turbulence is still fully modelled the improvement concerns low-turbulence cases. Moreover, the choice of the turbulence model is determinant for this approach [23].

2.3.2 Lagrangian methods

In Lagrangian modelling, the motion of each air parcel is described. The motion is driven by the wind field, that is described as a combination of two components: a mean (deterministic value) and a turbulent one. This second term, that is a stochastic variable, describes the fluctuation of wind field due to atmospheric turbulence [26]. In general, the displacement of the particle is given by [27]:

$$dx_i = (U_i + u_i) dt \quad (2.5)$$

In which U_i is the main velocity component and u_i is the turbulent one. This second term can be expressed as:

$$\frac{du_i}{dt} = a_i(x_i, u_i) dt + b_i(x_i, u_i) \xi_i(t) \quad (2.6)$$

Where u_i is the turbulent velocity, $a_i(x_i, u_i)$ is the deterministic term, $b_i(x_i, u_i) \xi_i(t)$ is the stochastic term in which ξ_i is a normally distributed random increment.

The main advantage of these methods is that they do not depend on the computational grid, making them useful tools for the evaluation of long-range dispersion but also short-range applications as an alternative to high-resolution Eulerian computations. In addition, they can take into account high temporal and spatial variations in the meteorological field without adding computational cost to the analysis. Nevertheless, the computational time required by Lagrangian models is higher with respect to Eulerian ones.

2.3.3 Other methods

Other models could be used, even if with limitations in their applicability due to the assumptions they are based on. Among these methods, box models, aerosol dynamic models, dense gas models can be recalled. In box models the domain is treated as a box in which emitted pollutants undergo chemical and physical processes. These models are based on the conservation of mass. Air is treated as well mixed, with uniform concentrations all over the domain. They can accurately describe the chemistry and physics of the particles in the atmosphere, but they do not take into account local concentrations of pollutants, resulting in lacks in the modelling in local environments, in which particles dynamics are influenced by local changes of wind field and emissions. Aerosol dynamic models and dense gas models are instead developed to solve dispersion for particulate matter and dense gases respectively.

Chapter 3

Design of the experiment

3.1 Assessment of the problem

3.1.1 Objectives of the analysis

The aim of the analysis consists in a critical review of the current French regulation that establishes the minimum height of industrial chimneys.

As shown in Chapter 1.2, the values prescribed in this decree are obtained by means of a specific analytical formula, Eq. 1.1, that involves several parameters linked to atmospheric dispersion. However, a deeper focus on the phenomena that occur during this process shows that many other parameters with respect to the ones considered in the formula of the regulation are involved (Chapter 2.2). The determination of the industrial chimney's height with Eq. 1.1 could then appear to be too simplistic.

In order to have a comprehensive overview of the effectiveness of the regulation three main questions should be addressed in the analysis:

- *Are all the most affecting parameters considered in the formula for the determination of the minimum chimney's height?*
- *Does the formula properly work in any possible situation it is assessed for?*
- *Is the minimum chimney's height enough to ensure the respect of air quality standards?*

To give an answer to these questions different types of evaluation should be performed. For the first two, a generic analysis (i.e. not referred to specific situations) should be carried out, in order to obtain universal results that can be applied to any situation. For the third question instead it is not possible to adopt this type of approach: the answer could be got through a comparison between the contribution to pollution deriving from the industrial plant and the European air quality standards (Table 1.1). However, since threshold values are expressed as averages in specific periods of time (one hour to one year), several factors as for example variable meteorological conditions or variable operational mode of the plant during that period of time should be considered. As it is not feasible to generalize this type

of information still obtaining reliable results (several hypotheses should indeed be made), a more specific analysis applied to particular locations for which real data is well known should be performed. Given the necessity of different approaches to have a comprehensive overview of the regulation, this work is then only aimed at the achievement of general results in order to answer to the first two questions, opening up new prospects for further analysis as a complement.

The starting point for the analysis is the data about real power plants provided by the enterprise *Poujoulat SA* (Appendix A.1). As the information is only available for two fuel types, namely natural gas and biomass, it is chosen to perform the analysis only for biomass plants because they involve the emission of three main pollutant species (NO_x , SO_x and *dust*), with respect to natural gas ones that only emit NO_x , giving the possibility to have a more extensive overview of the problem.

3.1.2 Methodology for the resolution

The regulation is introduced with the aim of preventing from risks to human health and environment. It is consequently chosen to consider as criteria for the evaluation of the regulation the peak of pollutant concentration at the ground, defined as the concentration in the breathing zone (in this analysis, it is intended as the pollutant concentration average from the ground up to 2,5 m based also on the considerations made in Chapter 1.1 regarding the sample position). The location of the peak is also determined for more qualitative considerations. The evaluation of the pollutant concentration is made through the use of numerical modelling, carried out with the support of the software Fluidyn-PANACHE.

To answer to the first question, it should be quantified the effect of the parameters involved in the dispersion process. In this way, the most affecting ones will be identified and a comparison with the terms used by formula in the regulation will be carried out. This evaluation is made by means of a parametric analysis. There are several methodologies used as support for this kind of study; in this analysis the Design of Experiments (DOE) will be implemented, in order to find the set of simulations to perform.

Concerning the second question instead, the regulation should be evaluated in several different situations that could realistically occur; then, a comparison with threshold values should be performed. The set of situations should include more common conditions and extreme ones in terms of production of peak of concentration. For this aim, the same DOE and also the results of the parametric analysis could be used as support: the identification of the configuration that gives the highest value of ground concentration peak could indeed be found with this analysis.

3.2 Design of Experiments methodology

The design of the problem, intended as the choice of the set of cases to perform in order to get an answer to the previously mentioned questions, is found through the application of a specific methodology generally used when performing parametric

analysis. It should be reminded that the objective of this type of study is to evaluate the effect of different input factors on a certain output. There are different methodologies at support of this type of study. The most common approach is to vary one variable at a time, keeping all the other variables of the experiment fixed (this method is called One-Variable-At-a-Time, OVAT). Nevertheless, this kind of approach requires a large number of experiments to obtain a limited amount of information about the process [28]. A more efficient way to run a parametric analysis is offered by the use of Design of Experiments (DOE), a methodology developed in early 1920s and based on statistical approaches. In this kind of analysis input parameters are intentionally varied in order to observe corresponding changes in the output response.

The DOE methodology consists in three different phases: a designing phase in which the design of the experiment itself is defined, a conducting phase consisting in the carry out of the experiment, an analysing phase in which the results are evaluated in order to obtain conclusions. The same steps are applied to the current analysis. For the designing phase different approaches could be used (mainly classical designs by Fisher or orthogonal array approaches by Taguchi). Classical methods are applied when the output behaviour is should be analysed in detail; Taguchi methods when the sensitivity of response of the analysis to noise factors (not controllable factors that affect the results) should be evaluated. The classical methods by Fisher will be used for this analysis because it is the most suitable one for the aims of the analysis (i.e. the evaluation of the pollution contribution of the plant when different parameters are varied).

The application of the DOE methodology allows to evaluate the weight of each parameter on the output response. In addition, the effect of interactions between parameters can be evaluated (an interaction occurs when the effect of one factor on the output is different at different levels of another factor). In practice, the parameters of the analysis can be evaluated at two or more different values, called levels, that can be quantitative or qualitative. When choosing the levels for a factorial design, the assumption is that the output has a quite linear behaviour in the range between the two extremes.

The number of runs needed to obtain the results depend on the choice of the experimenter; as the number of trials decrease the quality of resolution of the problem decreases as well, but the main results can still be obtained. In practice, to decrease the number of runs needed for the analysis the effect of some interactions should be “confounded” with main factors (aliasing process): in this way, a larger number of parameters can be considered without increasing the number of experiments needed. For a Full factorial design, that is the one in which all the possible combinations of levels of the parameters are performed, the number of runs can be determined as:

$$N_{runs} = L^k \quad (3.1)$$

Where N_{runs} is the number of runs requested by the design, L is the number of levels, k is the number of factors (or parameters) that are evaluated in the analysis. If the number of runs requested by the analysis is too large, a Fractional factorial design could be used. In this kind of experimental design the resolution of the problem is decreased by aliasing interactions with main factors. In practice, with this kind of design only $\frac{1}{L^p}$, where L is the number of levels and p the number of orders of interactions to neglect, of the number of experiments requested by the Full

factorial design is performed. For example, in a two levels, three factors design the third order interaction effect (AxBxC) could be neglected, reducing the number of experiments to $\frac{1}{2^3} = \frac{1}{8}$ of the total one. The number of runs needed is determined as:

$$N_{runs} = L^{k-p} \quad (3.2)$$

3.3 Choice of the parameters to analyze

Many parameters are involved in the dispersion process (Chapter 2.3) but the determination of the minimum height with Eq. 1.1 only takes into account some of them. If all the parameters involved in dispersion were considered in the analysis a very large number of simulations would be required, even if a Fractional factorial design were used. Thus, in order to make the analysis feasible in terms of time, only some of all the possible parameters will be explicitly evaluated in this work. The parameters to vary in the analysis are selected according to two main characteristics: their relation to the regulation and the independence of their value from the one of the others.

First of all, the regulation is considered in order to identify the terms involved. Recalling Eq. 1.1, it can be observed that the height of the stack is written in function of the following terms:

$$h_p = h_p(k, c_r, c_o, q, R, \Delta T) \quad (3.3)$$

Where k is the constant adopted in the regulation, c_r is the reference pollution value, c_o is the background pollution level, q is the specific pollutants flowrate at the emission, R is the smoke volumetric flowrate, ΔT is the temperature difference between the temperature of the source (T_{source}) and the mean annual ambient air temperature (T_{air}).

However, some parameters are linked to the others by specific relations; in particular:

- $q = \frac{c_x \cdot R_o}{10^6} = q(c_x, R, \text{smoke composition})$
- $R = \frac{\dot{m}}{\rho_{T_{source}}} = R(\dot{m}, T_{source}, \text{smoke composition})$
- $\Delta T = T_{source} - T_{air} = \Delta T(T_{source}, T_{air})$

Where c_x is the concentration of pollutant emitted at the source, \dot{m} is the smoke mass flowrate, $\rho_{T_{source}}$ is the smoke density evaluated at the source temperature, the smoke composition is given by the percentages of molecules that constitute the smoke.

In addition, k , c_r and c_o are constants, the first two depending on the type of pollutant, the third one depending on the pollution level in the location of the plant. Thus, Eq. 3.3 can be rewritten as:

$$h_p = h_p(c_x, \dot{m}, T_{source}, T_{air}, \text{smoke composition}, \text{background pollution level}, \text{type of pollutant}) \quad (3.4)$$

Since still 7 factors contribute to the determination of height, in order to decrease this number some simplifications of the problem are adopted:

- c_x : it is considered constant for a specific pollutant and equal to the maximum value allowed by regulations (the limit values indicated in the French regulation and used for this analysis, according to the size of the plant, are indicated in Figure A.4);
- T_{air} : it is considered constant for all the cases that will be simulated;
- *Smoke composition*: it is considered constant;
- *Type of pollutant*: considering biomass plants, NO_x , SO_x and dust emissions should be considered. In order to simplify the problem, these pollutants are approximated to NO_2 , SO_2 and PM_{10} respectively, because these pollutant species are the most important ones to consider when dealing with industrial pollution.

Considering all these assumptions, the equation for the height of the stack can be finally written as function of three parameters only:

$$h_p = h_p(\dot{m}, T_{source}, background\ pollution\ level) \quad (3.5)$$

The regulation does not explicitly take into account other parameters linked to atmospheric conditions or location characteristics. In particular, some of the parameters that could be considered are atmospheric stability, ground roughness, wind profile, ABL height; it is chosen to include the first three in the parametric analysis. The last one is not considered because it would result in several different plume profiles according to the stable atmospheric stability at the emission height, increasing too much the difficulty in the assessment of the problem because, as it will be better explained later, only two levels for each parameter will be considered.

The height of the stack will not be explicitly considered as a factor to vary, but it will be determined according to the values assumed by the background pollution level and the mass flowrate (that is assumed to be proportional to the plant nominal power). In this way, in all the configurations that will be simulated the height of the stack will be set to its minimum value according to the regulation. As a consequence, the results of each run will already represent the ground concentration obtained by applying the regulation. The same will be done for the other parameters that are dependent on the ones selected for the parametric analysis. In particular, the concentration of pollutants emitted by the source c_x corresponds to the maximum allowable value according regulations on emissions, that is different for different power sizes of the plant.

All the parameters could be evaluated considering a 2-level factorial design except for atmospheric stability, that would instead need a 3-level design to simulate stable, unstable and neutral configurations. Nevertheless, using a 3-level design would determine the use of a much larger number of simulations (for example, in a Full Factorial design it will be $3^6 = 729$ cases, instead of $2^6 = 64$ cases). Due to this reason, is chosen to decompose the stability parameter into two main factors, namely wind profile and solar radiation, expressed in terms of time of the day (to simulate morning and night). The wind profile will be considered as a logarithmic one, imposing a velocity value at a reference height ($10m$). A combination between wind profile and solar radiation corresponds indeed to a specific atmospheric stability when reference is made to Pasquill stability classes (Figure 3.1). The classes indicated by Pasquill cover a range from A to F. An A class corresponds to an ex-

tremely unstable case (in which a high dispersion process occurs), an F class to an extremely stable one (determining low dispersion phenomena); intermediate classes correspond to intermediate situations. In particular, a neutral stability corresponds to a D class.

Wind speed at 10 m (m s ⁻¹)	Night				
	Insolation			Thinly overcast or ≥ 4/8 low cloud	
	Strong	Moderate	Slight	≤ 3/8 cloud	≤ 3/8 cloud
< 2	A	A-B	B	—	—
2-3	A-B	B	C	E	F
3-5	B	B-C	C	D	E
5-6	C	C-D	D	D	D
> 6	C	D	D	D	D

Figure 3.1: Pasquill stability classes [29]

Summarising, the parameters considered in the analysis are:

- *source temperature*, T_{source}
- *mass flowrate*, \dot{m} (that is proportional to the nominal power of the plant, and thus determining different values for the minimum height according to Figure 1.1)
- *background pollution level* (used to refer to general or PPA locations and thus vary the height)
- *wind speed* at 10m
- *time of the day*
- *ground roughness* (expressed through the aerodynamic roughness length, z_0)

The two levels to assign to each of the parameters should represent two extreme cases.

For the choice of the levels for wind speed and time of the day reference is made to Pasquill stability classes with the aim of performing three different atmospheric stability regimes: extremely unstable, extremely stable case and neutral. In particular, the wind speed value at 10m is set to $2\frac{m}{s}$ (to include stable and unstable cases) and $7\frac{m}{s}$ (to include neutral cases). Concerning the time of the day instead, two opposite situations are considered: 2PM to simulate strong solar radiation and 2AM to simulate ground cooling during night. Using this strategy, it is possible to simulate all the desired atmospheric regimes: low wind velocity and high or low solar radiation indeed give rise to unstable and stable cases respectively, high wind velocity determines a neutral one regardless of the time of the day.

The flowrate levels are chosen according to the values provided by the enterprise *Poujoulat SA* for 2 MW and 20 MW plants (Figure A.1).

The extremes for the source temperature are chosen according to realistic situations for a biomass power plant, again suggested by *Poujoulat SA*: a low temperature of $45^{\circ}C$ when heat recovery techniques are used, a maximum operational temperature of $180^{\circ}C$.

The background concentration level is a dummy parameter used to considered both the heights indicated in the regulation for general locations and PPA areas. Given the relation between pollution level and minimum height demonstrated in Appendix A.1, this parameter is set to medium (low level) and high (high level). The first case

corresponds to general locations, the other one to PPA areas.

Finally, for the ground roughness it is possible to find in literature several tables that correlate this parameter to the value aerodynamic roughness length z_0 . In this analysis reference is made to a specific values assessed by Wieringa [30] (Figure 3.2). The first intention was to simulate two opposite and extreme situations such as a plant located close to the seaside and one located close to woods or highly urbanised towns. Nevertheless, it was noticed that Fluidyn-PANACHE seemed not to properly adapt the flow to the ground roughness when very high values of z_0 were considered (probably due to a bug). Due to this reason the values set for z_0 correspond to a bare soil with grass ($z_0 = 0.01m$) for the low level and a grain field ($z_0 = 0.15m$) for the high one. Even if the most extremes situations are not performed, the quite large variance between these two values could still give an idea of the influence of this parameter on dispersion.

Table 1. Range of homogeneous surface roughness z_0 -- Wieringa (1992).

Surface type	Roughness length (m)
Sea, loose sand and snow	≈ 0.0002 (V-dependent)
Concrete, flat desert, tidal flat	0.0002-0.0005
Flat snow field	0.0001-0.0007
Rough ice field	0.001-0.012
Fallow ground	0.001-0.004
Short grass and moss	0.008-0.03
Long grass and heather	0.02-0.06
Low mature agricultural crops	0.04-0.09
High mature crops ("grain")	0.12-0.18
Continuous bushland	0.35-0.45
Mature pine forest	0.8-1.6
Dense low buildings ("suburb")	0.4-0.7
Regularly-built large town	0.7-1.5
Tropical forest	1.7-2.3

Figure 3.2: Aerodynamic roughness length (z_0) related to the type of terrain (Wieringa, 1992)

A summary of all the parameters to vary in the analysis and the two levels that can assume is shown in Table 3.1.

Table 3.1: Summary of the parameters to evaluate and their levels

Parameter	Low level (-1)	High level (+1)
Wind speed [m/s]	2	7
Hour [-]	2:00AM	2:00PM
Flowrate [kg/h]	5500	54900
$T_{source}[^{\circ}C]$	45	180
Background concentration [-]	Medium	High
z_0 [m]	0.01	0.15

3.4 Final simulation matrix

Six parameters, any of them with 2 levels, will be used in the parametric analysis. Considering a Full factorial design, the total number of simulations required would be $2^6 = 64$, still too high. Thus, it is chosen to use a Fractional factorial design. In order to choose the most appropriate one, reference is made to Figure 3.3, in which a summary of the possible configurations and their resolutions is summarised.

TABLE D-1 Two-Level Orthogonal Array Selection

OA	Number of two-level factors*																
	1	2	3	4	5	6	7	8	9	10	11	12	13	14	15	16	17
L4	4**	1	Not possible														
L8	4	2															
L16	4	3	2	1													
L32	4	3	2	1													
L64	4 with repetitions	4	3	2													
L128	4 with repetitions	4	3	2													
L256	4 with repetitions	4	3	2													

*Consider each three- or four-level factor equivalent to 3 two-level factors; for example, 1 four-level factor and 5 two-level factors would have to use an L16 because that is equivalent to a total of 8 two-level factors

**Resolution number is a measure of the amount of confounding in a column:
 4 = all items are in separate columns (full factorial)
 3 = A and B × C × D × E, or A × B and C × D × E are in the same column
 2 = A and B × C × D, or A × B and C × D are in the same column
 1 = A and B × C are in the same column

Figure 3.3: Aiding table for the choice of the Fractional factorial design to use (highlight on the one used) [31]

Considering 6 parameters, either a L8 (corresponding to 8 runs), a L16, L32 or L64 (Full factorial design) matrix could be used. In practice, the number indicated for each case of the table (in the range from 1 to 4) indicates the resolution level of the problem; the higher this value, the higher the resolution but also the number of runs needed. Decreasing the resolution, some of the interactions are aliased with new factors. For example, considering a resolution 2, only some of all the possible interactions between two parameters can be explicitly evaluated.

Given the number of required simulations and the resolution level of the problem for each possible matrix configuration, it is chosen to use a 16-runs Fractional factorial design, in which only $\frac{1}{2^2} = \frac{1}{4}$ of the Full factorial design is considered. The implication is that only some of the two-parameters interactions can be evaluated. This choice is mainly justified by time constraints. For each simulation it was indeed observed that the time needed get a solution was quite long (variable depending on the case, but in the order of several hours). Moreover, as each simulation required the resolution of the wind field before the dispersion process, the number of simulations was even larger.

The standard final matrix to use for this study is shown in Figure 3.4. The parameters can assume two levels (-1 and +1), that correspond to their minimum and maximum value respectively. In order to facilitate the lecture of the matrix, the value of each parameter is made explicit in Figure 3.5. In this table it is also shown

for each case the corresponding atmospheric stability (according to the combination of wind speed and time of the day) and stack height (according to the combination of flowrate value and background pollution level).

	A Wind speed	B Time of the day	C Flowrate	D Source temperature	E Background pollution level	F z_0
1	-1	-1	-1	-1	-1	-1
2	+1	-1	-1	-1	+1	-1
3	-1	+1	-1	-1	+1	+1
4	+1	+1	-1	-1	-1	+1
5	-1	-1	+1	-1	+1	+1
6	+1	-1	+1	-1	-1	+1
7	-1	+1	+1	-1	-1	-1
8	+1	+1	+1	-1	+1	-1
9	-1	-1	-1	+1	-1	+1
10	+1	-1	-1	+1	+1	+1
11	-1	+1	-1	+1	+1	-1
12	+1	+1	-1	+1	-1	-1
13	-1	-1	+1	+1	+1	-1
14	+1	-1	+1	+1	-1	-1
15	-1	+1	+1	+1	-1	+1
16	+1	+1	+1	+1	+1	+1

Figure 3.4: Simulation matrix used for the analysis ($\frac{1}{4}$ factorial design with 2 levels)

Case	Wind velocity [m/s]	Time of the day [-]	Flowrate [kg/s]	Source temperature [°C]	Pollution level [-]	z_0 [m]	Atmospheric stability [-]	Height of the stack [m]
1	2	2 AM	1.53	45	MEDIUM	0.01	STABLE	10
2	7	2 AM	1.53	45	HIGH	0.01	NEUTRAL	15
3	2	2 PM	1.53	45	HIGH	0.15	UNSTABLE	15
4	7	2 PM	1.53	45	MEDIUM	0.15	NEUTRAL	10
5	2	2 AM	15.25	45	HIGH	0.15	STABLE	24
6	7	2 AM	15.25	45	MEDIUM	0.15	NEUTRAL	20
7	2	2 PM	15.25	45	MEDIUM	0.01	UNSTABLE	20
8	7	2 PM	15.25	45	HIGH	0.01	NEUTRAL	24
9	2	2 AM	1.53	180	MEDIUM	0.15	STABLE	10
10	7	2 AM	1.53	180	HIGH	0.15	NEUTRAL	15
11	2	2 PM	1.53	180	HIGH	0.01	UNSTABLE	15
12	7	2 PM	1.53	180	MEDIUM	0.01	NEUTRAL	10
13	2	2 AM	15.25	180	HIGH	0.01	STABLE	24
14	7	2 AM	15.25	180	MEDIUM	0.01	NEUTRAL	20
15	2	2 PM	15.25	180	MEDIUM	0.15	UNSTABLE	20
16	7	2 PM	15.25	180	HIGH	0.15	NEUTRAL	24

Figure 3.5: Summary of the cases to perform

Chapter 4

Numerical model assessment

After the determination of the cases to perform, the numerical model should be assessed. The simulations are carried out by means of the CFD software Fluidyn-PANACHE. In the following a description of its main characteristics as well as the methodology adopted for the assessment of the numerical model are presented.

4.1 Fluidyn-PANACHE

Fluidyn-PANACHE is a modelling software suitable for the simulation of the atmospheric flow and pollutants dispersion in complex environments, used for the prediction or diagnosis of the impact due to accidental or chronic release of hazardous gases and particulates into the atmosphere [32].

The software solves the 3-dimensional Reynolds Average Navier-Stokes (RANS) equations for the conservation of species concentration, mass, and energy using a finite volume numerical scheme [33]. The modeling of Reynolds stresses is made under the hypothesis of linear eddy viscosity model [34].

The version used to perform simulations for this analysis is *Fluidyn PANACHE-SUPER 5.2.2.5* (release date in March 2019).

4.2 Setting of the model

In this analysis different configurations with different source characteristics and environmental conditions should be simulated. As a consequence, is not possible to use the same model for all the cases, but a common methodology can be applied for all of them. This can be made in particular for the choice of the dimensions of the domain and the grid, the imposition of inlet and boundary conditions, the physical models, the assessment of the atmospheric stability. The choice of the input models is aimed at running a realistic simulation at the lowest computational cost. Since these two objectives are in contrast with each other, a compromise is found by applying opportune simplifications and considering the constraints of the software.

4.2.1 Simulation mode

The problem can be set as steady or transient. In the first case the solution is independent of time (resulting the same at each instant of the analysis), while in

the transient case it can be evaluated the evolution of the solution in time. For the analysis it is chosen to apply stationary conditions, assuming that wind direction and intensity don't change in time. This hypothesis can be considered realistic when dealing with simulations aimed at representing a short period of time.

4.2.2 Domain

As some settings related to the domain such as the dimensions or the type of terrain depend on the case to be performed, the choice is not unique for all the simulations. To set the dimension, preliminary simulations with a coarse grid have been performed. Then, according to the results obtained, the choice is made in such a way to capture all the relevant information with the lowest allowable dimension. Concerning the terrain instead, Fluidyn-PANACHE gives the possibility to set different types (a general one imposing the aerodynamic roughness length value z_0 , a field type, a forest type, a water body type or an urban area), each of them presenting some specific characteristics. It is chosen to refer to the value of z_0 , estimated according to the reference table provided by Wieringa (Figure 3.2). However in practice, as some problems of adaptation of the flow were observed when setting the z_0 parameter to high levels, the terrain of the domain for these cases was modified by including as a new type of terrain (a field type one) with an equivalent value of z_0 at a short distance from the inlet. This approach was indeed observed to be the only way to obtain a fully developed wind profile, despite the higher computational cost.

No obstacles are considered in the domain in order not to incur the modifications of the regulation for this kind of configurations. Neglecting the presence of obstacles results in considering a surface with homogeneously distributed elements.

4.2.3 Setting of the source

Fluidyn-PANACHE gives the possibility to choose among different types of source, listed in Figure 4.1. Any of these have specific properties; it is thus important to choose the most appropriate for the application. Two different types of sources could be used for an industrial stack, namely *Point* or *Stack*.

Shape	Source in PANACHE	Description
Point	Point	Emissions occur at a point in vertical, horizontal, or other direction
Stack	Stack	Emission from a stack of industries and others
Area	Area Urban Area	Emissions occur on a surface patch on the ground or on an obstacle
Volume	Volume	Instantaneous release in a volumetric region
General	General	Emissions occur on a surface patch on the ground or on an obstacle

Figure 4.1: List of possible types of sources [35]

In this case it is chosen to use a *Point* source, according to the definition given in the User Manual of Fluidyn-PANACHE: *0-dimensional in shape. Though in reality, emission occurs over a surface (rupture in a pipe, stack exit), the size of the release area is negligible when compared to the study area. Use point source when you are not interested in the flow around the releasing object* [35]. In a first approach it is then assumed that the presence of the stack does not significantly affect wind flow. For a *Point* source, different characteristics should be specified (the height and direction of emission, the mass flowrate, the exit velocity, the species emitted and their concentration, the instant of release and duration in the case of transient mode). In the software, the concentration at the emission cannot be expressed in $\frac{mg}{Nm^3}$, that is the unit generally used for sources. Due to this reason a conversion of units is made under the assumption of modelling gaseous pollutants as ideal gases (Appendix B.1). For the definition of species, either a database of Fluidyn-PANACHE with information about the most common pollutants or new species definition could be used. The pollutants to study for a biomass plant are NO_x , SO_x and dust, approximated to NO_2 and SO_2 and PM_{10} as mentioned in Chapter 3.3. All these species are already defined in the database of Fluidyn-PANACHE and can immediately be used. It is important to notice that in the software PM_{10} is defined as an equivalent gas specie.

4.2.4 Inlet conditions

Inlet conditions are applied at the inlet of the domain and can be imposed when setting weather conditions. In particular, the imposition concerns the wind, turbulence and temperature vertical profiles.

The choice of the inlet profiles is made considering the assumption used by the software itself: *PANACHE models the structure of the surface layer using Monin-Obukhov similarity theory* [35]. Since the height used for the stacks is not excessively high (the maximum value used is 28m) it is assumed that the emission occurs in the surface layer, where Monin-Obukhov similarity theory can be applied. In this part of the atmospheric boundary layer the profile that better represents the real wind velocity profile is the logarithmic one [36], defined as it follows:

$$u(z) = \frac{u^*}{\kappa} \left[\ln\left(\frac{z}{z_0}\right) - \Psi_m(z) \right] \quad (4.1)$$

where u^* is the friction velocity, z_0 the aerodynamic roughness height, κ the Von Karman constant (about 0.41), $\Psi_m(z)$ the correction function for stability if it is not neutral).

For the temperature profile instead, a lapse rate is imposed. This value represents the gradient of temperature with the height, resulting in a linear temperature profile. This imposition assures the control of the atmospheric stability (imposing a logarithmic profile with the software for temperature did not allow to set the desired profiles for stable and unstable atmosphere).

Finally, for the choice of the turbulence vertical profile two main options were given by Fluidyn-PANACHE: an *Arya* profile and a *Prognostic* one. In the *Arya model*, the similarity relationship (Monin-Obukhov theory) is used to describe the vertical profile of the mean turbulence fields as function of the dimensionless groups $\frac{z}{L}$ and $\frac{z}{h}$ (with z the elevation above the ground, L the Monin-Obukhov length, h the height

of the ABL). These profiles are applied at the whole ABL, including the surface boundary layer [37]. All the profiles are found from experiments. According to the atmospheric stability a different equation is used for this kind of modelling (see Appendix B.2). On the other hand, prognostic models predict values for meteorological variables by solving the atmospheric dynamic equations [38]. The prediction does not require extensive observation networks, however, it can be affected by inaccuracy due to errors in the imposed input values (i.e. physical parametrizations, boundary or initial conditions). Considering the methodology used to obtain the two turbulence profiles, the *Arya* profile is preferred because of its applicability to the Monin-Obukhov similarity theory.

4.2.5 Initial conditions

Initial conditions represent the configuration before the simulation starts to run. They are defined according to inlet conditions and ambient air properties that can be set by the user. The software applies the inlet wind profile on the whole domain. Ambient air is defined according to its temperature and pressure, cloud cover, relative humidity and rainfall rate. These values are kept constant for all the simulations and summarized in Table 4.1.

Table 4.1: Initial ambient air conditions

Parameter	Imposed value
Ambient temperature [$^{\circ}\text{C}$]	15
Ambient pressure [<i>bar</i>]	1
Cloud cover [<i>10's of</i> %]	0
Relative humidity [%]	0
Rainfall rate [$\frac{\text{mm}}{\text{hour}}$]	0

It is chosen to consider dry air (relative humidity is set to 0%) in order to neglect the influence of the vapor phase on dispersion; in addition, no rain or clouds are considered in order to simulate general cases. The air temperature and pressure values are chosen with the aim to represent realistic annual mean values for a generic location.

4.2.6 Boundary conditions

The software automatically sets the boundary conditions, not allowing the user to impose specific ones. The conditions are set to open boundary for all the sides of the domain except for the inlet one, in which inlet conditions are imposed.

4.2.7 Physical models

The physical models formulate the problem in terms of differential equations or auxiliary equations solved by the numerical solver. The software allows the user to choose among different options concerning the modelling of air, the resolution of temperature and wind velocity equations, the choice of gravity and turbulent models. The list of parameters that can be set is shown in Table 4.2.

Table 4.2: List of physical models

Parameter	Possible model
Air	Compressible Incompressible
Temperature	Freeze Solve
Wind	Freeze Solve
Buoyancy	No gravity Buoyancy Boussinesq Full gravity
Turbulence	Laminar $k - Diff$ $k - L$ $k - \epsilon$

Since taking into account all the physical processes involved in the problem would result in a high computational cost, some approximations were made. In particular:

- *Air*: it is modelled as incompressible, in order to neglect air density variations. This choice is made considering that the effect of heat exchange between pollutants and external air do not produce significant variations.
- *Temperature*: air temperature changes due to the heat exchange process with the smoke emitted and the ground. Due to this reason, it is chosen to solve the temperature equation.
- *Wind*: it is solved until the wind field reaches a fully developed condition.
- *Buoyancy*: two main effects should be taken into account for the buoyancy model, namely the gravity effect due to the weight of particles and the convective term due to temperature difference between external air and pollutants. In this analysis both gaseous and solid pollutants are involved. For the first ones the volume forces could be neglected, especially if thermal convection plays an important role; for solid particles instead, the weight can represent an important contribution. A *Full gravity model* should be in general used; nevertheless, it was observed that in the software PM_{10} is modelled as a gaseous pollutant with a molar weight similar to the one of air. Since for industrial emissions the source temperature can reach very high values, and considering the model adopted by Fluidyn-PANACHE for dust, it is assumed that

the main buoyancy contribution is due to temperature gradient between ambient air and smoke. The Boussinesq model is consequently chosen according its definition: *it assumes that variations in density have no effect on the flow field, except that they give rise to buoyancy forces. In more practical terms, this approximation is typically used to model liquids around room temperature, natural ventilation in buildings, or dense gas dispersion in industrial set-ups* [39].

- *Turbulence*: among all the possible models, it is chosen to apply the standard $k - \epsilon$ turbulence model because it is widely used for this kind of applications.

All the physical models used in this analysis are summarised in Table 4.3.

Table 4.3: Summary of physical models used in the analysis

Parameter	Possible model
Air	Incompressible
Temperature	Solve
Wind	Solve
Buoyancy	Boussinesq
Turbulence	$k - \epsilon$

4.2.8 Choice of the grid

The grid used is in general different for all the simulations because it is adapted to the specific needs of the case, but a common methodology has been adopted. First of all, it is chosen to use an uniform structured mesh (square cells) due to the absence of obstacles in the domain of analysis. In order to evaluate the good dimension of the cell it was studied one of the cases provided by the enterprise (Table A.1), namely a 2 MW natural gas plant. For this case a $100x50x100m$ domain was used, and neutral atmospheric stability with a logarithmic wind profile of $2\frac{m}{s}$ velocity at the reference height of 10 m was considered. The mesh was refined on the horizontal and vertical direction in order to improve the accuracy of the results only where needed. The ratio between the less refined cell and the most refined one is set to 2 for the horizontal plane; on the vertical instead the mesh is refined close to the ground, with cells progressively larger as the height increases.

The dimension of the cells is chosen according to a grid independence study. It is chosen as reference case a $1x1x0.5m$ cell (at the ground); then, a 1.2 times more refined and 1.5, 2, and 4 times less refined meshes for all the directions have been used. In all this cases the wind profile was evaluated. Figure 4.2 shows the results of the grid independence analysis for wind profiles up to 10 m in order to better appreciate the differences close to the ground, where the most significant effects of the cell size are found.

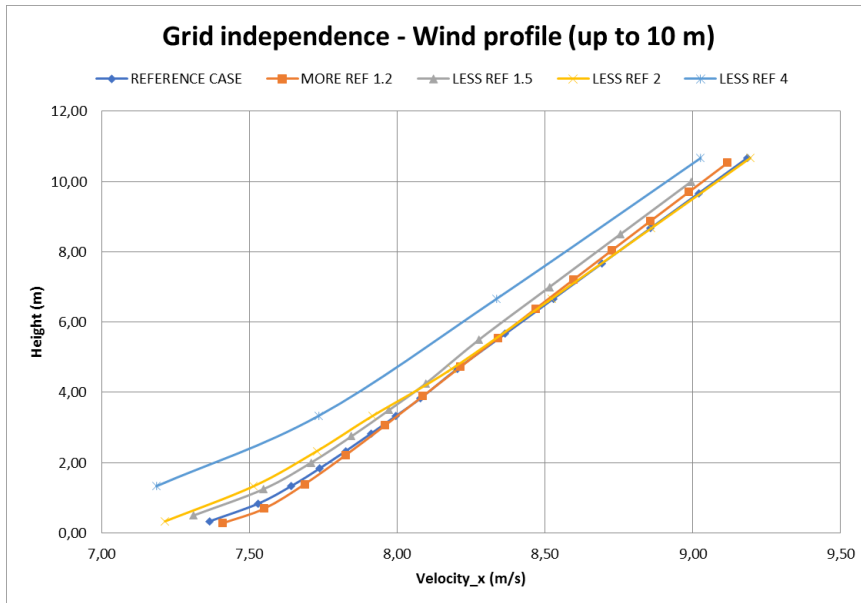


Figure 4.2: Grid independence results

According to the results, it is chosen to consider $1x1x0.5m$ cells at the ground because of the small difference in comparison to the most refined mesh (about 0.6% as max difference). Finally, the mesh used for this domain is shown in Figure 4.3.

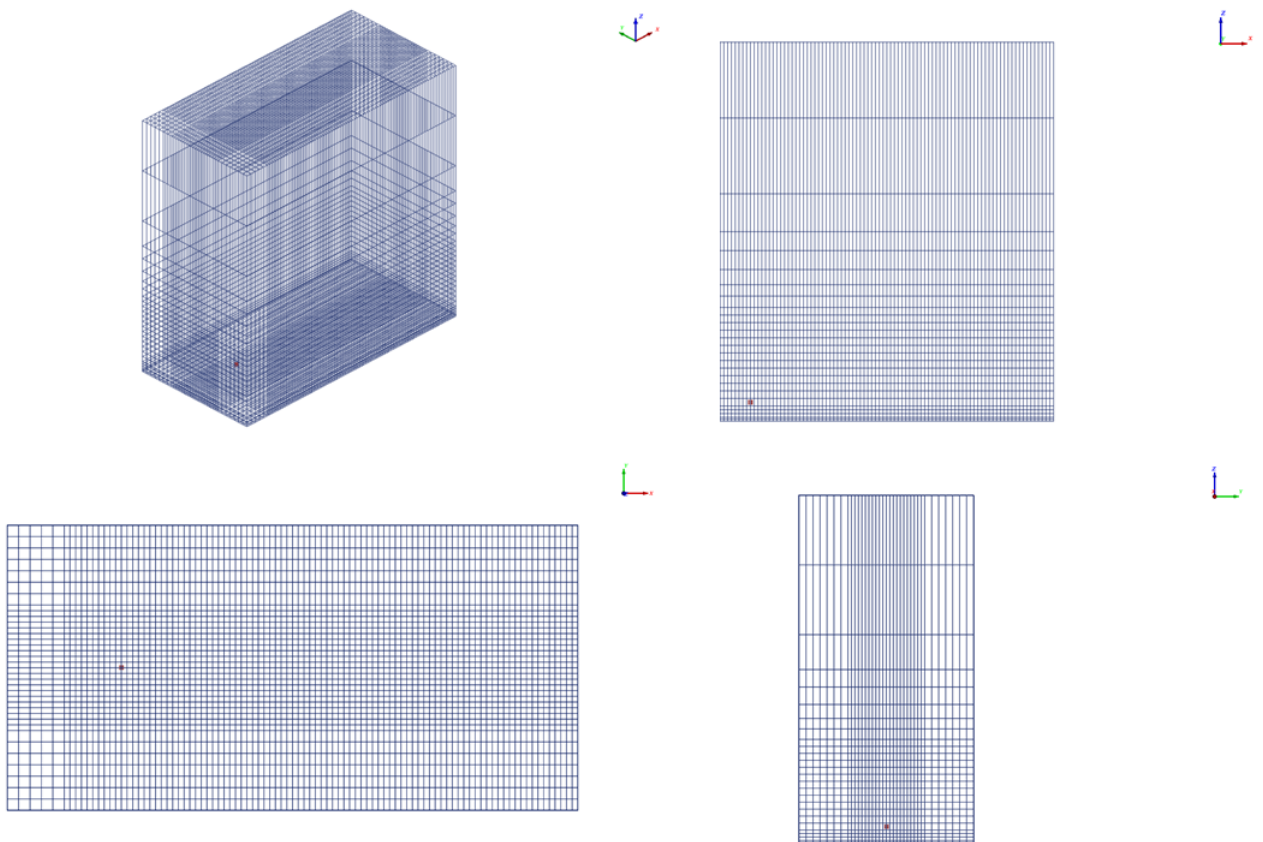


Figure 4.3: Reference grid

4.2.9 Atmospheric stability assessment

The imposition of atmospheric stability on Fluidyn-PANACHE depends on the setting of two main parameters, namely wind profile and vertical temperature profile. The first one is set to a logarithmic profile based on Eq. 4.1; for the vertical temperature profile instead a lapse rate is imposed. For an unstable atmospheric stability this value is set to $\frac{0.01^\circ\text{C}}{m}$; for a stable one the opposite profile is chosen in order to have the same and opposite intensity of the effect [40]. For neutral stability instead, a uniform vertical profile is set in order not to have a temperature variation with height.

To check the correctness of the setting for atmospheric conditions, the potential temperature profile, that is the parameter that is commonly used to determine stability, is evaluated. This parameter can be estimated as:

$$T_{pot} = T \cdot \left(\frac{10^5}{p}\right)^{\frac{R}{c_p}} \quad (4.2)$$

Where T_{pot} is the potential temperature at the evaluated height, T and p are the respective temperature and pressure, R is the ideal gas constant, c_p is the specific heat capacity at constant pressure. Atmospheric stability is determined according to the variation of potential temperature with the height ($\theta = \frac{\Delta T_{pot}}{z}$). θ must be:

- $\theta < 0$ for unstable atmospheric stability
- $\theta > 0$ for stable atmospheric stability
- $\theta = 0$ for neutral atmospheric stability

The results for different stabilities are shown in Figure 4.4.

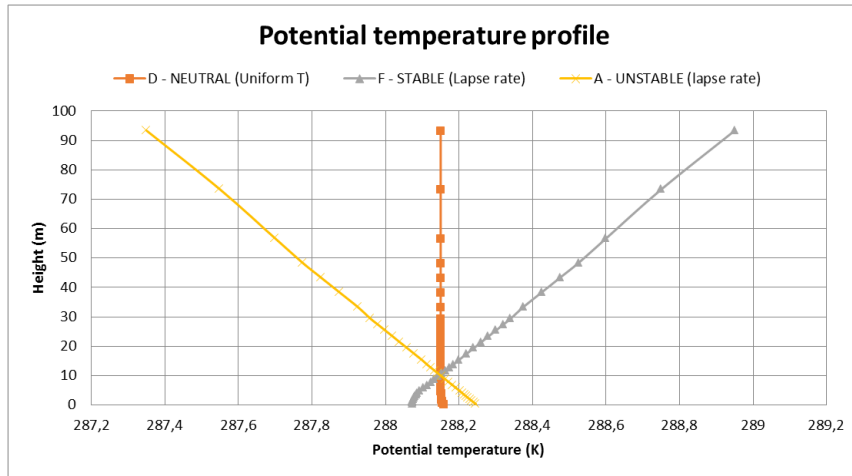


Figure 4.4: Evaluation stability through potential temperature vertical profile

Figure 4.4 shows that the potential temperature profile effectively corresponds to the desired case (negative variation for the unstable case, positive one for the stable, no variation for neutral case). A comparison of the lateral profiles of dispersion in the three cases (obtained considering a coarse mesh) is shown in Figure 4.5.

The profiles obtained show that in the unstable profile the dispersion process is much stronger than in the other cases, resulting in a higher expansion of the plume with height. In the stable case instead, the profile is smoother and more elongated due to low dispersion of pollutants in the atmosphere. The pollutants are expected

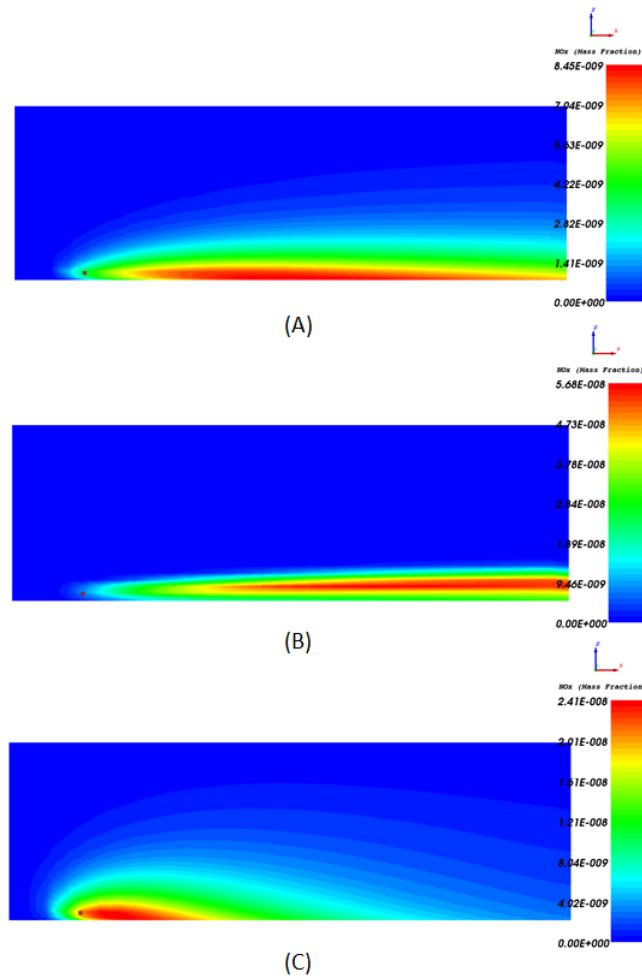


Figure 4.5: Dispersion profile on the XZ plane, where: (A) neutral case; (B) stable case; (C) unstable case

to reach higher distances in this second configuration. The neutral case presents instead an intermediate profile between the two.

4.2.10 Wind field development

The numerical model requires the resolution of all the equations at each iteration; due to this reason, the steady state solution that is looked for is only found after several calculations. In addition, a stable wind field should be imposed before considering the emission of pollutants from the source. Due to this reason, for all the simulations the wind field should be calculated before evaluating the pollutants dispersion process.

The wind field is evaluated considering a steady state problem assessment without source emissions (null flowrate); then the obtained profile is evaluated in order to select the best location for the source. As an example, it is considered a $300m$ long profile (Figure 4.6) with logarithmic profile ($7 \frac{m}{s}$ at $10m$). It can be observed that the wind progressively develops along the domain, reaching a stable configuration after a certain distance from the inlet. As a high wind velocity at the reference height is imposed, the flow needs large distances to fully develop, especially in the higher part of the domain.

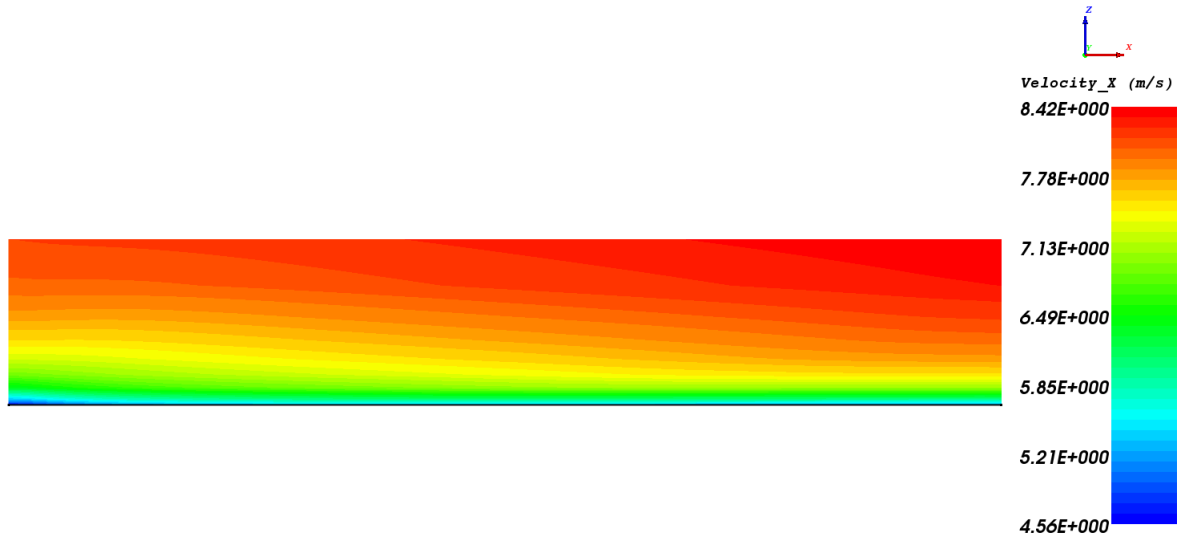


Figure 4.6: Example of developing wind profile

For all the configurations the source is put where the relative difference between the outlet and the selected location presents a relative difference of less than 5%. Same considerations are made for other properties, like turbulent kinetic energy or viscosity. After the determination of the developed wind field, the source contribution is added by continuing the previous simulation.

4.2.11 Convergence criteria

For all the simulations a convergence criteria to stop the numerical resolution should be imposed. In the analysis it is considered that a simulation has converged when the residuals for all the variables are lower than 10^{-3} . In order to verify that this value is good enough, a monitor point (that acts like a sensor, that evaluates all the properties in a specific location) is put at the end of the domain. If all the properties remain constant after a certain number of iterations the solution is considered as converged. Figure 4.7 shows an example of convergence evaluation, in which turbulent kinetic energy is evaluated (it was observed to be the slowest parameter to converge). It can be noticed that after about 3000 iterations the solution remains the same for the case considered; the simulation is then considered as converged and the convergence criteria adequate. This evaluation is made for all of the simulations performed in the analysis.

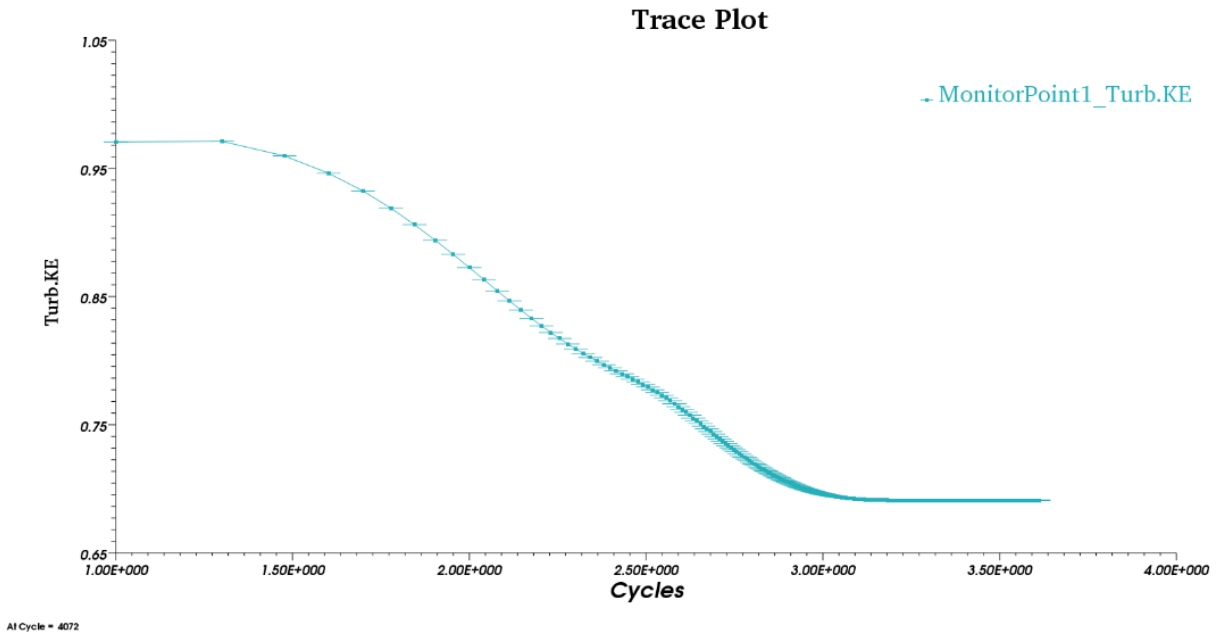


Figure 4.7: Evaluation of convergence through monitor point

4.2.12 Validation of the results

As the analysis involves the performance of parametric studies, it is not possible to compare the results with reference cases or experiments, as usually done in CFD simulations for validation. Even if all the verifications (grid independence, convergence of the solution, wind field development) were made for all the cases, an uncertainty in the results of the simulations still persists, related both to the choices for the numerical model and the constraints of the software. For the last consideration, references for specific applications (dense gases dispersion) were found, in which comparison matrixes with a confidence level of 80% in the results were showed [33].

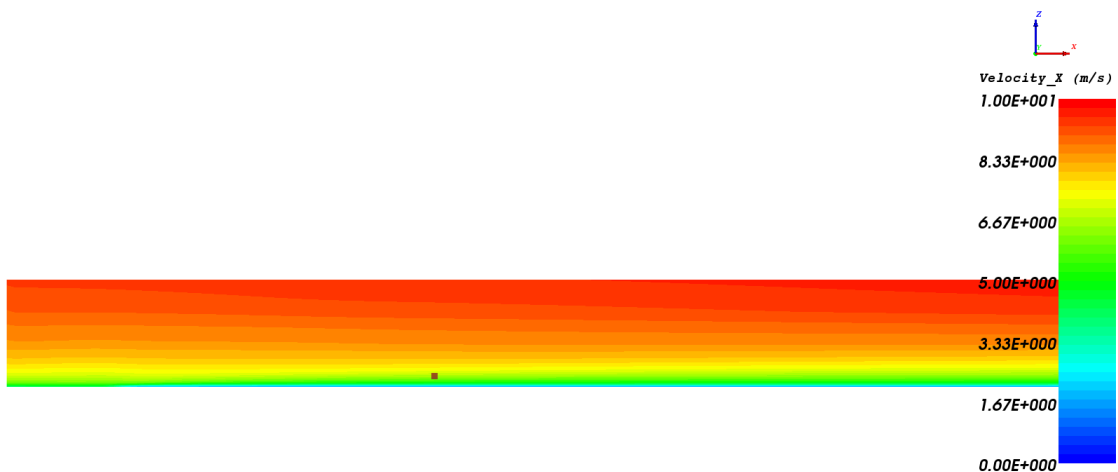
Chapter 5

Results of the analysis

After the determination of the results of all the simulations to perform the results can finally be analyzed in order to critically review the regulation. In the following, the results are presented.

5.1 Analysis of simulations results

For each performed simulation, different information were extracted in order to evaluate the correctness of the results and to compare different configurations. As each case required the resolution of the wind field before the introduction of the source, it was firstly checked that this one was developed. In this regard, the most critical simulations were the ones in which high values of aerodynamic roughness length had to be used, due to the previously mentioned problems of adaptation of the flow for high z_0 configurations. Figure 5.1 shows an example of fully developed wind profile in the case of high aerodynamic roughness length (plane at $y = 0$).



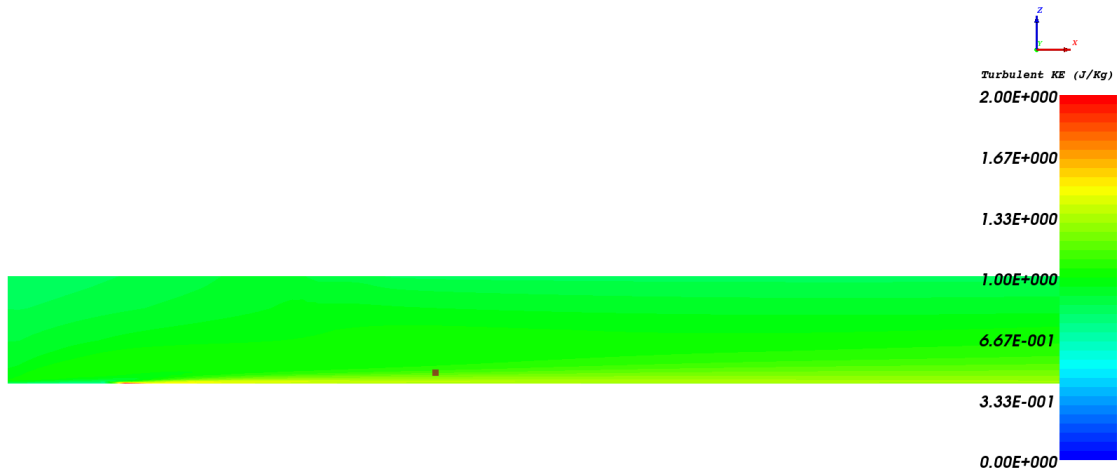
At Cycle = 3532

Figure 5.1: Wind field for high z_0 cases (case 4)

It can be noticed that after a short distance from the inlet the profile slightly changes (especially close to the ground), up to a final adaptation. The source po-

sition should be located in a spot in which the wind profile is fully developed for all the cases. The maximum value of velocity involved in the profiles was $10 \frac{m}{s}$ at a height of more than 100 m, obtained in low z_0 configurations.

As the dispersion process depends on the turbulence in the flow, also the turbulent kinetic energy profile was extracted for all the cases. It was observed a large variance in the values of this parameter among the cases: the range goes from a value in the order of the $10^{-2} \frac{J}{kg}$ for stable cases, up to about $2 \frac{J}{kg}$ for neutral ones. The high value obtained for the neutral cases can be explained by the high wind velocity imposed at the inlet ($7 \frac{m}{s}$), but also by the fact that when high roughness was imposed, as the type of terrain changed (as explained in Chapter 4.2.2) a turbulent effect was generated. This effect is highlighted in Figure 5.2.



AtCycle = 3231

Figure 5.2: Turbulent kinetic energy profile for a neutral case with high z_0 (case 4)

From each simulation two main information were extracted for the analysis, namely the peak of concentration for the three pollutants and their distance from the source. Fluidyn-PANACHE considers as ground the plane corresponding to $z = 0m$, but this height is out of the range indicated by the regulation for the measurements of pollutants concentration (1,5 to 4m). Due to this reason, for each case and for each pollutant, the ground concentration was evaluated considering the average value between the measures in the cells from the ground up to 2.5m, that is chosen as reference because close to the breathing zone but also to eliminate the dependency on cells size. After the determination of the peak, its location is defined; this value is about the same for all the species due to the buoyancy model used for the analysis, that considers only thermal effects.

In Figure 5.3 the ground concentration plot for one simulation obtained from the software and the evaluation of its mean value are showed. It was noticed that the peak values can vary significantly, especially when stable configurations, characterized by low diffusion effects, are performed (for example, in case 9 the peak evaluated with the software corresponds to $61,1 \frac{\mu g}{m^3}$, that is about $15 \frac{\mu g}{m^3}$ less than the one obtained by evaluating the average).

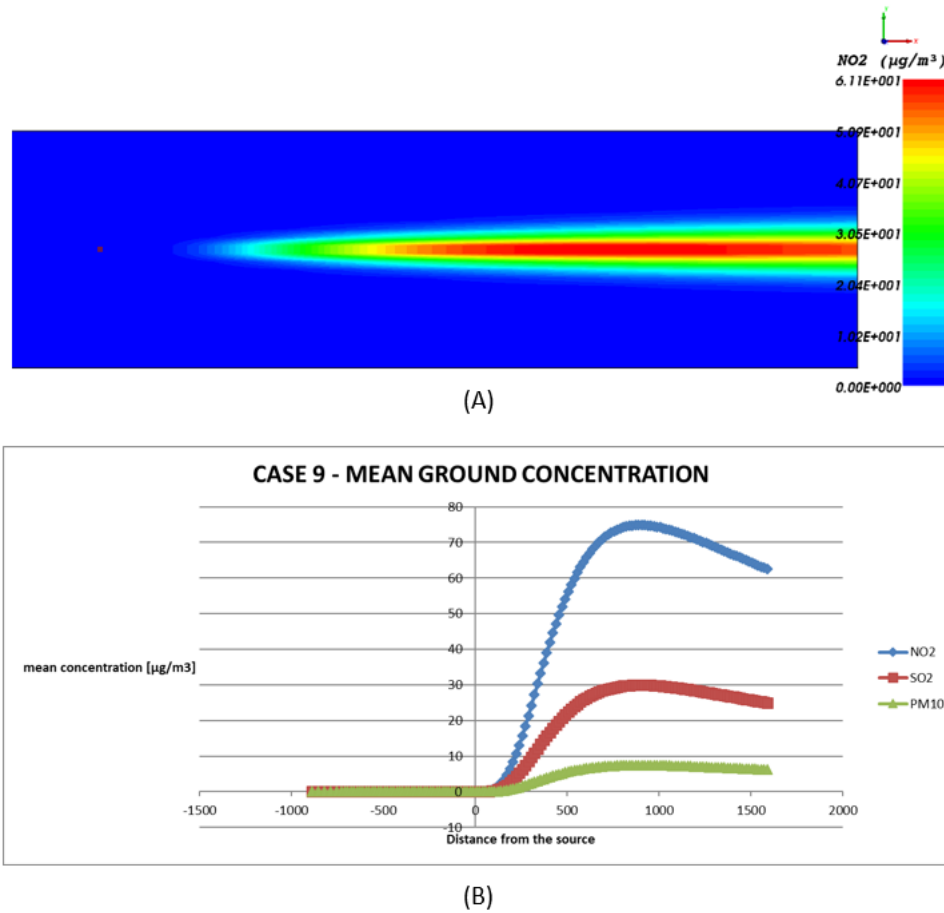


Figure 5.3: Example of ground concentration profile on Fluidyn-PANACHE (A) and evaluation of mean ground concentration (B) (case 9)

The exact values for each examined parameter are reported in Appendix C.1, and the results of each of them for all the cases are shown in Appendix C.2. The final results for ground concentration are instead summarised in Figure 5.4; for PM_{10} , since very low values with respect to the other pollutants were obtained, the results are multiplied by a factor of 10 to better evaluate the trend.

It can be observed the same trend for all the pollutant species, characterized by a quite large variance in the results, especially for NO_2 (the maximum peak of concentration, corresponding to case 1, is about $380 \frac{\mu g}{m^3}$, the lowest one, case 13, about $6 \frac{\mu g}{m^3}$). The general trend also shows that in the first cases performed (case 1 to 8) the concentration is higher than in the rest of the cases. In case 1 the value is however much elevated (it is almost three times larger than the second higher concentration obtained, case 7). Such results can be explained considering the settings for this configuration: a stable atmosphere (low wind and night time) with low effective height of emission (low height of the stack, low flowrate, low source temperature). Moreover, a small aerodynamic roughness length is imposed, resulting in low turbulent effects close to the ground. In such a configuration the dispersion is expected to be low and, as a mean concentration from the ground up to a specific height is considered, a larger concentration value will be detected. However, the results for this case were compared to the ones that can be obtained using an analytical Gaussian model, in order to check the expected order of magnitude. Also using this

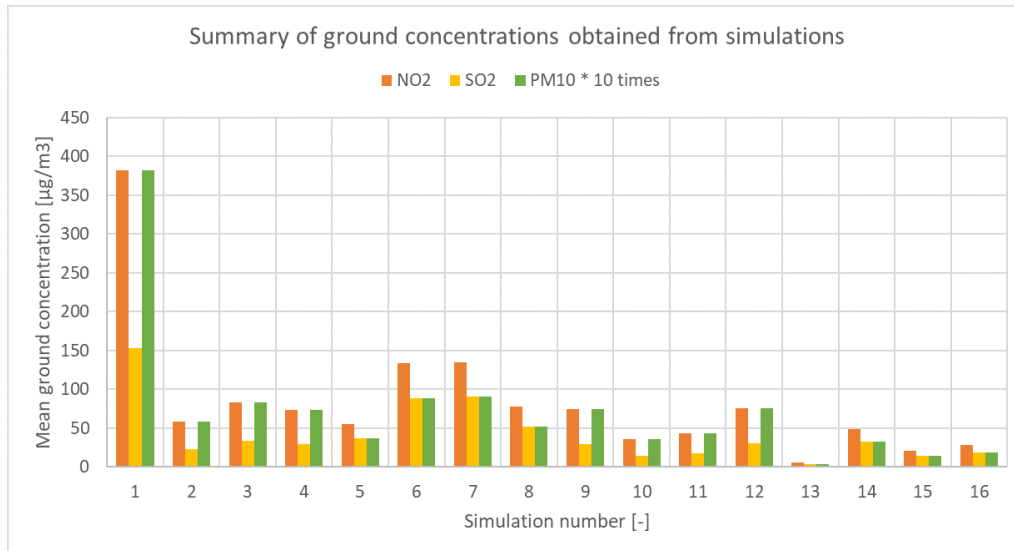


Figure 5.4: Summary of the results for mean ground concentration peak

model the results provide very high ground concentrations (Appendix C.3).

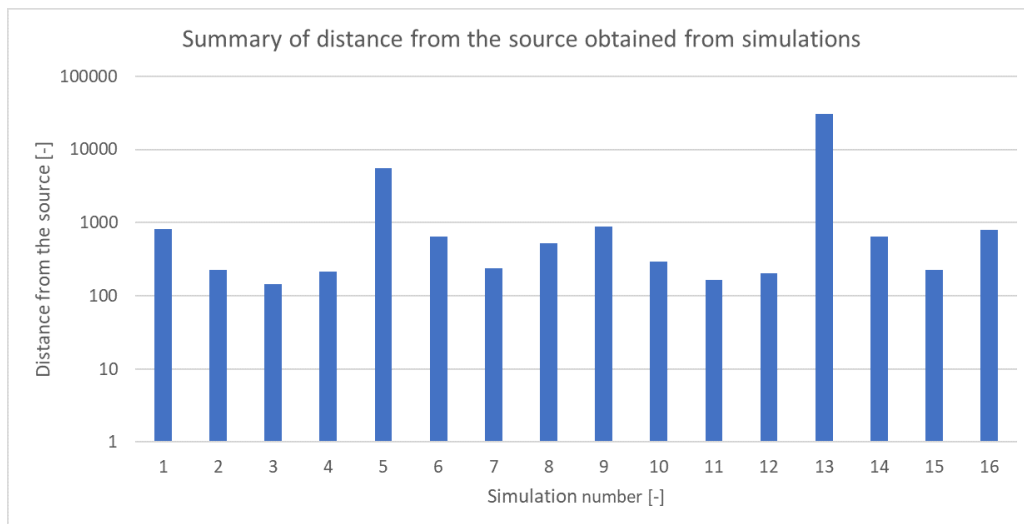


Figure 5.5: Summary of the results for mean ground concentration peak

A large variance in the results can be also observed in the distance of the peak of concentration from the source, that varies from about 140 m to slightly more than 30 km (graphically showed in Figure 5.5, where the y axis is in logarithmic scale). As expected, when stable atmospheric stability, characterized by low turbulent effects, is imposed (case 1, 5, 9, 13) a large distance from the source is observed. However, the results obtained for case 13 could still surprise. It should be kept in mind that a very extreme configuration was considered in this simulation (very high effective emission point and very smooth ground roughness, in addition to the fact that there are no obstacles in the domain).

Finally, it can be noticed that when the aerodynamic roughness length is higher the peak of concentration occurs in a location closer to the source.

5.2 Parametric analysis

5.2.1 Main effects plot

To explain the behaviour of the results obtained the effect of each parameter on dispersion should be evaluated with the parametric analysis. The results will allow to answer to the first question addressed to in this study. To simplify the evaluation, the study is carried out with the aid of the software *Minitab 18*, a mathematical tool that is suitable for this kind of applications (it is mainly used in the statistical field).

In the first part of the analysis, the effect of each parameter is quantified according to the variance that it can produce when set to different levels. For this purpose, a value of the output variable (i.e. mean ground concentration) is computed considering the average result of all the simulations in which a chosen parameter is set to a specific level. Mathematically:

$$\bar{C}_{p,Lx} = \frac{\sum_{i=1}^N \bar{C}_{i,Lx}}{N} \quad (5.1)$$

where $\bar{C}_{p,Lx}$ is the average value obtained by the calculation for the parameter p set to the fixed level Lx , N is the total number of simulations that present the same level for the parameter p (in this case, 8 simulations for each parameter to analyse), $\bar{C}_{i,Lx}$ is the mean ground concentration obtained in the i -th simulation in which the parameter was set to that specific level. By applying this formula, for each of the parameters two different values (referred to the two levels imposed) are computed. In DOE, the results for this kind of evaluation are summarised in a graph that is called *Main effects plot* (Figure 5.6). On the x-axis for each parameter the corresponding two values are indicated; the y-axis refers to the mean concentration evaluated with Eq. 5.1.

A large gradient between the mean values of the two levels indicates that the parameter under evaluation significantly affects the result; if the difference between them is small instead, the evaluated effect does not strongly affect the results. Considering the main effects plot obtained for NO_2 for example, the analysis suggests that the most influencing parameter for mean ground concentration is the temperature of the source, followed by the background pollution level of the location. However, all the parameters have an impact on the results (the slope is never flat for NO_2). A deeper evaluation of the results obtained suggests that the emission point plays a significant role on dispersion. An increase in the temperature of the source indeed produces a higher elevation of the plume above (Chapter 2.2.1), that in turn allows a larger dispersion in the atmosphere. The pollution level instead determines the minimum height of the stack (in PPA areas it was used the value in parenthesis in Figure 1.1, that is higher); even in this case the increase of the effective height produces a lower peak for mean ground concentration. As the results indicate a significant impact of the height of emission on dispersion, the importance of an efficient regulation is emphasised.

Considering the graphs obtained for the other pollutants the same conclusions could be derived, except for the flowrate, whose impact on the results is different for all the species. Such a result could be explained considering the allowed concentration of pollutants at the emission, that by regulation changes according to the nominal

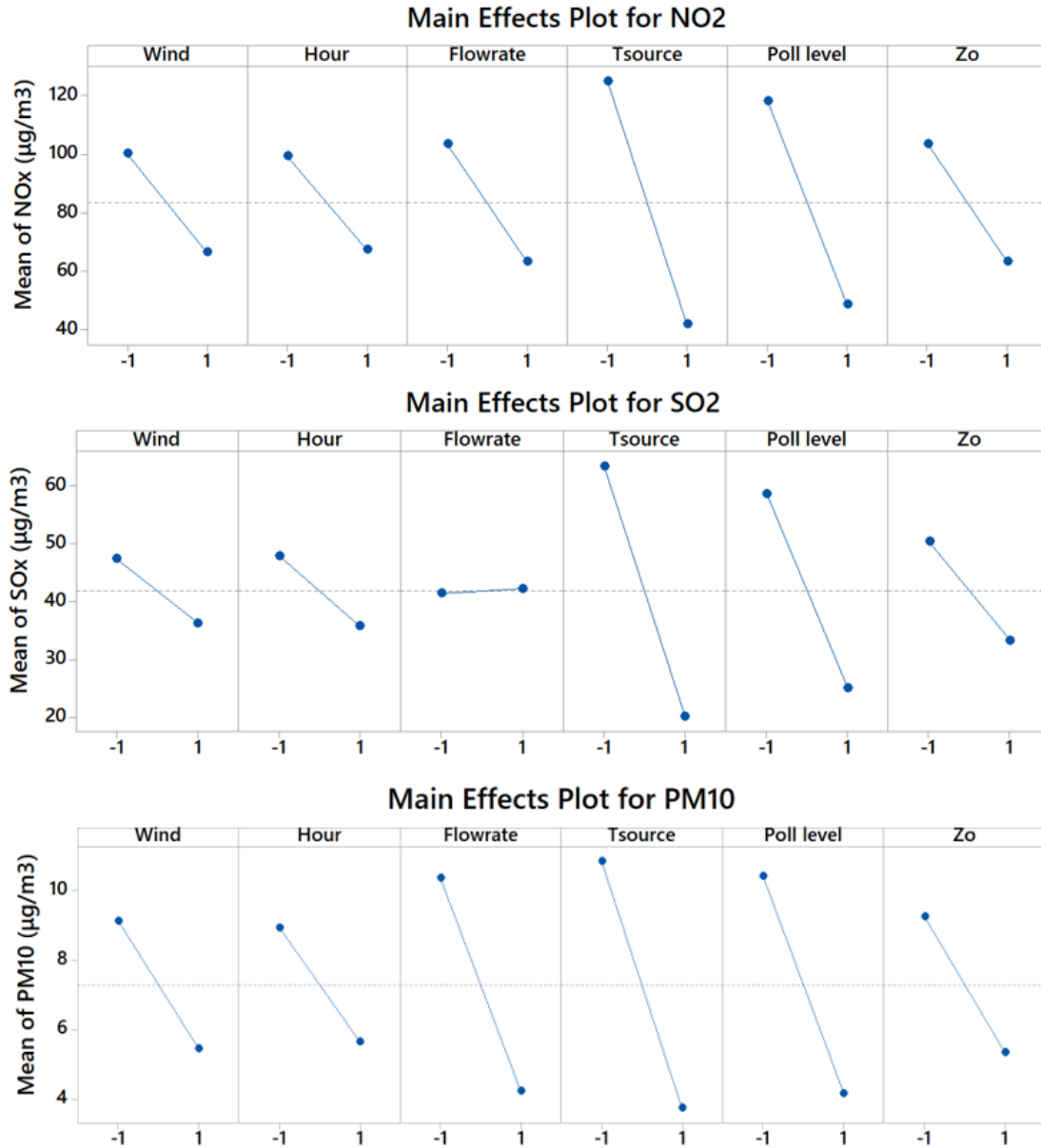


Figure 5.6: Main effects plot for all the pollutant species under evaluation

power of the plant (and thus according to the flowrate imposed, because it was assumed a proportional relation between the variables). For NO_2 and PM_{10} , as the nominal power increases the allowed concentration at the emission decreases [4]. For the first pollutant, the reduction of allowed emission from 2 MW plants to 20 MW ones is 40%; for PM_{10} the reduction is larger (-60%). Considering SO_2 instead, the limit for emitted concentration does not change when the nominal power increases. These results suggest that rather than the variation of flowrate, that can depend on other parameters (velocity of emission, diameter of the chimney, pollutants density), what affects the mean pollutants concentration at the ground is the amount of pollutants emitted. When the decrease is larger (like in the case of PM_{10}) the effect of the parameter flowrate becomes more important. The emission limits for each pollutant can be found in Appendix A.2.

The graph can also provide information on how to optimize the configuration accord-

ing to the analysis of the values of the output obtained in the simulations. The best case to maximise the output is indeed the one obtained when all the parameters are set to the level that maximises the average value estimated with Eq. 5.1. Opposite considerations could be made if the objective is to minimize the results. Considering again the plot for NO_2 , it can be seen that the configuration that maximises the mean ground concentration is the one in which all the selected parameters are set to a low level (a small power plant with low height of the stack and source temperature, located in a quite flat environment and in stable atmosphere conditions), that corresponds to case 1. However, as the concentration at the ground obtained in this configuration is very high in comparison with the other cases, it could be thought that case 1 altered the results of the parametric analysis. Thus, to evaluate the reliability of the results, the same study was carried out modifying the results for this case in order to eliminate its influence on the results (in practice, the mean ground concentration obtained for each specie was set to an average value calculated as a mean between the concentrations obtained for the other cases) (Appendix C.4). The result indicates that the most affecting parameters are the same as for the first analysis, but some differences for the other parameters can be noticed, especially for the flowrate. Such procedure confirms that the temperature of the source and the height of the stack are the most affecting parameters for this study.

Other considerations could be made for the distance of the peak of concentration from the source (Figure 5.7). In this case the analysis suggests that all the parameters play an important role for the determination of this output. In particular, it is shown that in order to obtain a peak very distant from the source the best configuration would be a stable case (low wind and night time) in a highly polluted, bare environment and with a large nominal power, emitting pollutants at high temperature. Even in this case it can be indirectly obtained that the emission point plays an important role. All of the parameters related to the source indeed (ejection temperature, background pollution, flowrate) when set to high levels produce a high effective height of emission, that allows the plume to attain longer distances before reaching the ground. A stable atmospheric stability and a low ground roughness contribute to the spread over long distances of the plume as well.

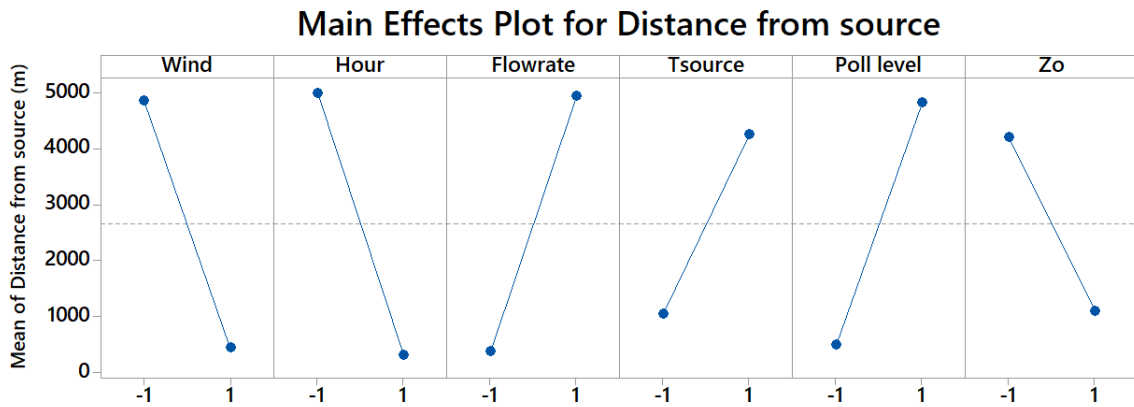


Figure 5.7: Main effects plot for the distance of the peak from the source

5.2.2 Pareto chart

The results obtained with the Main effects plot give an idea of the most affecting parameters on dispersion. The analysis can be further deepened with a quantification of the effects. This is made by considering a normalization of the gradients generated by each parameter at different levels. In this way, the percentual weight of each factor is evaluated; the sum of all the quantified effects clearly gives 100%. First of all, the difference in absolute terms $\Delta\bar{C}_p$ between the two average concentrations evaluated with Eq. 5.1 is calculated:

$$\Delta\bar{C}_p = |\bar{C}_{p, +1} - \bar{C}_{p, -1}| \quad (5.2)$$

where $\bar{C}_{p,\pm 1}$ is the average concentration for the parameter p when set at the level $+1$ or -1 . This variance is evaluated for all the parameters of the analysis. The weight of each parameter \bar{E}_p is then evaluated by normalizing all the gradients:

$$\bar{E}_p = \frac{\Delta\bar{C}_p}{\sum_{i=1}^N \Delta\bar{C}_{p_i}} \quad (5.3)$$

with N the total number of parameters, $\Delta\bar{C}_{p_i}$ the gradient of the i -th parameter (evaluated with Eq. 5.2). The normalized effects for all the examined outputs are summarised in the *Pareto charts* of Figure 5.8.

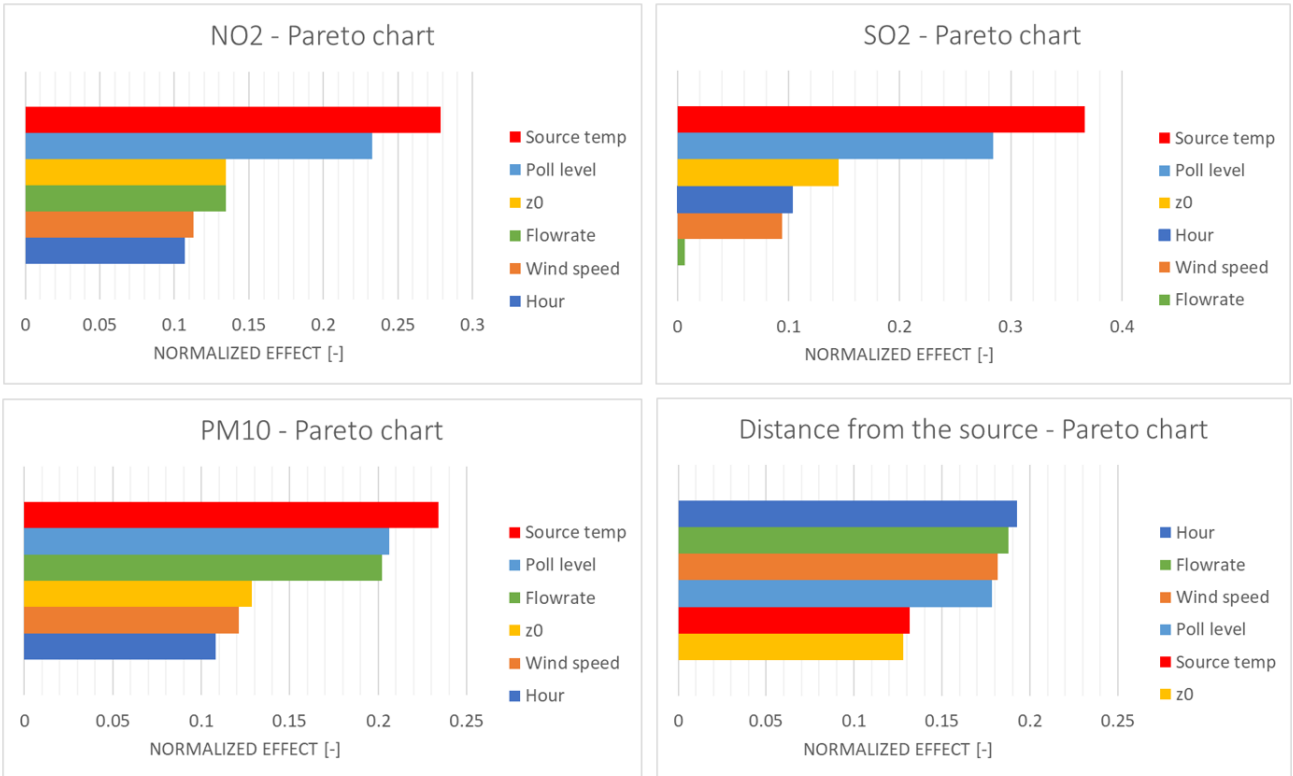


Figure 5.8: Pareto chart of the normalized effects

First of all, it can be noticed that the source temperature, that is the most affecting parameter for the peak of concentration of all the species, can account up to almost 37% of the total variation of concentration (for SO_2). For NO_2 and PM_{10} the weight of the source temperature is about two to three times larger than

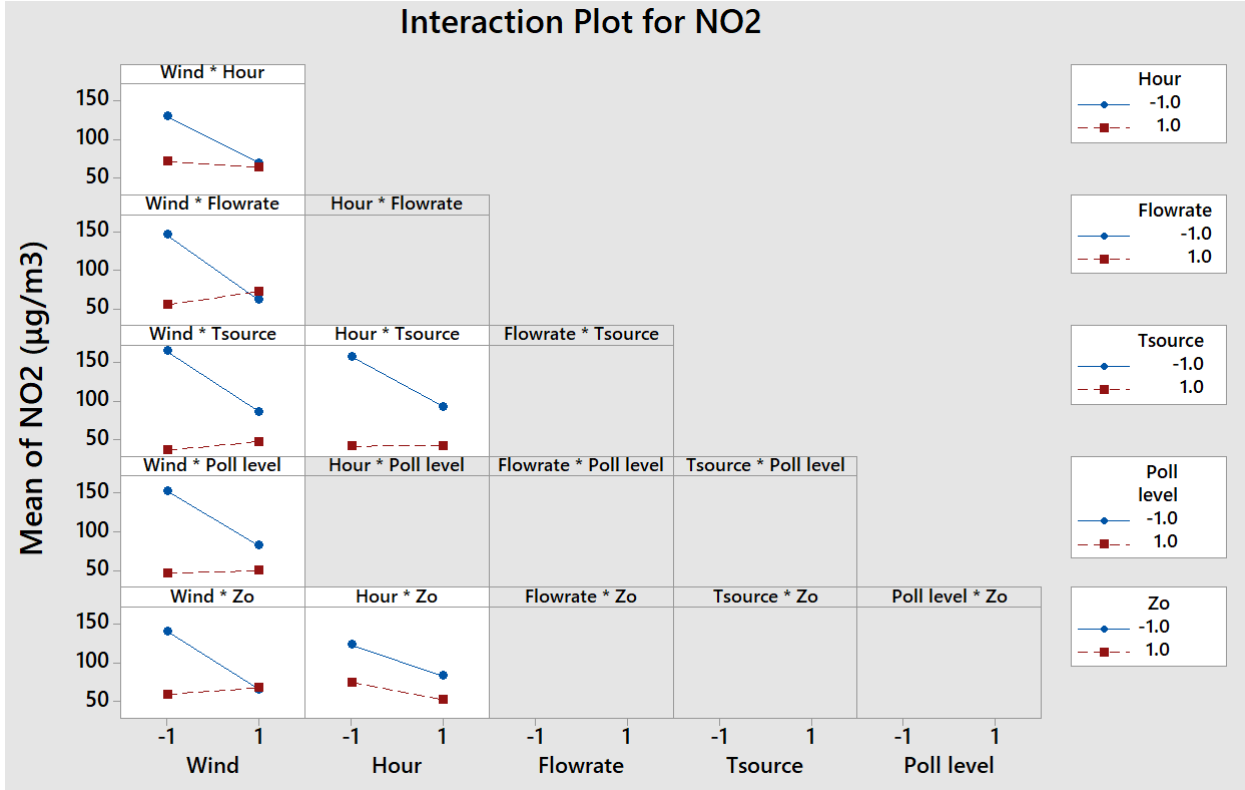
the least affecting parameter (time of the day); for SO_2 it is about 37 times larger than flowrate (that in this case is almost not affecting at all the results). In the case of SO_2 there is a larger difference between the most significant parameters and the least influencing ones, probably due to the independency of the results on the emitted mass of pollutants. Considering the distance of the peak of concentration from the source instead, the difference between the most affecting parameter and the least affecting one is much smaller: the time of the day affects as about 1,5 times more than the z_0 .

5.2.3 Interaction plot

The number of simulations chosen in the Fractional factorial design allows to study also some interactions between parameters. An interaction consists in an observed variation in the output value due to the combined effect of two or more factors. In practice, all the possible combinations between the levels of each two or more parameters are studied: evaluating factor at fixed levels, the level of the other ones is changed. For the design used in this work, this analysis can be made for the interaction of the wind with all the other factors and the one of the time of the day with the source temperature and z_0 (AB, AC, AD, AE, AF, BC, BF). The combined effect of different factors can be easily detected using the *Interaction plot*. In this plot, the average output obtained from Eq. 5.1 is plotted for different combinations of parameters. When fixing one of the factors at different levels, the variation produced by the change of the other parameter generates some curves. If the curves are quite parallel it means that no significant interaction exists; if they tend to cross each other an interaction, whose intensity depends on the degree of departure between the curves, exists.

It was observed that for all the species considered in the analysis the same interactions occurred, even if the significance can vary among the cases (for example, the interaction between flowrate and wind velocity is much more significant in the case of SO_2 , probably due to the consideration above mentioned about the emitted concentration). As an example, the interactions evaluated in the analysis for NO_2 are shown in Figure 5.9.

In this case it can be observed that for the wind the interaction with all the other parameters is not negligible, being important especially for the combination with the flowrate. The time of the day instead is more independent from the other evaluated parameters (especially for the combination $Hour - z_0$). In general, it can be observed that when the wind is set to high level the curves tend to converge. Such a configuration corresponds to a neutral atmospheric static stability. According to the results, in this situation the change in other parameters has a lower effect on the output concentration; it can probably be explained by the smaller relative importance of the diffusion process with respect to advection in neutral cases. The wind velocity is set to a low value instead (stable or unstable atmosphere), the variance in the results is larger; this consideration is valid also for the hour, meaning that especially for stable cases a large variance in the results is produced. As an example, considering the interaction plot $Wind - Hour$, it can be seen that the stable case (hour set to -1) produces much larger peaks of concentration, as already discussed above. Moreover, it can be observed that in general, when changing the level of the fixed parameter, the variance in the output is much less significant


 Figure 5.9: Interaction plot for NO_2

if the other parameter is set to high level (in the graph, the slope of the red curves is quite flat for all the cases). These observations refer mainly to the interactions if wind velocity, but it would be interesting to deepen the analysis by evaluating all the possible interactions between parameters.

All the evaluated interactions for all the species and distance from the source can be found in Appendix C.5. The same considerations as for NO_2 and the other species can be made for the distance from the source, in which also the time of the day significantly interacts with the other parameters.

It is possible to build the pareto chart also for interactions. In this case, the quantification of the effects can be made with the following formula [39]:

$$I_{A,B} = \frac{1}{2}(E_{A,B(+1)} - E_{A,B(-1)}) \quad (5.4)$$

in which $E_{A,B(+1)}$ represents the effect of the parameter A when the parameter B is set to high level, $E_{A,B(-1)}$ is the effect of A when B is set to low level. In practice, the two effects are evaluated as the average of the difference between the mean results of parameter A at a fixed B value ($E_{A,B(+1)} = \frac{1}{2}(\bar{C}_{A,+1} - \bar{C}_{A,-1})_{B,+1} = (\Delta\bar{C}_A)_{B,+1}$ and $E_{A,B(-1)} = \frac{1}{2}(\bar{C}_{A,+1} - \bar{C}_{A,-1})_{B,-1} = (\Delta\bar{C}_A)_{B,-1}$). This calculation is made for all the combination of parameters analysed (AB, AC, AD, AE, AF, BC, BF). After that, the relative weight of each effect and interaction is evaluated (Eq. 5.3). Figure 5.10 shows the results of this analysis for NO_2 .

Considering also some of the interactions, the two most affecting parameters remain the source temperature and the pollution level. Their percentage contribution is though about decreased of the half. It is interesting to notice that some interac-

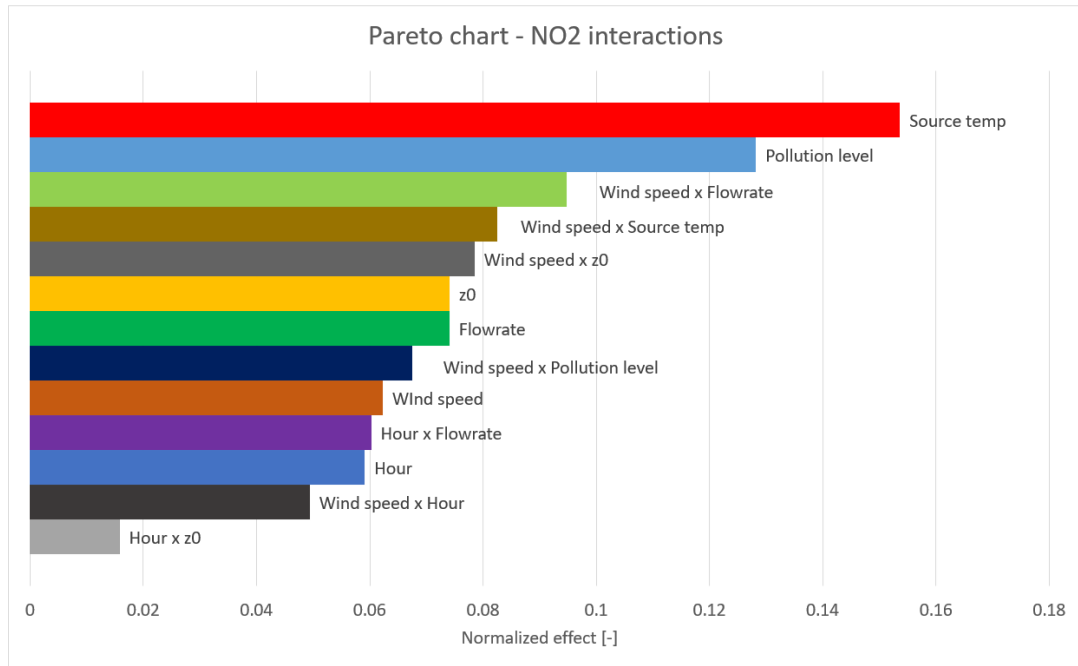


Figure 5.10: Pareto chart of main factors and interactions for NO_2

tions are more affecting than the single main parameters considered separately, as in the case of the interaction between wind and flowrate. This interaction produces indeed an affect that is about 26% larger than the effect of the flowrate, and about 50% larger than the effect of the wind.

Since only 16 simulations have been performed, over the 64 needed to have a complete analysis, it was possible to evaluate only these interactions. The results show that some of the combined effects are not negligible. It would be interesting to deepen the analysis with the evaluation of all the other possible interactions.

In the light of the results obtained with the parametric analysis the first objective of this study has finally been achieved: it is indeed shown that the most affecting parameters are explicitly considered in the determination of the minimum chimney's height.

5.3 Discussion of the regulation

The second step of the analysis is to evaluate the effectiveness of the regulation with respect to the targets it is assessed for. Given the relation between the heights imposed by the regulation under evaluation [4] and the formula that can be found in the same regulation for particular plants [5], it can be useful to refer to Eq. 1.1 to better understand the reliability of the regulation for industrial chimneys height.

5.3.1 Comparison with reference values

The calculation of the minimum chimney's height involves the parameter c_m , defined as the maximum allowable pollutant concentration at the ground only due to the emission of the stack (without taking into account other sources in the surroundings). This term is evaluated for all the pollutants involved in the dispersion. In the regulation, this threshold value is defined as:

$$c_m = c_r - c_0 \quad (5.5)$$

c_r represents a reference value provided by the regulation and c_0 the mean annual background pollution in the location in which the plant is built. Considering the definition of c_m and c_0 , it is possible to conclude that c_r represents the threshold value of pollutant concentration at the ground.

In order to understand if the regulation is precautionary enough, the peak of mean ground concentration (obtained by summing of the contribution of the source and the background pollution of the area) can be compared to the threshold value imposed by the regulation, c_r . As an alternative, the contribution of the source only can be compared to c_m . It is chosen to apply the second method. For this purpose, the results obtained with the simulations can be used, having the advantage of providing information both on the most frequent situations and extreme ones (i.e. case 1, 13). As the analysis does not refer to specific locations (the distinction is only made between general areas and PPA ones), the values provided by the regulation [5] are used for c_r and c_0 (a conversion from $[\frac{mg}{Nm^3}]$ to $[\frac{\mu g}{m^3}]$ referred to the thermodynamic conditions of the simulations is made). All the values involved in Eq. 5.5 for each case are summarised in Table 5.1.

Table 5.1: Reference values used for the examination of the formula for chimneys height (from regulation)

		$c_r [\frac{\mu g}{m^3}]$	$c_0 [\frac{\mu g}{m^3}]$	$c_m [\frac{\mu g}{m^3}]$
NO_2	General locations	131	47	84
	PPA areas	131	94	37
SO_2	General locations	140	37	103
	PPA areas	140	65	75
PM_{10}	General locations	140	37	103
	PPA areas	140	75	66

The comparison between the results of the simulations and the threshold value c_m is separately made for general locations (simulation 1, 4, 6, 7, 9, 12, 14, 15, in which the background pollution level was set to *medium*) and PPA areas (cases in which the background pollution level was set to *high*).

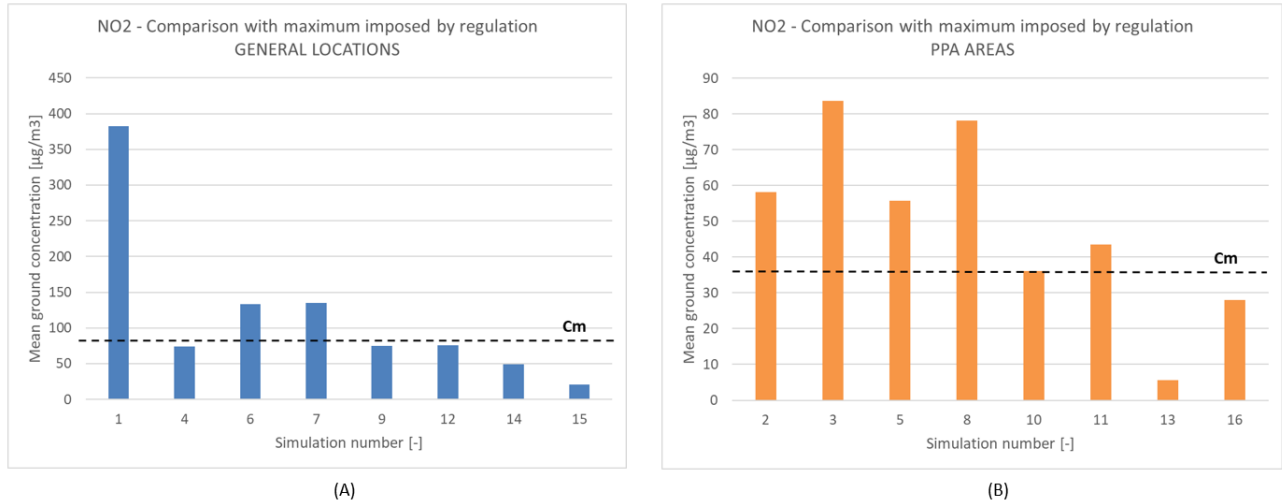


Figure 5.11: Comparison between peak of NO_2 at the ground and threshold value from regulation: (A) simulations in general locations; (B) simulations in PPA areas

In the case of NO_2 (Figure 5.11) the limit is exceeded in 50% of the considered situations and approached in most of the cases. The exceedance occurs especially when dealing with PPA areas (5 cases over 8), in which the excess is up to more than 2 times the threshold. Considering general areas instead the exceedance is generally lower with respect to the limit (up to about 60%) except for case 1, characterized by a very high peak of concentration at the ground (about 4.5 times more than the threshold).

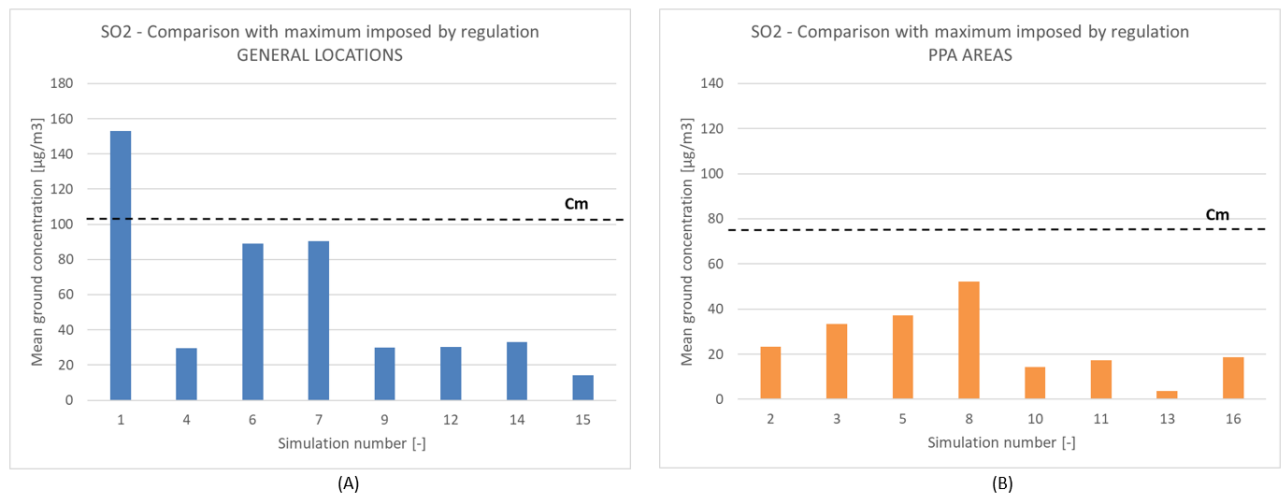


Figure 5.12: Comparison between peak of SO_2 at the ground and threshold value from regulation: (A) simulations in general locations; (B) simulations in PPA areas

The same comparison has been carried out for SO_2 (Figure 5.12). In this case it

can be observed that the only exceedance occurs in case 1; in all the other situations the limits are respected and almost approached only in case 6 and 7. Moreover, considering PPA areas a better performance can be observed with respect to NO_2 , since for SO_2 no exceedances occur.

Finally, the comparison has been made for PM_{10} (Figure 5.13). In this case no exceedances occurred, neither in general locations nor in PPA areas. Even in the worst situation (case 1) there is a difference of about 60% between the limit and the peak of concentration at the ground.

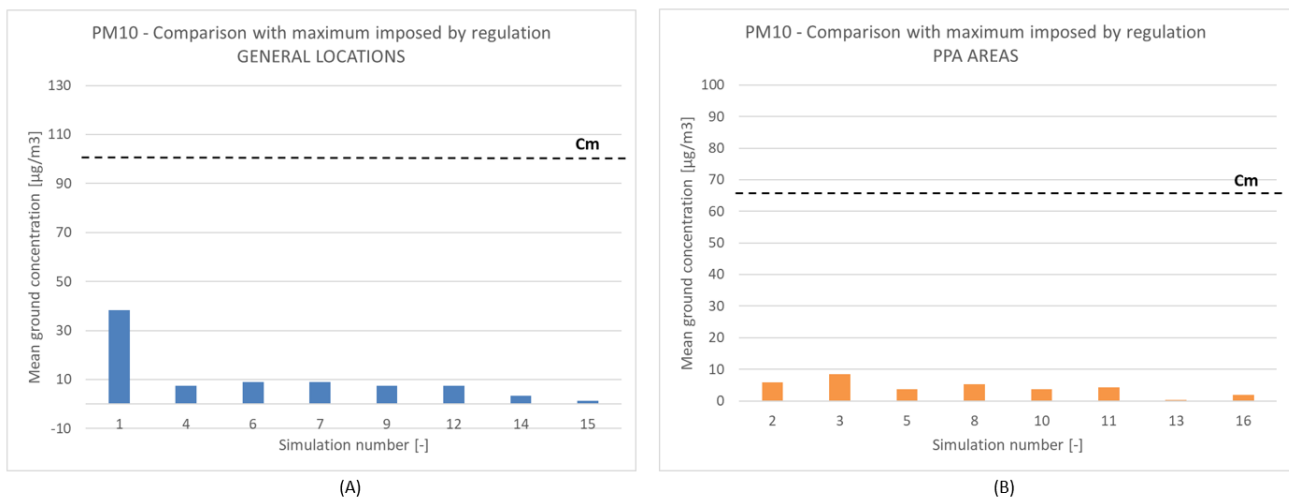


Figure 5.13: Comparison between peak of PM_{10} at the ground and threshold value from regulation: (A) simulations in general locations; (B) simulations in PPA areas

These results give rise to different considerations about the general performance of the formula used for the determination of the height of the chimneys. It is shown that the regulation allows not to exceed the objective value c_m in most of the cases when SO_2 and PM_{10} are involved. On the other hand, when dealing with NO_2 several breaches of the thresholds occur, especially in PPA areas. Such results could surprise, especially when considering PM_{10} , that is commonly recognized to be the most critical pollutant when dealing with pollution events.

The difference in the performance for different pollutants can be explained remembering that the calculation of the height (Eq. 1.1) is separately made for all the species. For each of them a value of height is obtained; then the highest one is chosen. The results suggest that the driver for the determination of the chimney height is probably NO_2 ; for the other species the chimney is oversized, allowing a higher dispersion process. This hypothesis is also confirmed by the parametric analysis, that shows the importance of the height of the chimney on the value of pollutants concentration at the ground. Such consideration can in part justify the large difference between the threshold value and the plant contribution to pollution obtained for PM_{10} .

Overall, it can be concluded that the formula used for the determination of the height of industrial chimneys is not able to guarantee in all the cases the respect of the threshold limit c_r that is aimed at. Given the large number of exceedances

that can occur, especially when dealing with NO_2 , an improvement of the formula is needed. In this regard it can be observed that most of the breaches occur when the temperature of the source is set to low level (case 1 to 8), due to its strong influence on the determination of ground concentration. An improvement of Eq. 1.1 could then involve a change in the weight of the thermal buoyancy term (ΔT). Moreover, as observed with the parametric analysis, the effect of some interactions not taken into account in the formula could be relevant.

However, some considerations could be made about the determination of the threshold term c_m used as a reference for the evaluation of the performance of the regulation.

The first one regards the background pollution value c_0 . The values in Figure 1.1 are determined using the values indicated in the regulation itself (Table 5.1), but it can be questioned either these values are realistic for real applications or not. For this purpose, information about the mean annual background pollution for locations that are representative of the situation in terms of pollution in France have been looked for. In general, power plants could be found either in rural or industrial areas or close to urban ones. According to this consideration, information on the mean annual concentration have been obtained for three different cities, namely Paris, Lyon and Nantes and in rural areas within their respective regions (Ile de France, Rhone-Alps, Pays de la Loire). The concentration is obtained by consulting pollution maps (Appendix D), provided by different regional entities of the country. For SO_2 , only information about Nantes was found. It is important to notice that pollution maps are statistically obtained starting from experimental data in limited locations, so the value of concentration in a specific location is only indicative.

These data show that cities are the most polluted areas whereas surrounding rural areas present lower peaks of concentration. Moreover, both in cities and rural areas the values can significantly vary at different spots (for example, close to the main roads the concentration of NO_2 and PM_{10} is generally much higher than in the surroundings). Assuming that cities correspond to PPA areas and rural areas correspond to general locations, the values provided for c_0 in the regulation can be compared with the ones of pollution maps. As the external conditions for the evaluation of the mean annual concentrations in the maps are not specified, it is assumed that they refer to the conditions of the simulations ($15^\circ C$, $1bar$). Such a comparison shows that even when considering the maximum values of concentration detected on the maps for urban and rural areas a large difference exists: the values provided by the regulation result indeed much higher (Table 5.2).

In particular, considering NO_2 the c_0 values given in the regulation for general areas and PPA ones are about twice and 1.5 times respectively the corresponding ones in the pollution maps; for PM_{10} the value provided by the regulation is about 1.5 times larger in both situations. It can be supposed that c_0 has been set to a precautionary value in order to obtain larger heights for the stacks from Eq. 1.1 (an increase in c_0 indeed determines an increase in the minimum height of the chimney), but it is probably not representative of reality.

A second consideration concerns the reference value c_r , that represents the threshold value of pollutant concentration at the ground. This limit is defined by the regulation as a constant value never to be exceeded, but it is not explicated how

Table 5.2: Comparison between the value of c_0 given in the regulation and peak of concentration detected on maps of concentration

General locations				
	c_0 regulation [$\frac{\mu g}{m^3}$]	Ile de France [$\frac{\mu g}{m^3}$]	Rhone-Alps [$\frac{\mu g}{m^3}$]	Pays de la Loire [$\frac{\mu g}{m^3}$]
NO_2	47	22	24	20
SO_2	37	na	na	na
PM_{10}	37	20	23	20
PPA areas				
	c_0 regulation [$\frac{\mu g}{m^3}$]	Paris [$\frac{\mu g}{m^3}$]	Lyon [$\frac{\mu g}{m^3}$]	Nantes [$\frac{\mu g}{m^3}$]
NO_2	94	60	60	48
SO_2	65	na	na	10
PM_{10}	75	50	40	45

it was set.

The large difference between the threshold value and the plant contribution to pollution obtained for PM_{10} can be especially justified by this observation: a very large value is indeed assigned to c_r for this pollutant in the regulation.

For a more extensive evaluation of the impact of the chimney on air quality (third question addressed to in this work), reference should be made to the limits imposed by the EU Directive for ground concentration (Table 1.1). Nevertheless, to perform this analysis another type of approach would be needed, as argued in Chapter 3.1. Given the generality of this analysis, even under different assumptions a comparison with these limits can only give general trends. A more comprehensive study performed using data for specific sites, that take into account the variance of external and operational conditions in time, would complete the critical analysis of the regulation.

5.3.2 General regulation trends

More general considerations on the performance of the regulation can be made considering the pollutant concentration produced at the ground for different heights. The two levels chosen for the flowrate allowed to simulate two different power sizes of the plants (2 MW and 20 MW). For each size of the plant, the minimum stack height is applied according to the background pollution level of the area (for 2MW power plants, 10 m for general locations or 15 m for PPA ones; 19 m or 28 m for 20 MW power plants). In Figure 5.14, the blue points indicate the pollutant concentration or distance measured in one of the simulations; the orange ones are calculated as the mean of the outputs obtained in configurations with a fixed height.

The graphs for ground concentration show a general decrease of the mean value for each pollutant as the minimum height imposed by the regulation increases. It can be observed both when considering a fixed power size (so passing from a medium background pollution location to a PPA zone) and when considering different sizes of a plant built in the same location (comparison between mean peak values given by stacks of 10 m or 19 m in medium background pollution areas, or by stacks of 15 m or 28m in PPA zones). The first consideration can be easily explained by the larger

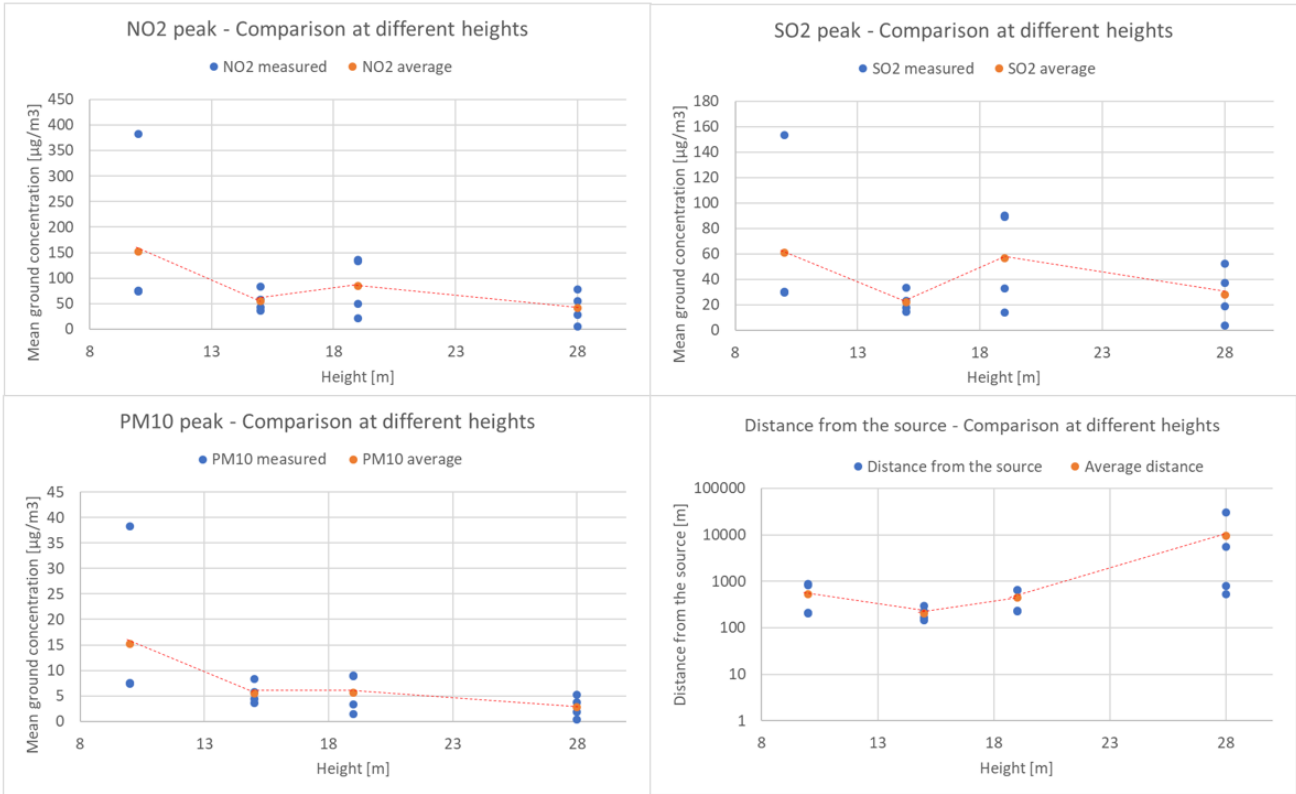


Figure 5.14: Trend of mean ground concentration and distance from the source according to the stack height

dispersion process that can occur when the emission height increases. Especially when small power plants (2MW) are considered, the decrease in concentration peak is quite high (about -63% for all the pollutants; it is probably the same for all the pollutants because only thermal buoyancy effects have been considered in the simulations). When dealing with higher plants the percentage decrease is slightly lower (-51% for all the pollutants). The second consideration can instead be explained by the fact that as the nominal power of the plant increases the concentration emission limits at the source become stricter. The decrease is relevant especially for PM_{10} (-63% for general locations, -49% for PPA zones), probably because for this pollutant the regulation imposes a more significant decrease in the emissions, as previously observed. For SO_2 instead, the variation is much smaller, and in the case of PPA areas an increase in ground concentration can even be detected ($+26\%$).

Opposite considerations can be done for the distance from the source: it is observed a general increasing trend as the minimum height increases (when passing from general location to PPA zones in small power plants the results seem to indicate a decrease in the distance opposite to what expected, but it is probably due to the weight of the results of case 1 on the mean concentration for 10 m sources).

From all these considerations it is possible to conclude that for higher power plants the regulation results more precautionary, even if this effect is mostly due to the limitations on pollutants emission.

Chapter 6

Conclusions

Considering the extreme importance of air quality assessment for the prevention of health and environmental risks, the aim of this analysis was to critically evaluate the effectiveness of a specific regulation adopted in France for the determination of minimum industrial chimneys height.

The study was carried out through two different analysis by considering the peak of pollutant concentration at the ground as criteria for the evaluation. Firstly, a question was raised whether the equation used for the determination of the minimum chimney's height takes into account all the most affecting parameters. To look for an answer, a parametric analysis was performed, through which it was possible to evaluate the contribution of different parameters on pollutants dispersion and to find configurations that are likely to produce larger peaks of pollutant concentration. After that, the effectiveness of the regulation in realistic applications was investigated. For this purpose, a comparison of the ground concentration peak produced by stacks respecting the minimum chimney's height in different situations and for different pollutants with the maximum allowable ground concentration defined in the regulation was performed. The *Design of Experiments* was used as support methodology in order to find the set of simulations to perform. The estimation of the ground concentration for the cases considered in the analysis was made with the support of numerical simulations, performed with the software Fluidyn-PANACHE 5.2.2.5.

The results showed that a large variance in pollutants ground concentration peak can be obtained when considering different situations. The parametric analysis indicated that for this study the most affecting parameters were the temperature of the source, directly related to the variation of plume rise, and the background pollution level, that is involved in the choice of the minimum height of the stack for a specific power plant. Moreover, the quantification of the effects of the parameters analysed showed that some interaction effects are not negligible; it would be interesting to deepen the analysis in order to study all the possible interactions. Summarising the results, it was shown that the effective height of the stack, depending both on the physical height of the stack and the plume rise effect, significantly affects the pollutants ground concentration, emphasising the importance of a proper regulation on chimneys height. Considering the formula used for the determination of the height it is concluded that all the most affecting parameters are taken into account.

Starting from the formula used for the determination of the chimney height and using reference background pollution values [5], all the performed cases are compared to the maximum allowable ground concentration defined in the regulation (c_m). It was observed that in some situations the threshold values were exceeded, especially when dealing with NO_2 . For this pollutant the exceedance occurs in half of the analysed cases, suggesting that the formula provided for the determination of the height should be improved. A possible modification of the formula could consist in a change in the formulation of thermal effects.

However, a deeper analysis on the determination of the c_m value defined in the formula is needed. This term is indeed based on the difference between two values, the background pollution level c_0 , and the reference threshold not to be exceeded at the ground, c_r . Concerning the first term, it was observed that in the regulation it is overestimated if compared to mean values of pollution in France. Secondly, there are doubts on the determination of the c_r values in the regulation: the European regulation on air quality sets indeed different thresholds at the ground. Further analysis could then be focused on the analysis of the determination of these values. Moreover, the study of the effectiveness of the regulation on chimneys height should be deepened by performing a comparison with European limits in order to check the respect of air quality standards. However, this kind of evaluation would require a different approach to the analysis with respect to the one used for this work: reference should be made to specific locations for which meteorological and operational data are well known during long periods of time, in order to obtain realistic average values for concentration to be compared with European thresholds. Given the generic nature of the present work, this type of evaluation was not feasible.

An additional qualitative evaluation of the regulation was made by comparing the ground concentration for different heights. In this case it was observed that, as a general trend, the French regulation is more precautionary when power plants with high nominal power are considered, even if this effect is mostly due to the reduction of emitted pollutants for power plants with higher nominal power. Considering the general nature of this analysis, to have a more comprehensive overview of the industrial pollution contribution to air quality further analysis should include more detailed data.

It is important to keep in mind that the results depend on the choices and sometimes on the constraints related to the setting of the problem. The assessment is made in order to attain the best possible results considering time and software limitations, but still some simplifications were necessary to perform the analysis.

Concerning the design of the experiment, a Fractional factorial design was implemented in order to choose the simulations to perform. This methodology results very convenient in terms of time, because it allows to get a large amount of information about the influence of all the parameters under evaluation on dispersion performing a limited number of simulations. Nonetheless, the choice of the cases to perform is based on a statistical approach; although this methodology is conceived to obtain satisfactory information about a process, the results of the parametric analysis are still subject to uncertainty, especially concerning the exact quantification of the effects and in the evaluation of the interactions between parameters. The complete

information could only be obtained implementing a Full factorial design, in which all the possible combinations between parameters are considered. However, such detailed results are beyond the scopes of this analysis.

Even the choice of the parameters to evaluate affects the results. It is important to underline that the selection was oriented through the evaluation of regulation: firstly, the terms explicitly considered in the formula for the determination of the minimum chimney height were considered; then additional parameters were included in the model. Moreover, to decrease the number of simulations to perform different assumptions were then made (constant ambient air temperature, fixed smoke composition, no chemical reactions in the atmosphere, air treated as an ideal gas). The effect of some of these parameters or their interaction with other ones could maybe be relevant for the dispersion process, but only an analysis specifically oriented to the evaluation of the effects of all the parameters on dispersion could clarify it. However, considering the main phenomena produced by these effects, it could be expected a lower influence on the pollutant ground concentration with respect to other parameters that have been instead considered in the analysis. On the other hand, one of the main limitations of this analysis consists in the fact that the effect of atmospheric inversion layer on dispersion is not taken into account, due to the difficulty of the implementation in such a study (the effect on dispersion depends on the height of emission with respect to the inversion layer, that was not possible to evaluate with this design of the experiment). Considering the presence of the obstacles instead, even if several studies demonstrated their importance on the dispersion process, the evaluation of their effect was not suitable for a general analysis as the present one.

Finally, the results are affected by the choices made for the setting of the numerical model. The most important simplification used for the setting concerns the use of the Boussinesq model, that does not allow to consider the buoyancy effect related to the mass of different species on the dispersion process. The results could significantly vary (both in terms of ground peak value and distance from the source) especially in the case of solid particles like PM_{10} , in which the weight of the pollutant could play a very important role. However, the results show that the most relevant pollutant for the analysis is NO_2 , that is less affected by this approximation due to its gaseous state. Another consideration concerns the modelling of the source as a point one. Such an approximation results in neglecting some phenomena (as, for example, wakes) that can occur close to the source itself. However, since the regulation under evaluation does not take into account the presence of obstacles, this effect would not be extremely relevant for the plants considered in the analysis.

All these considerations suggest that, despite all the simplifications adopted for the resolution of the problem, the results obtained could still be considered reliable in qualitative terms.

Appendix A

Application of the regulation to real data

A.1 Comparison of the height obtained from the two different French regulations

The chimney heights indicated in the Article 54 of the French regulation [4] are compared to the values obtained through the application of the formula of the Article 23 to search for a possible relation between the two. It is made by applying the formula to real power plants data, that have been provided by the enterprise Poujoulat SA (Figure A.1).

	WOOD 35%			NATURAL GAS ($\lambda = 1.25$)		
Power rate (MW)	2	6	20	2	6	20
Flue gas flow (kg/h_wet)	5500	27500	54900	3635	18167	36350
(Nm ³ /h)	4326	21632	43184	2919	14586	29186
(kg/s_wet)	1.53	7.64	15.25	1.01	5.05	10.10
Ro (Nm ³ /h 6%O ₂)	4569	22847	45610			
(Nm ³ /h 3%O ₂)				3058	15281	30576
Temperature (°C)	160	160	160	120	120	120
Nitrogen (%vol)	66.2%	66.2%	66.2%	71.3%	71.3%	71.3%
Oxygen (%vol)	6.8%	6.8%	6.8%	3.8%	3.8%	3.8%
Argon (%vol)	0.8%	0.8%	0.8%	0.9%	0.9%	0.9%
Carbon Dioxide (%vol)	10.6%	10.6%	10.6%	7.9%	7.9%	7.9%
Water (%vol)	15.6%	15.6%	15.6%	16.1%	16.1%	16.1%
Dust (mg/Nm ³)	50	30	30			
(kg/h)	0.228	0.685	1.368			
NOx (mg/Nm ³)	500	300	300	100	100	100
(kg/h)	2.285	6.854	13.683	0,306	1,528	3,058
SOx (mg/Nm ³)	200	200	200			
(kg/h)	0.914	4.569	9.122			
Chimney height (m)	10	14	16	4	6	8
Exhaust velocity (m/s)	6	6	6	5	5	5

Figure A.1: Power plants data

Application of *Art. 23 - Hauteur de cheminée*

(Arrêté du 3 août 2018 relatif aux installations de combustion d'une puissance thermique nominale totale inférieure à 50 MW soumises à autorisation au titre des rubriques 2910, 2931 ou 3110 ; Chapitre IV - conditions de rejet à l'atmosphère)

Calculation of the parameter s :

$$s = k \cdot \frac{q}{c_m} \quad (\text{A.1})$$

Where k is a constant provided by the regulation ($k = 340$ for gaseous pollutants, $k = 680$ for dust), q is the emission rate of pollutant ($\frac{kg}{h}$), c_m is the maximum admissible concentration at the soil ($\frac{mg}{Nm^3}$). The parameter s is evaluated for each different pollutant; it is then considered the maximum value obtained in order to estimate the height of the chimney.

For the evaluation of c_m :

$$c_m = c_r - c_0 \quad (\text{A.2})$$

where c_r is a reference value, c_0 is the mean annual concentration at the considered location. The first term is constant, indicated in the regulation (Figure A.2.). For the second term, the regulation provides indicative values in the case the information on the concentration in the location is missing (Figure A.3).

Polluants	Valeur de c_r
Dioxyde de soufre	0,15
Oxydes d'azote	0,14
Poussières	0,15
Acide chlorhydrique	0,05
Composés organiques	1
Métaux toxiques (Pb, As, Hg, Cd)	0,0005

Figure A.2: Table provided by the regulation for the determination of c_r

En l'absence de mesures de la pollution, c_0 peut être prise forfaitairement de la manière suivante :

	SO _x	NO _x	Poussières
Zone peu polluée	0,01	0,01	0,01
Zone moyennement urbanisée ou moyennement industrialisée	0,04	0,05	0,04
Zone très urbanisée ou très industrialisée	0,07	0,10	0,08

Figure A.3: Table provided by the regulation for the determination of background pollution c_0

It is then evaluated the height of the chimney according to the formula:

$$h_p = s^{\frac{1}{2}} \cdot (R \cdot \Delta T)^{-\frac{1}{6}} \quad (\text{A.3})$$

where R is the gas flowrate referred to the emission temperature ($\frac{m^3}{h}$), ΔT is the difference between the temperature of emission of gases and the mean annual air temperature (if this value is smaller than $50K$, it will be considered $\Delta T = 50K$). As mean annual air temperature $15^\circ C$ is considered.

For the estimation of R , it is considered the provided exhaust flowrate in $\frac{kg}{h}$ (referred to moist air smoke mixture) and it is divided by the density of smoke at the source temperature:

$$R = \frac{\dot{m}}{\rho_{T_{source}}} \quad (A.4)$$

where \dot{m} is the mass flowrate at the source conditions, $\rho_{T_{source}}$ is the temperature of emission of pollutants.

Determination of moist air density

The density of moist air at the source temperature should be determined. This is made by considering air as a perfect gas with the following procedure:

- Evaluation of the molar weight of moist air:

$$MW_{air} = \sum_{i=1}^n x_i \cdot MW_i \quad (A.5)$$

MW_i represents the molar weight of the $i - th$ component of the mixture, x_i .

- Calculation of the volume per unit mole (Ideal gas law):

$$\frac{V}{n} = \frac{R \cdot T}{p} \quad (A.6)$$

- The density of the air (in $\frac{g}{m^3}$) is evaluated according to the formula:

$$\rho_{air} = \frac{MW_{air}}{\frac{V}{n}} \quad (A.7)$$

Comparison of the height evaluated with the two regulations

As an example, it is evaluated the height using the formula in Article 23 for two ranges of nominal power of the plant. The value is computed considering the upper value of the range (i.e. 2 MW and 20 MW respectively). The differences can be due to the consideration of different values for mean ambient temperature, flowrates or smoke composition.

- Biomass plant

		Height determined by Article 23 [5]	Regulation [4]
Medium background pollution	$1 < P < 2$ MW	10 m	10 m
	$15 < P < 20$ MW	15 m	14 m
High background pollution	$1 < P < 2$ MW	14 m	14 m
	$15 < P < 20$ MW	24 m	24 m

- Natural gas plant

		Height determined by Article 23 [5]	Regulation [4]
Medium background pollution	$1 < P < 2$ MW	4 m	4 m
	$15 < P < 20$ MW	9 m	8 m
High background pollution	$1 < P < 2$ MW	6 m	6 m
	$15 < P < 20$ MW	13 m	14 m

A.2 Emission limits

For the most important pollutant species the regulation [5] imposes a maximum mass amount that can be emitted by the power plant. This limit depends on the size of the power plant and on the type of fuel. For biomass and natural gas (the fuel types whose data is provided by Poujoulat SA, Figure A.1) the limits imposed for different power sizes are shown in Figure A.4.

	Power, P (MW)	SO ₂ (mg/Nm ³)	NO _X (mg/Nm ³)	Poussières (mg/Nm ³)	CO (mg/Nm ³)
Biomass	$P < 5$	200	500 (3)	50	250
	$5 \leq P < 10$		300 (3)	30 (8)	
	$10 \leq P < 20$				
	$20 \leq P$	300 (4)	20 (9)	200	
Natural gas	$P < 5$	-	100	-	100
	$5 \leq P < 10$				
	$10 \leq P < 20$				
	$20 \leq P$				

Figure A.4: Concentration limits at the emission (Art. 10.II) [5]

Appendix B

Complements to the numerical model

B.1 Units conversion for source definition in Fluidyn-PANACHE

The available pollutants concentrations are provided in $\frac{mg}{Nm^3}$ (Figura A.1). This unit cannot be directly used on Fluidyn-PANACHE, thus a conversion is required. The possible units accepted by the software are listed in the table below.

Table 3-11 pollutant emission composition description

Units	Description
Micro g/g	Micrograms/gram
%Yi	Percentage mass fraction
Yi	Mass fraction
Micro- m ³ / m ³	Micro cubic meter/cubic meter
%Xi	Percentage volume fraction
Xi	Volume fraction
Bq/ m ³	Becquerel/cubic meter

Figure B.1: Concentration units used on Fluidyn-PANACHE [32]

It is chosen to obtain the concentration in $\frac{\mu g}{g}$. Exploiting the calculation for air density (Eq. A.7) and considering a constant pressure and number of moles, it is then evaluated the density at normal conditions:

$$\rho_{air,0} = \rho_{air} \frac{T}{T_0} \quad (B.1)$$

The new concentration for the pollutant can be obtained by dividing the initial concentration for the density of air at normal conditions:

$$NO_x = \frac{c_{in}[\frac{mg}{Nm^3}]}{\rho_{air,0}[\frac{g}{Nm^3}]} \cdot 1000[\frac{\mu g}{mg}] \quad (B.2)$$

B.2 Turbulence modelling

For the vertical profile of turbulence imposed at the inlet, reference is made to the *Arya* profiles. The equations can be found in the NASA document *An estimation of turbulent kinetic energy and energy dissipation rate based on atmospheric boundary layer similarity theory*, by J. Han, S.P. Arya, S. Shen and Y. Lin. The extract of the document for the formulas can be found in the following.

are suggested in the following subsections; some of the expressions are adopted directly from those references, whereas the others are derived using the similarity relationships of turbulence variables other than TKE and EDR.

2.1 Neutral and Stable Boundary Layers ($z/L \geq 0$)

The boundary layer may be subdivided into a surface layer (in which stress is nearly constant with height) and an outer layer. A separate set of algorithms is assigned to each sublayer as follows.

2.1.1 Surface Layer ($z \leq 0.1h$)

In the surface layer, the TKE (e) and EDR (ϵ) are given by (Hogstrom, 1996; Rao and Nappo, 1998)

$$e = 6u_*^2, \quad (1)$$

$$\epsilon = \frac{u_*^3}{kz} \left(1.24 + 4.3 \frac{z}{L} \right), \quad (2)$$

where $k \simeq 0.4$ is von Karman constant. The friction velocity, u_* , is defined as

$$u_*^2 = \left[(\overline{u'w'})_s^2 + (\overline{v'w'})_s^2 \right]^{1/2}, \quad (3)$$

where the right hand side of Eq. (3) represents the total vertical momentum flux near the surface (the subscript s denotes the ground surface). The Obukhov length L depends on both the momentum and heat fluxes near the surface and is defined later; the ratio z/L is the fundamental similarity parameter of the Monin-Obukhov similarity theory.

2.1.2 Outer Layer ($z > 0.1h$)

Expressions for the outer layer can be assigned according to the level of stratification.

(1) Neutral and Stable Boundary Layer

In the neutral and moderately stable boundary layer, the TKE and EDR are given by (Hogstrom, 1996; Rao and Nappo, 1998)

$$e = 6u_*^2 \left(1 - \frac{z}{h} \right)^{1.75}, \quad (4)$$

$$\epsilon = \frac{u_*^3}{kz} \left(1.24 + 4.3 \frac{z}{L} \right) \left(1 - 0.85 \frac{z}{h} \right)^{1.5}. \quad (5)$$

Alternatively, *Eqs.*(4) and (5) may also be used for the entire boundary layer, including the surface layer.

(2) Very Stable and Decoupled Layers

In the very stable boundary layer and decoupled layers, the TKE and EDR can be expressed by extension of *Eqs.*(1) and (2) as

$$e = 6u_L^2, \quad (6)$$

$$\epsilon = 4.3 \frac{u_L^3}{kL_L}, \quad (7)$$

where u_L is the local (friction) velocity scale and L_L is the local buoyancy length scale. Under very stable conditions, the elevated layers of turbulence are decoupled from the surface and the local fluxes and scales cannot be reliably estimated. Perhaps, an empirical relationship between the overall turbulence intensity ($e^{1/2}/\bar{u}$) and Richardson number should be explored. It is worthwhile to note that some experimental results show that *Eq.*(5) can be still used to estimate ϵ even in a very stable boundary layer.

2.2 Unstable Boundary Layer ($z/L < 0$)

The unstable ABL such as during daytime surface heating can be divided into three regimes depending upon the stability parameter, z/L or h/L .

2.2.1 Strongly Unstable (Convective) Regime ($|z/L| > 0.5$)

The structure of the convective regime is dominated by buoyancy. The mean wind velocity and potential temperature profiles are nearly uniform with height. For this reason, the convective outer layer is called the “mixed layer.” The mixed layer is topped by an inversion layer in which temperature increases with height. A broad maximum of TKE is usually found in the middle of the mixed layer, while EDR decreases slightly with height.

(1) Surface Layer ($z \leq 0.1h$)

In the surface layer, the TKE and EDR are given by (Arya, 2000)

$$e = 0.36w_*^2 + 0.85u_*^2 \left(1 - 3\frac{z}{L}\right)^{2/3}, \quad (8)$$

$$\epsilon = \frac{u_*^3}{kz} \left(1 + 0.5\left|\frac{z}{L}\right|^{2/3}\right)^{3/2}. \quad (9)$$

(2) Mixed Layer

In the mixed layer, the TKE is given by (Arya, 2000)

$$e = \left(0.36 + 0.9\left(\frac{z}{h}\right)^{\frac{2}{3}} \left(1 - 0.8\frac{z}{h}\right)^2\right) w_*^2, \quad (10)$$

or, for most practical purposes,

$$e = 0.54 w_*^2. \quad (11)$$

The EDR decreases slowly with height at a linear rate (Sorbjan, 1989), i.e.,

$$\epsilon = \frac{w_*^3}{h} \left(0.8 - 0.3\frac{z}{h}\right), \quad (12)$$

where the convective velocity scale w_* is defined as

$$w_* = \left(\frac{g}{T_0} \overline{(w'\theta_v')}_s h\right)^{1/3}. \quad (13)$$

Here g is the gravitational acceleration, T_0 is the reference temperature, and $\overline{(w'\theta_v')}_s$ is the mean surface heat flux.

2.2.2 Moderately Unstable Regime ($0.02 < |z/L| \leq 0.5$)

In this regime, the mechanical production of TKE is comparable with buoyancy production of TKE, i.e., turbulence generation from vertical wind shear is comparable to that generated from surface heating. The TKE in this regime is more or less uniform over the boundary layer or may decrease slightly with height, and the boundary layer structure may be more uncertain.

2.2.3 Weakly Unstable (Near-Neutral) Regime ($|z/L| \leq 0.02$ or $|h/L| \leq 1.5$)

This regime often occurs during the transition period of early morning and late afternoon or during overcast days with strong winds. The lapse rate for temperature tends to be near-neutral. In this regime, mechanical (shear) production dominates the TKE budget.

Appendix C

Complements to the results

C.1 Summary of the results of simulations

For all the performed cases, the average ground concentration and the distance of the peak of concentration from the emission point are summarised in Figure C.1.

CASE	NOx [$\mu\text{g}/\text{m}^3$]	SOx [$\mu\text{g}/\text{m}^3$]	PM10 [$\mu\text{g}/\text{m}^3$]	Distance from source [m]
1	382.6	153.1	38.2	830
2	58.1	23.3	5.8	220
3	83.7	33.5	8.4	140
4	73.8	29.5	7.4	210
5	56.3	37.6	3.8	6470
6	133.4	88.9	8.9	650
7	135.4	90.3	9.0	240
8	78.2	52.1	5.2	530
9	74.9	30.0	7.5	890
10	36.0	14.4	3.6	290
11	43.6	17.4	4.4	160
12	75.8	30.3	7.6	200
13	5.6	3.8	0.4	30800
14	49.4	32.9	3.3	650
15	21.2	14.1	1.4	230
16	28.0	18.7	1.9	790

Figure C.1: Summary of the results obtained with numerical simulations

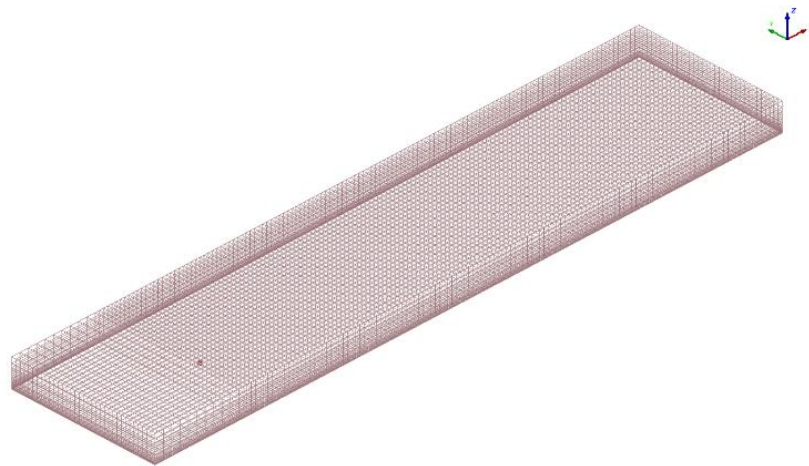
C.2 Main parameters evaluated for each simulation

In the following all the most relevant information for each simulation is shown.

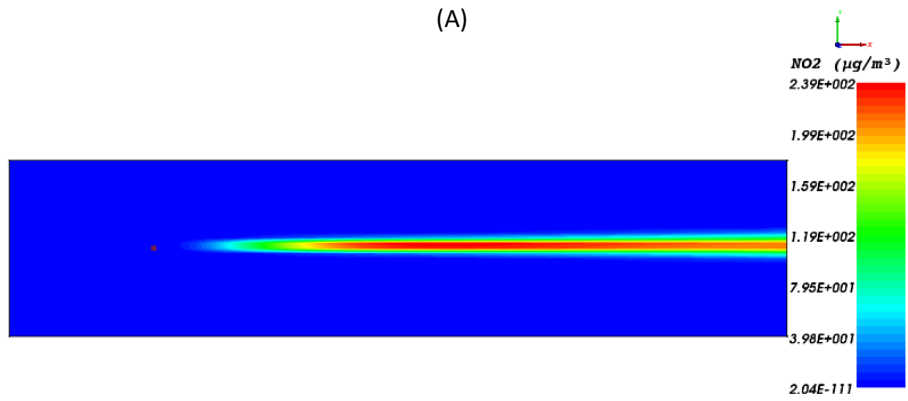
For each case it is possible to evaluate the following characteristics:

- (A) Domain grid
- (B) NO_2 ground concentration (i.e. pollutant concentration on the plane XY , $z=0$ m)
- (C) SO_2 ground concentration
- (D) PM_{10} ground concentration
- (E) NO_2 lateral concentration profile (i.e. pollutant concentration on the plane XZ , $y=0$ m)
- (F) SO_2 lateral concentration profile
- (G) PM_{10} lateral concentration profile
- (H) Turbulent kinetic energy profile on the plane XZ , $y=0$ m
- (I) Horizontal velocity profile on XZ plane, $y=0$ m
- (J) Temperature vertical profile (XZ plane, $y=0$ m)
- (K) Mean pollutants ground concentration (average value from the ground to about 2.5 m)

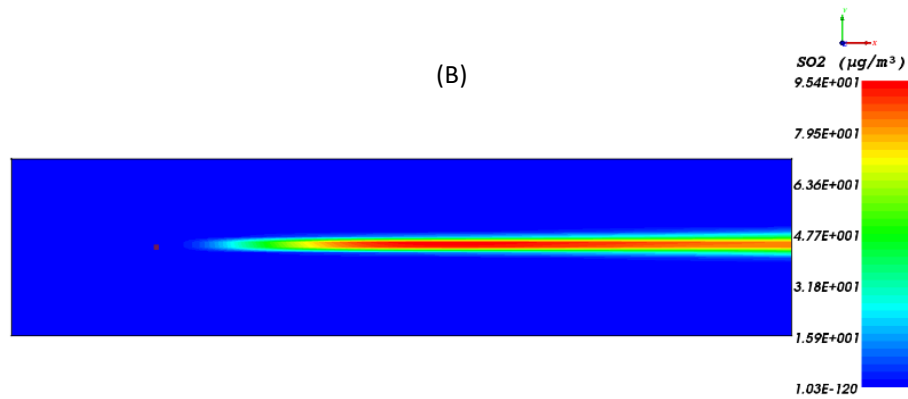
CASE 1



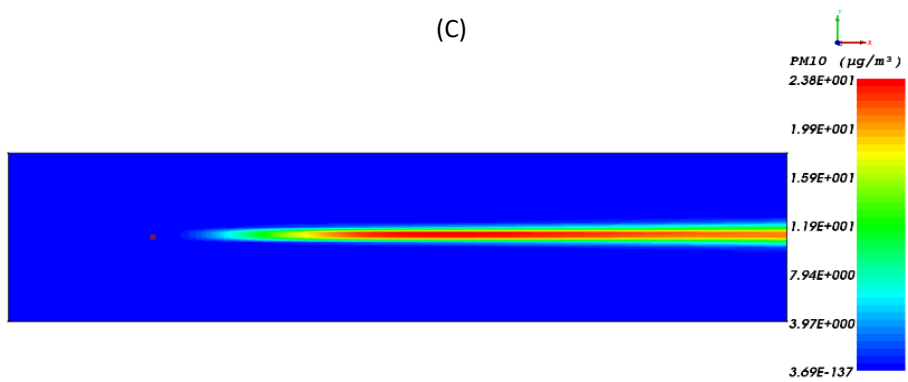
(A)



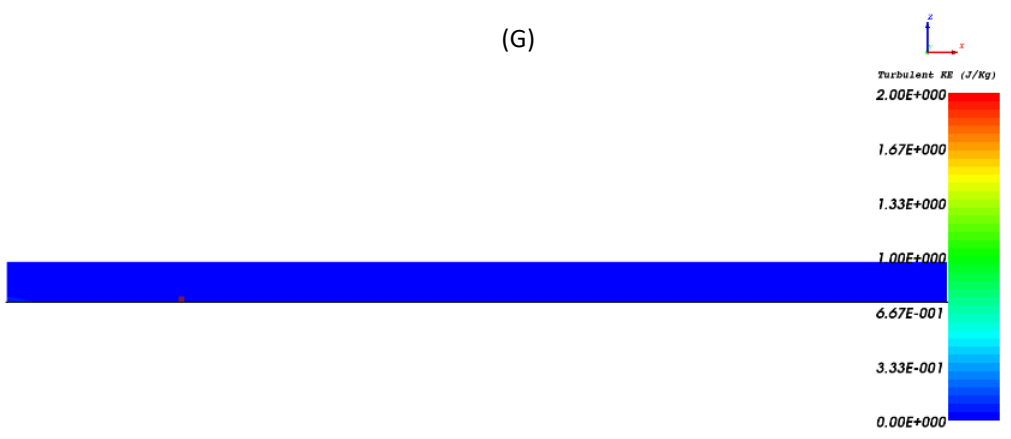
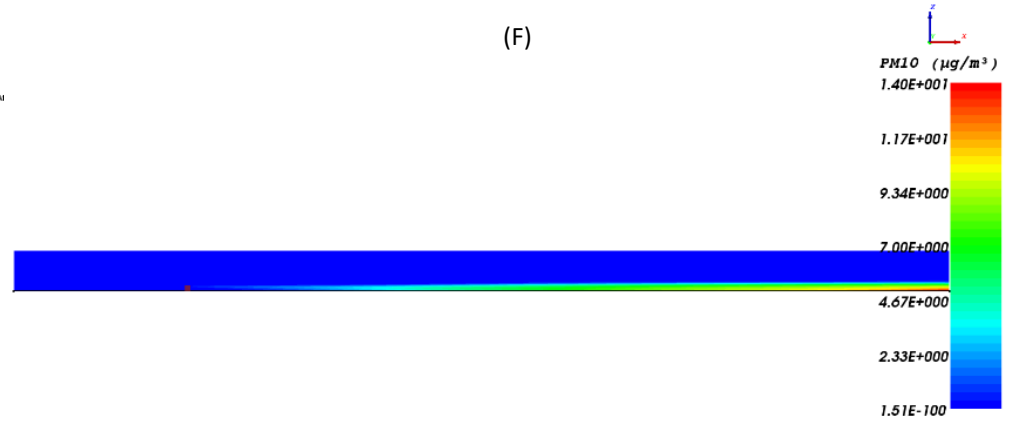
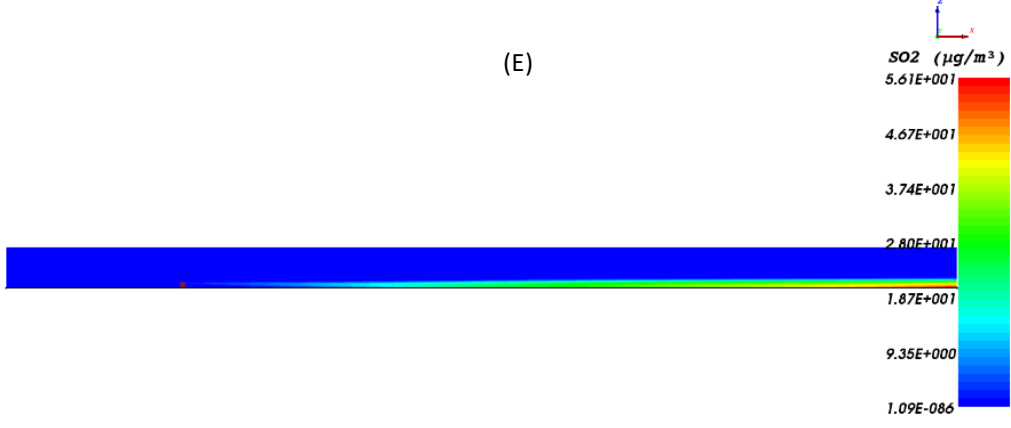
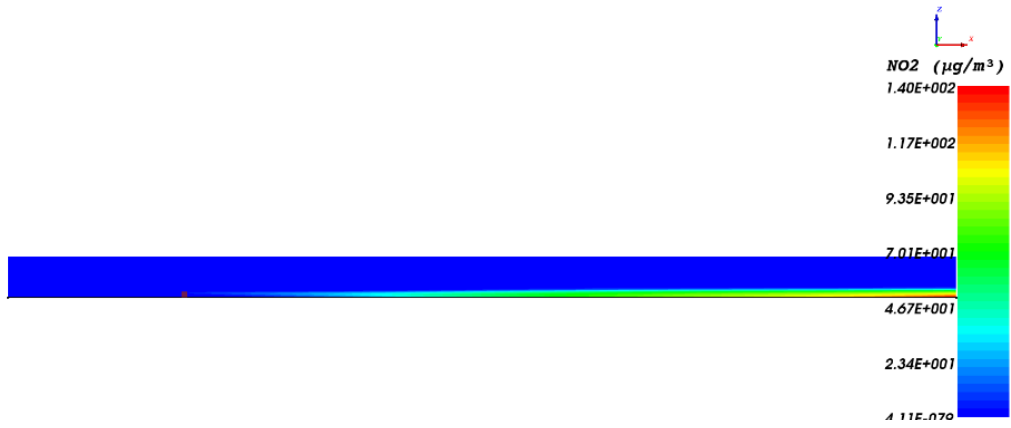
(B)

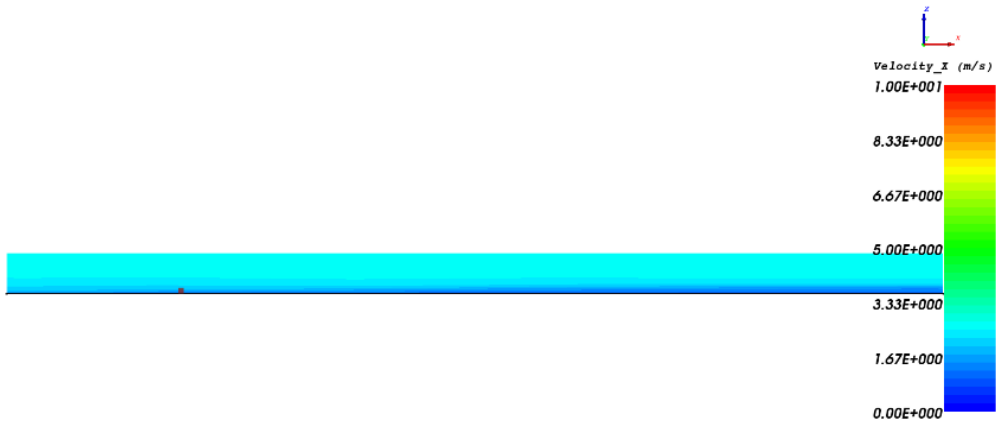


(C)

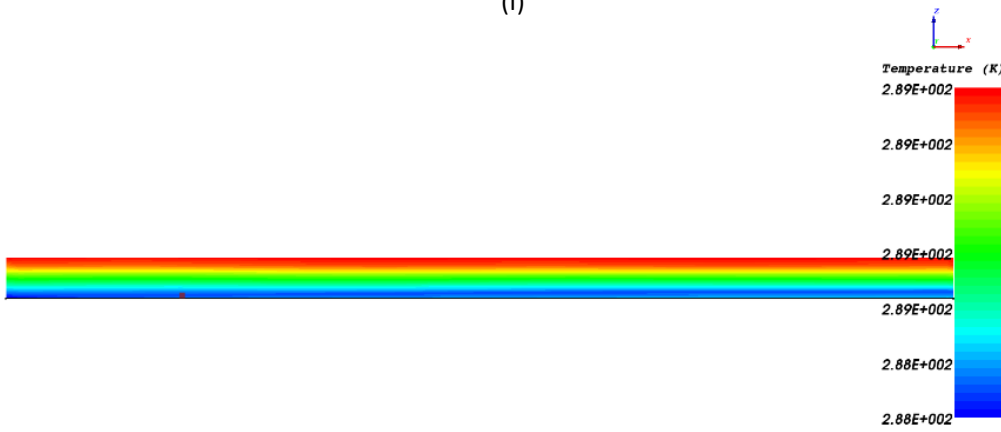


(D)

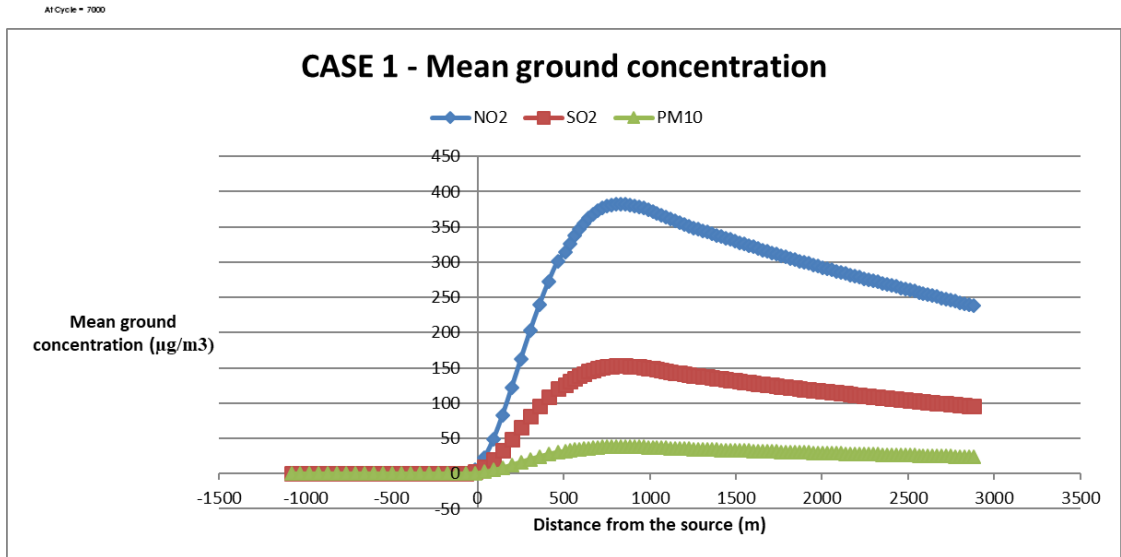




(I)

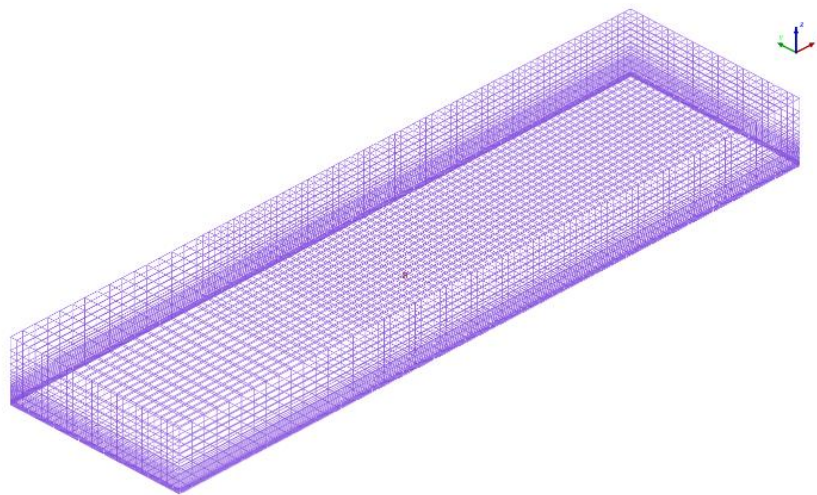


(J)



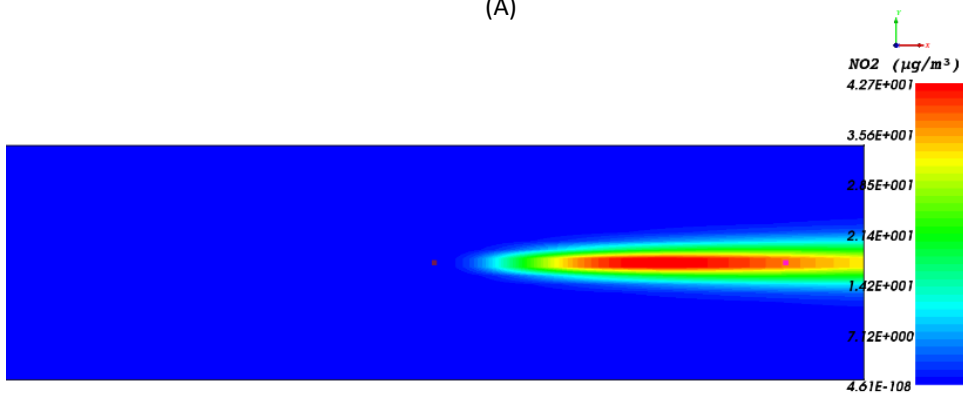
(K)

CASE 2

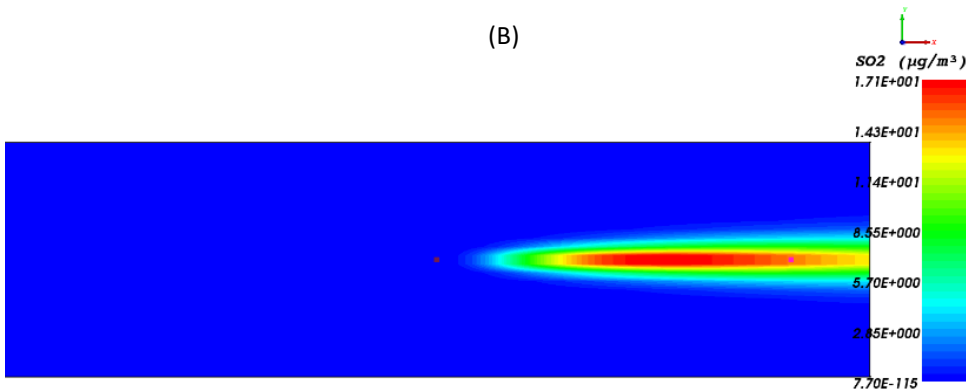


AtCycle = 3231

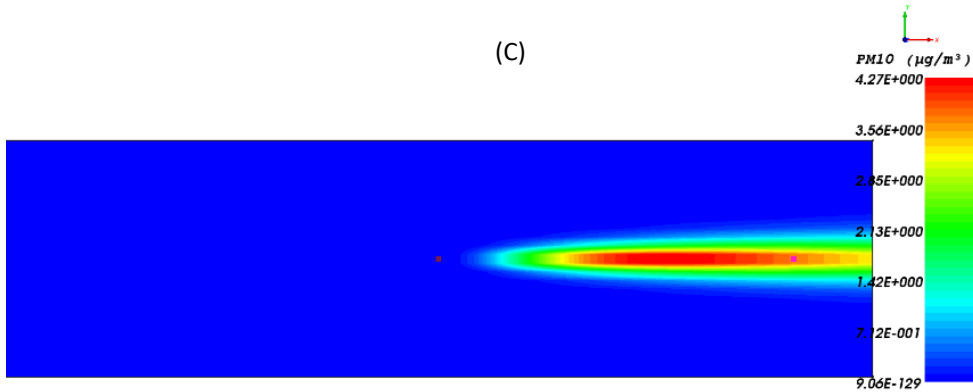
(A)



(B)

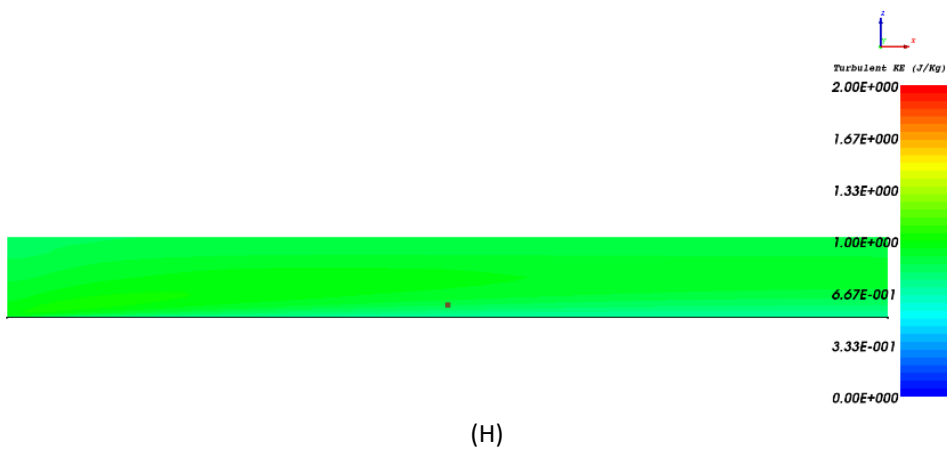
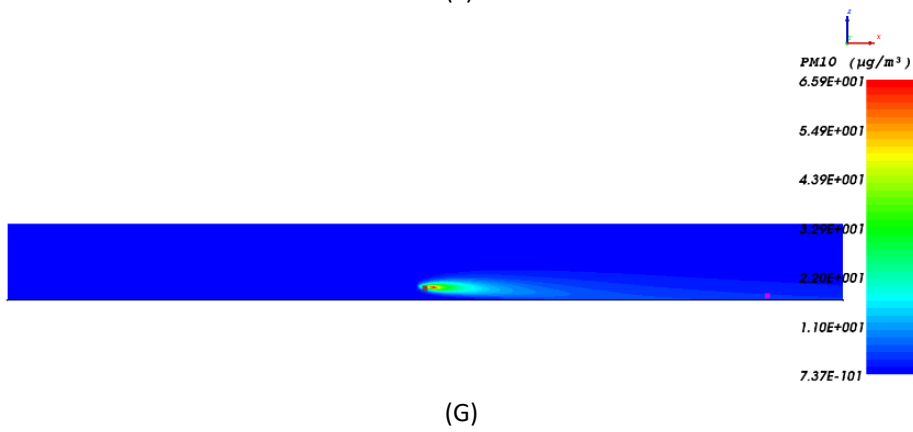
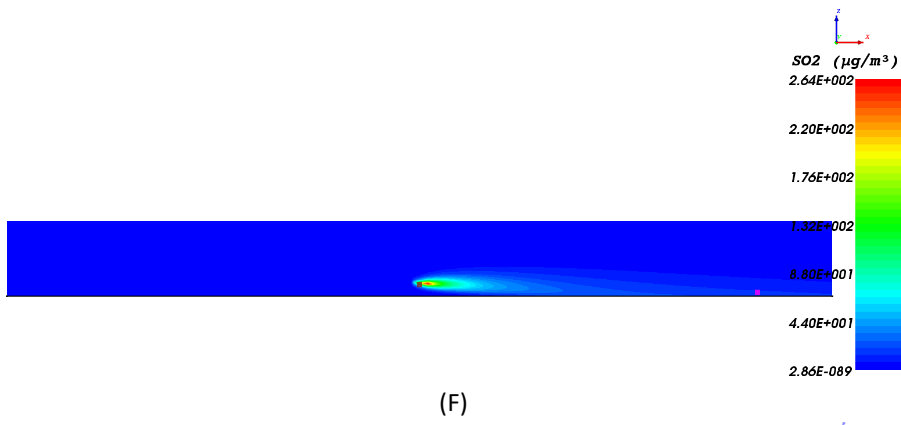
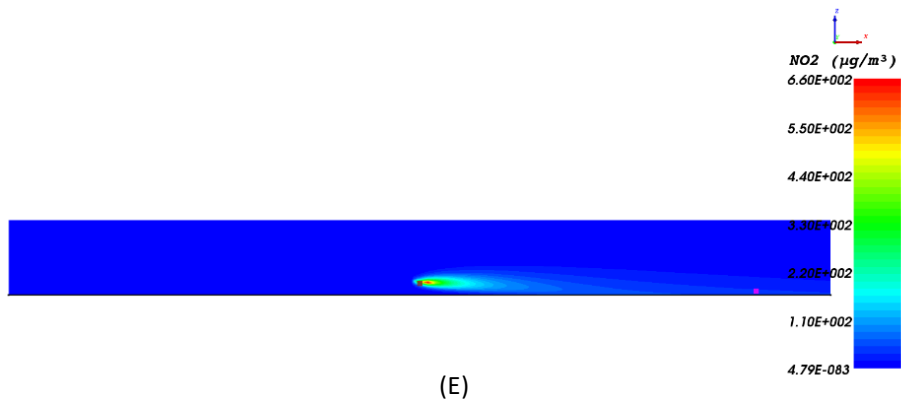


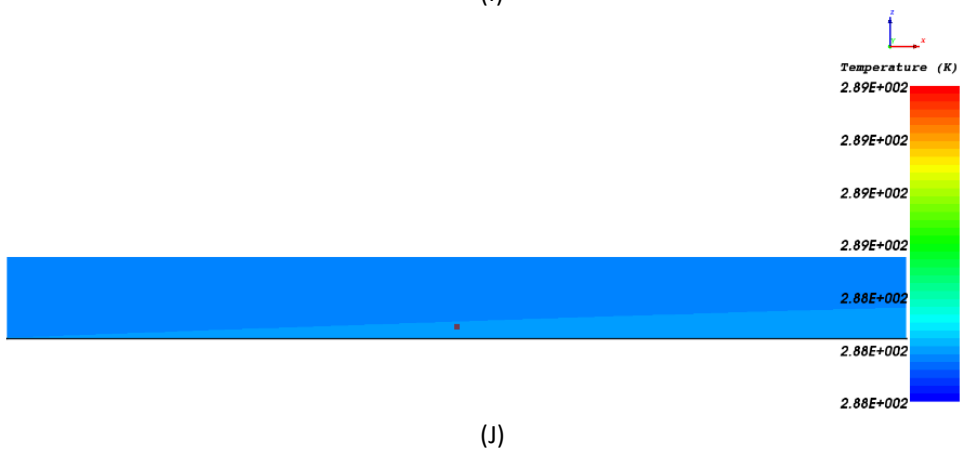
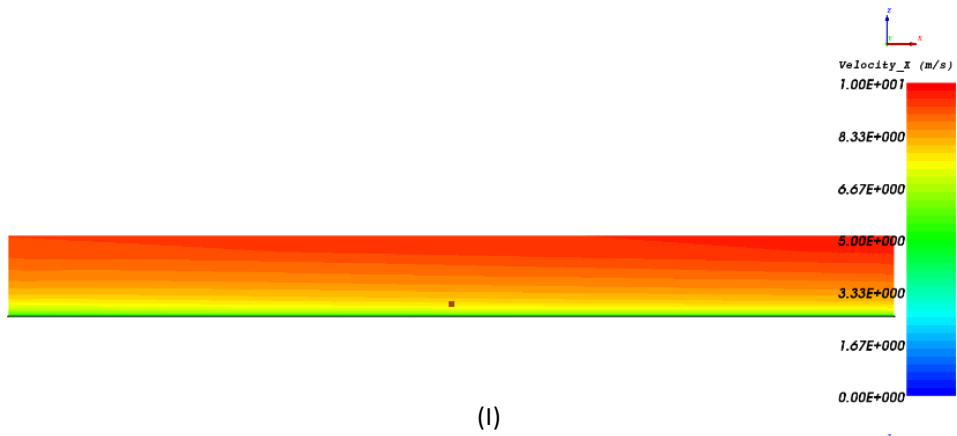
(C)



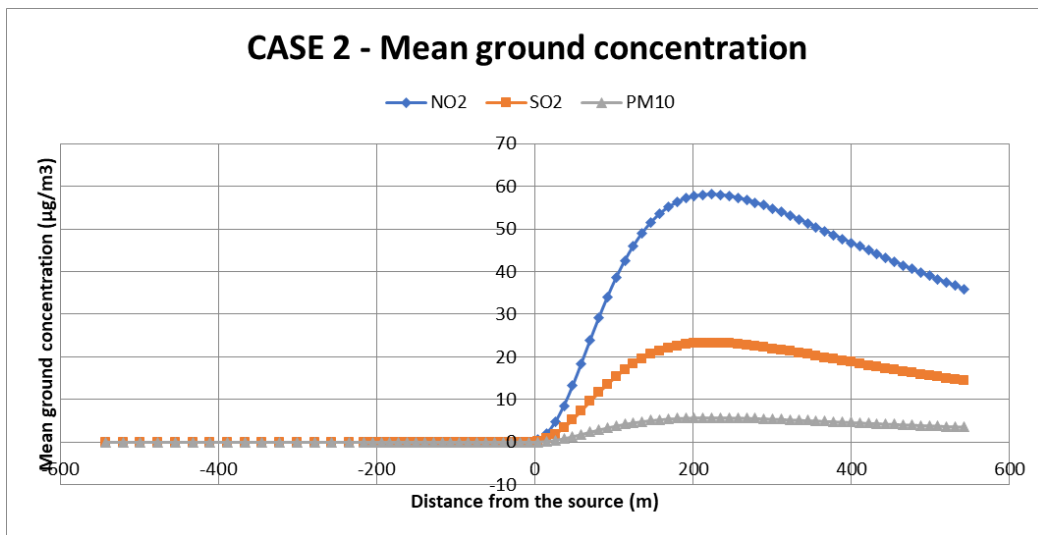
(D)

AtCycle = 3231



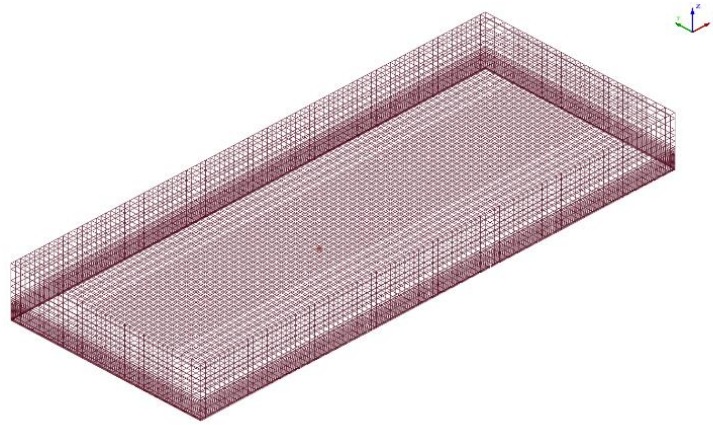


AI Cycle - 3211

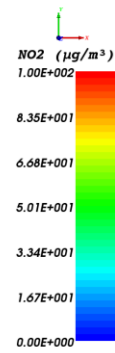
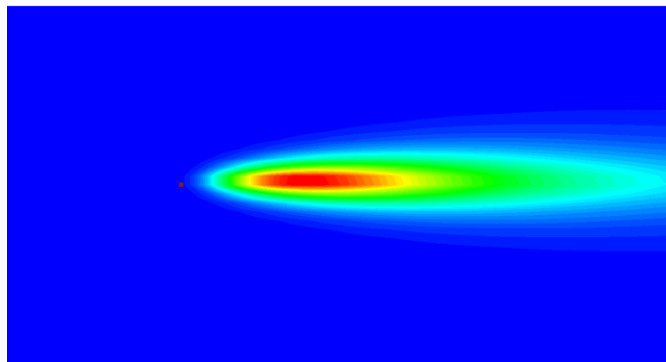


(K)

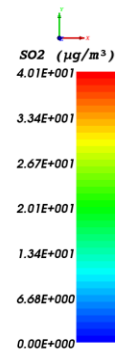
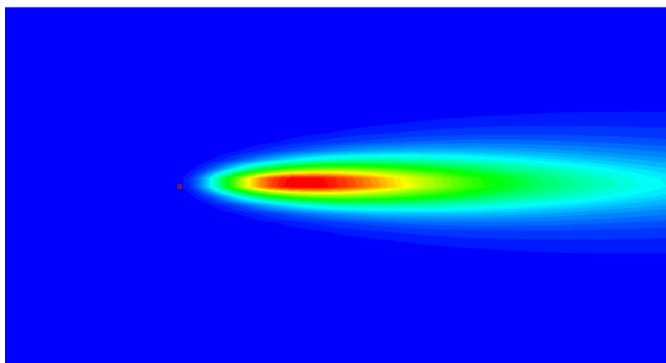
CASE 3



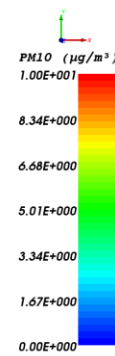
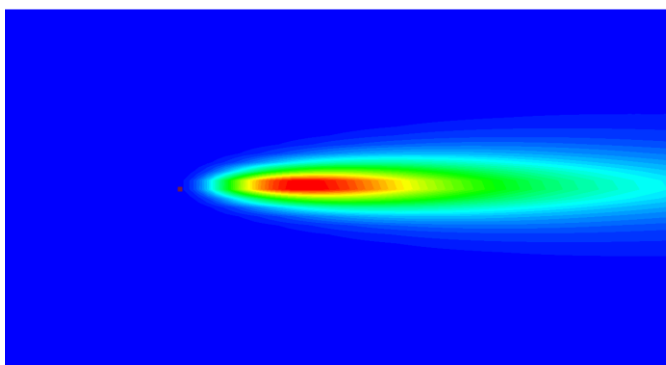
(A)



(B)

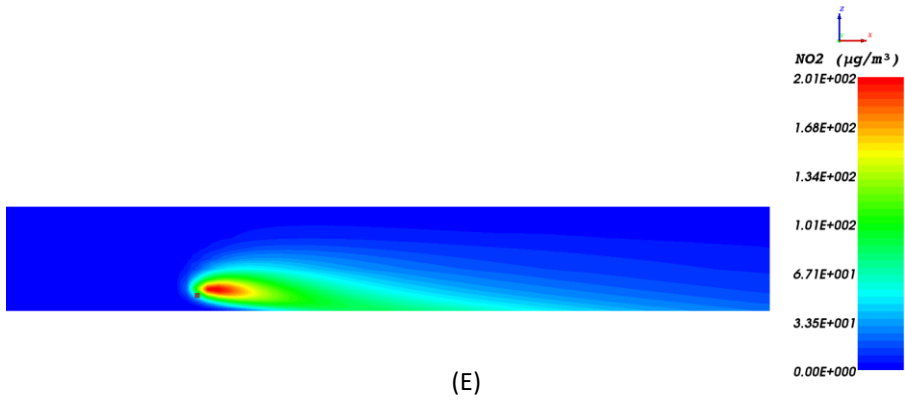


(C)

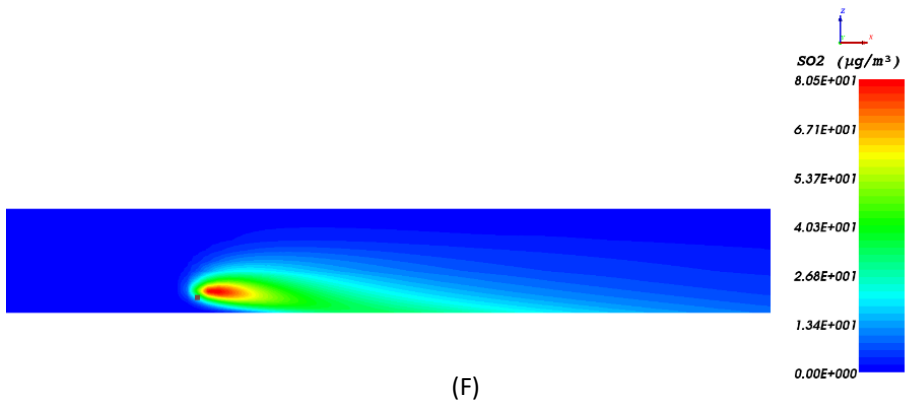


At Cycle = 6740

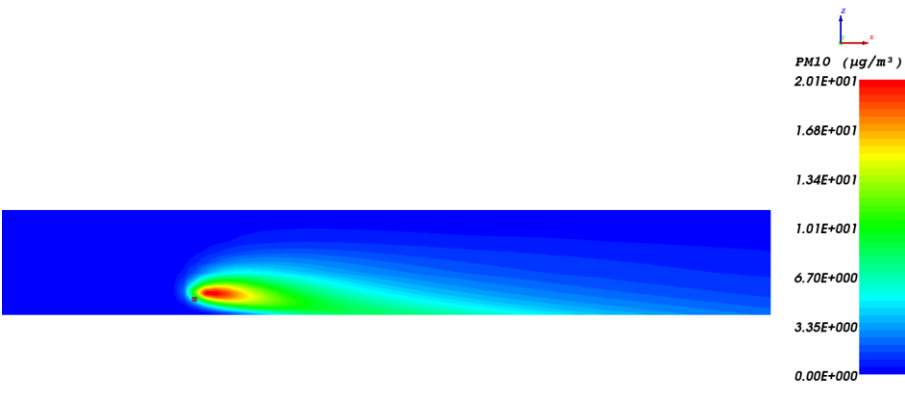
(D)



(E)



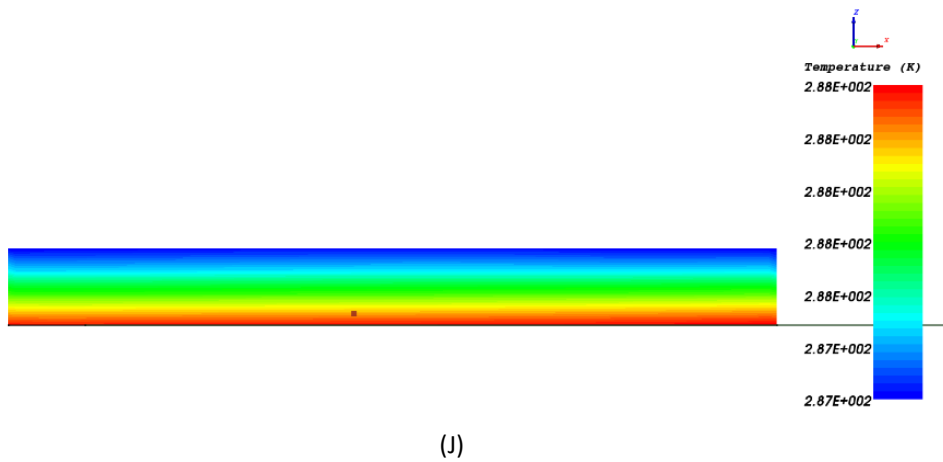
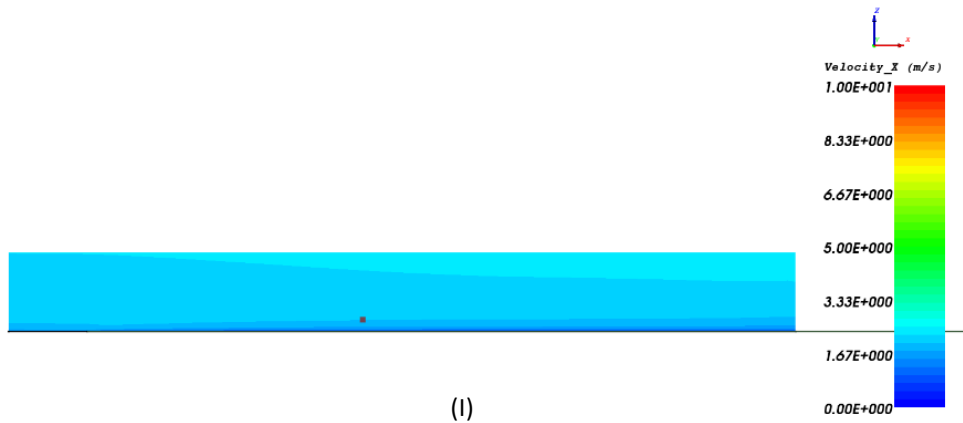
(F)



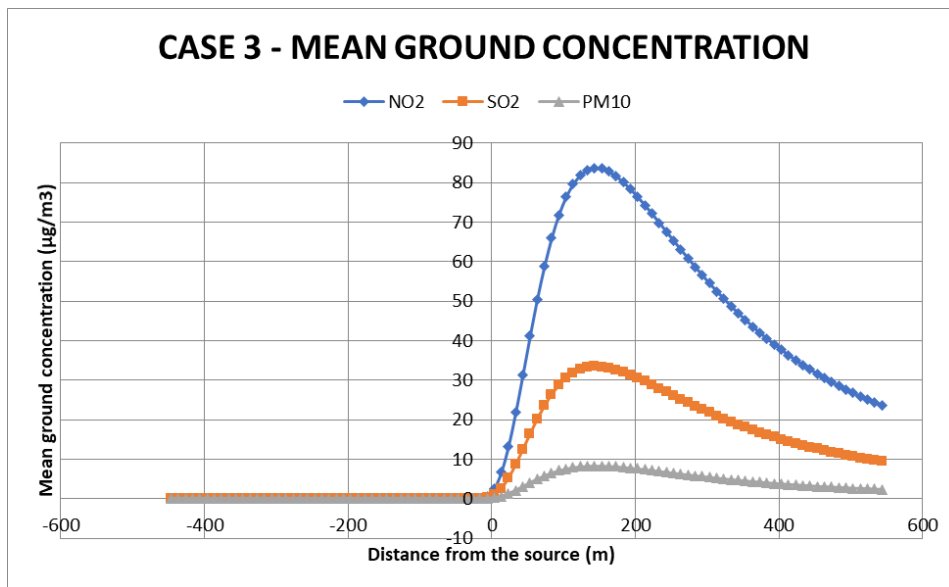
(G)



(H)

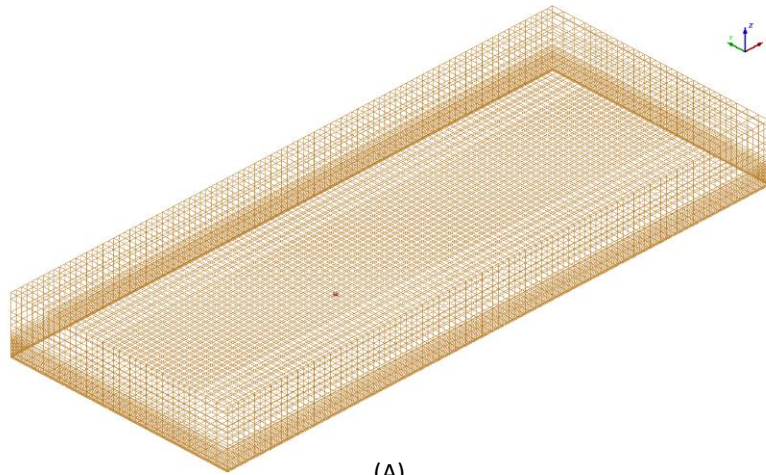


All Cycle = 3231



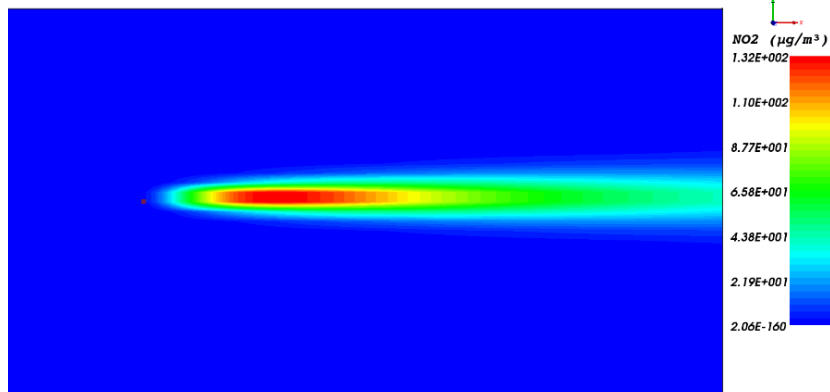
(K)

CASE 4



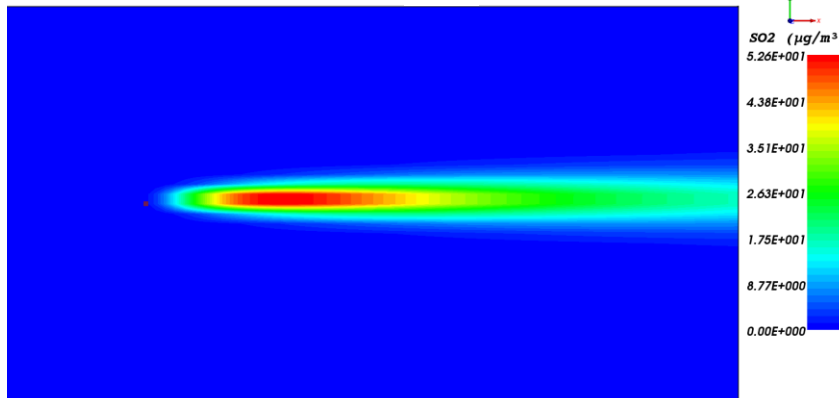
At Cycle = 0740

(A)

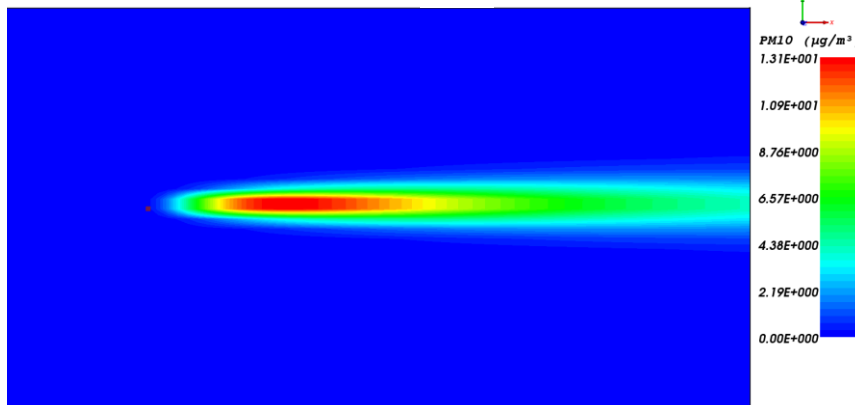


At Cycle = 3832

(B)

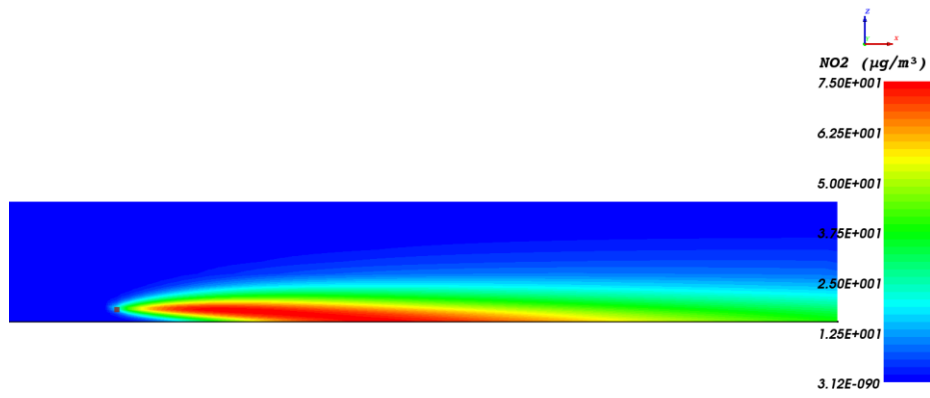


(C)

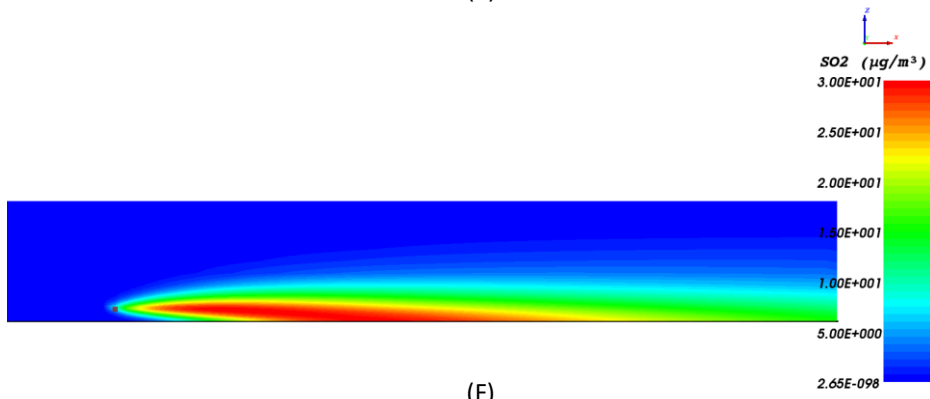


At Cycle = 3832

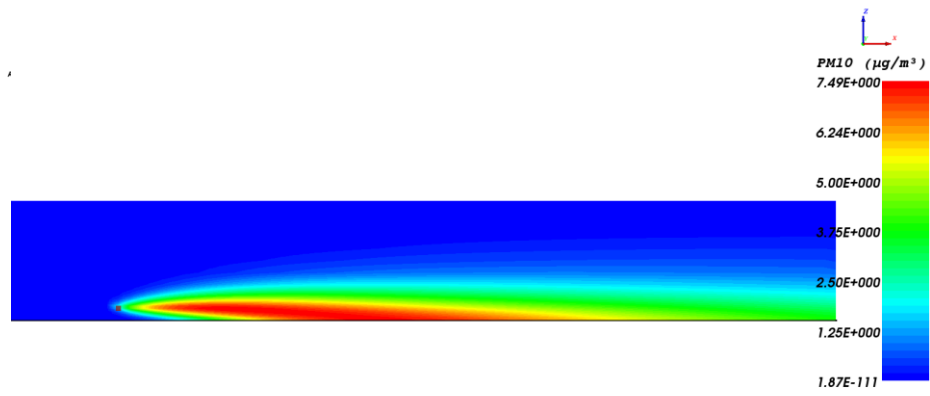
(D)



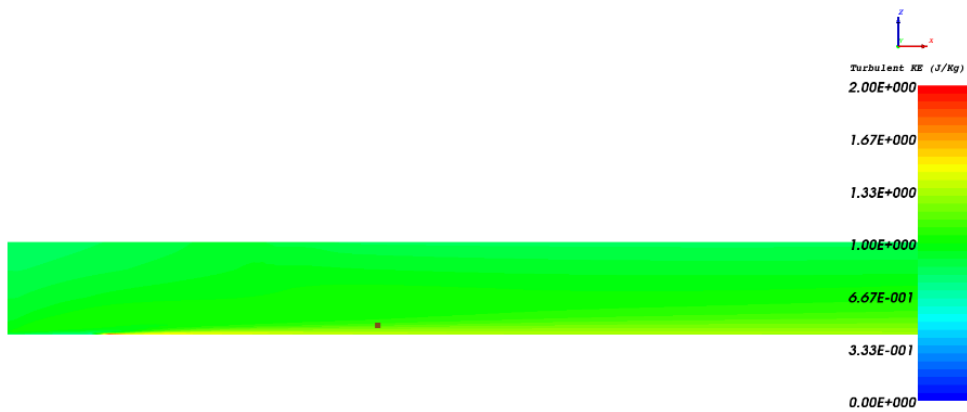
(E)



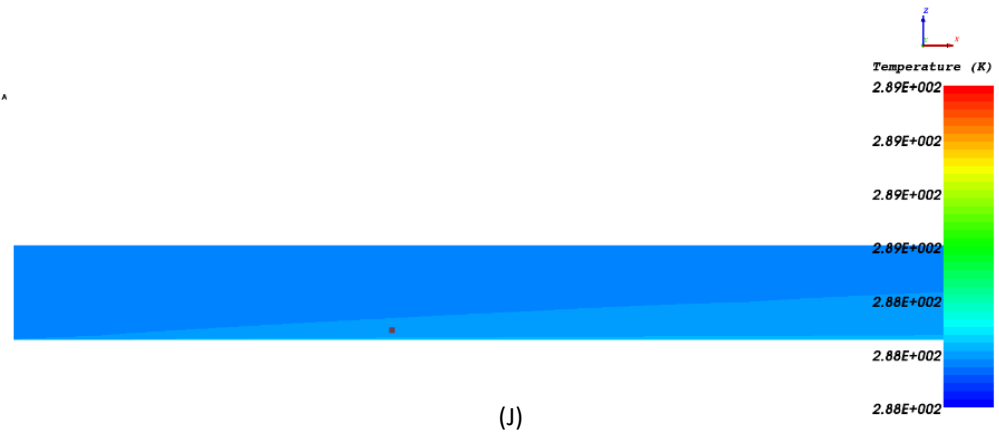
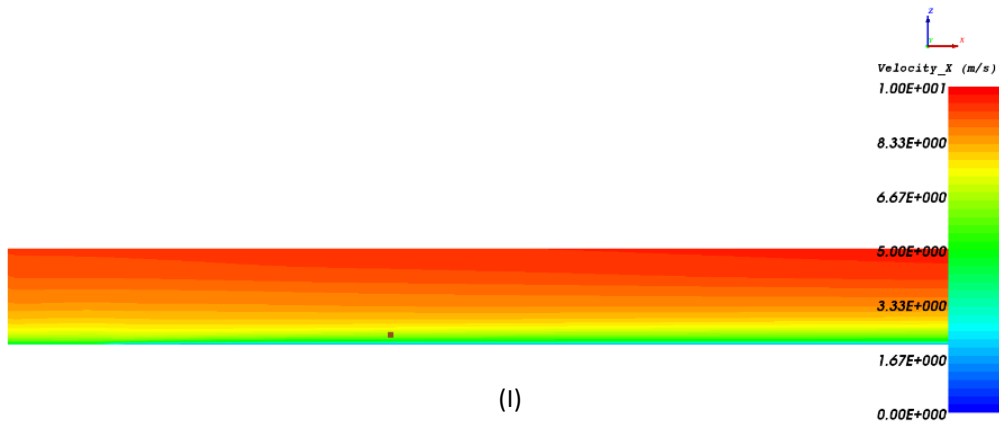
(F)



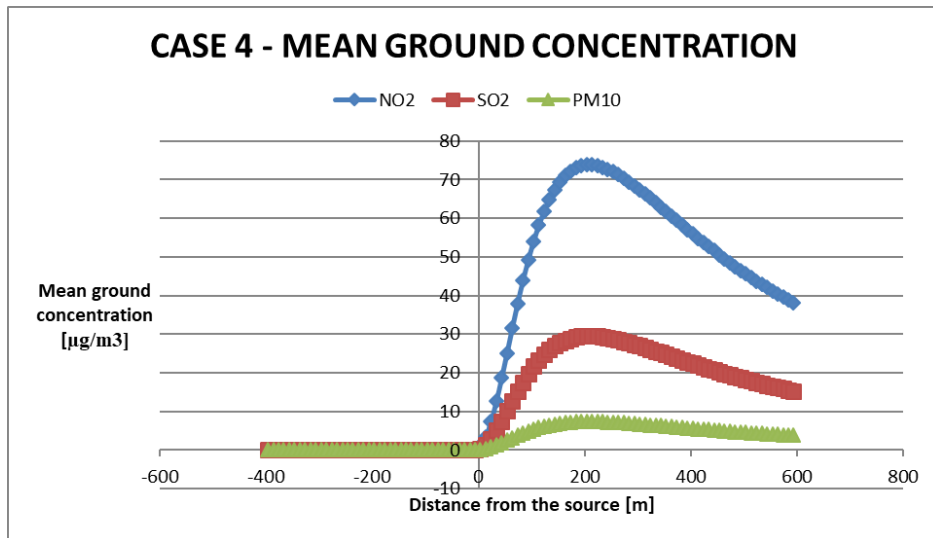
(G)



(H)



AI Cycle = 3532

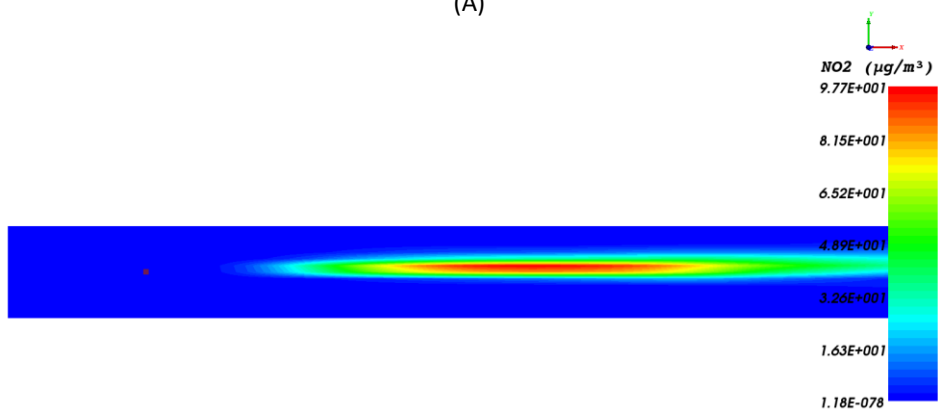


(K)

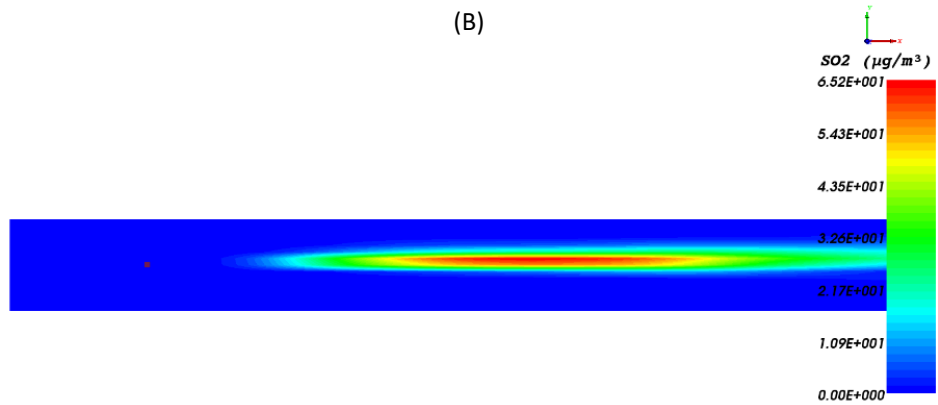
CASE 5



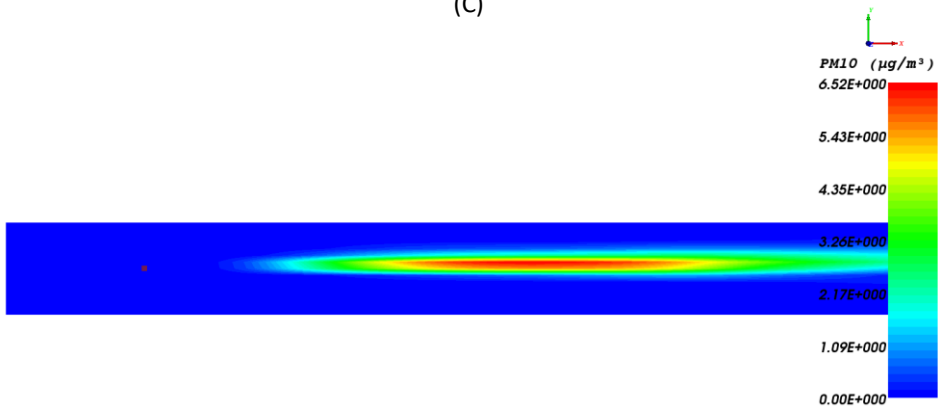
(A)



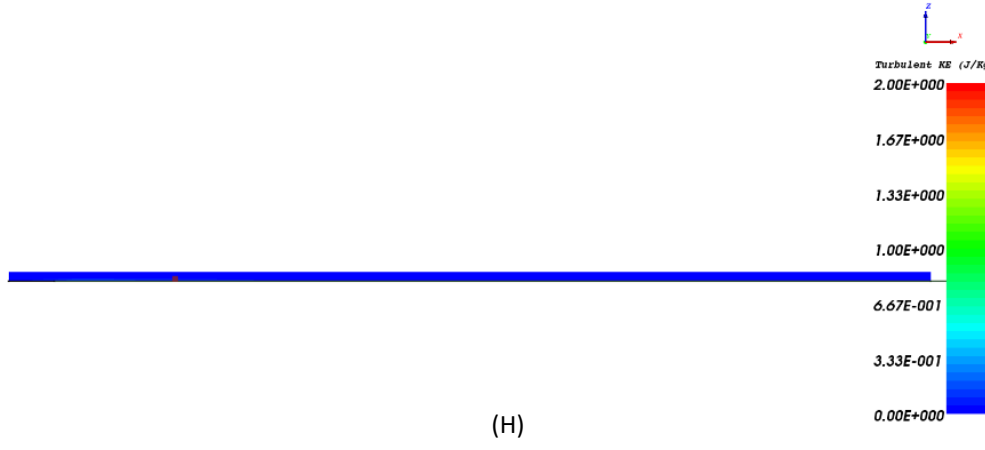
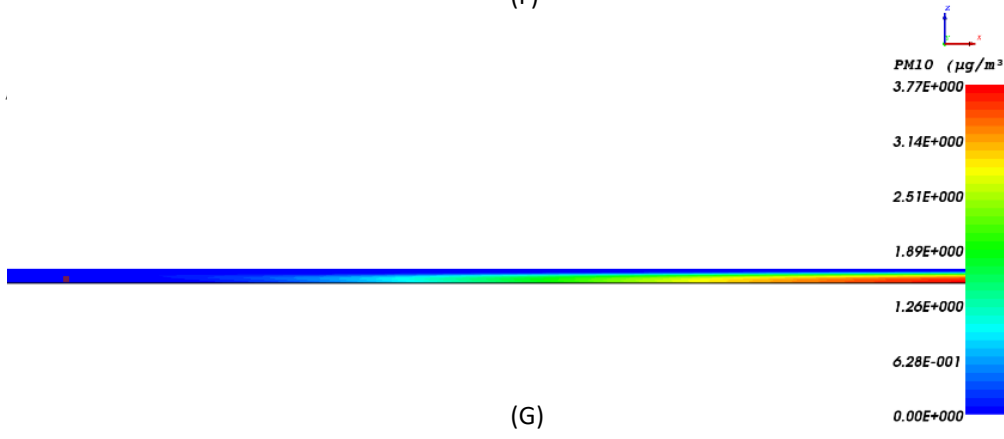
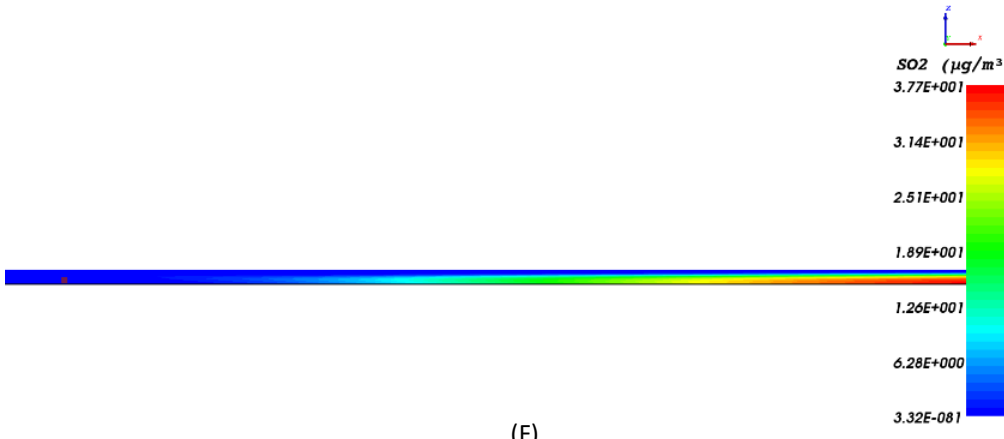
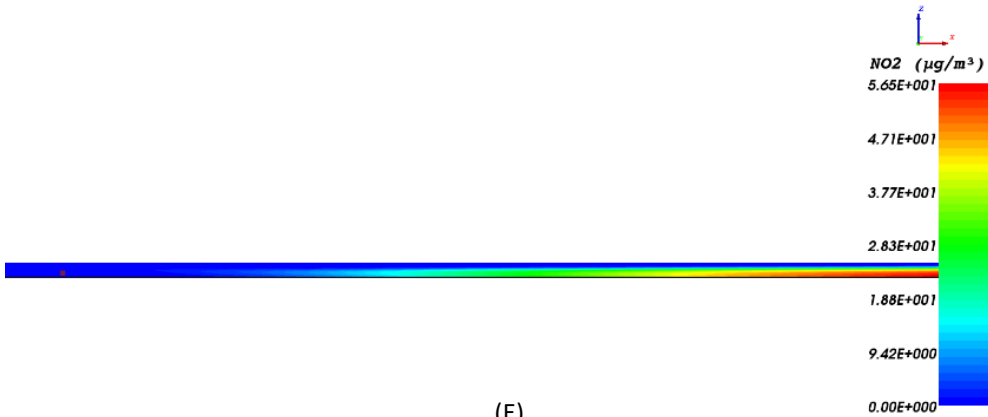
(B)

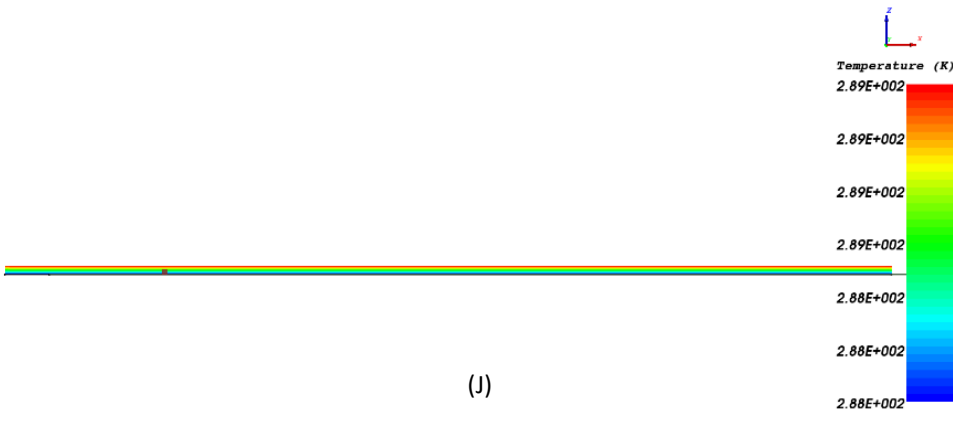
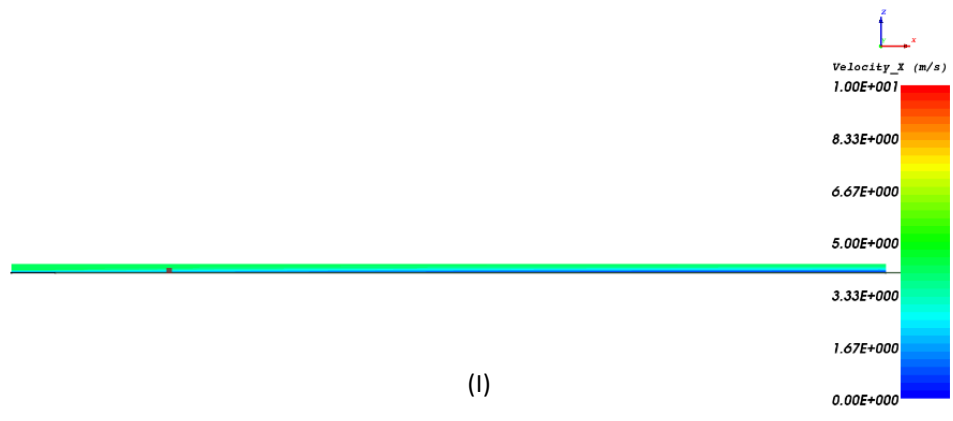


(C)

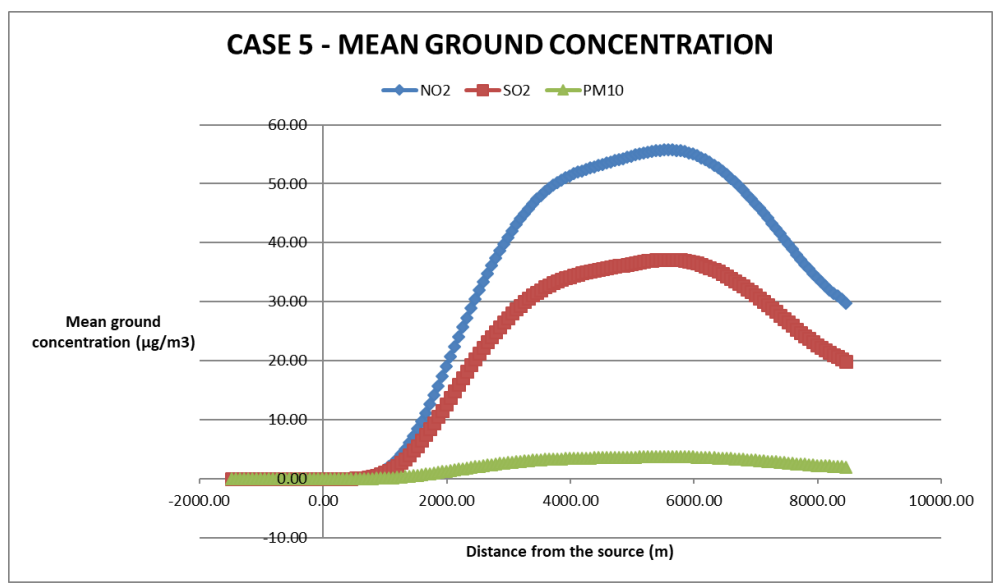


(D)



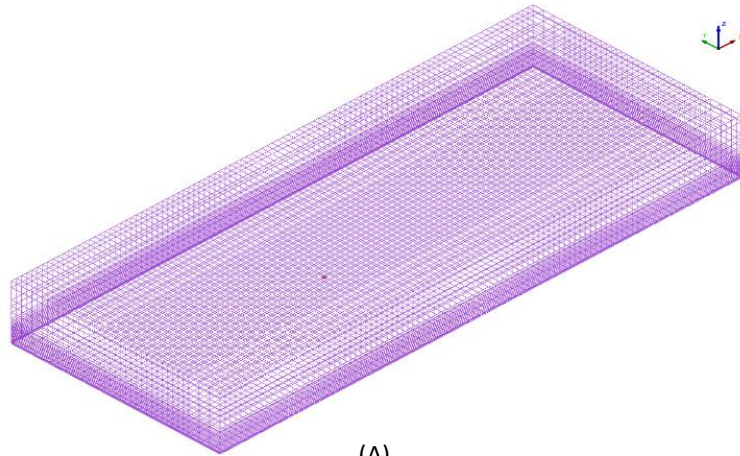


At Cycle = 478



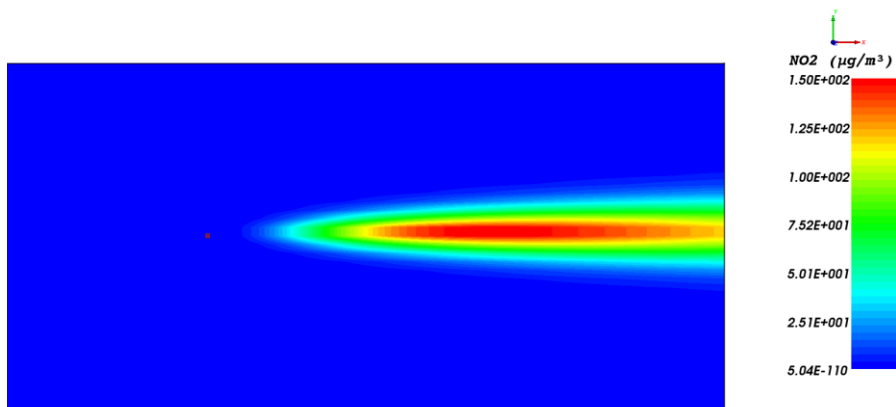
(K)

CASE 6

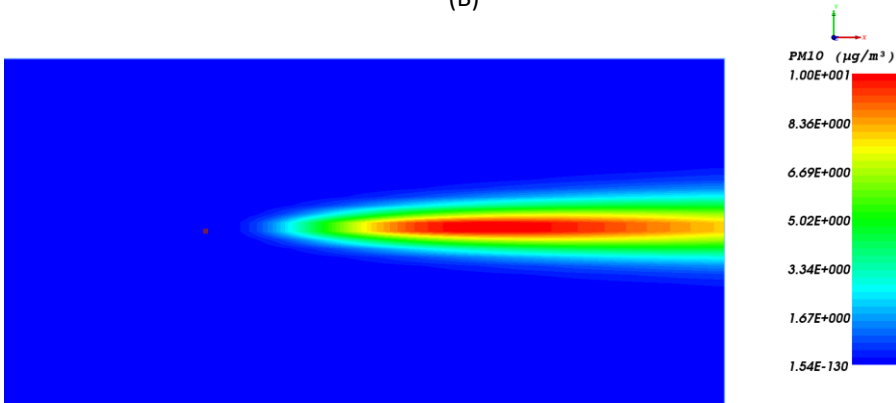


At Cycle = 3844

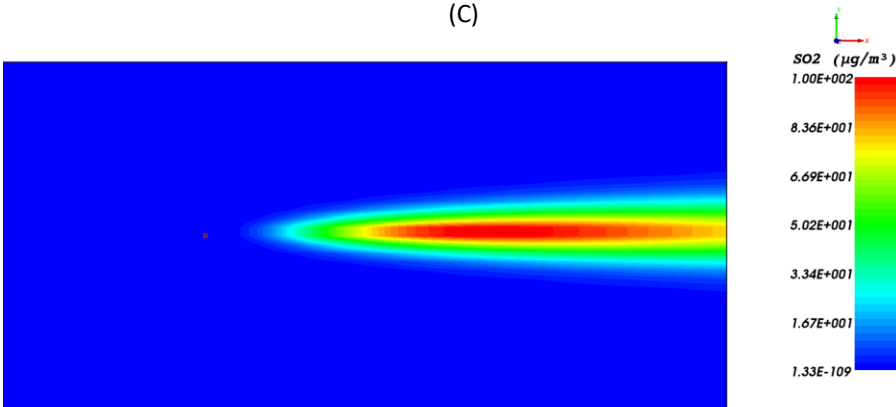
(A)



(B)

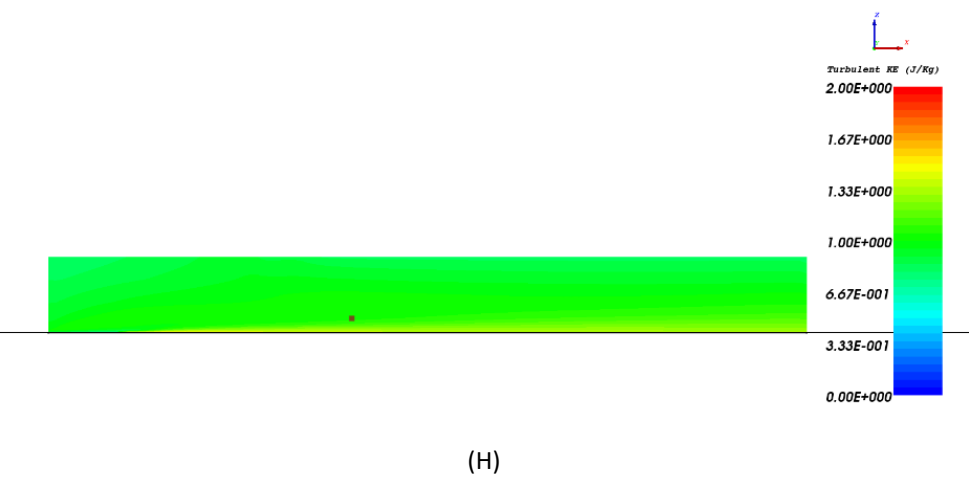
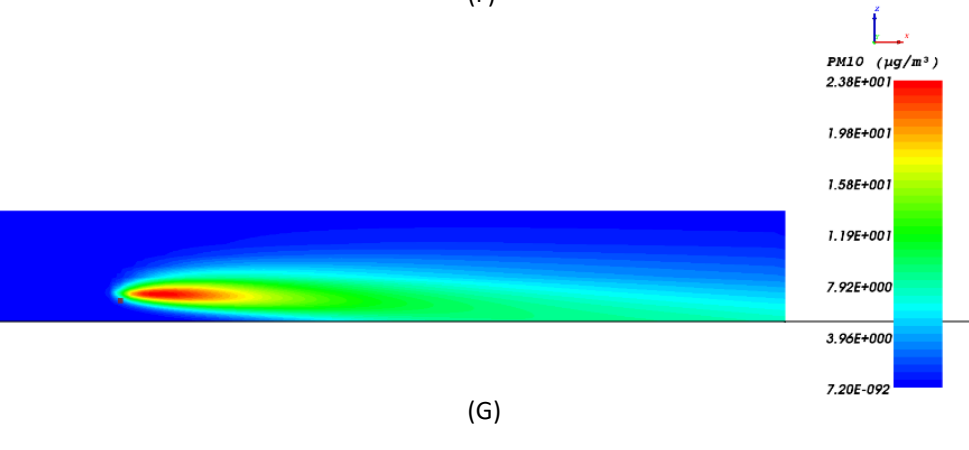
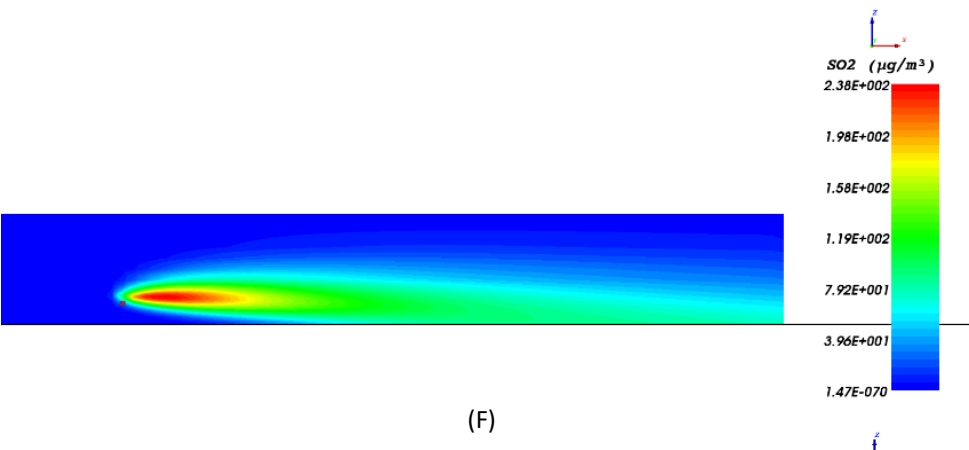
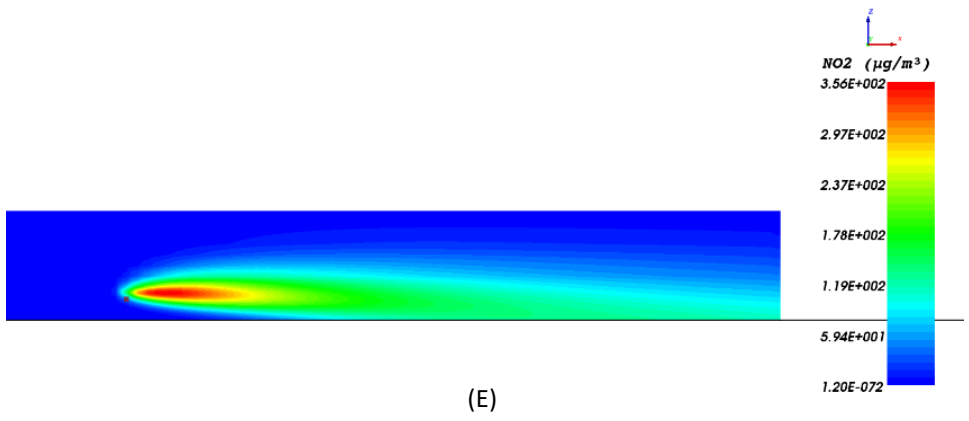


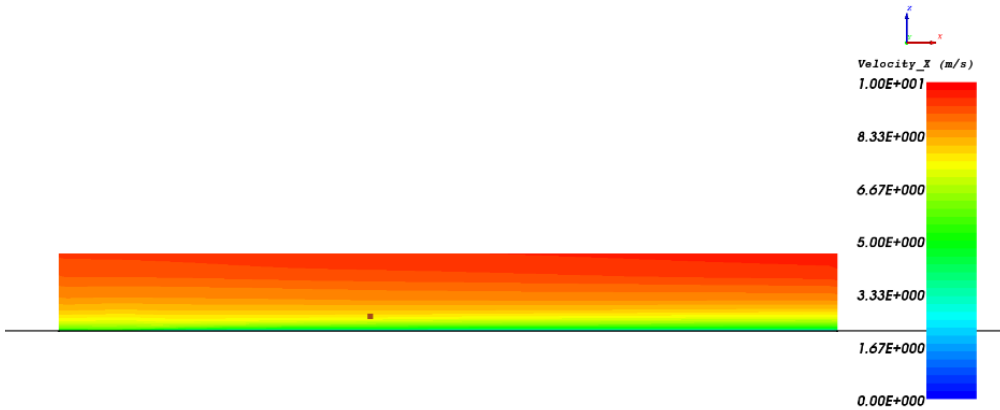
(C)



(D)

At Cycle = 3844



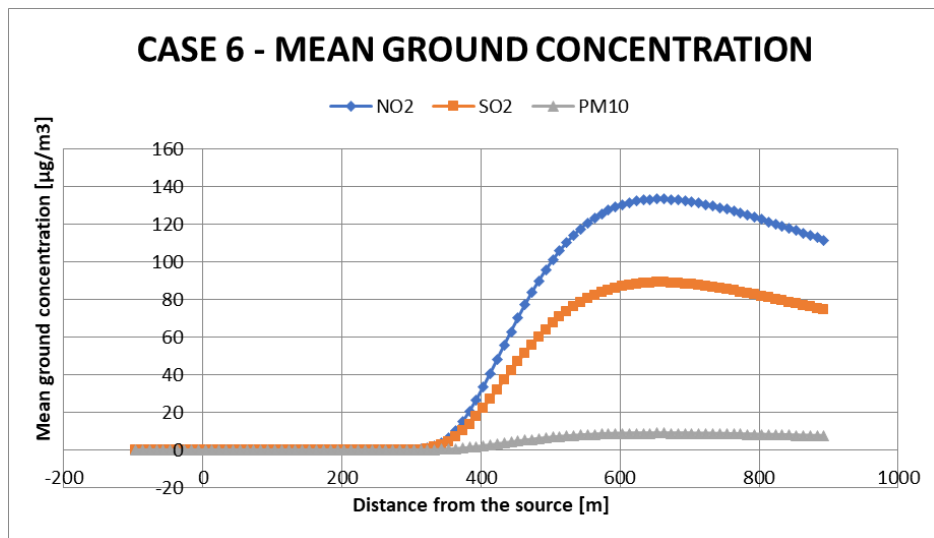


(I)



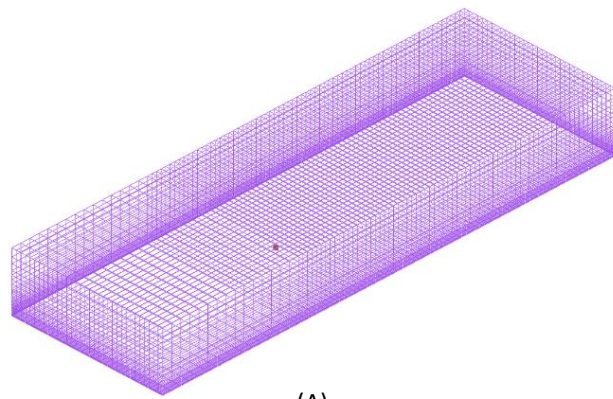
(J)

All Cycle = 3844

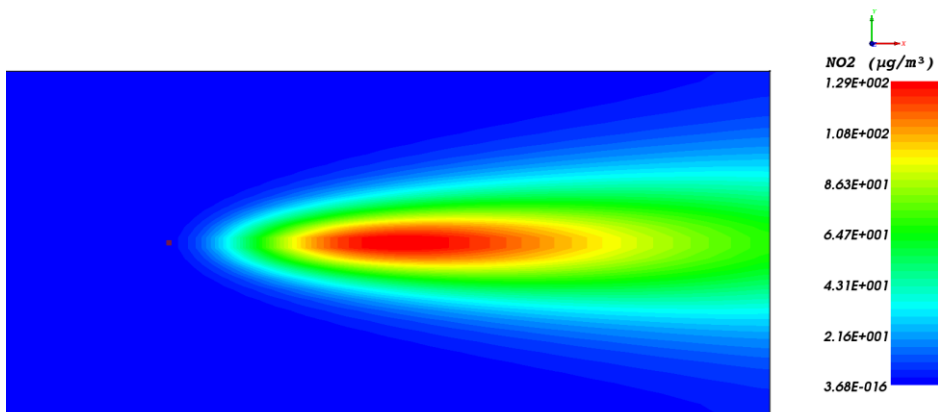


(K)

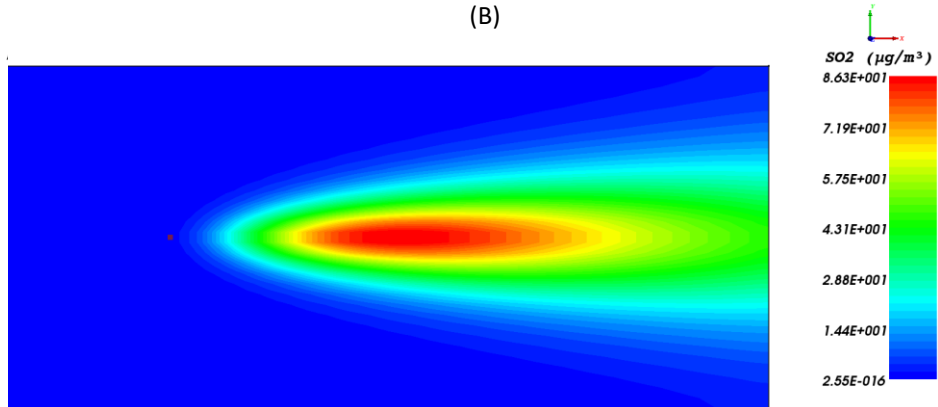
CASE 7



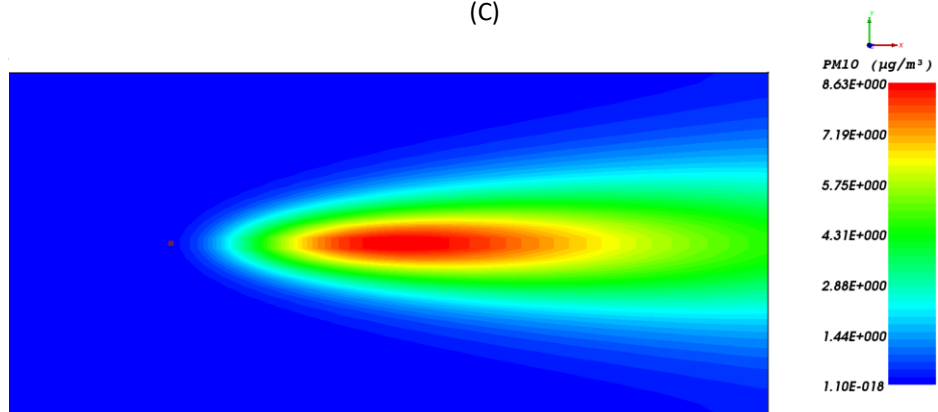
(A)



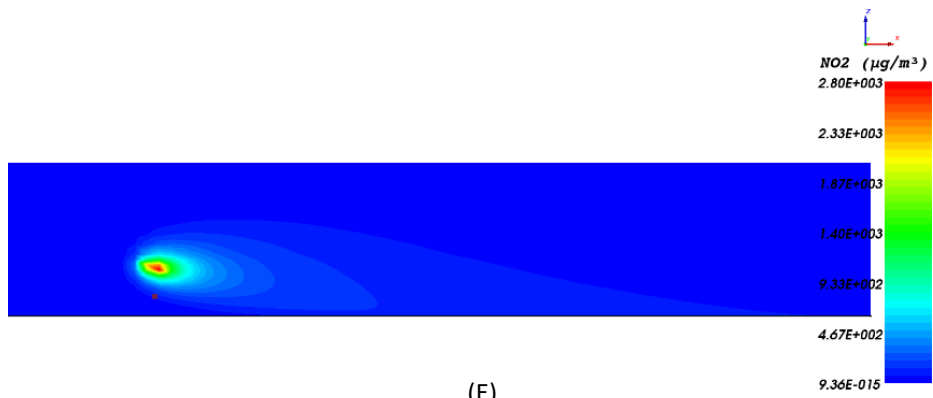
(B)



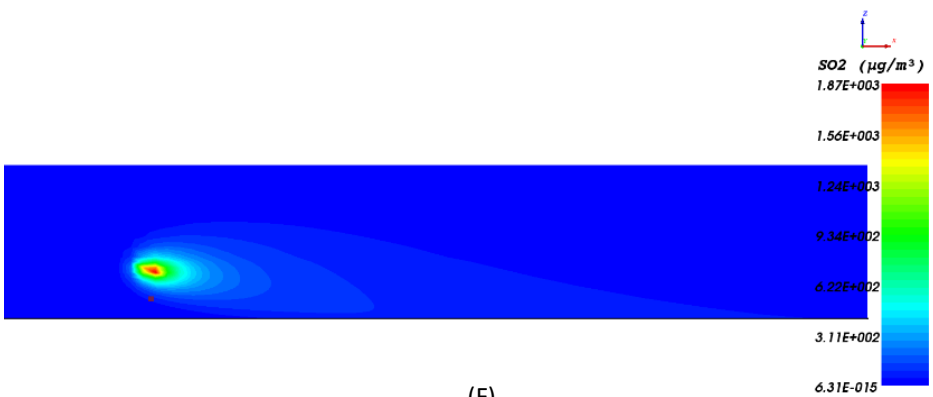
(C)



(D)



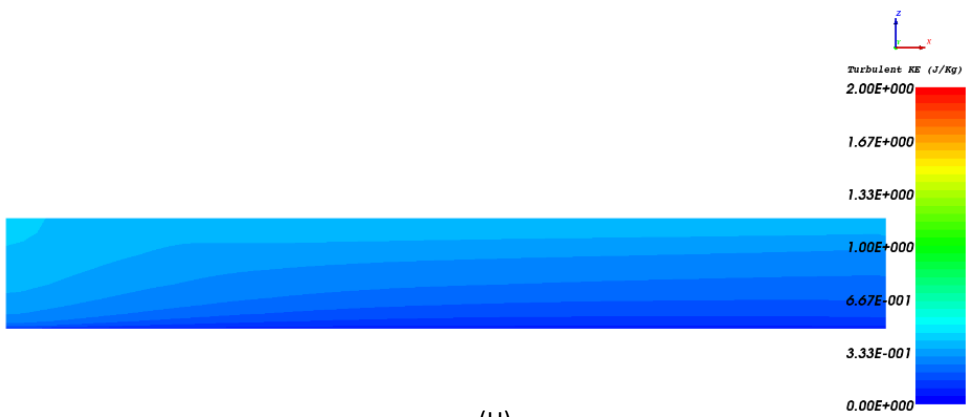
(E)



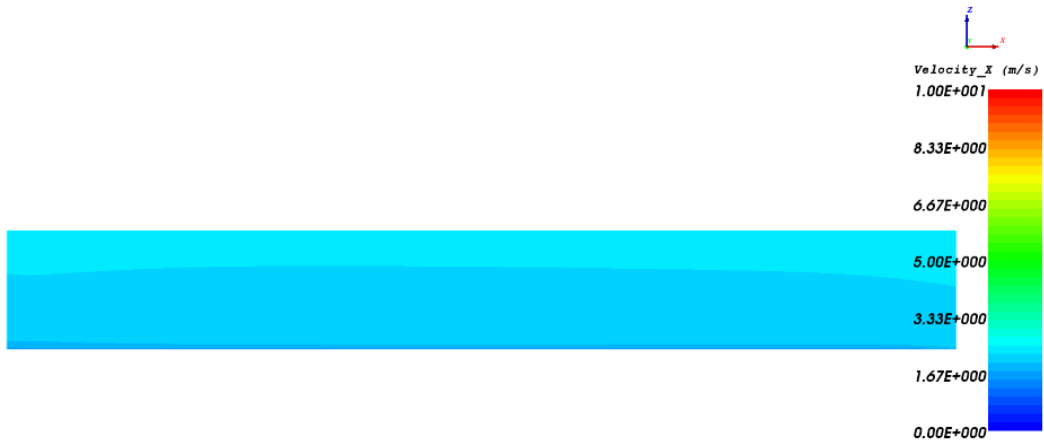
(F)



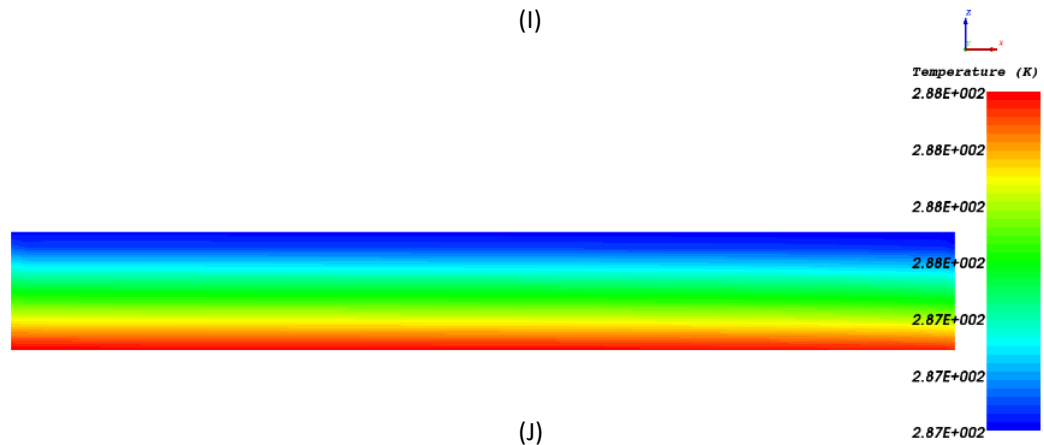
(G)



(H)

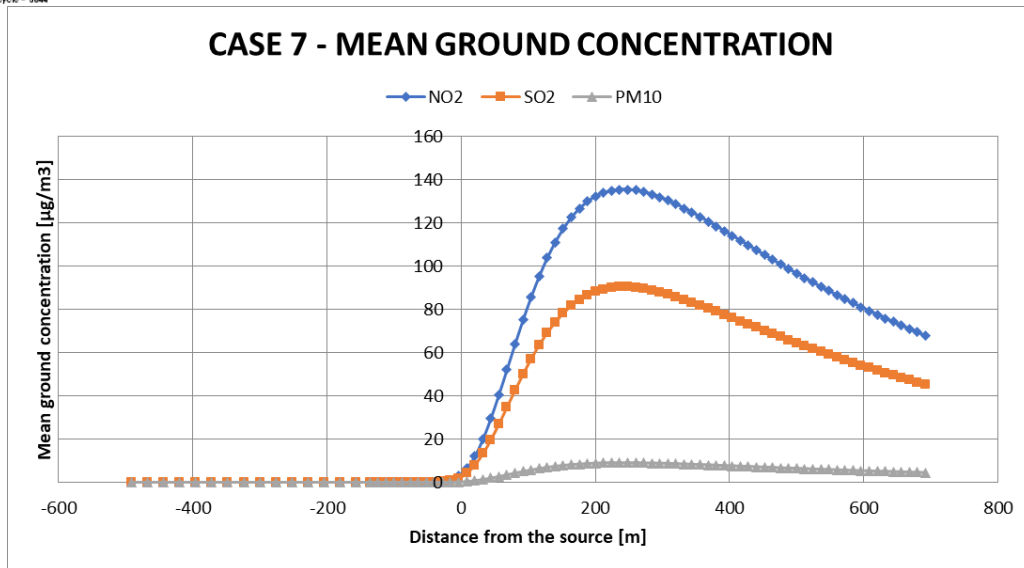


(I)



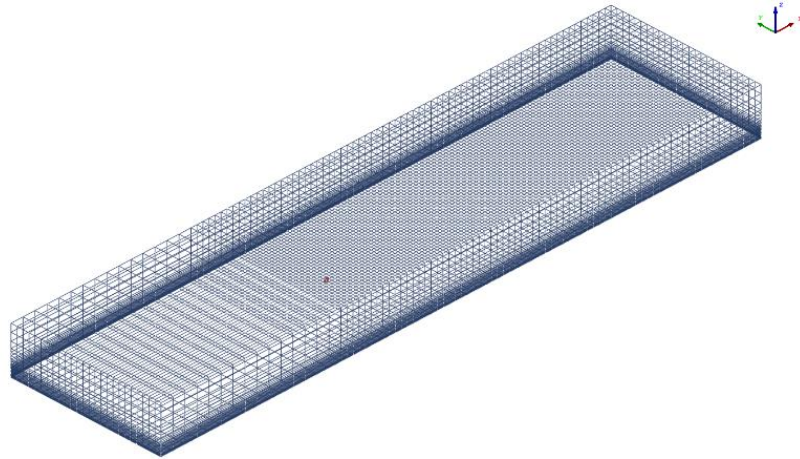
(J)

At Cycle = 3844



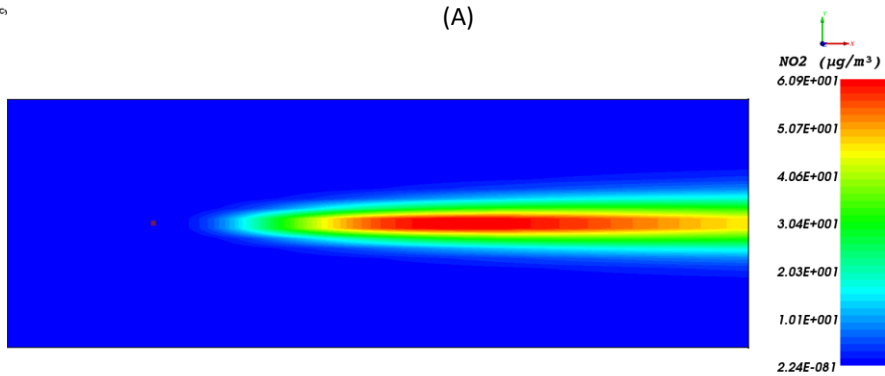
(K)

CASE 8

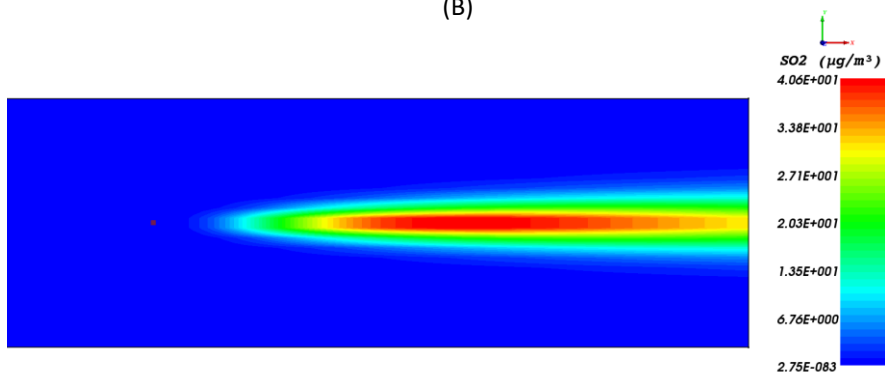


At 0

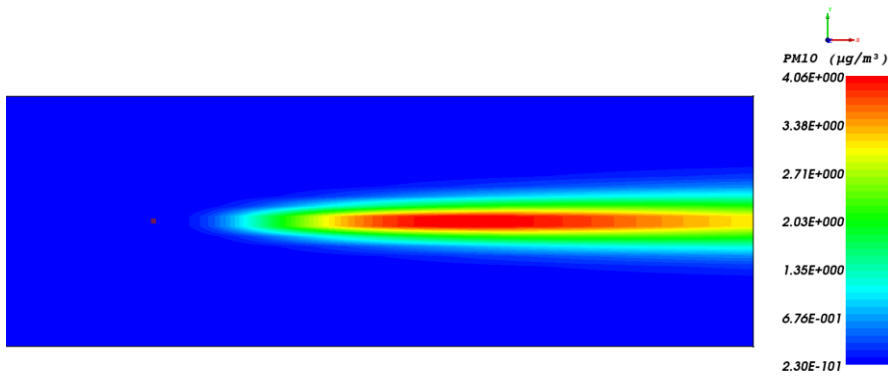
(A)



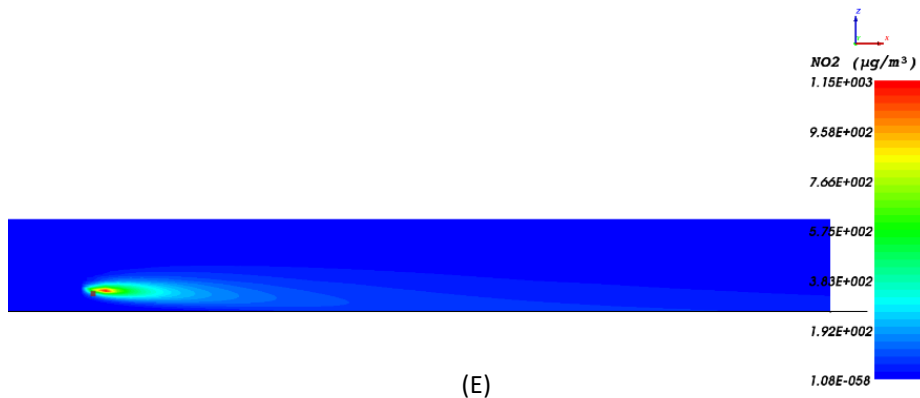
(B)



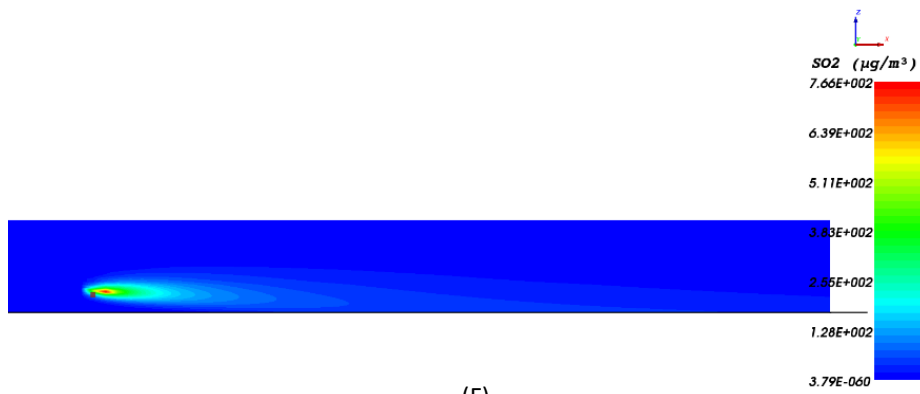
(C)



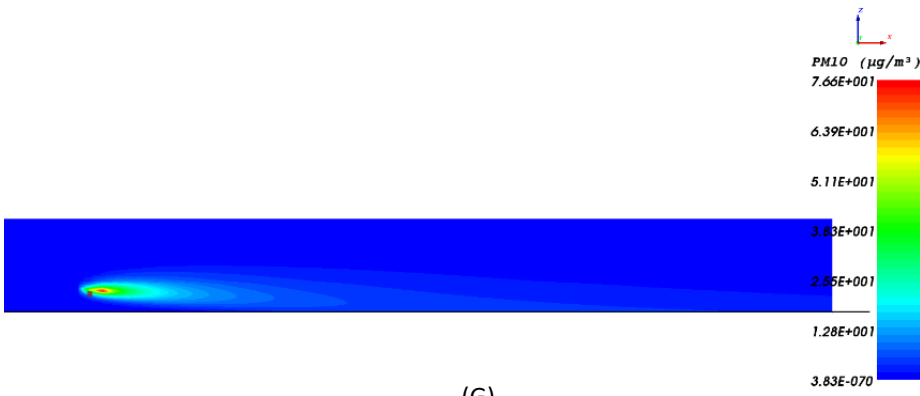
(D)



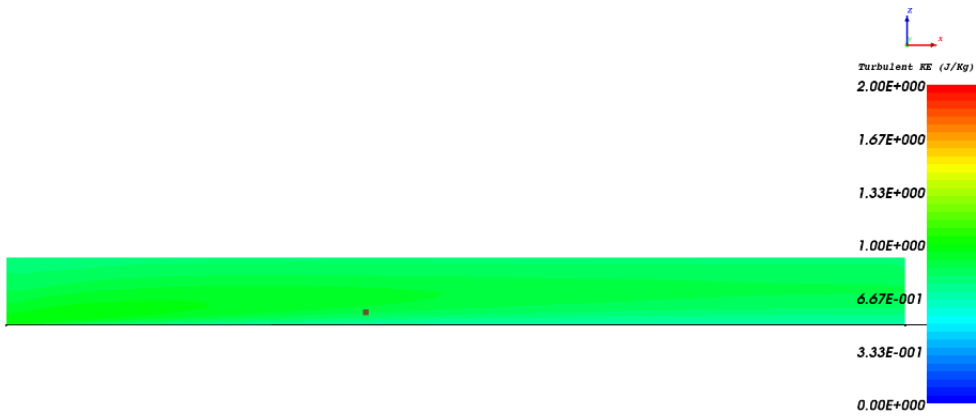
(E)



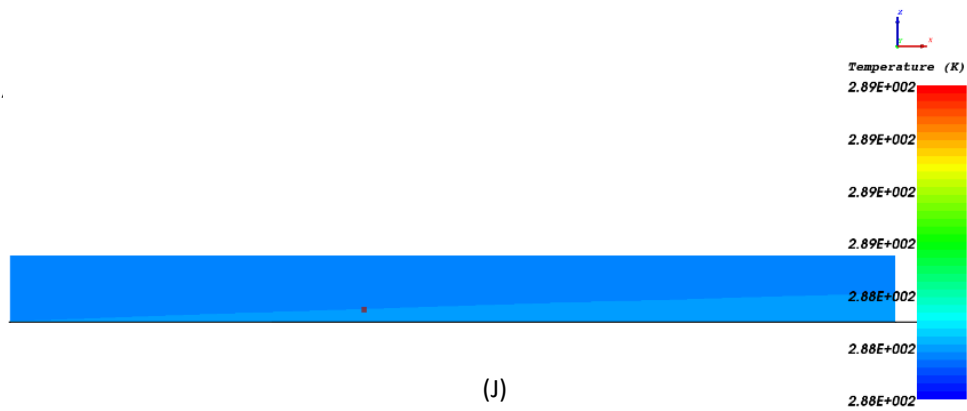
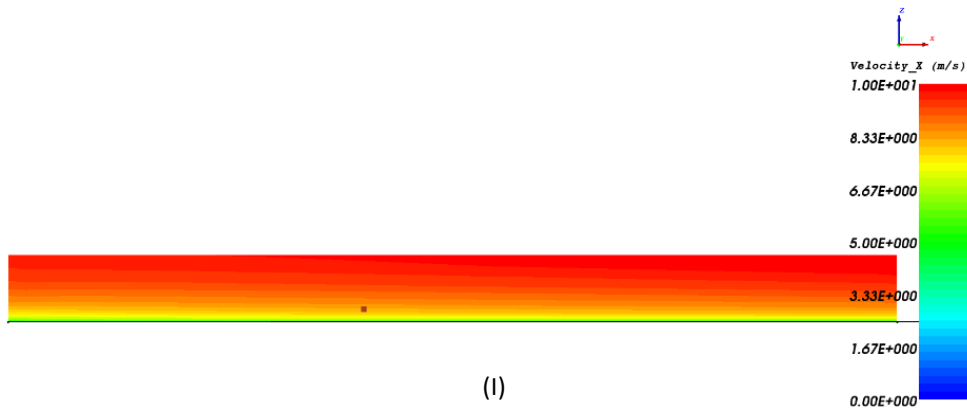
(F)



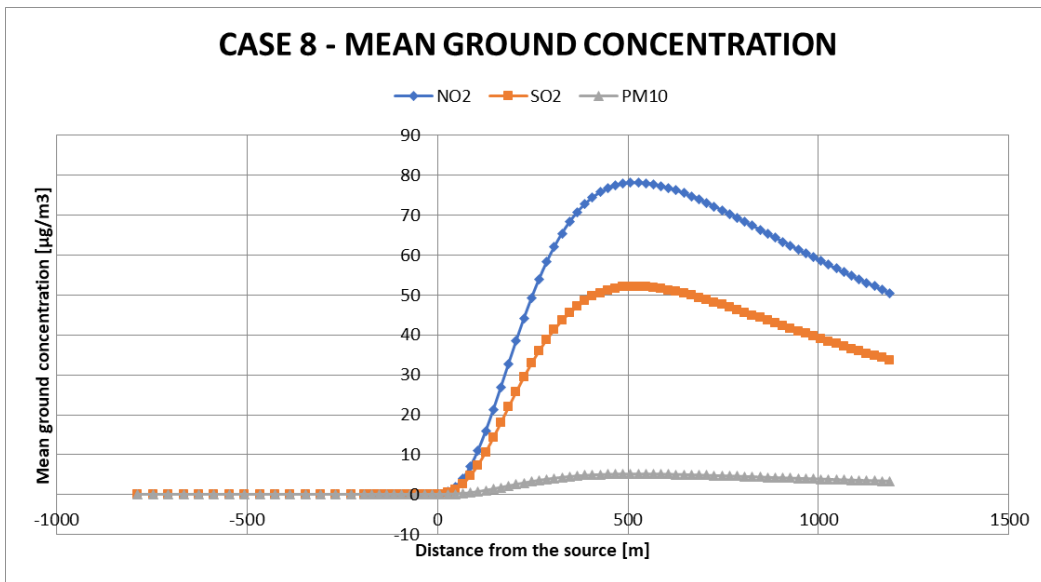
(G)



(H)

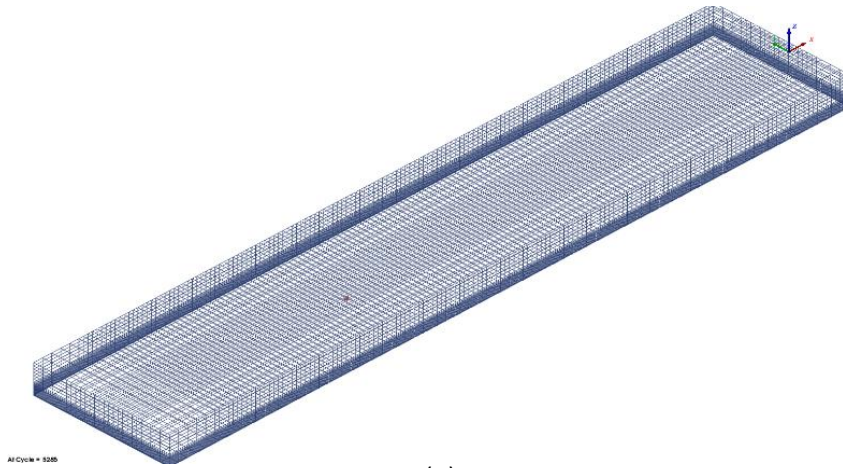


AI Cycle = 4073

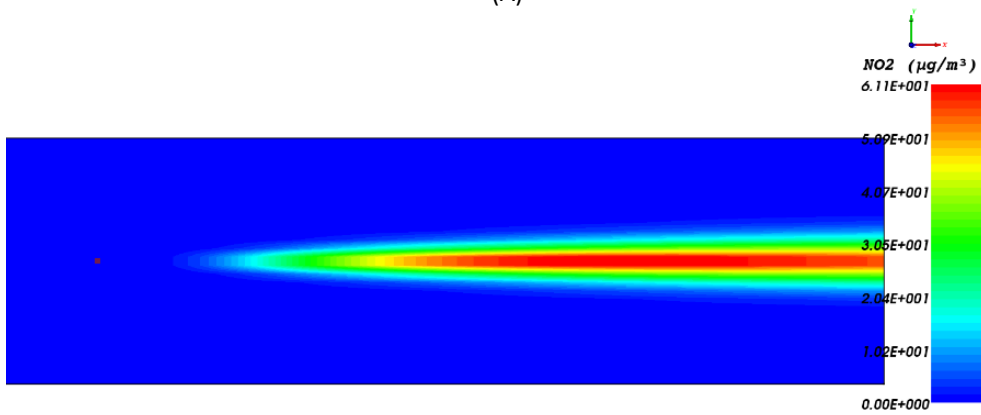


(K)

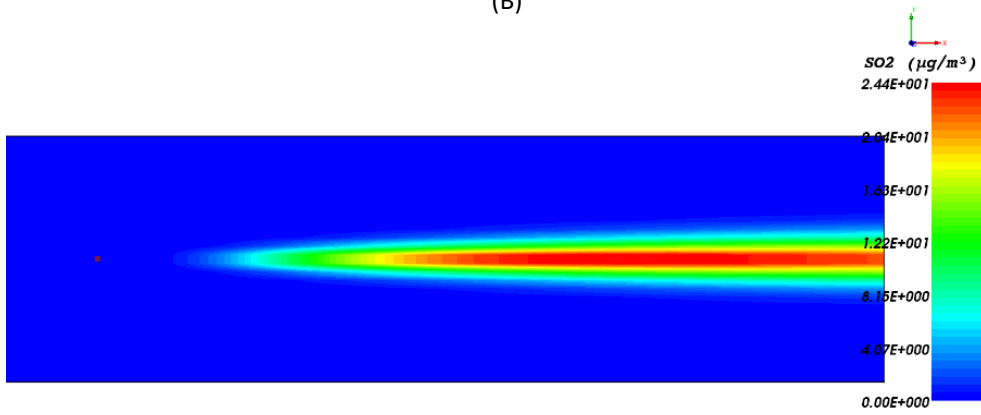
CASE 9



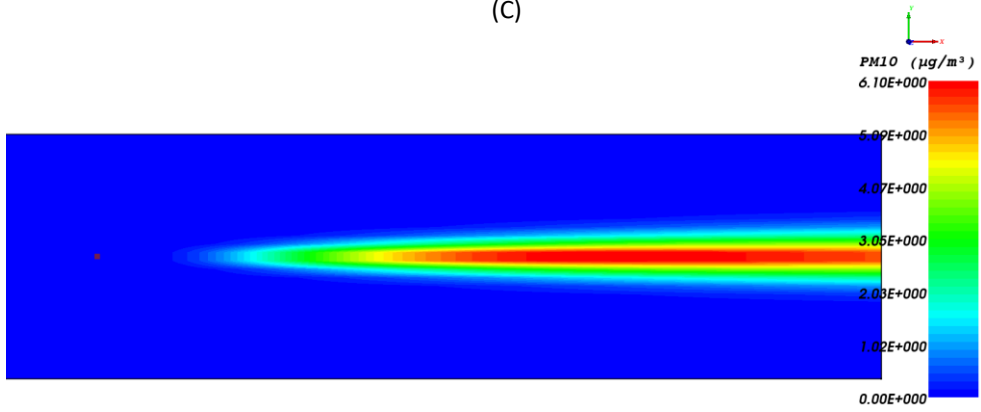
(A)



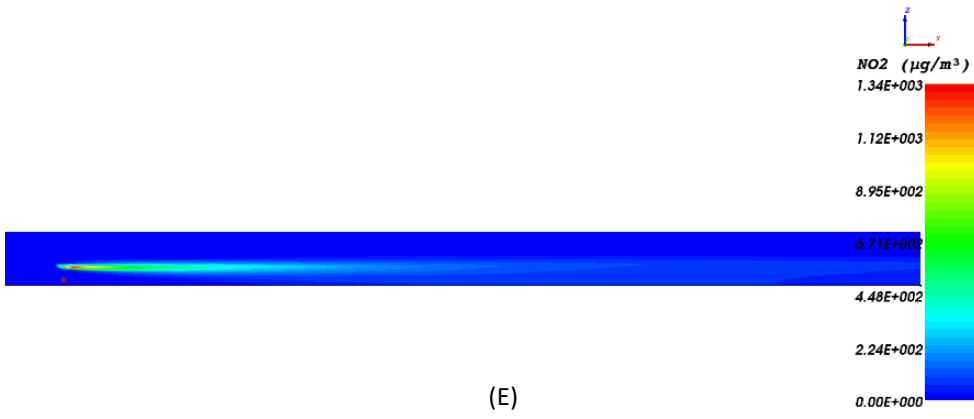
(B)



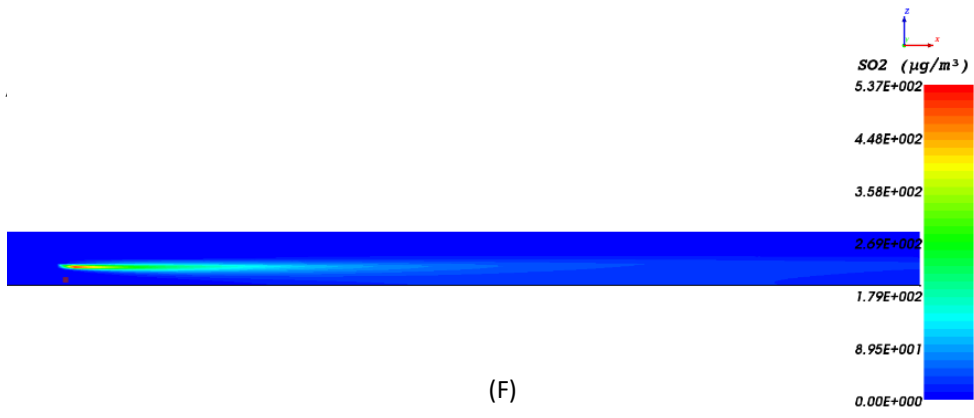
(C)



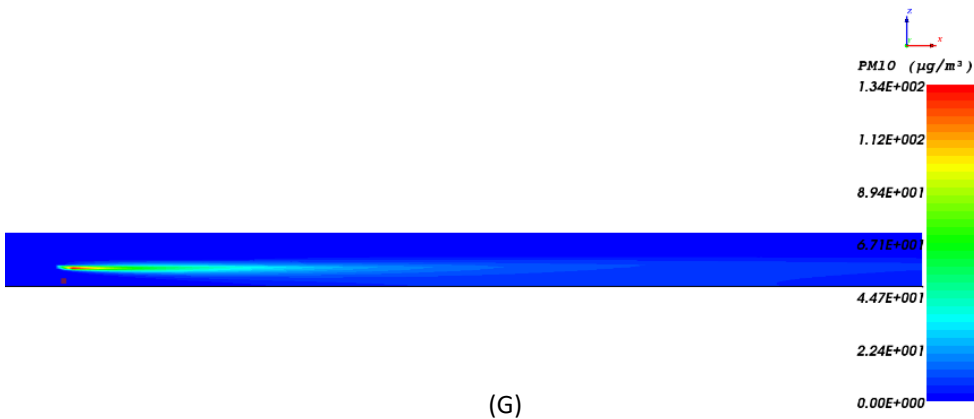
(D)



(E)



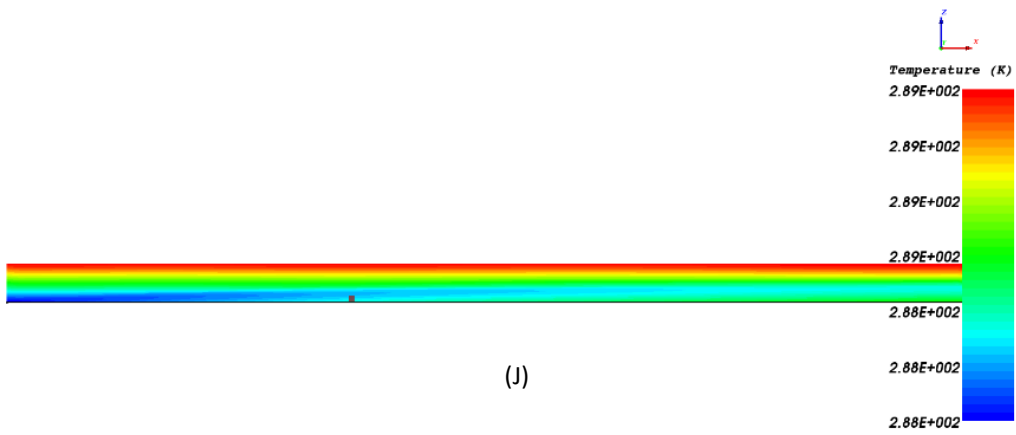
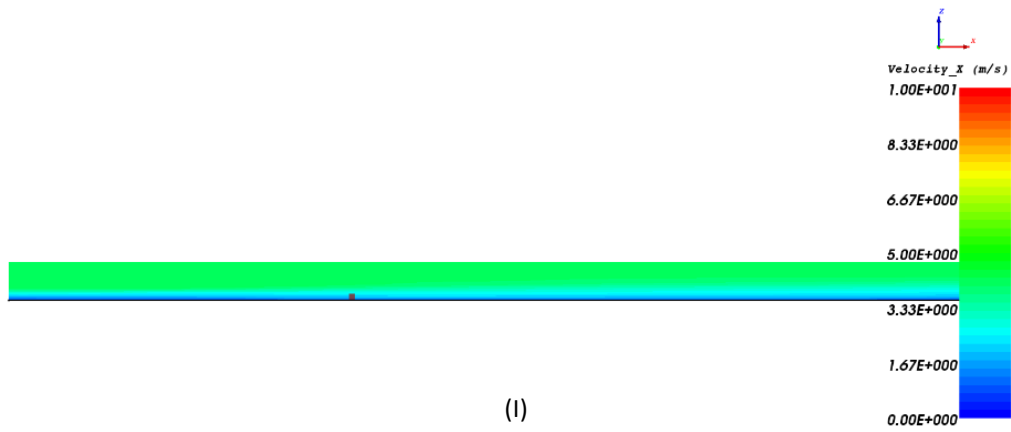
(F)



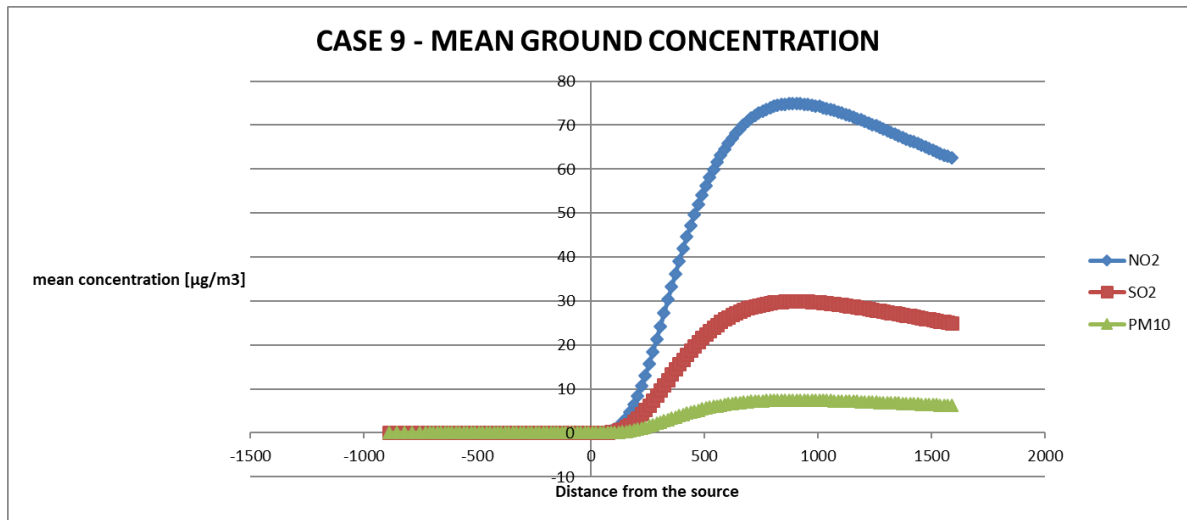
(G)



(H)

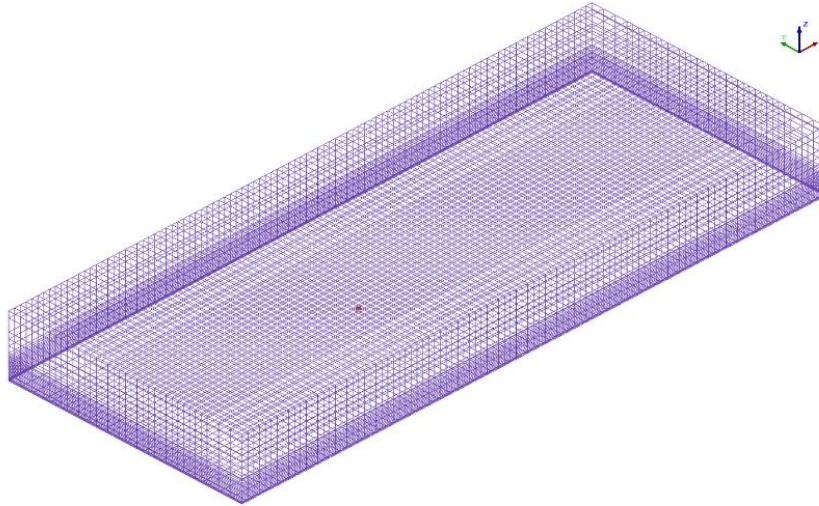


AtCycle = 5285



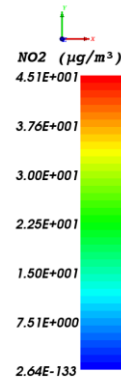
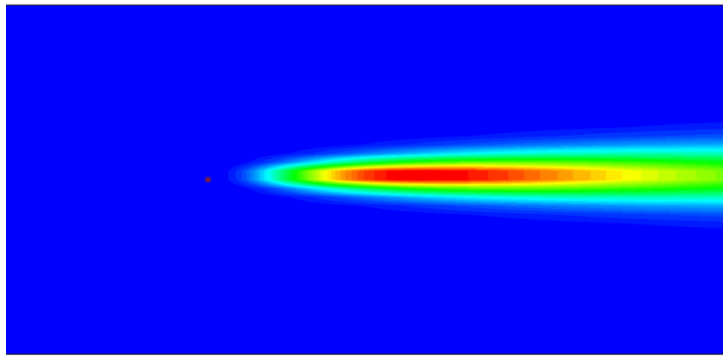
(K)

CASE 10

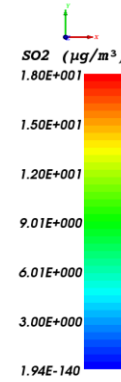
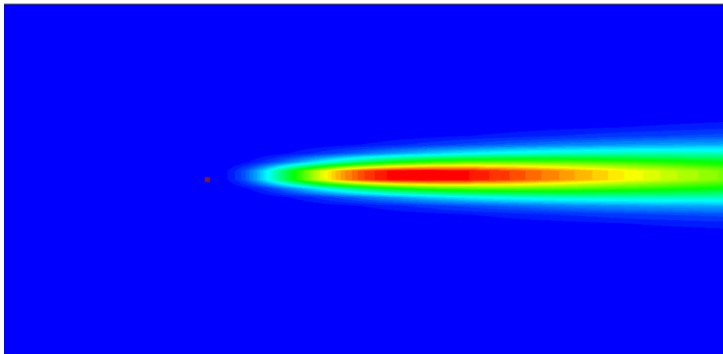


At Cycle = 3440

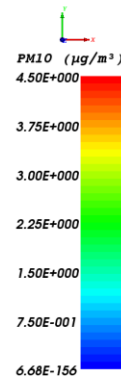
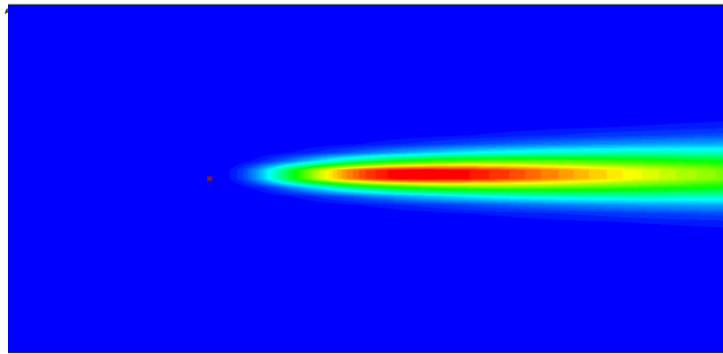
(A)



(B)

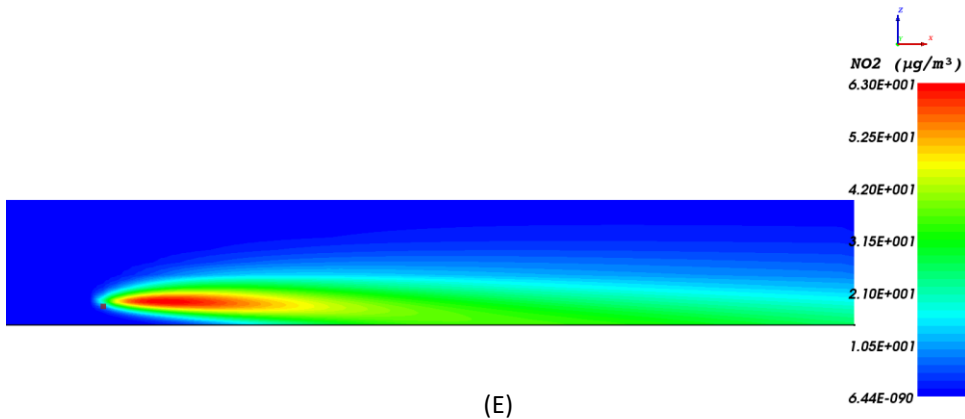


(C)

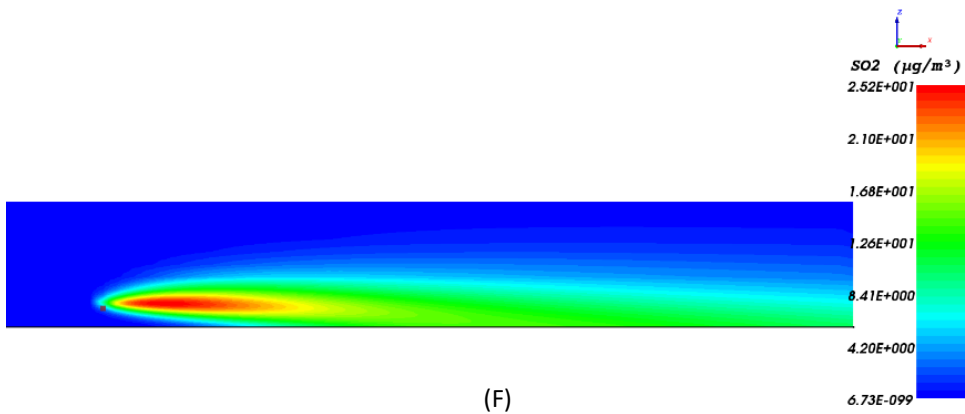


At Cycle = 3440

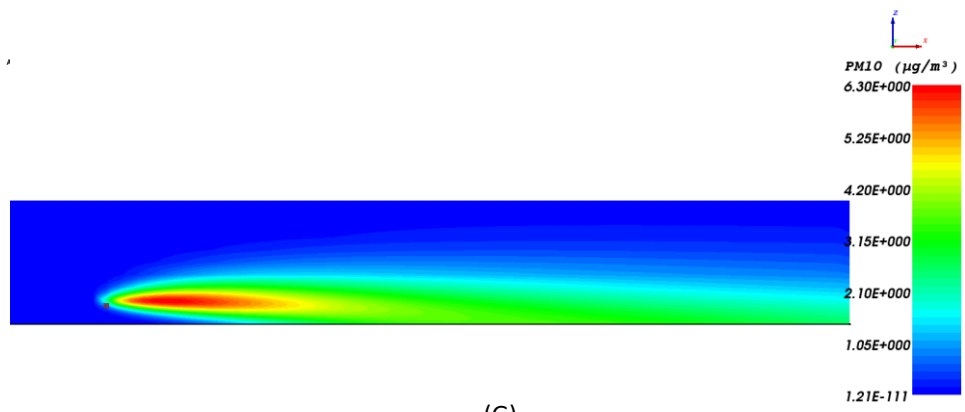
(D)



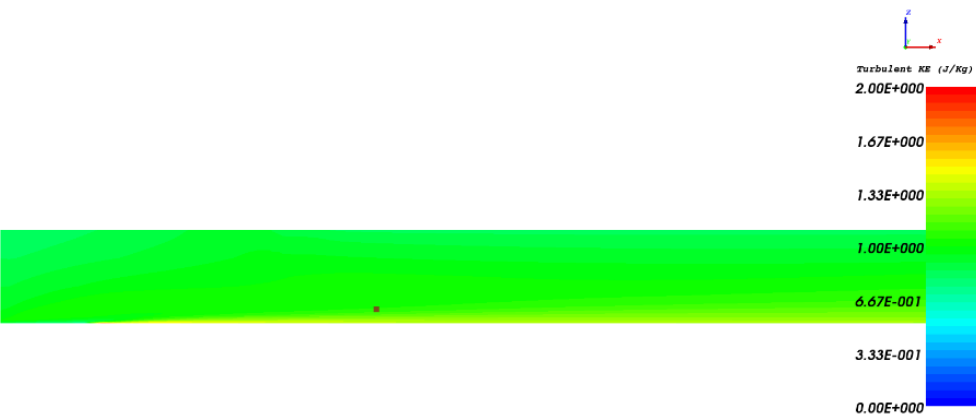
(E)



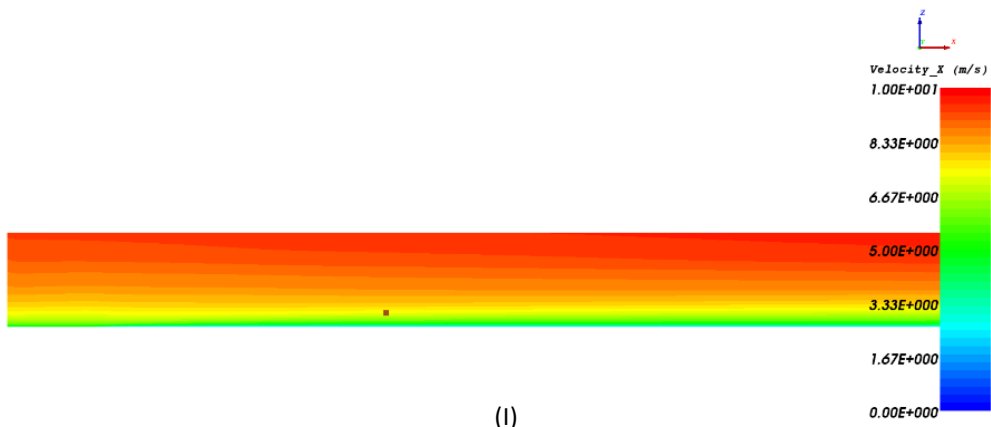
(F)



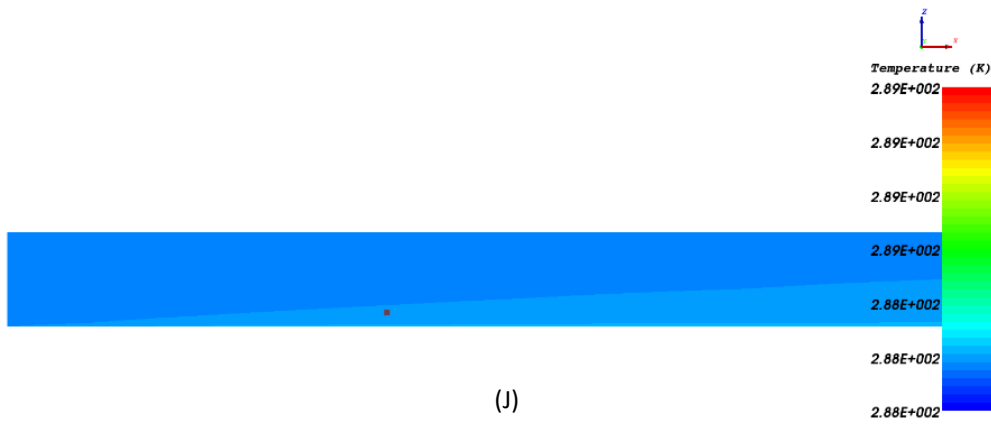
(G)



(H)

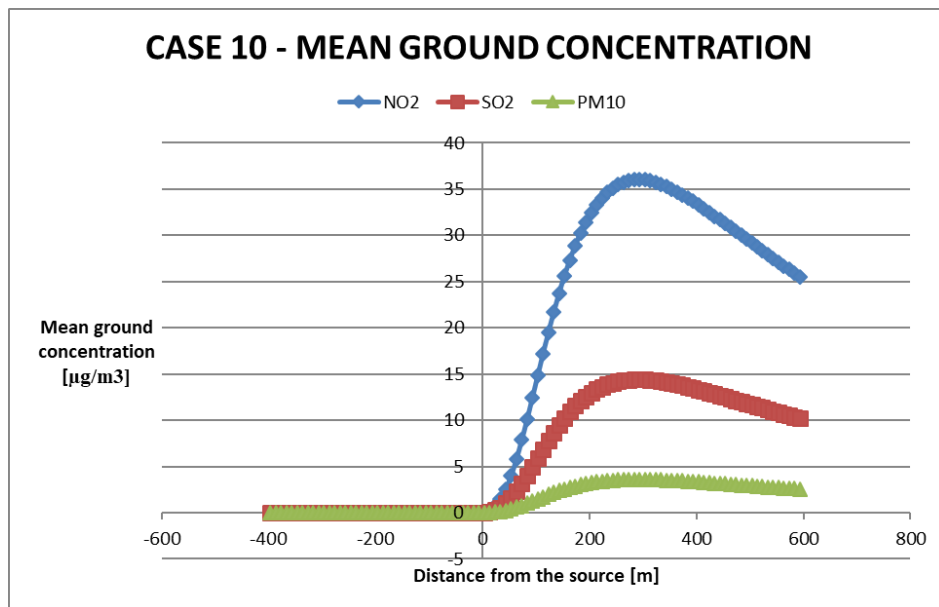


(I)



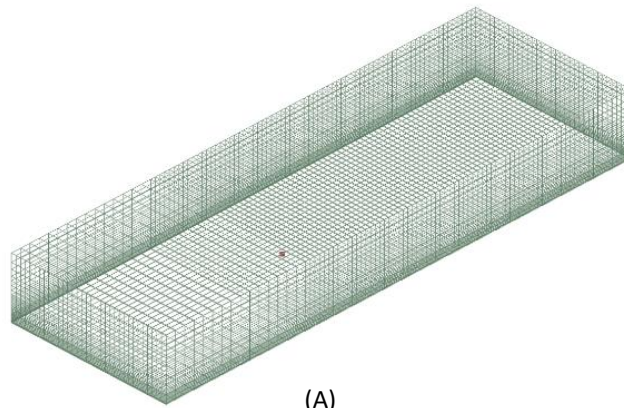
(J)

All Cycle = 3440

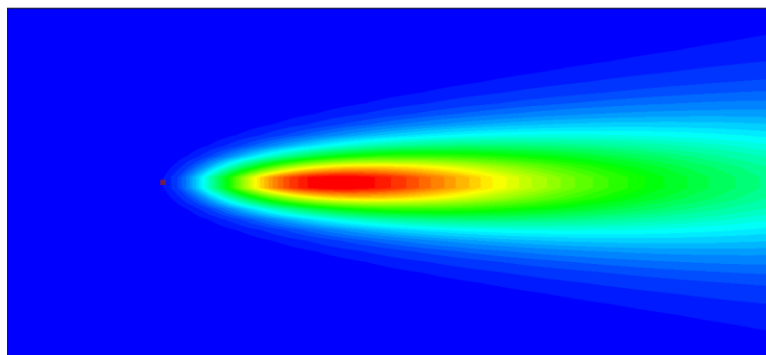


(K)

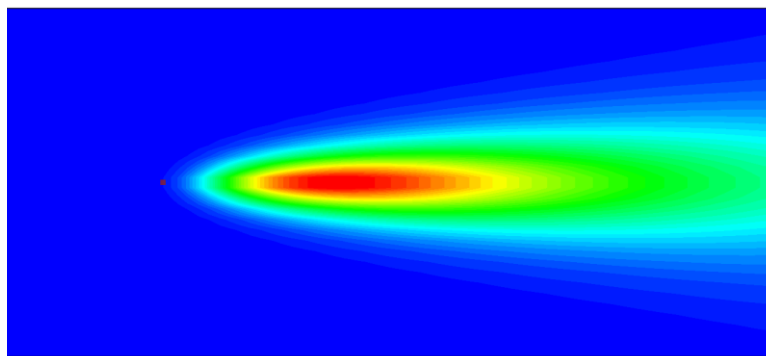
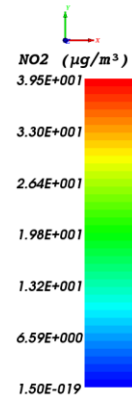
CASE 11



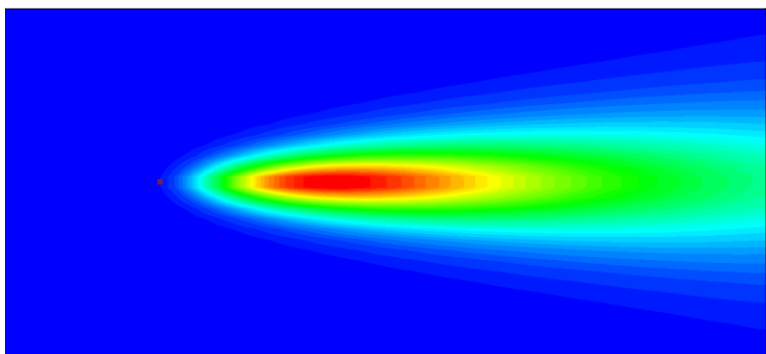
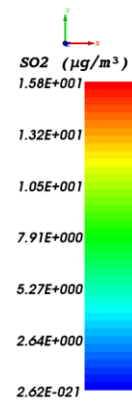
(A)



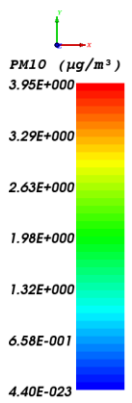
(B)

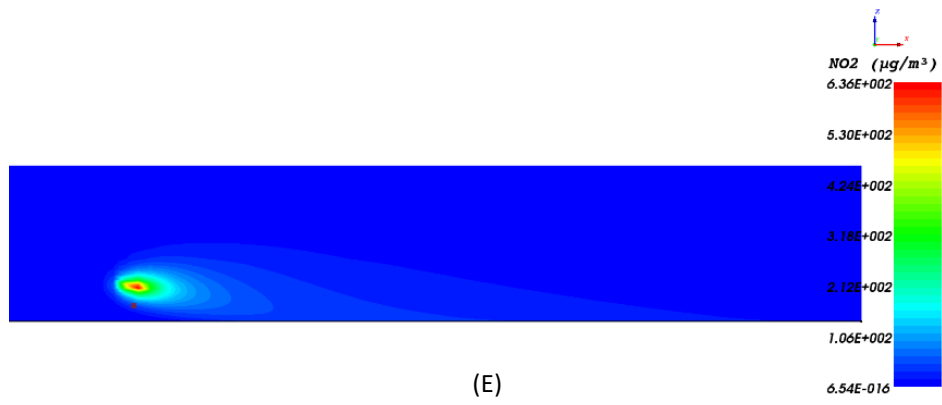


(C)

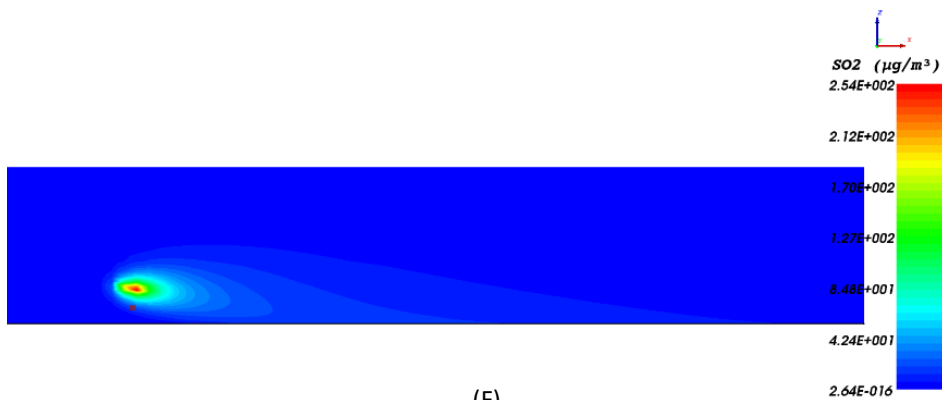


(D)

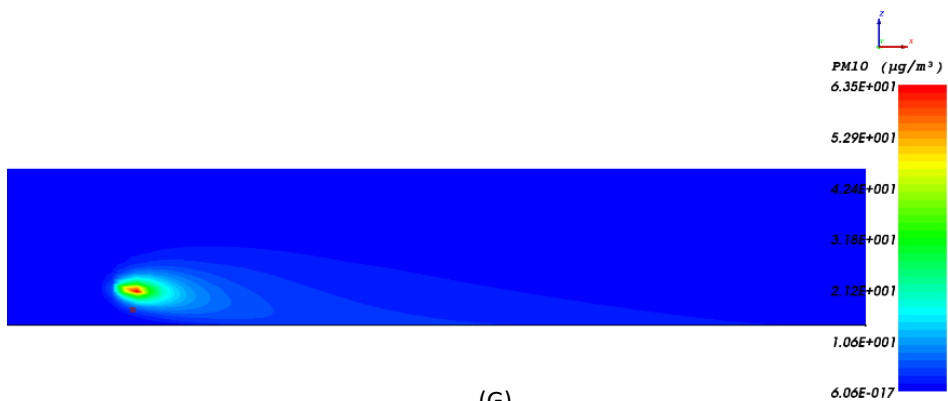




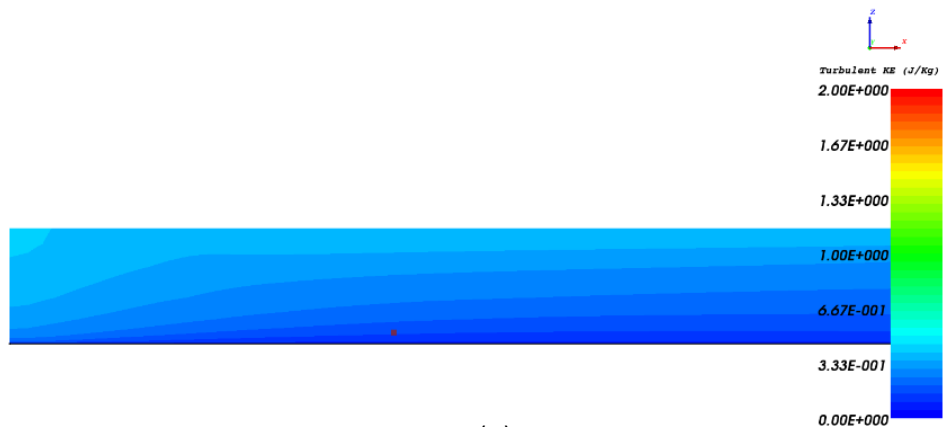
(E)



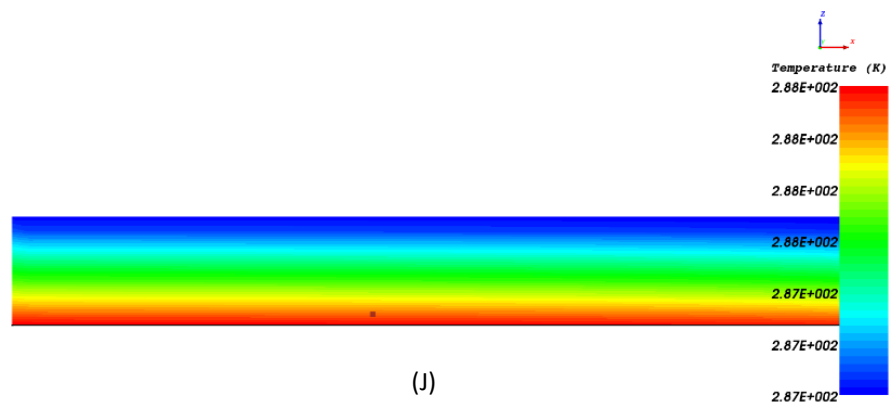
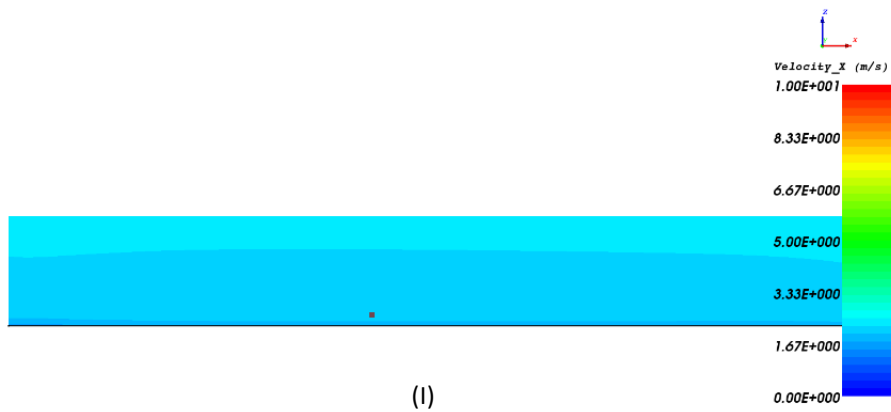
(F)



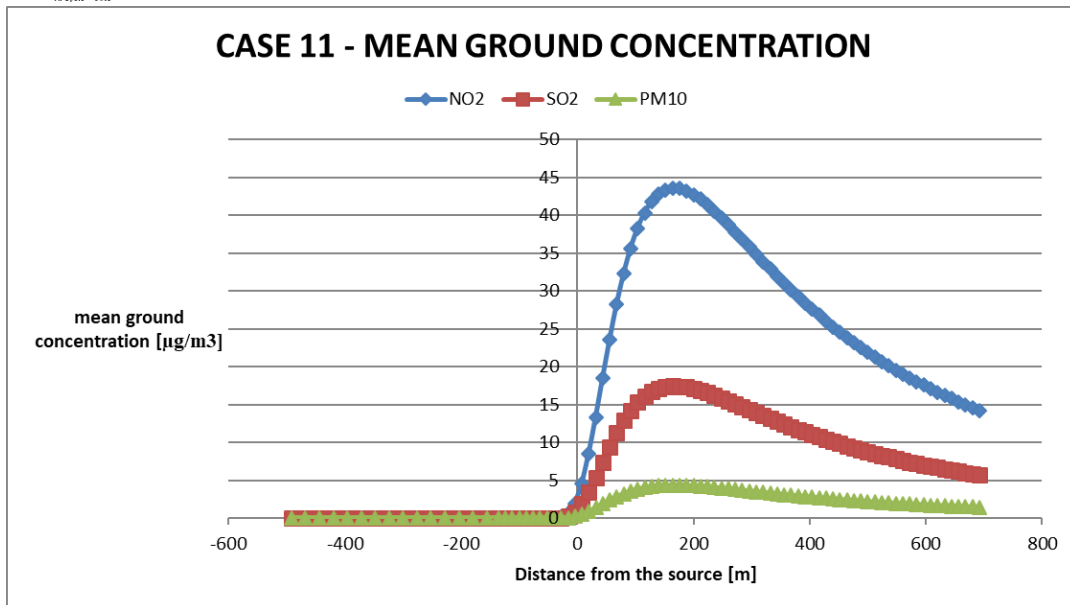
(G)



(H)

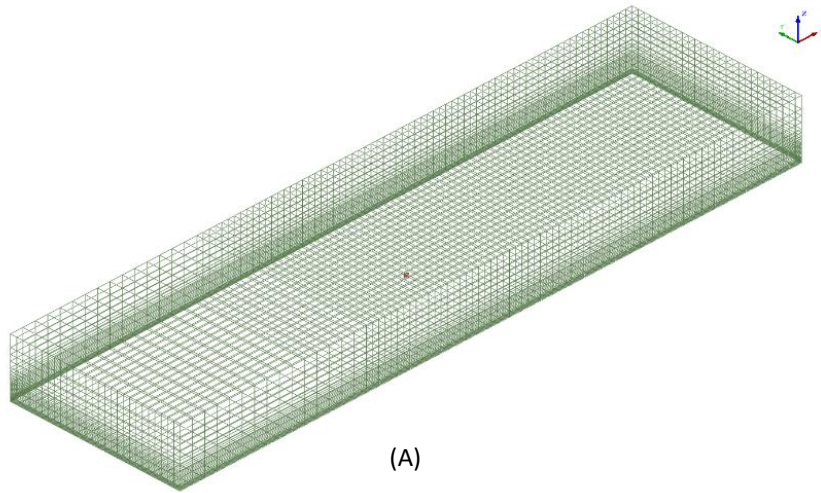


At Cycle = 3440



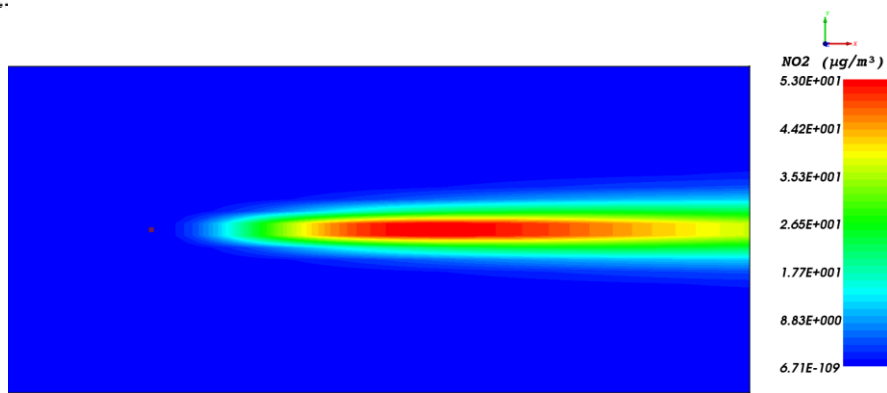
(K)

CASE 12

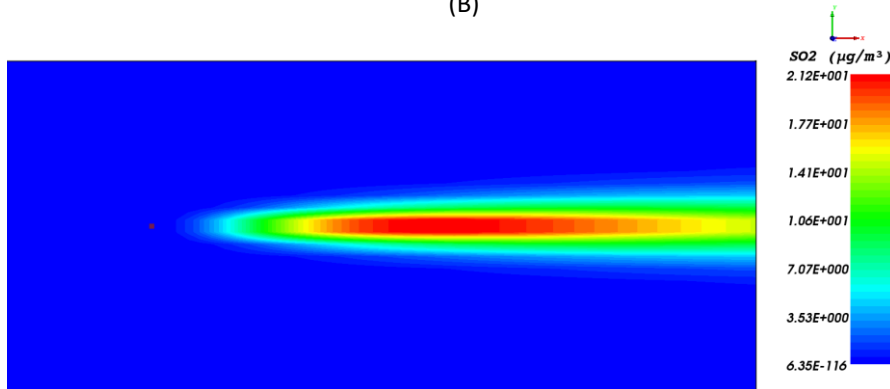


(A)

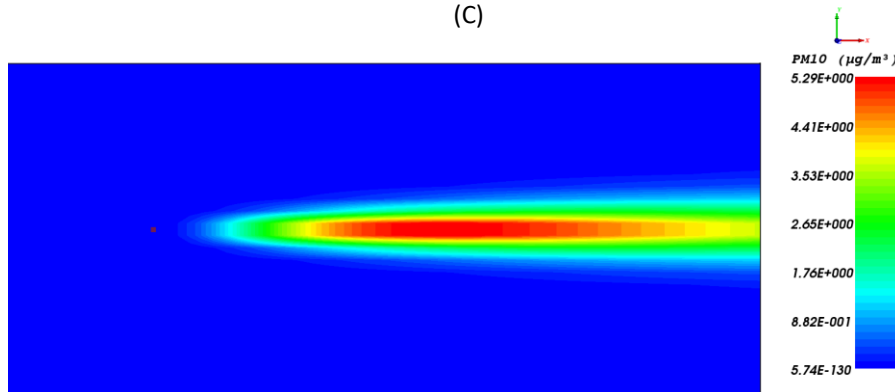
At Cycle =



(B)

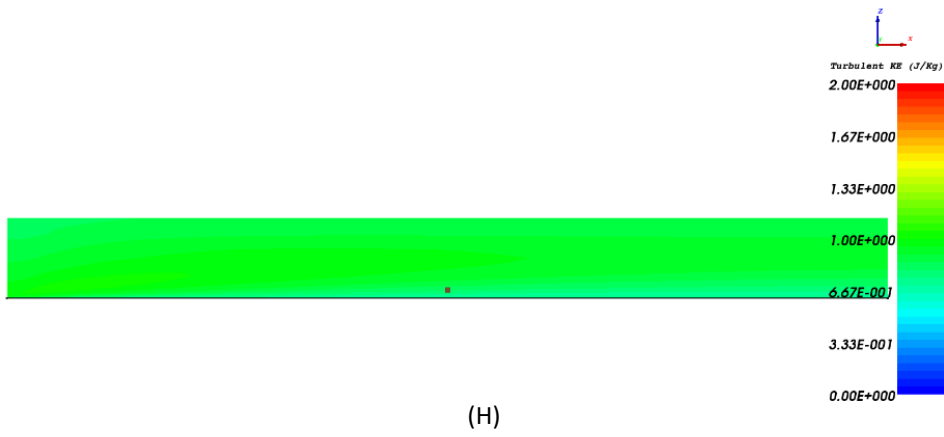
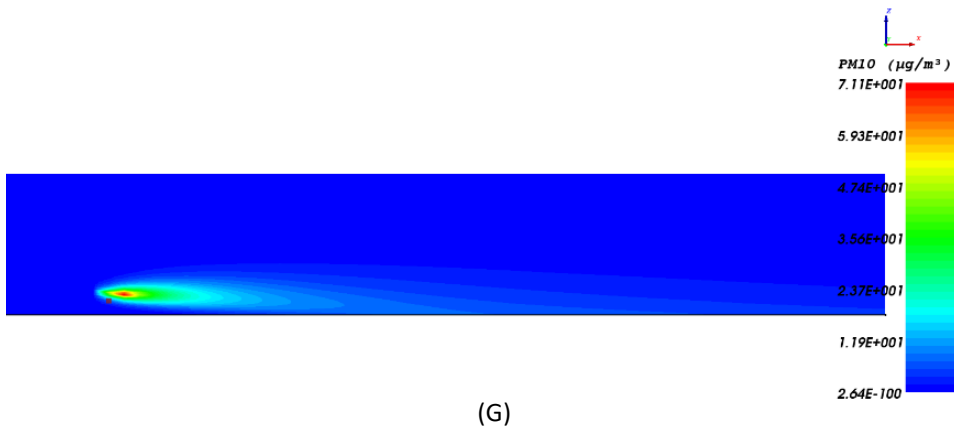
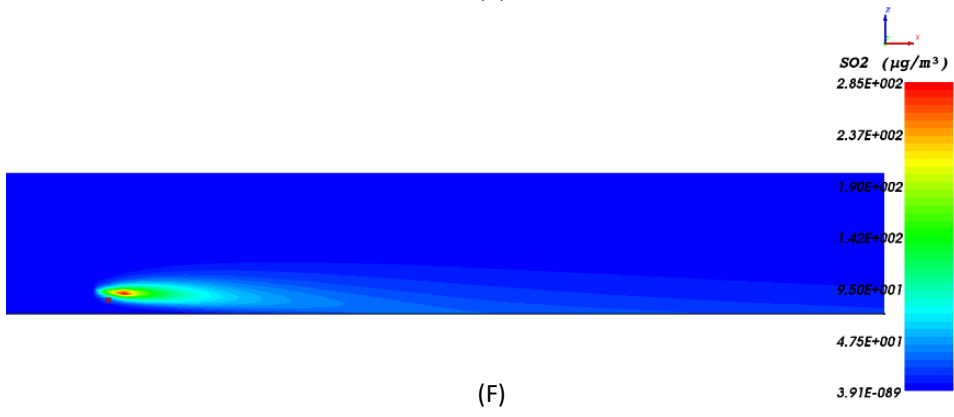
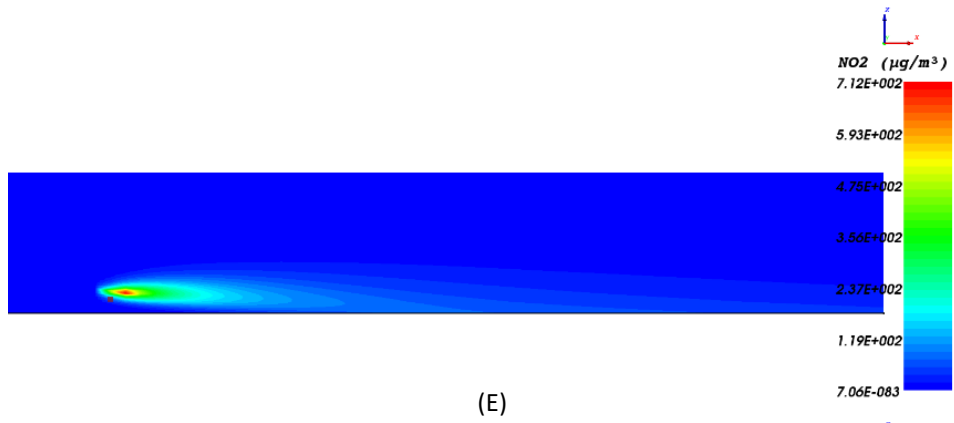


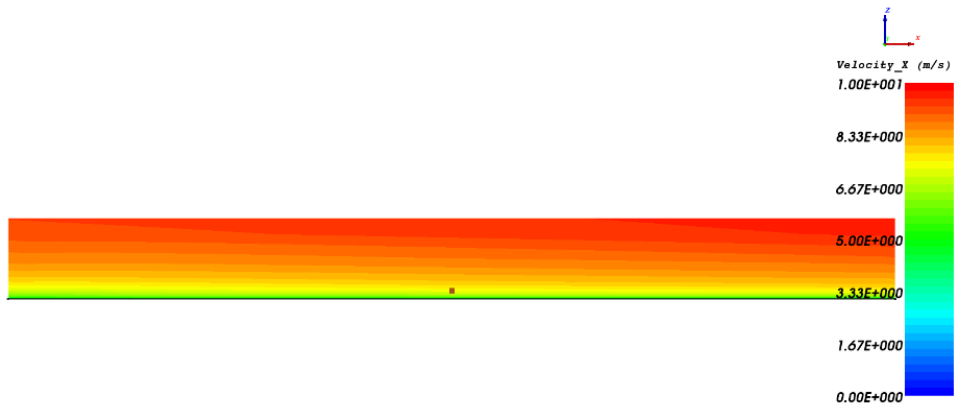
(C)



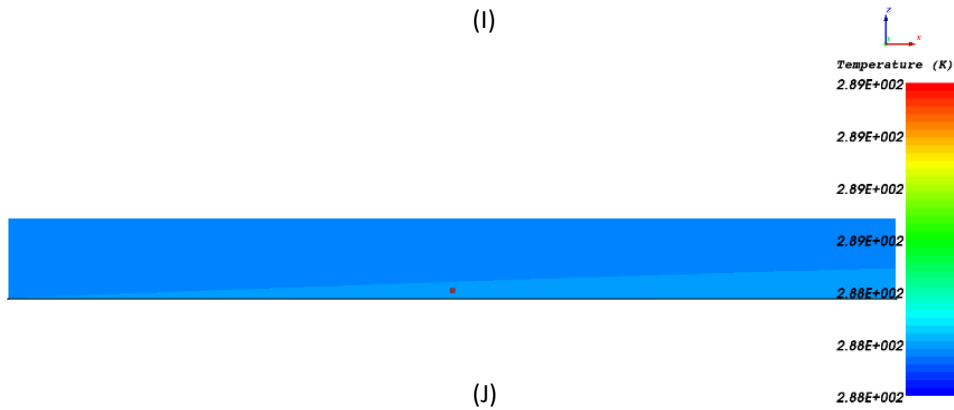
(D)

At Cycle = 3446



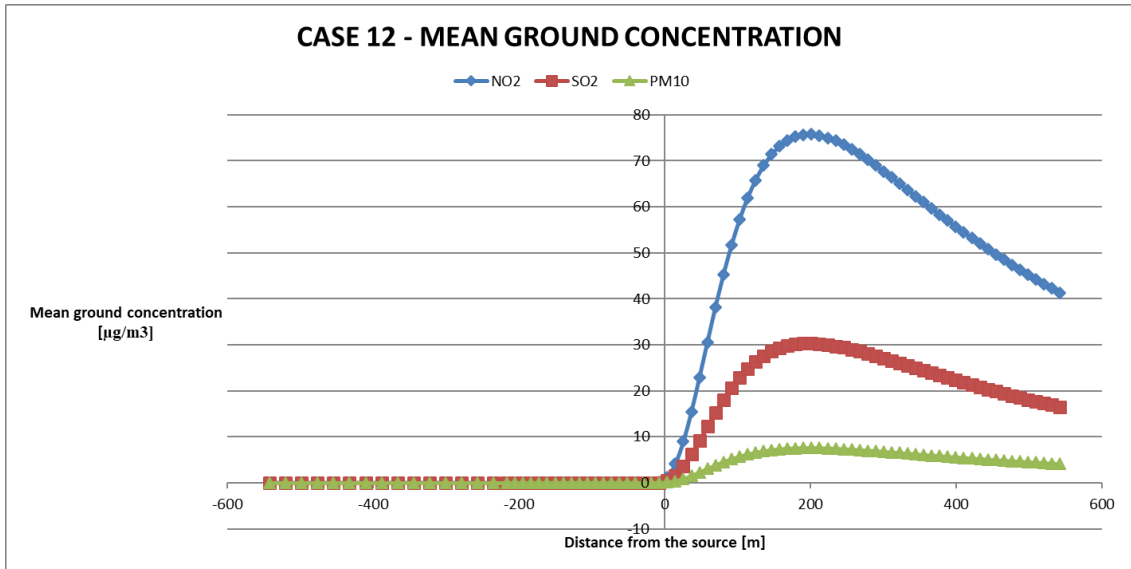


(I)



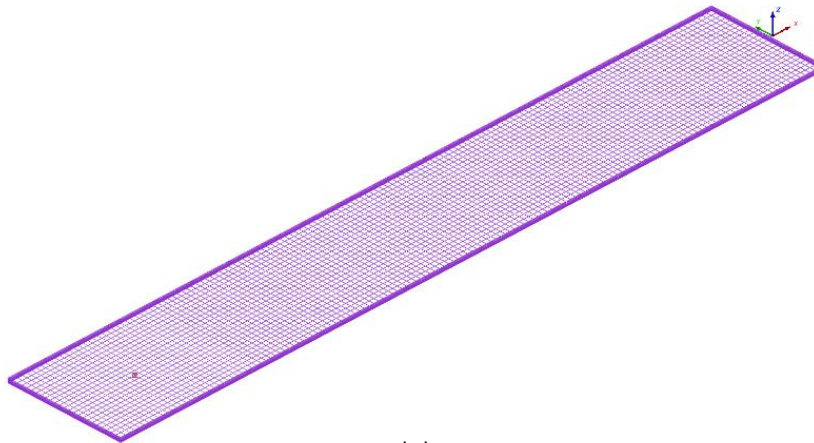
(J)

At Cycle = 3231

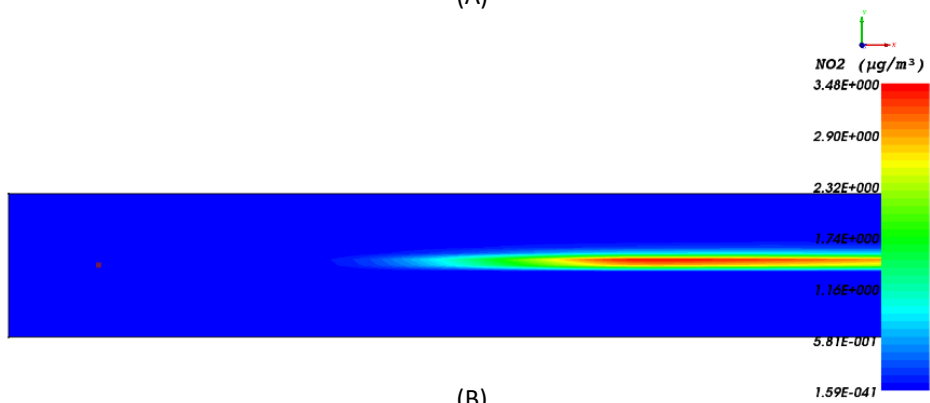


(K)

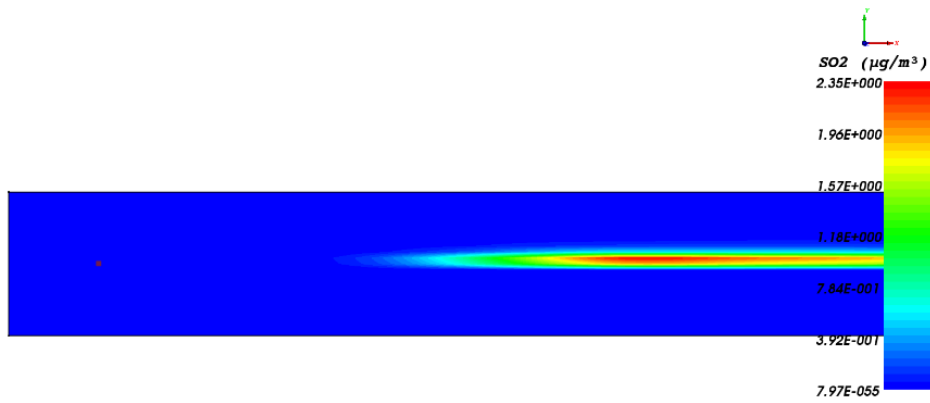
CASE 13



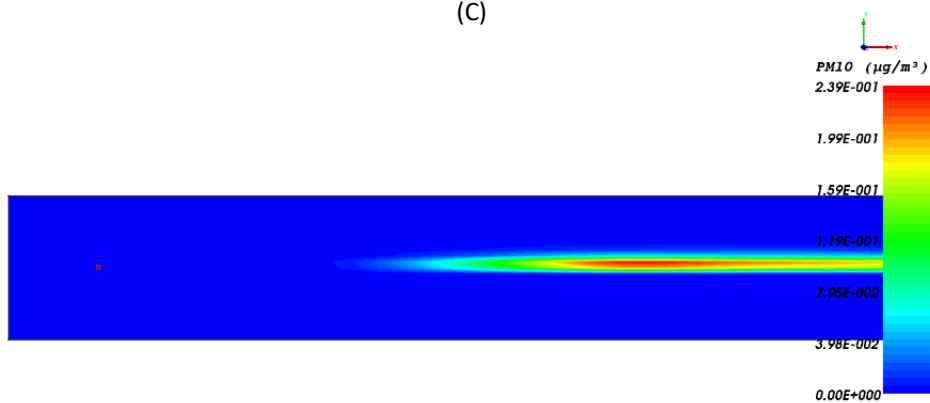
(A)



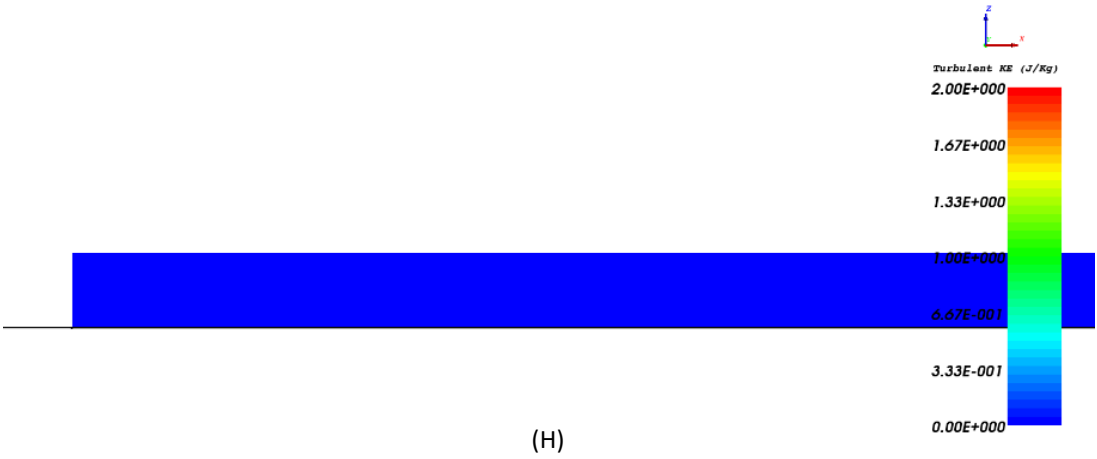
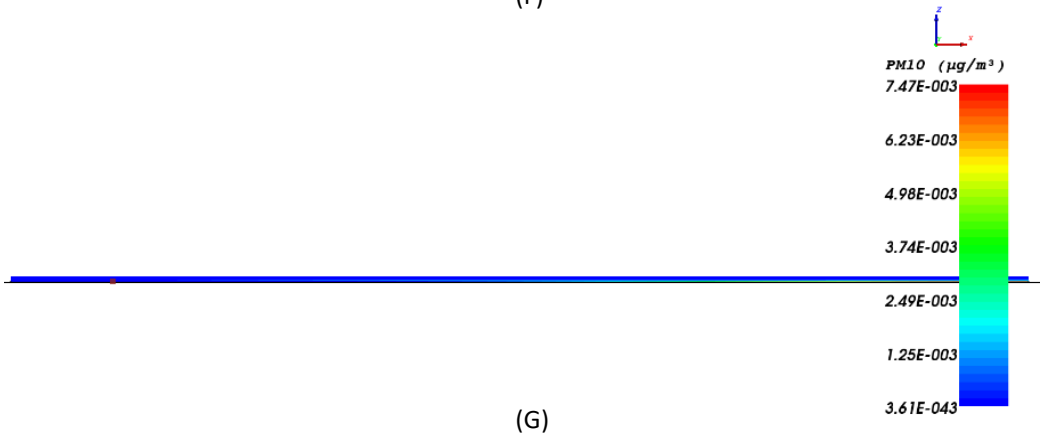
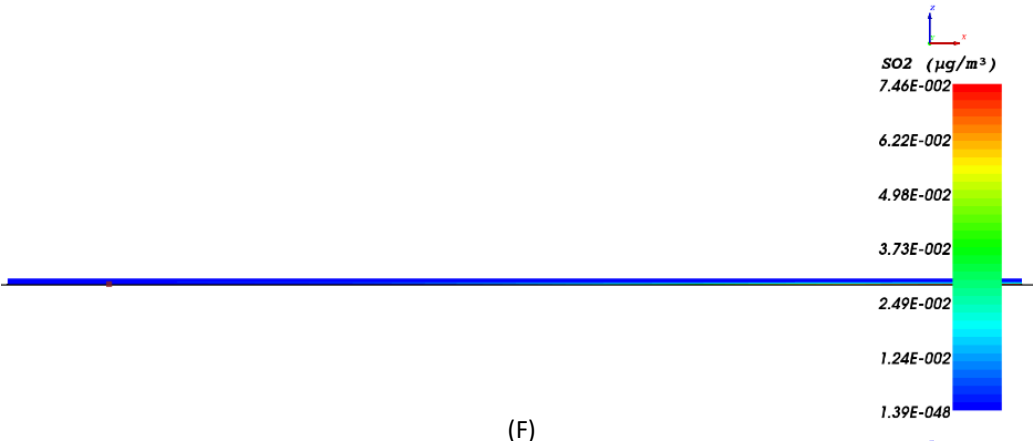
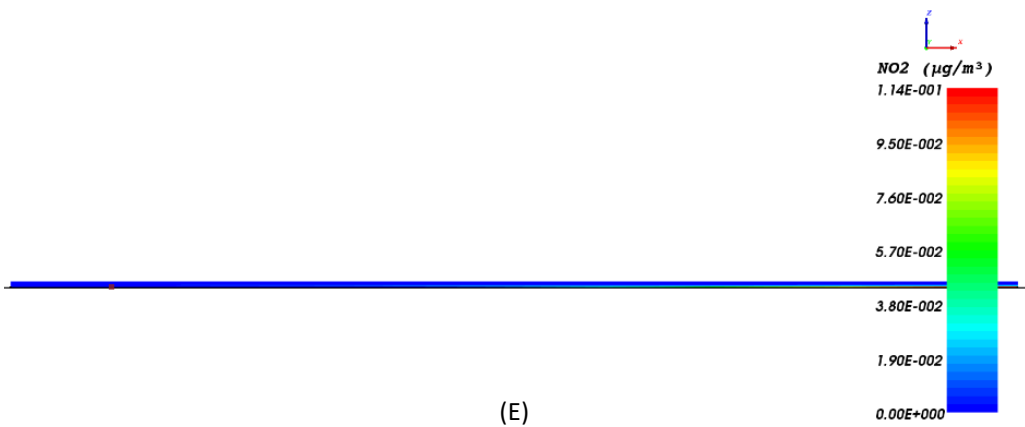
(B)

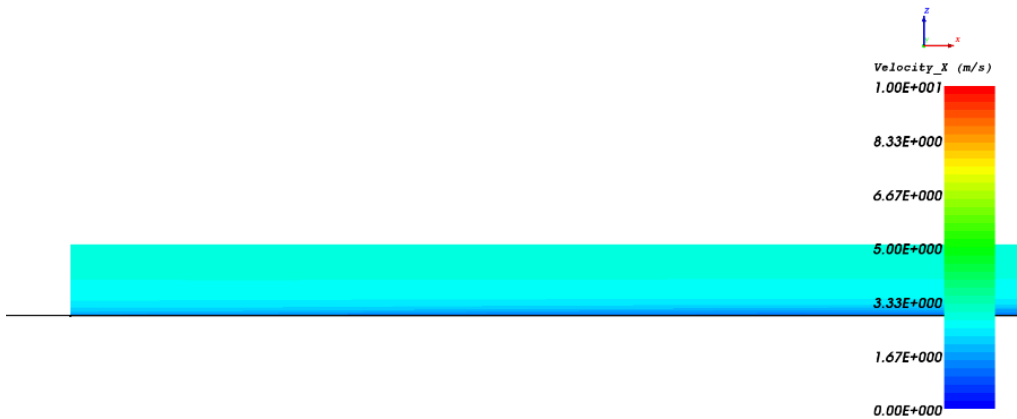


(C)

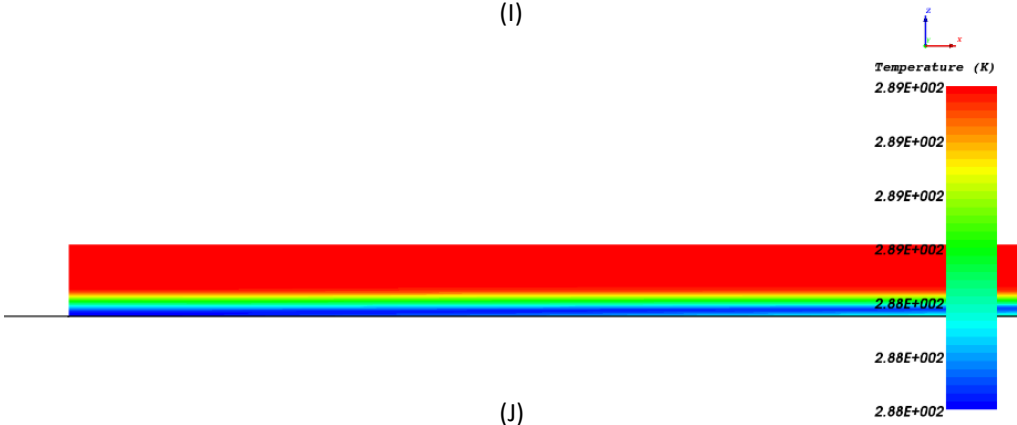


(D)

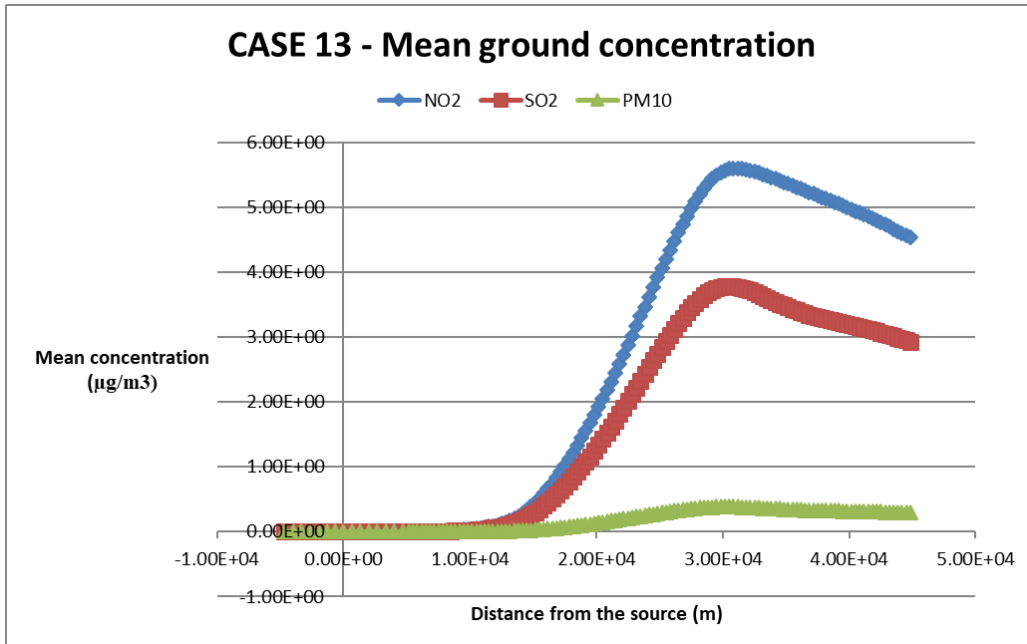




(I)

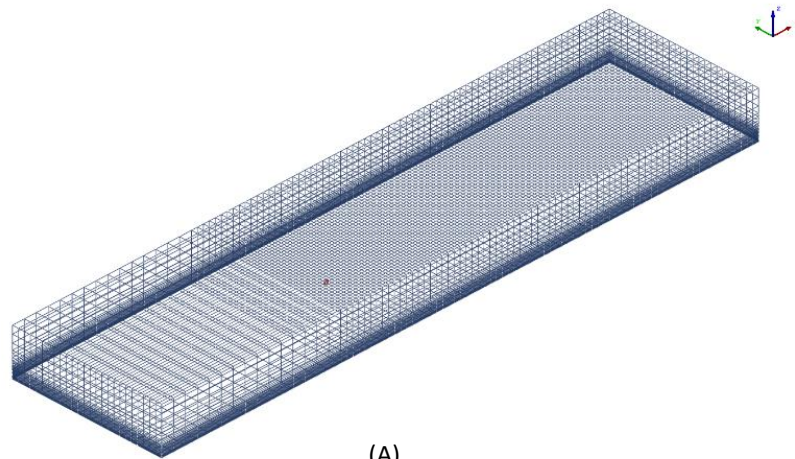


(J)



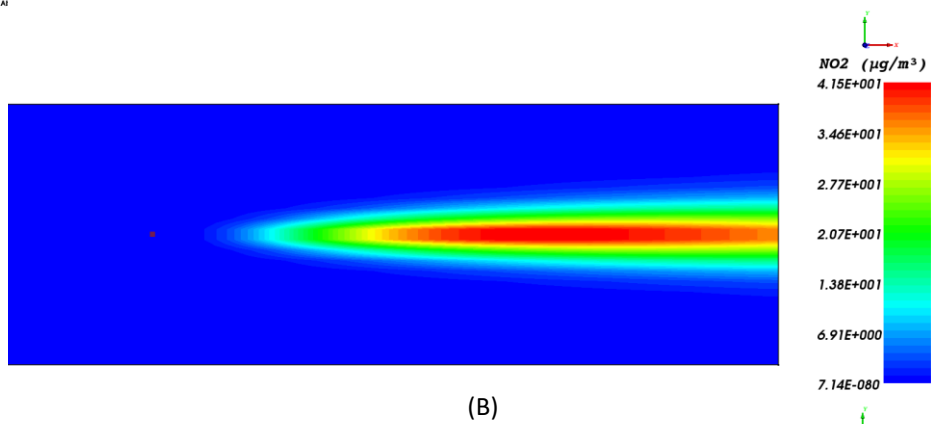
(K)

CASE 14



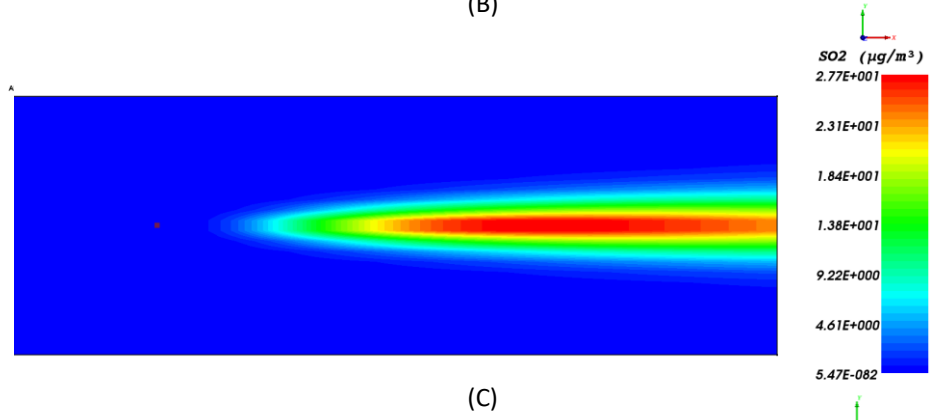
(A)

A



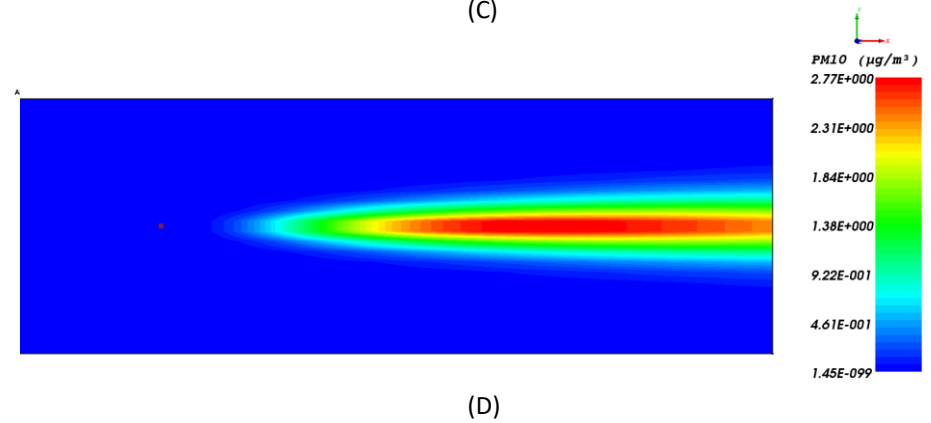
(B)

A

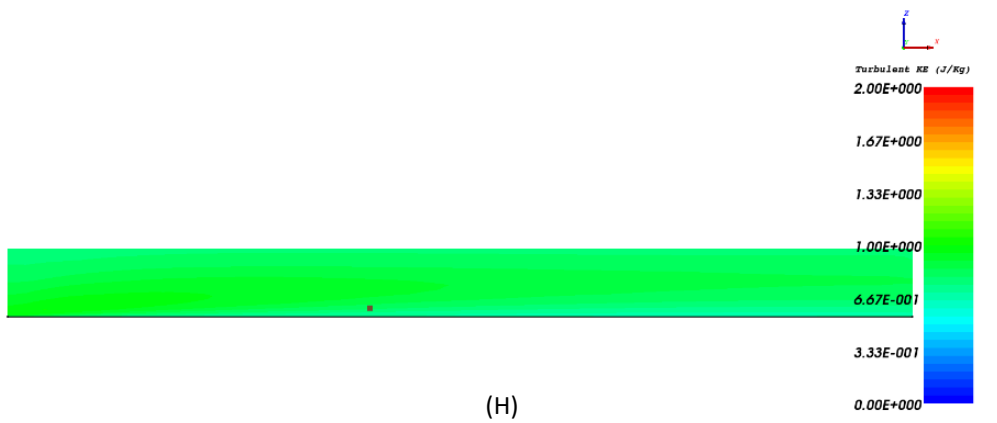
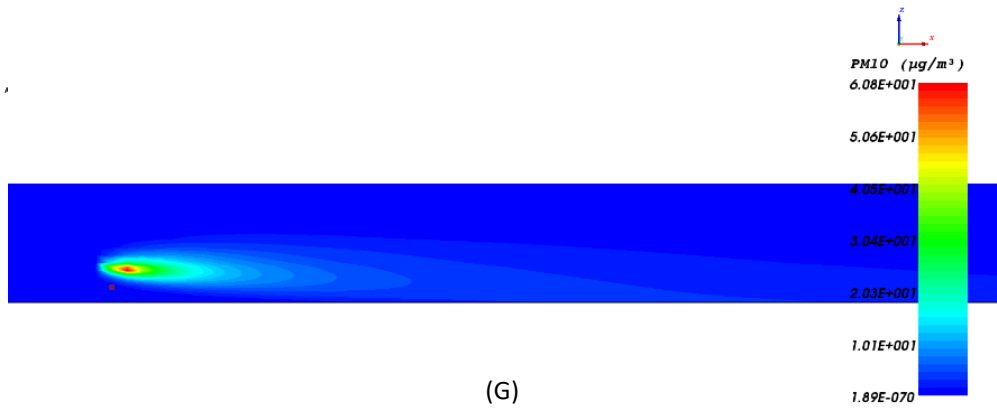
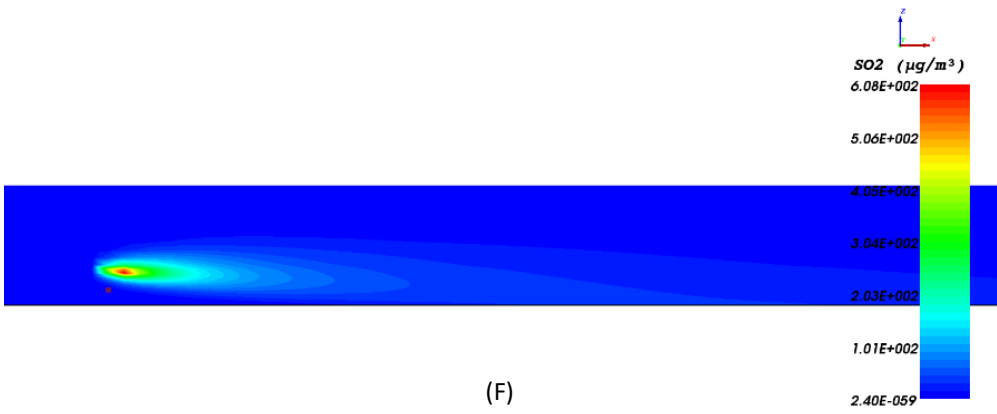
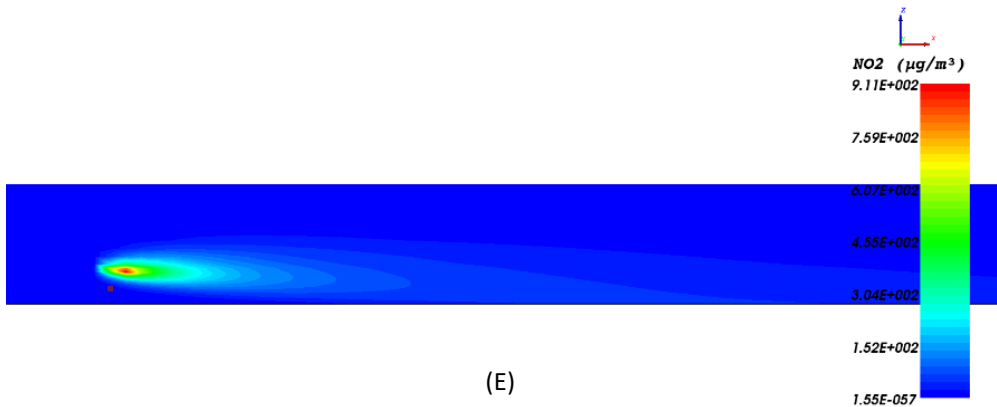


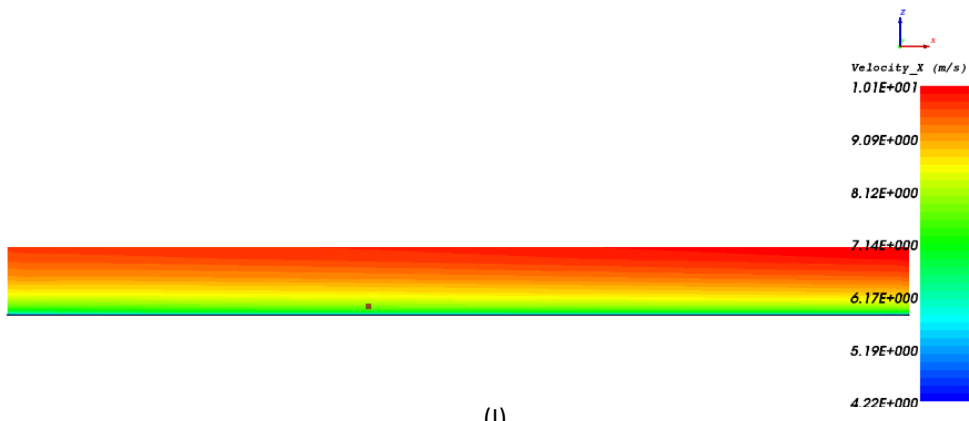
(C)

A

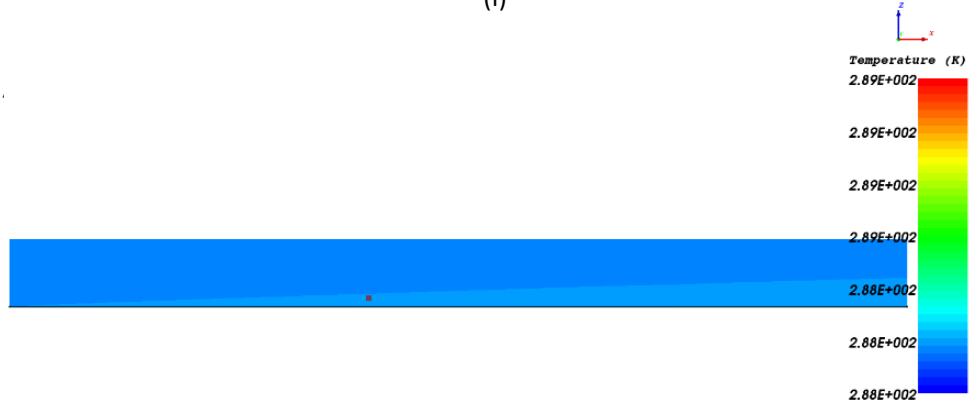


(D)



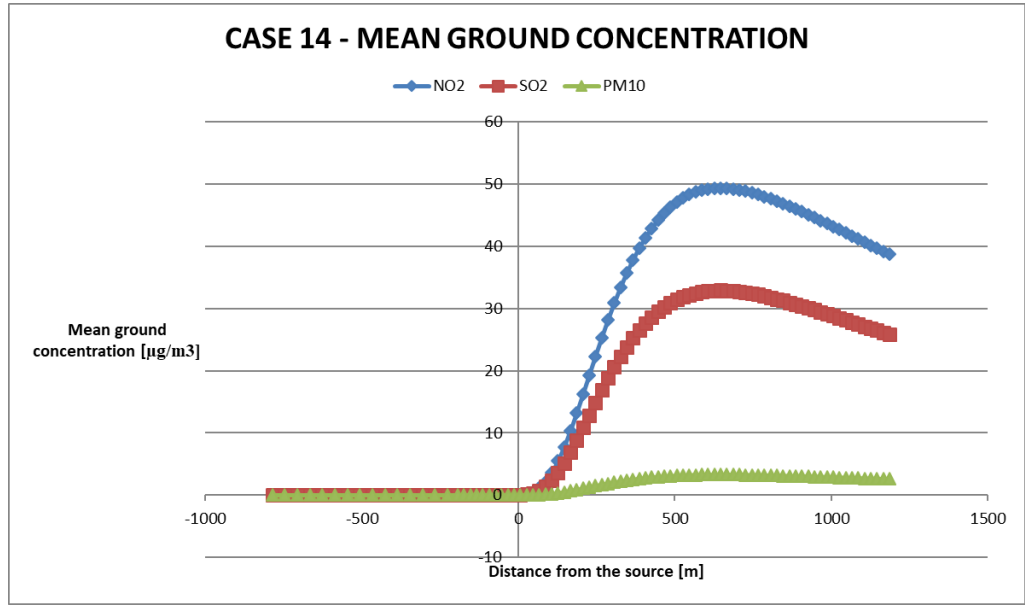


(I)



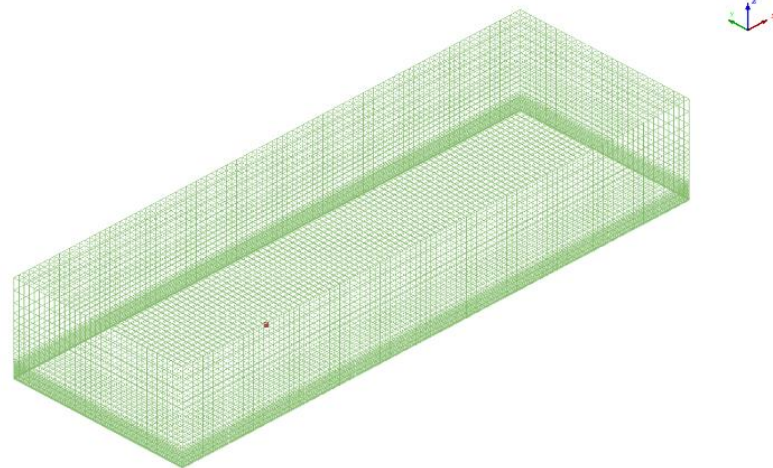
(J)

All Cycle = 4072

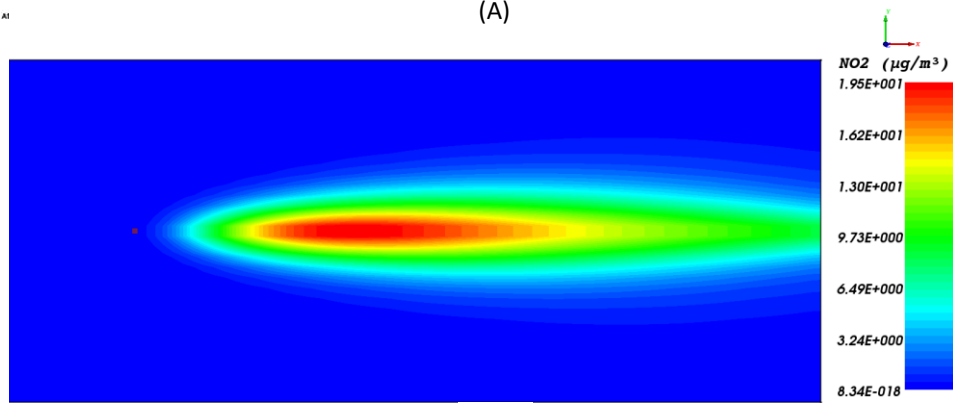


(K)

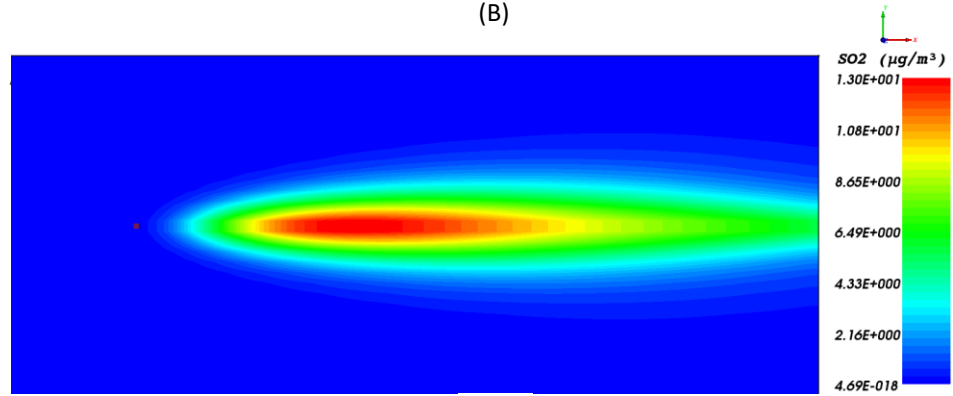
CASE 15



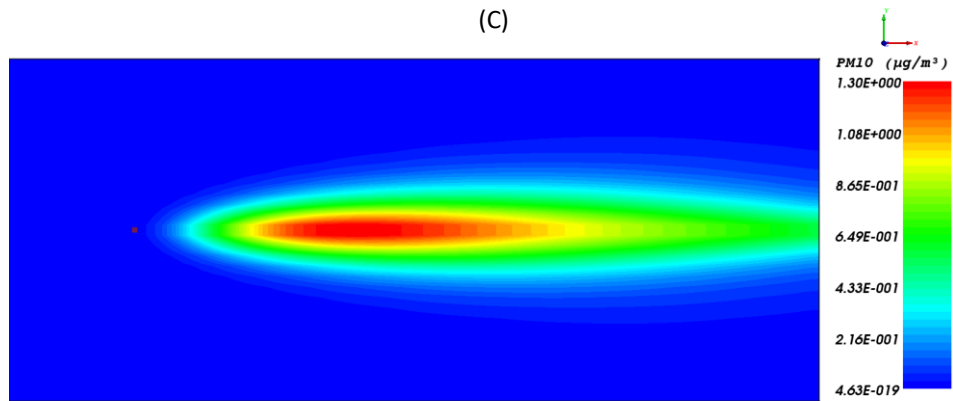
(A)



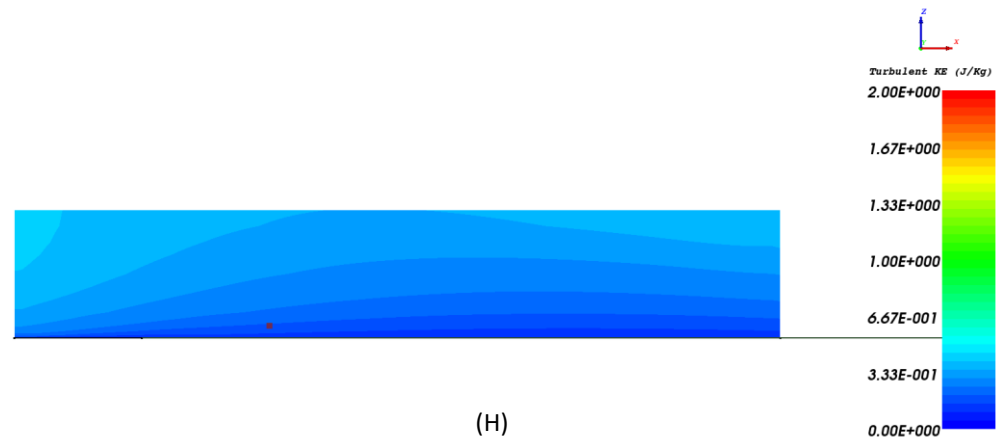
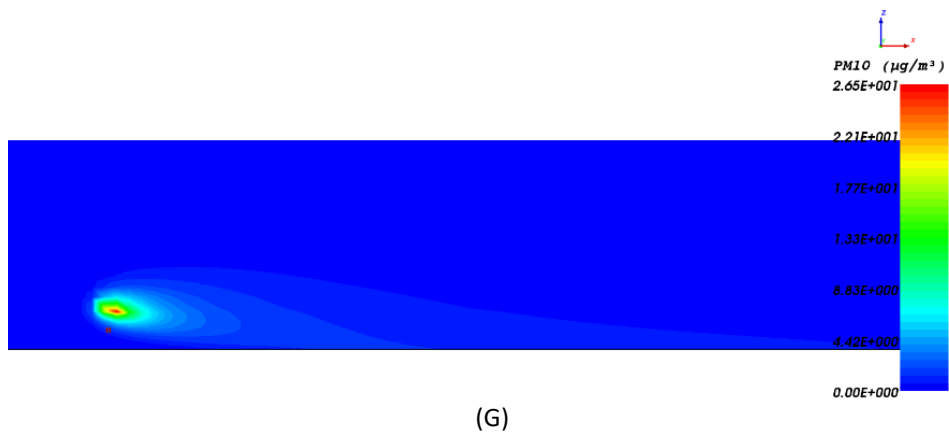
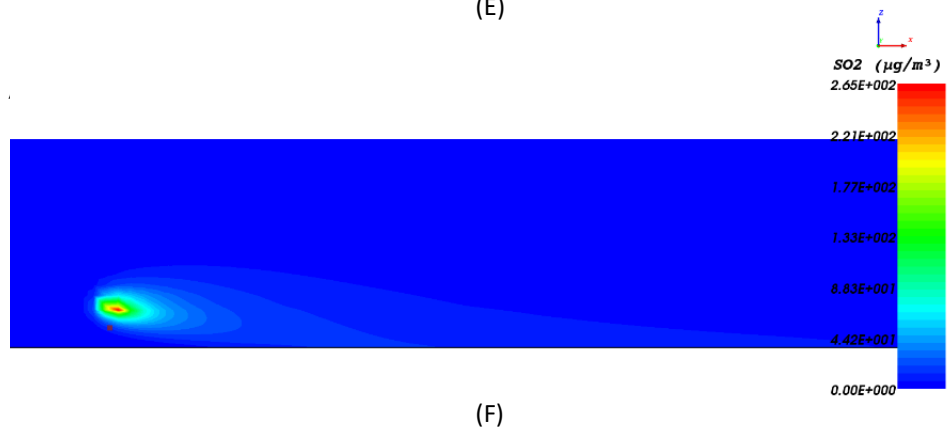
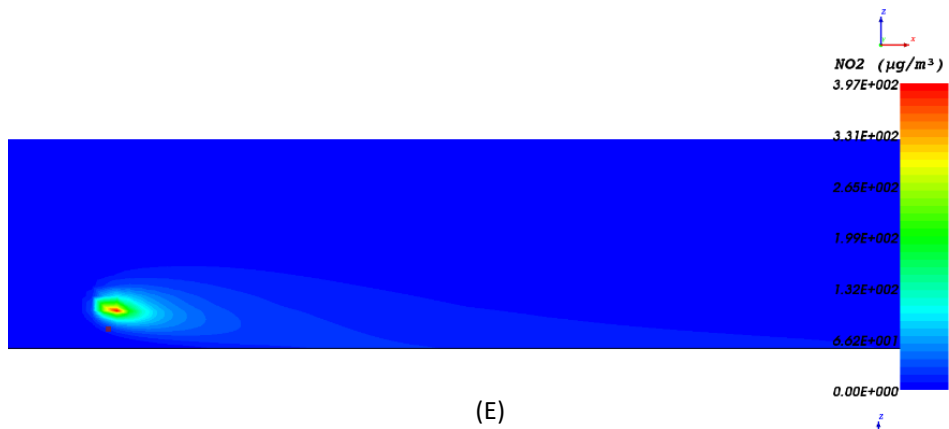
(B)

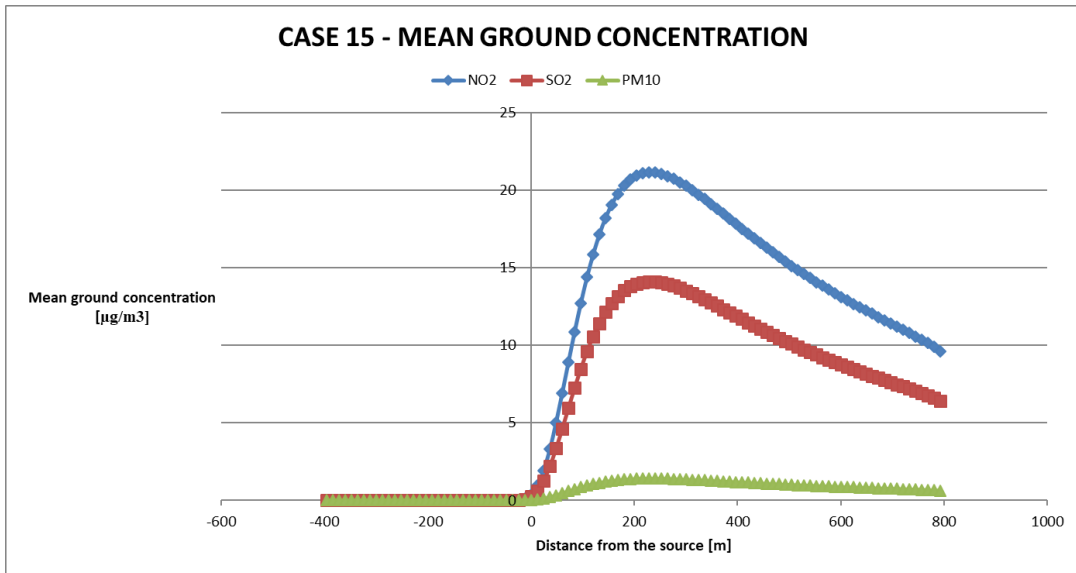
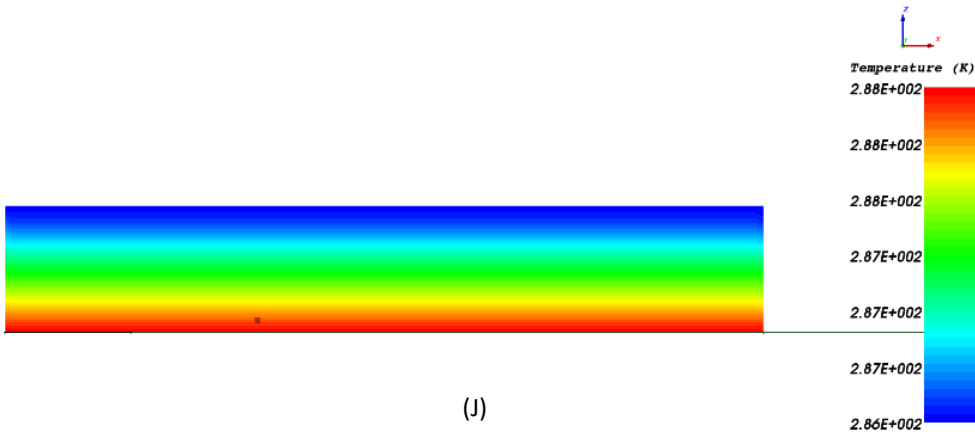
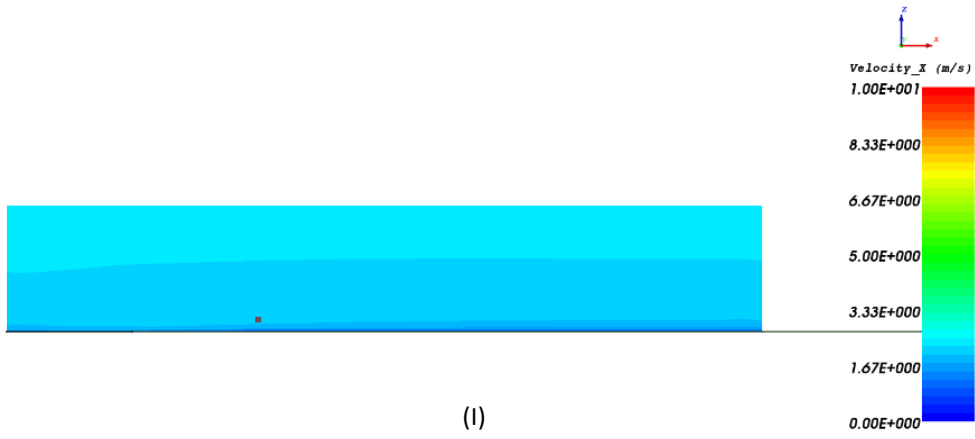


(C)



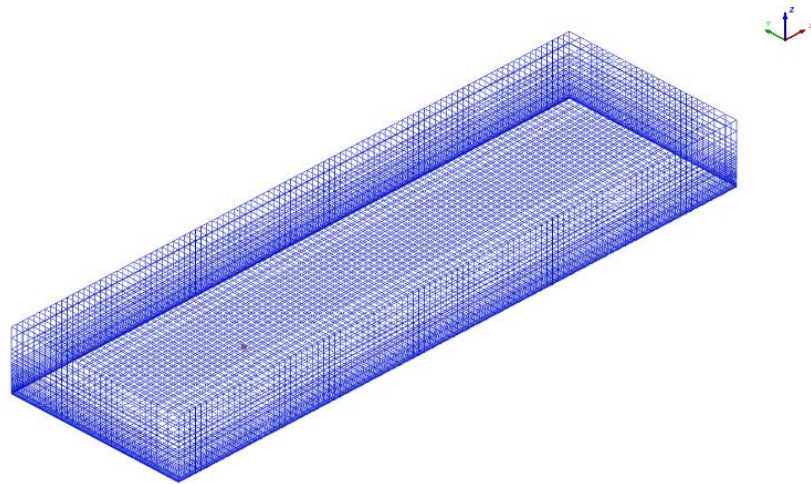
(D)





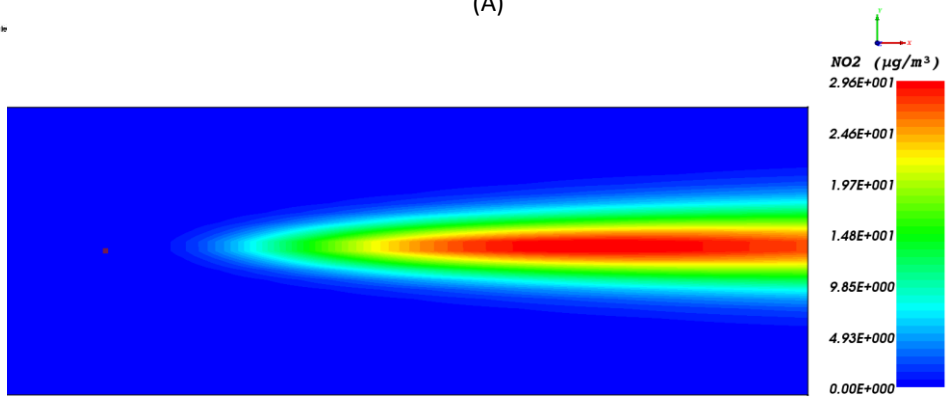
(K)

CASE 16

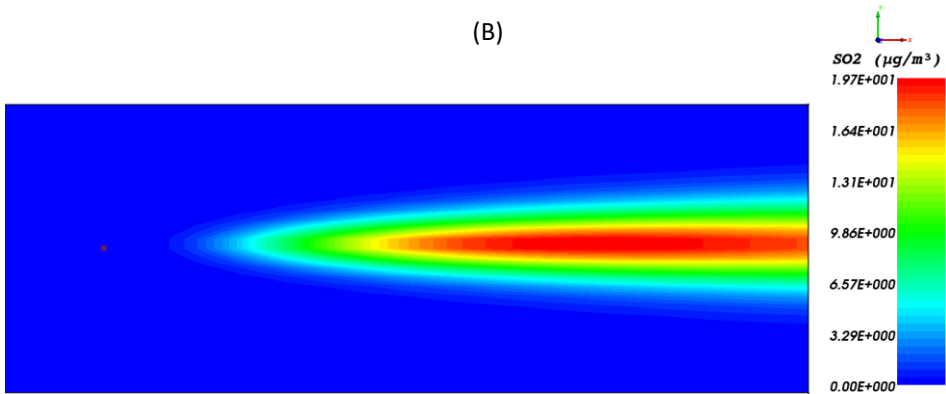


(A)

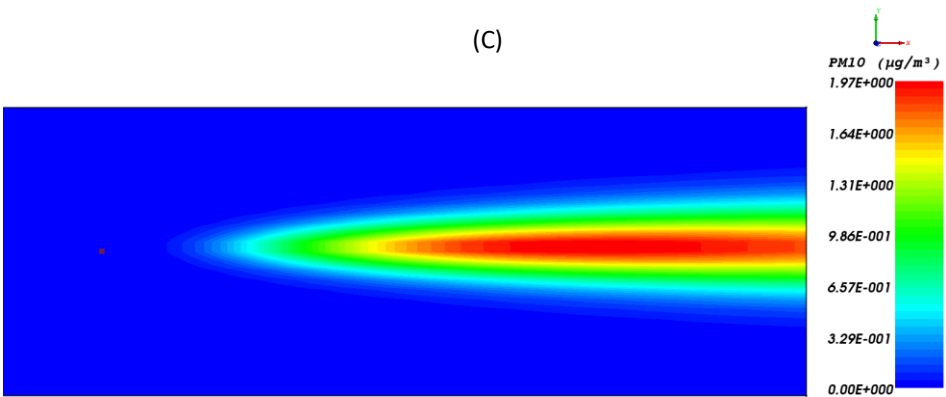
All Cycle



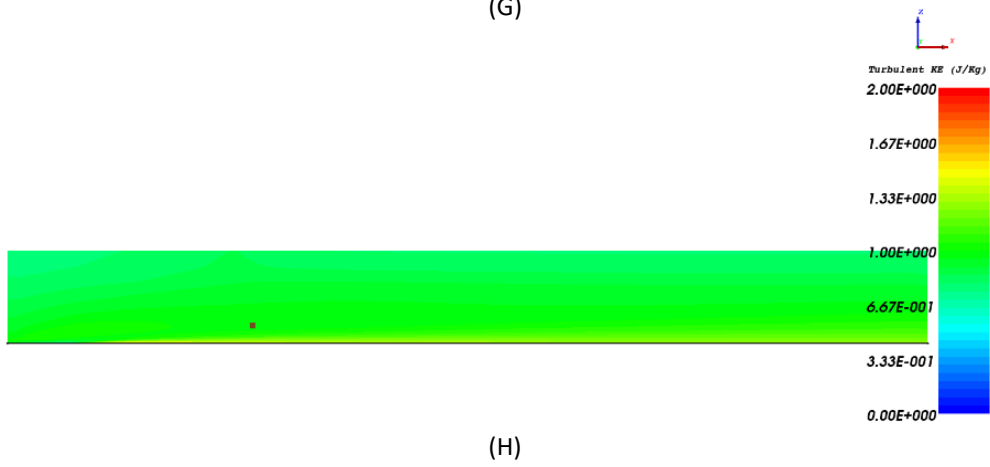
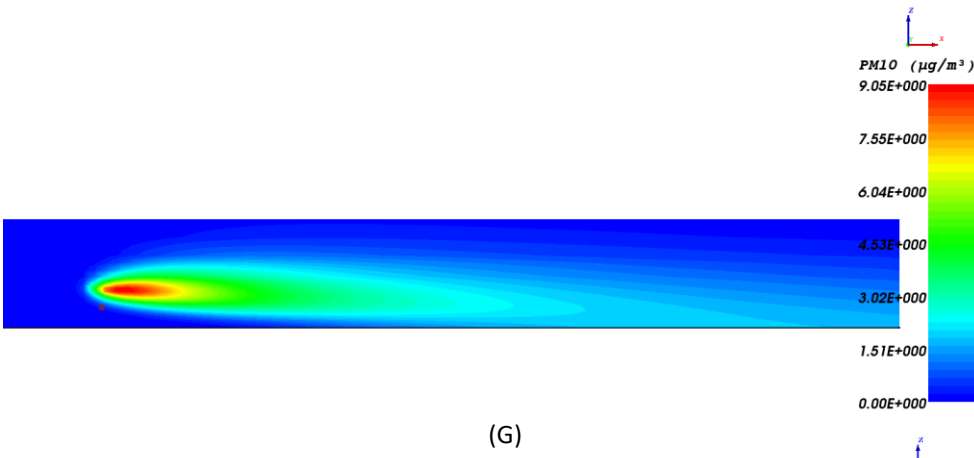
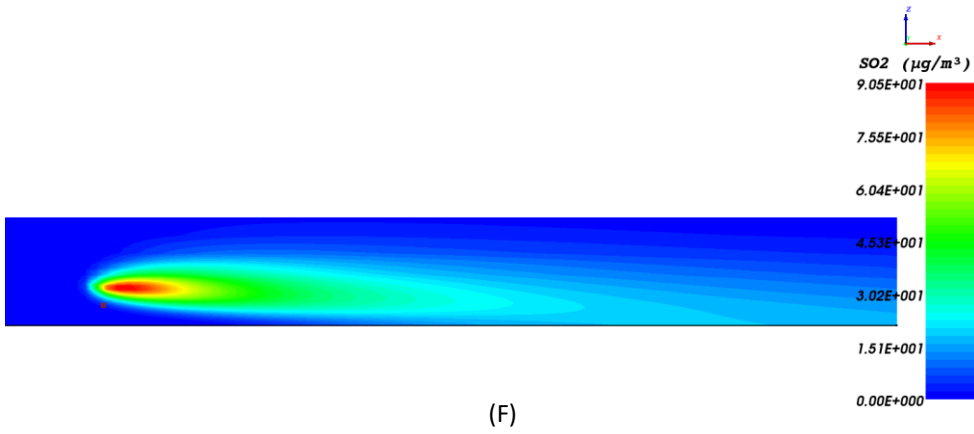
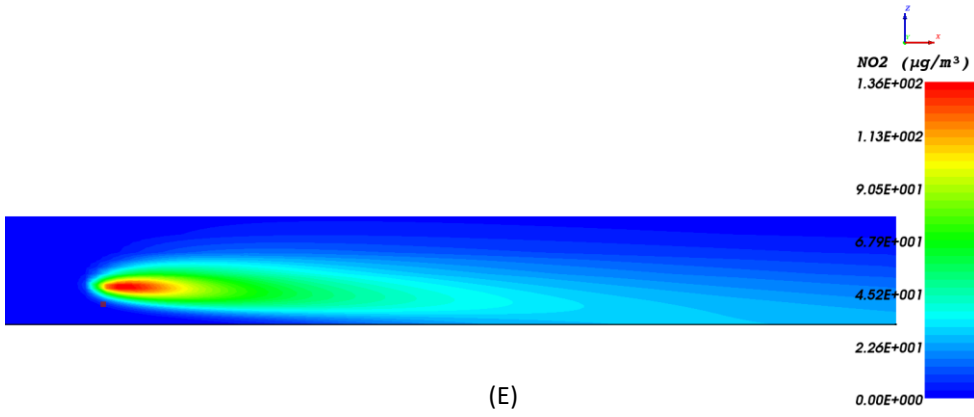
(B)

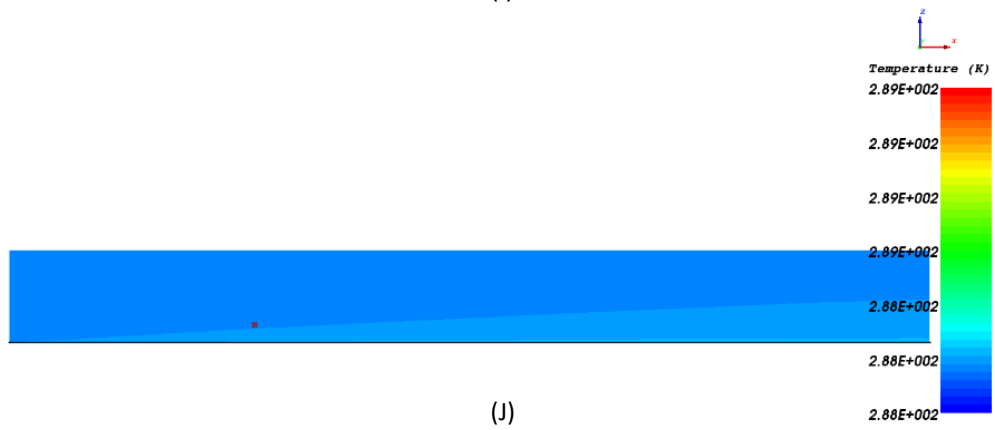
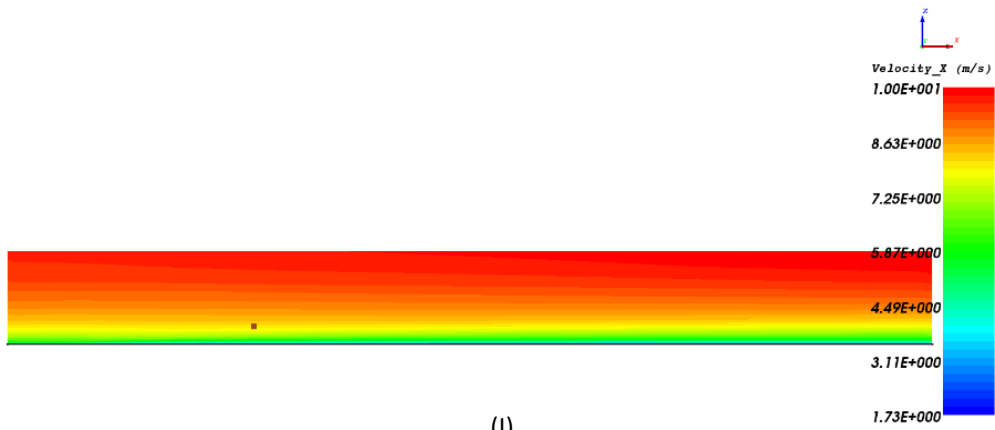


(C)

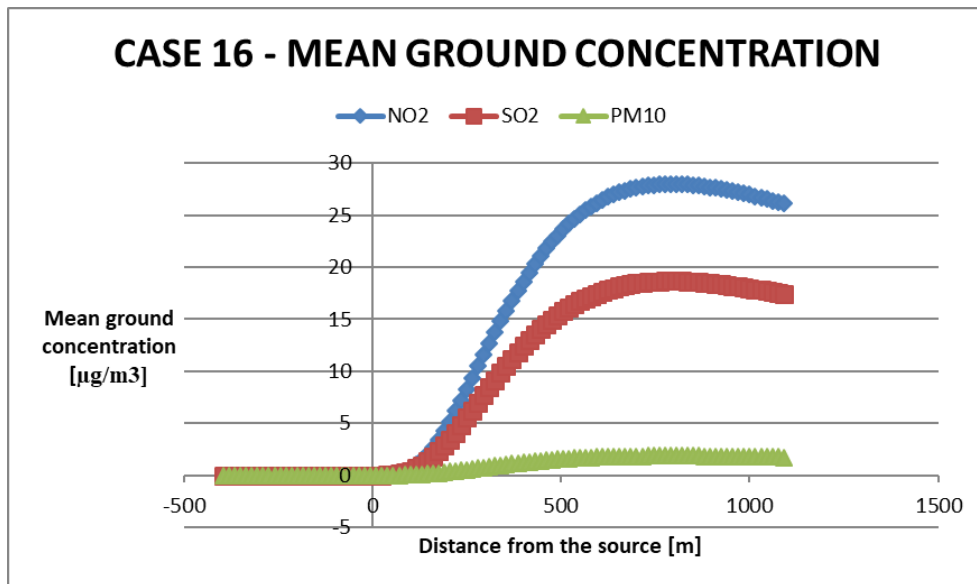


(D)





At Cycle = 4072



C.3 Evaluation of Case 1 with the Gaussian plume model

The value of mean ground concentration obtained from the numerical model for Case 1 is really high compared to the other cases. This observation introduces some doubts on the reliability of this result. In order to evaluate the order of magnitude of the expected result for this case the Gaussian Plume model is performed. It is an analytical model in which it is considered a continuous release of pollutants from a point source. This model is based on the following assumptions:

- the pollutant has the same density of air
- the domain is infinite in order to consider constant turbulent diffusion coefficients
- the emission rate of pollutants is constant in time

Considering a point source located at (x_0, y_0, z_H) and reflection at the ground the mean concentration in the plume, $\bar{C}(x, y, z)$, can be expressed as:

$$\bar{C}(x, y, z) = \frac{Q}{2\pi\bar{u}\sigma_y\sigma_z} \cdot \exp\left[-\frac{(y - y_0)^2}{2\sigma_y^2}\right] \left[\exp\left(-\frac{(z - z_H)^2}{2\sigma_z^2}\right) + \exp\left(-\frac{(z + z_H)^2}{2\sigma_z^2}\right) \right] \quad (\text{C.1})$$

where Q is the emission rate and σ_y and σ_z are the lateral and vertical dispersion coefficients respectively, \bar{u} is the mean wind velocity.

The model is implemented on Python; the code is written with reference to already existing ones, in particular the one by Connelly [41]. Also for choice of the experimental values of the dispersion coefficients reference is made to this model. The results of the application of the Gaussian Plume model to Case 1 for NO_2 are shown in Figure C.2.

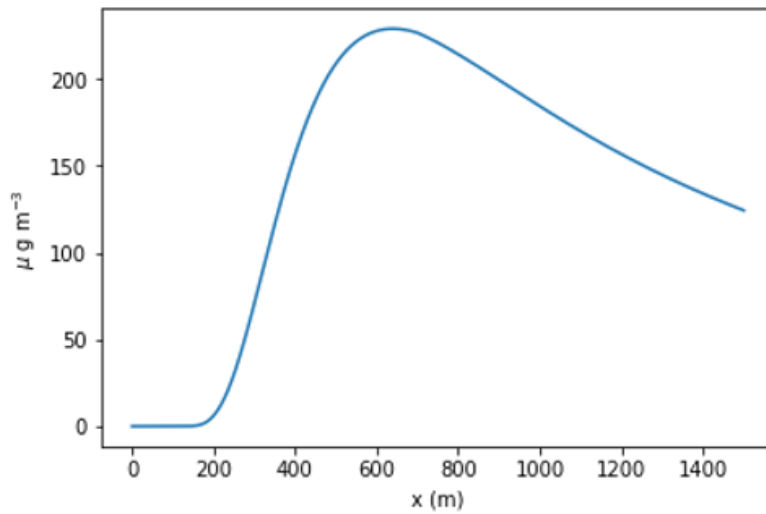


Figure C.2: Evaluation of NO_2 concentration at the ground (1 m) with Gaussian plume model (source at $x=0$ m)

C.4 Main effect plots with lower concentration for Case 1

In order to see the influence of the results of Case 1 on the parametric analysis it is attempted to "dump" its effect. This is made by setting the results of Case 1 to the average between the outputs of all the other simulations. It is made for all the parameters taken into account in the study. With this procedure the pollutant concentration for Case 1 has been set to $63.5 \frac{\mu\text{g}}{\text{m}^3}$ for NO_2 , to $34.5 \frac{\mu\text{g}}{\text{m}^3}$ for SO_2 and to $5.2 \frac{\mu\text{g}}{\text{m}^3}$ for PM_{10} . The new results are shown in Figure C.3.

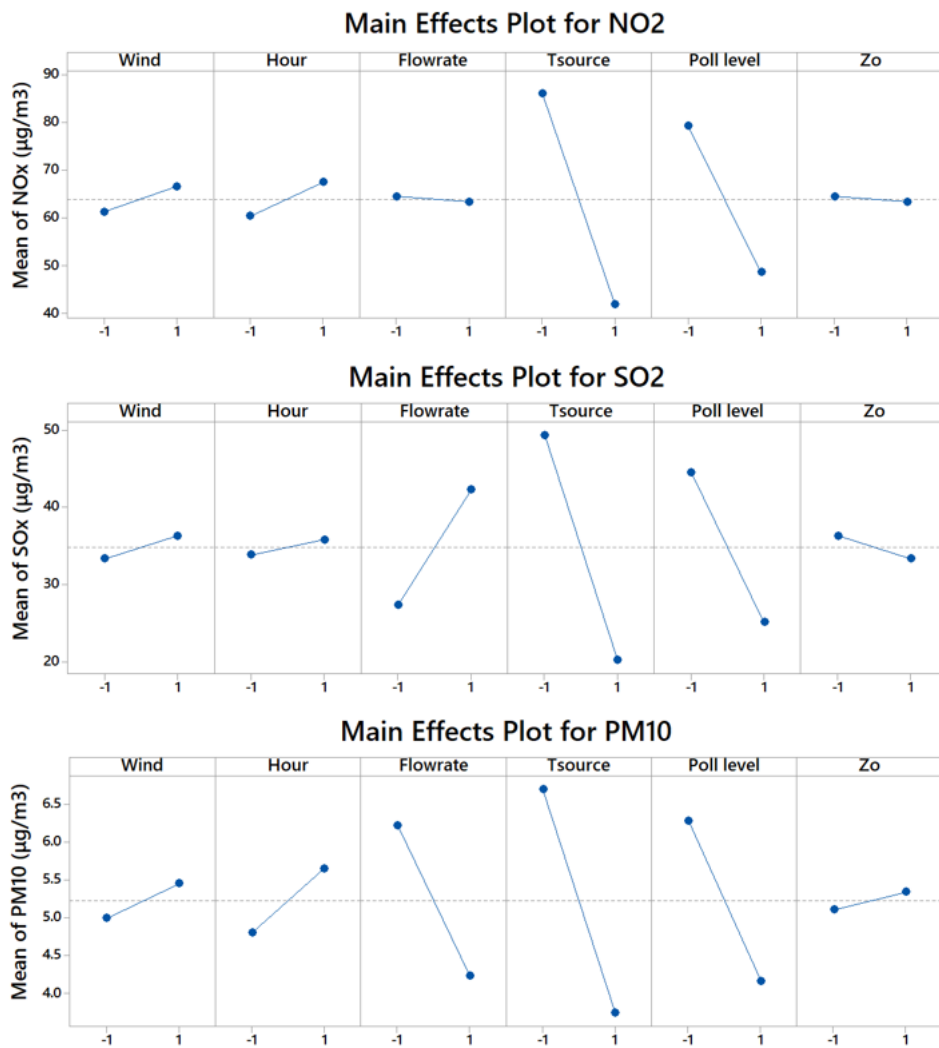


Figure C.3: Main effect plots for mean peak of ground concentration without the effect of case 1

C.5 Interaction plots for the other species under evaluation

The interaction plot has been obtained for all the parameters considered in the analysis. Figure C.4 shows the results for SO_2 , Figure C.5 shows the ones for PM_{10} and Figure C.6 the ones for the distance of the peak of concentration from the source.



Figure C.4: Interaction plot for SO_2

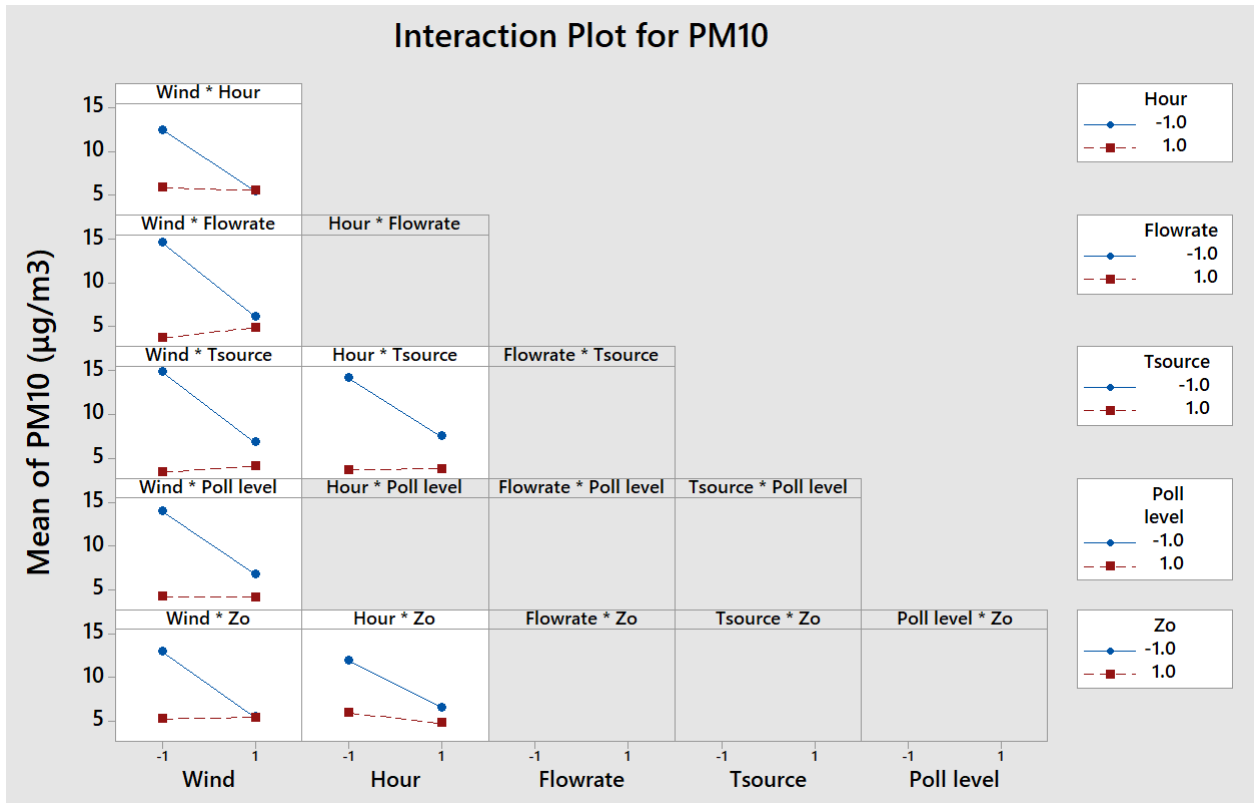


Figure C.5: Interaction plot for PM_{10}

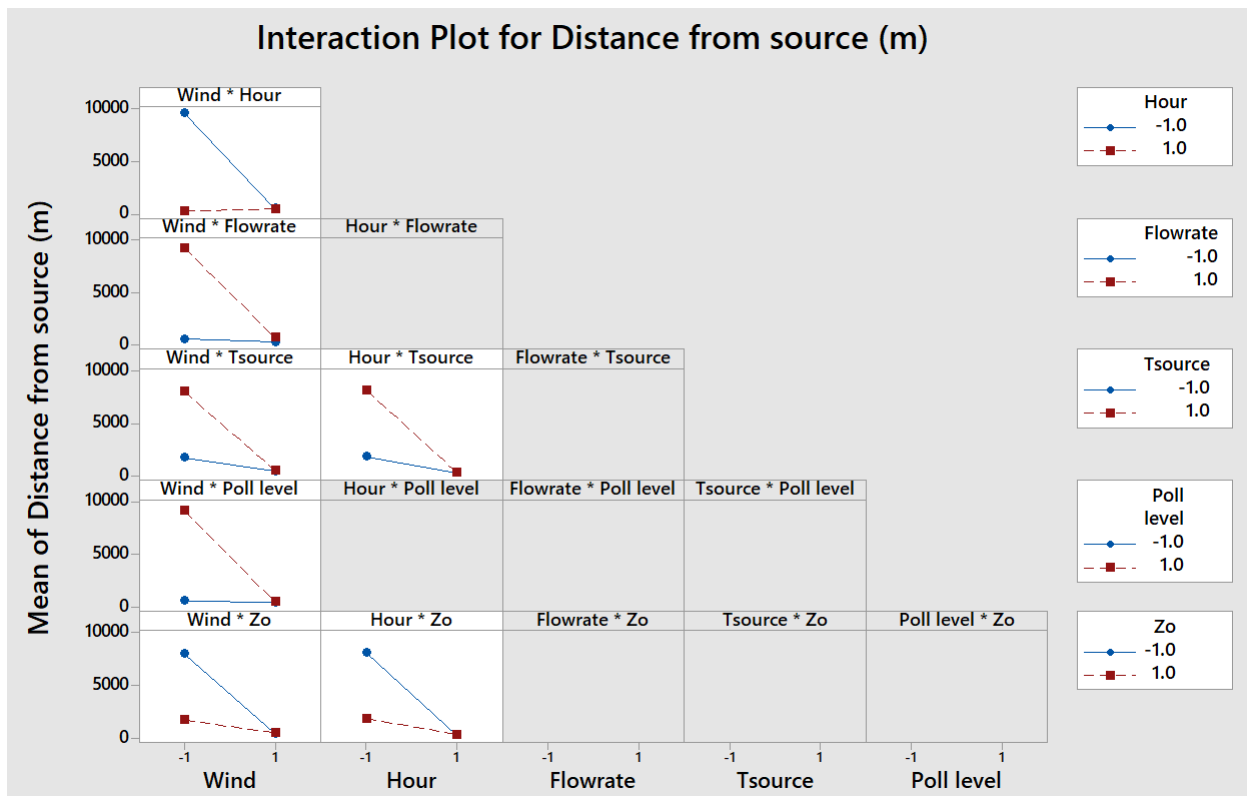


Figure C.6: Interaction plot for *Distance from the source*

Appendix D

Maps of concentration

In the following the maps of concentration used for the evaluation of the maximum ground concentration allowed by the regulation at the ground, c_m are shown. The maps represent the mean annual pollutant concentration in urban areas (Nantes, Paris, Lyon) and rural ones (the entire regions corresponding to the cities chosen for the analysis: Pays de la Loire, Ile de France, Rhone-Alpes). Each map refers to a specific pollutant (NO_2 , PM_{10} ; SO_2 is only available for Nantes).

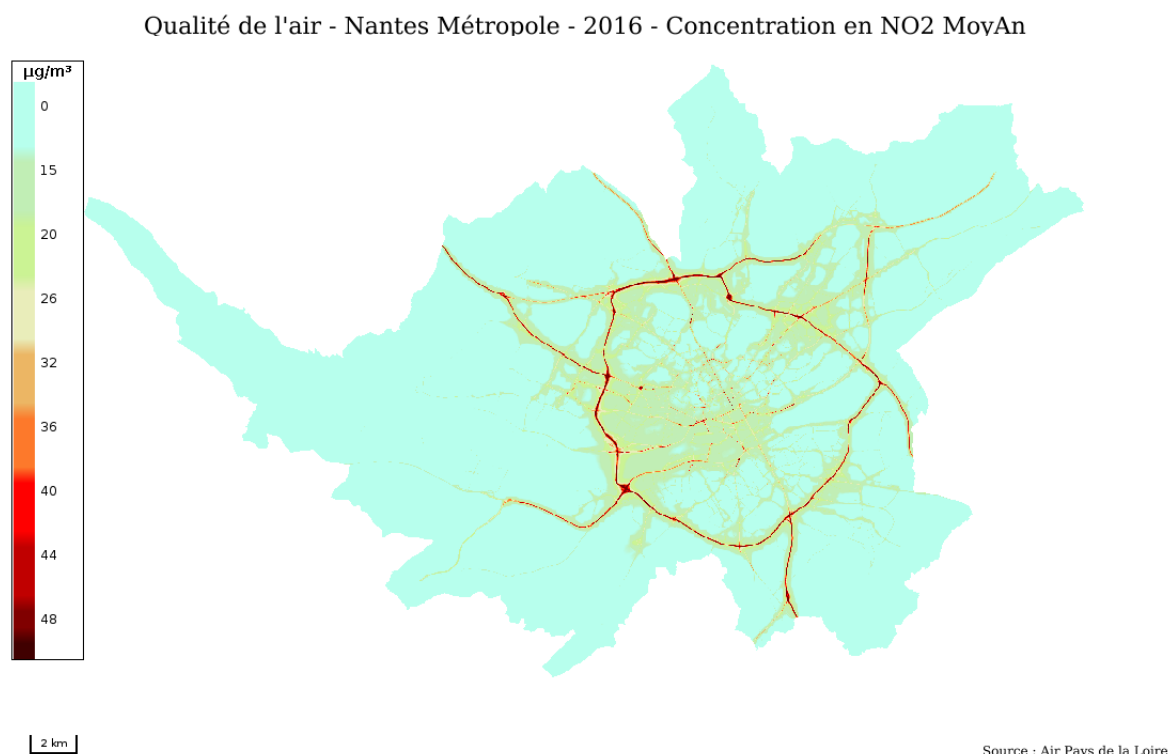


Figure D.1: NO_2 mean annual concentration in Nantes [42]

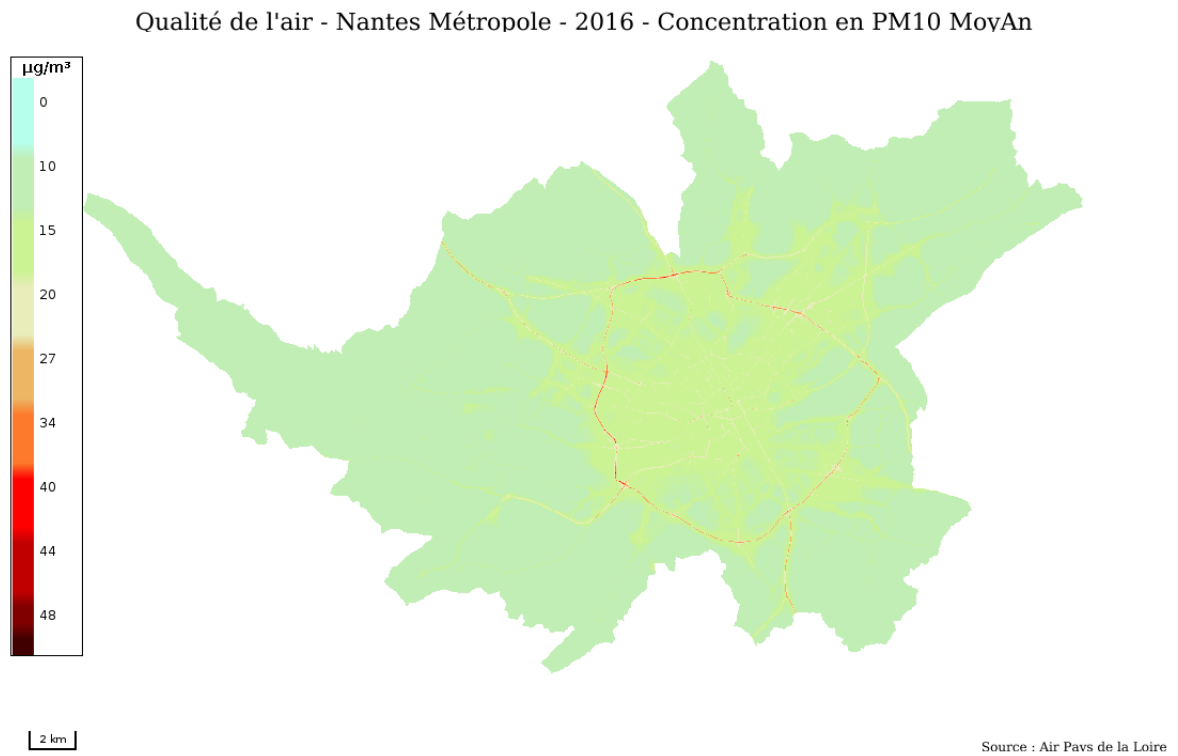


Figure D.2: PM_{10} mean annual concentration in Nantes [42]

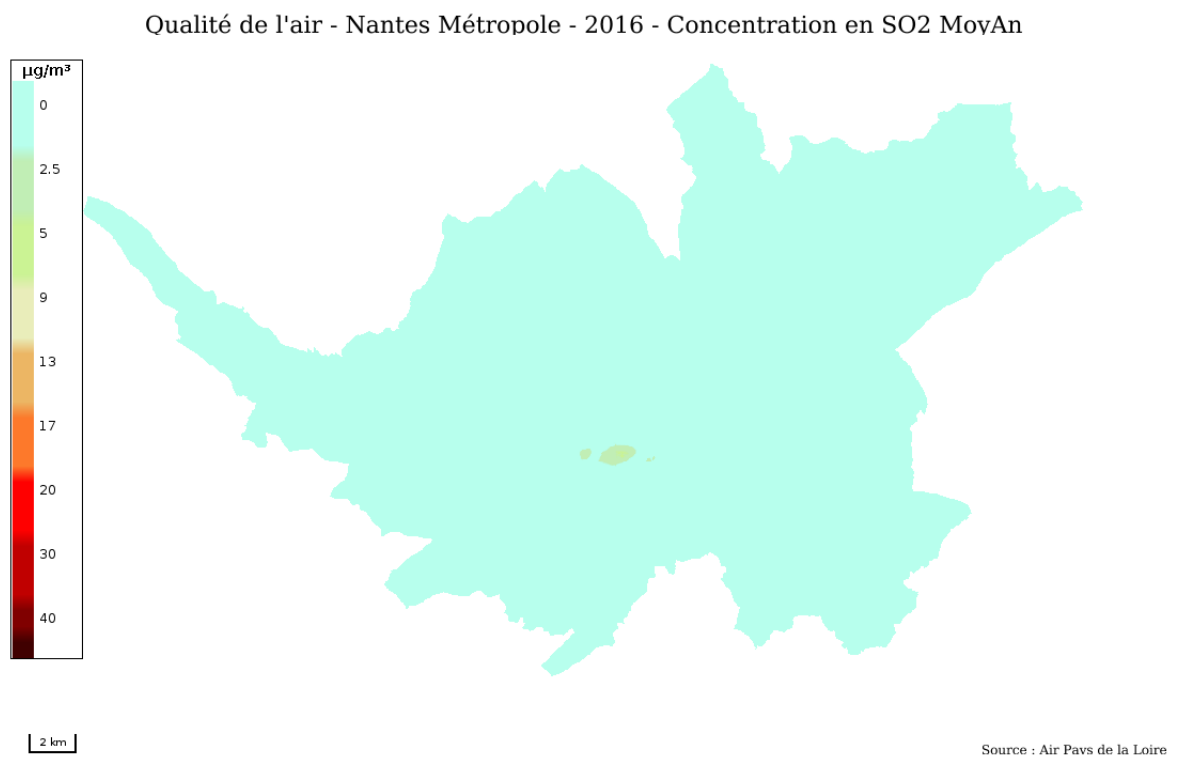


Figure D.3: SO_2 mean annual concentration in Nantes [42]

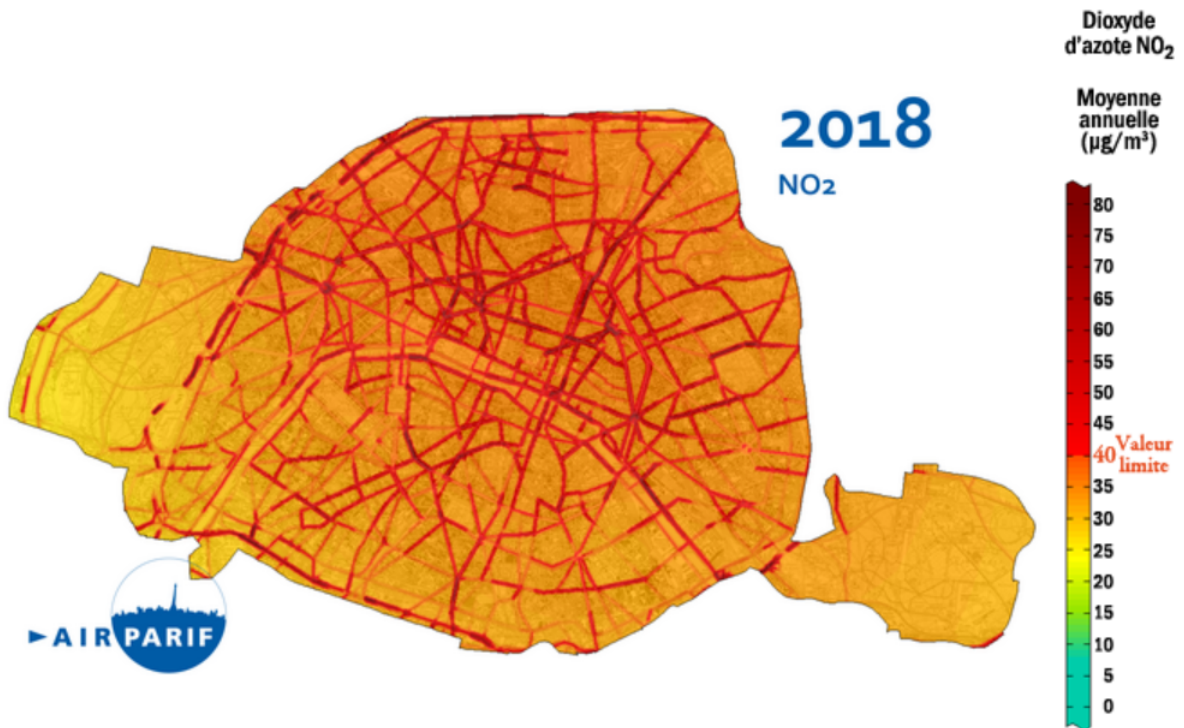


Figure D.4: NO₂ mean annual concentration in Paris [43]

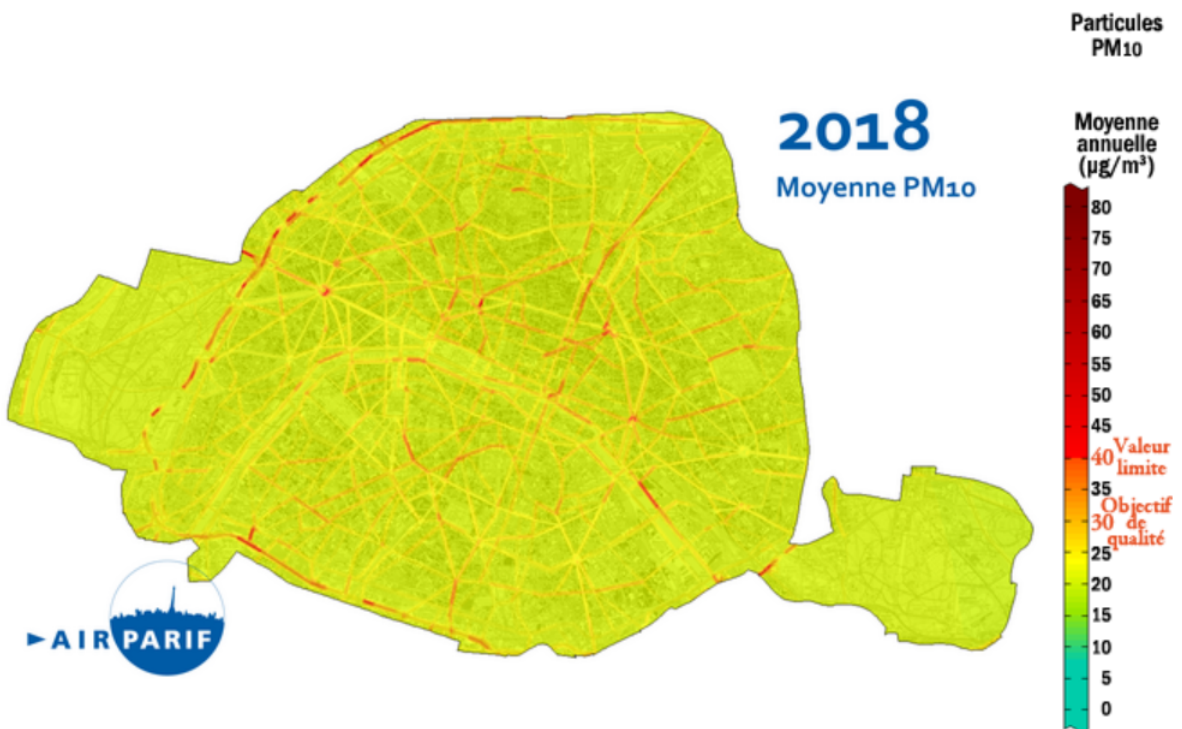


Figure D.5: PM₁₀ mean annual concentration in Paris [43]

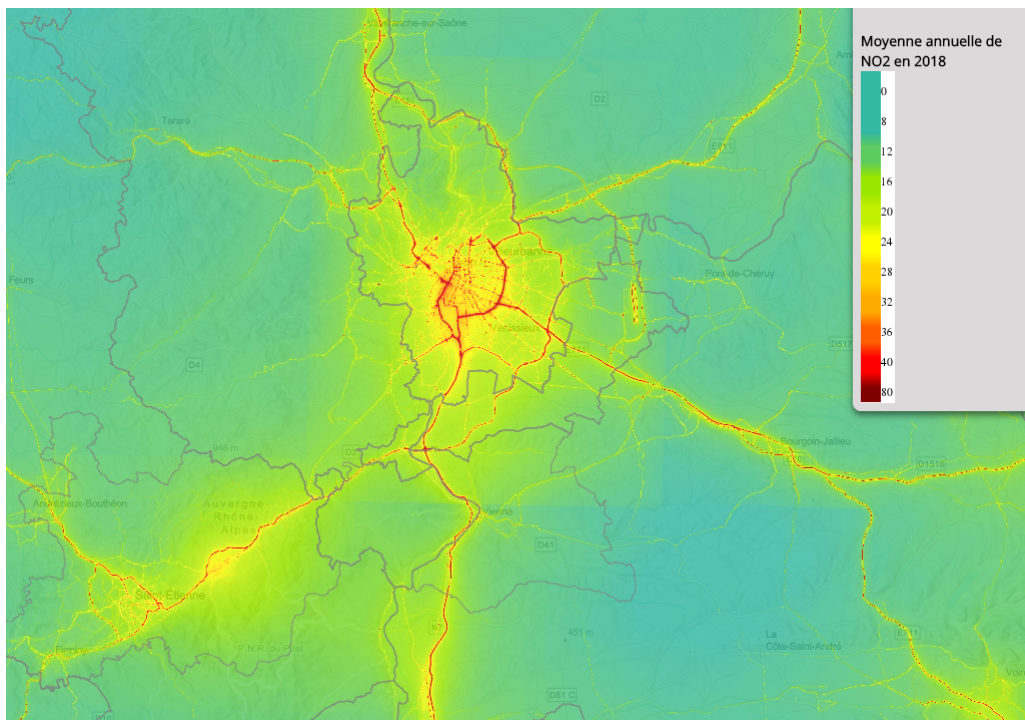


Figure D.6: NO_2 mean annual concentration in Lyon [44]

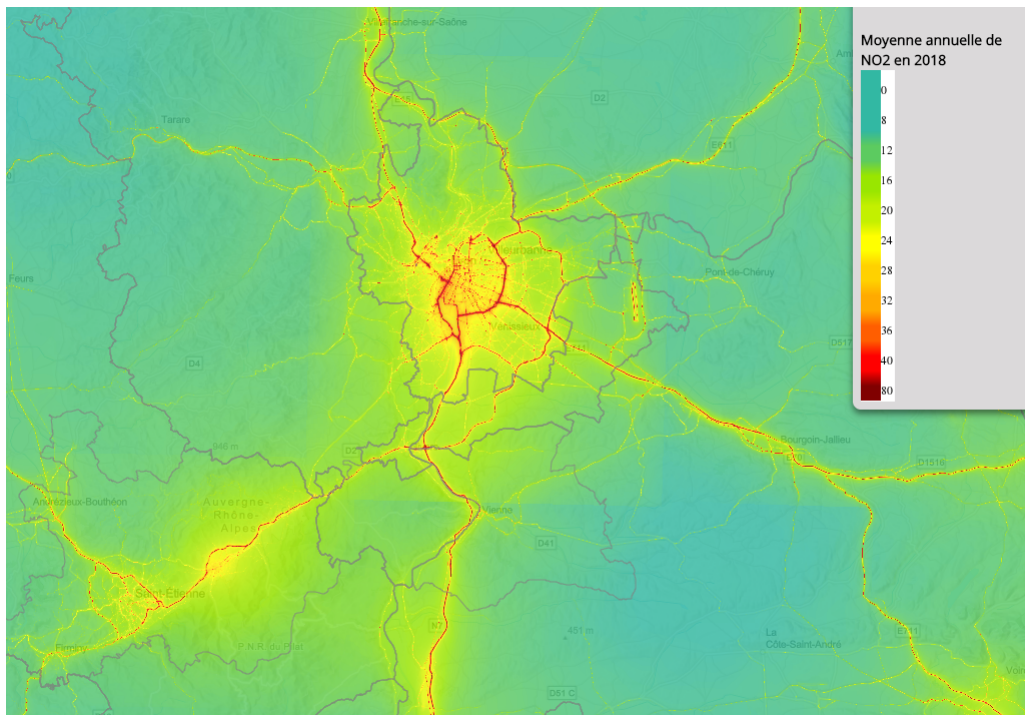


Figure D.7: PM_{10} mean annual concentration in Lyon [44]

Qualité de l'air - Pays de la Loire - 2017 - Concentration en NO₂ MoyAn

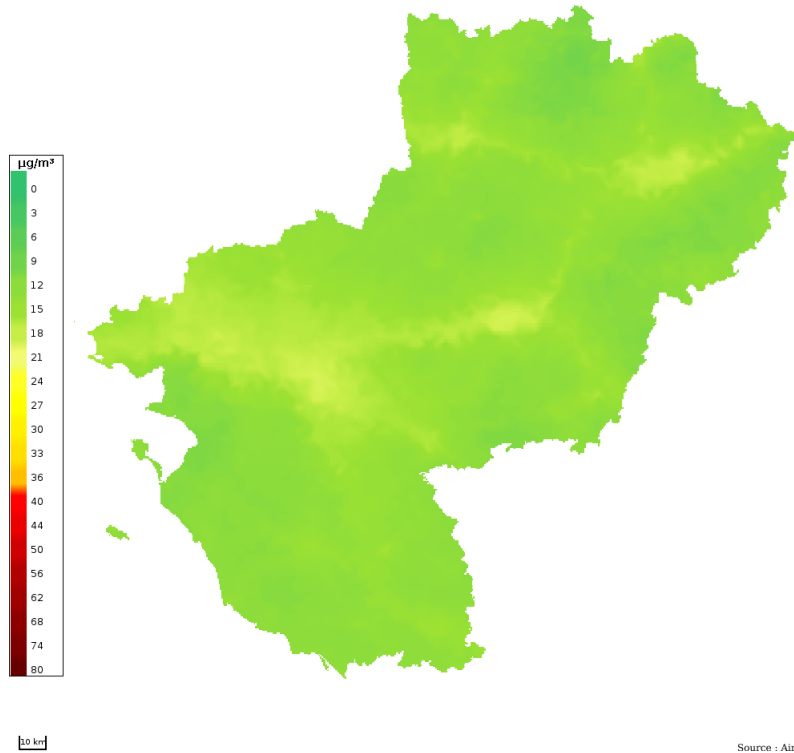


Figure D.8: NO₂ mean annual concentration in Pays de la Loire [42]

Qualité de l'air - Pays de la Loire - 2017 - Concentration en PM₁₀ MoyAn

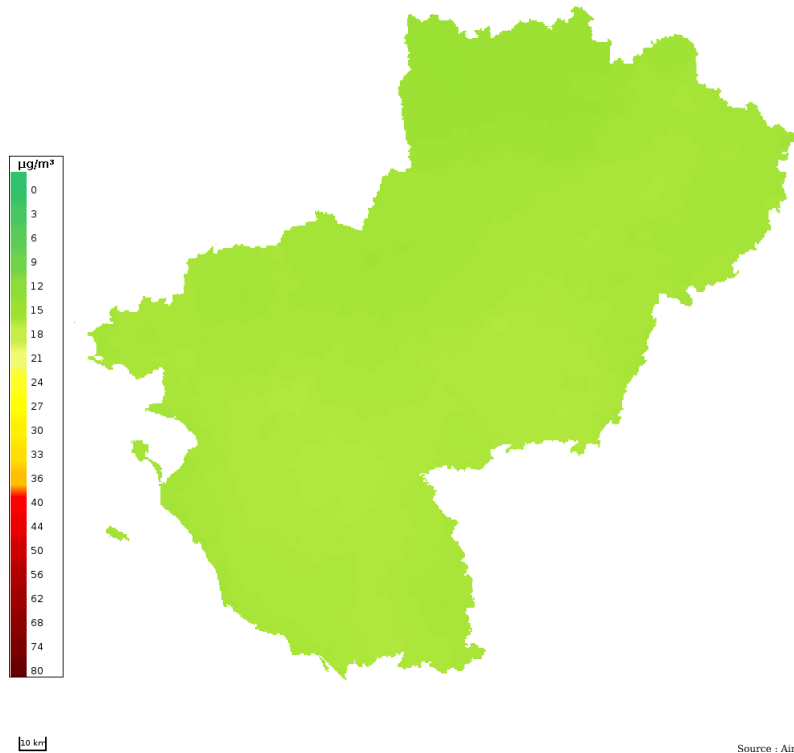


Figure D.9: PM₁₀ mean annual concentration in Pays de la Loire [42]

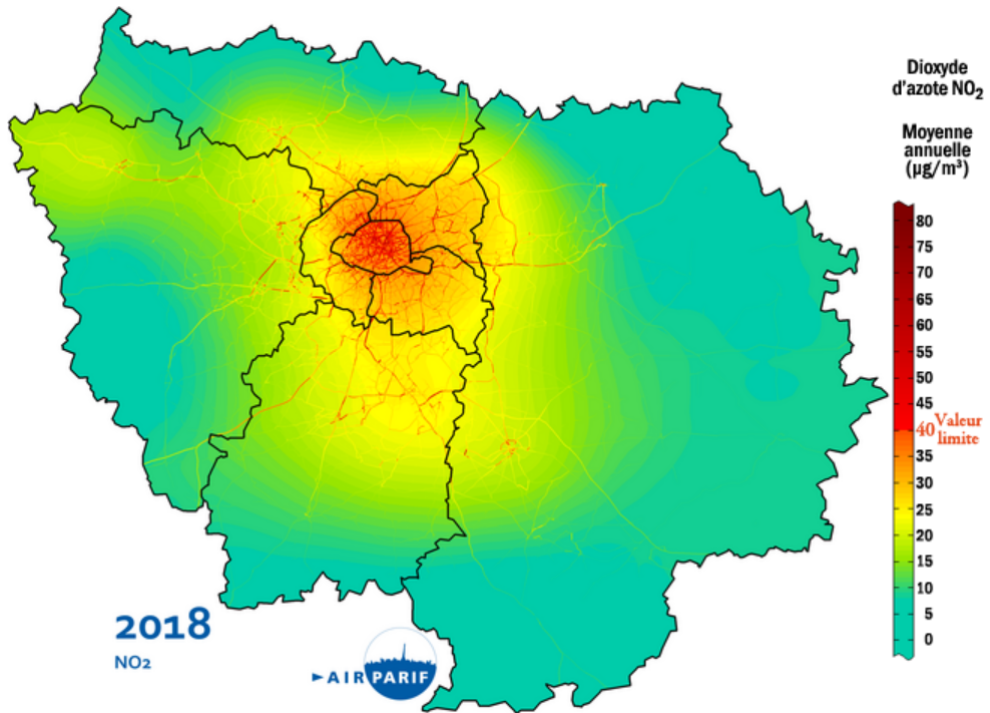


Figure D.10: NO_2 mean annual concentration in Ile de France [43]

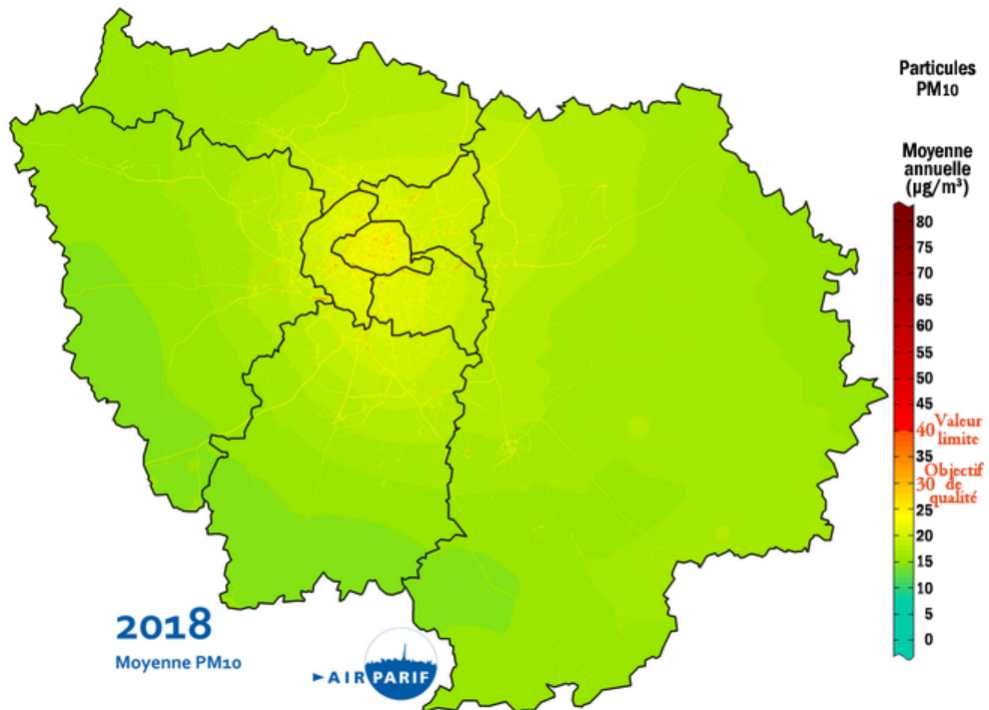


Figure D.11: PM_{10} mean annual concentration in Ile de France [43]

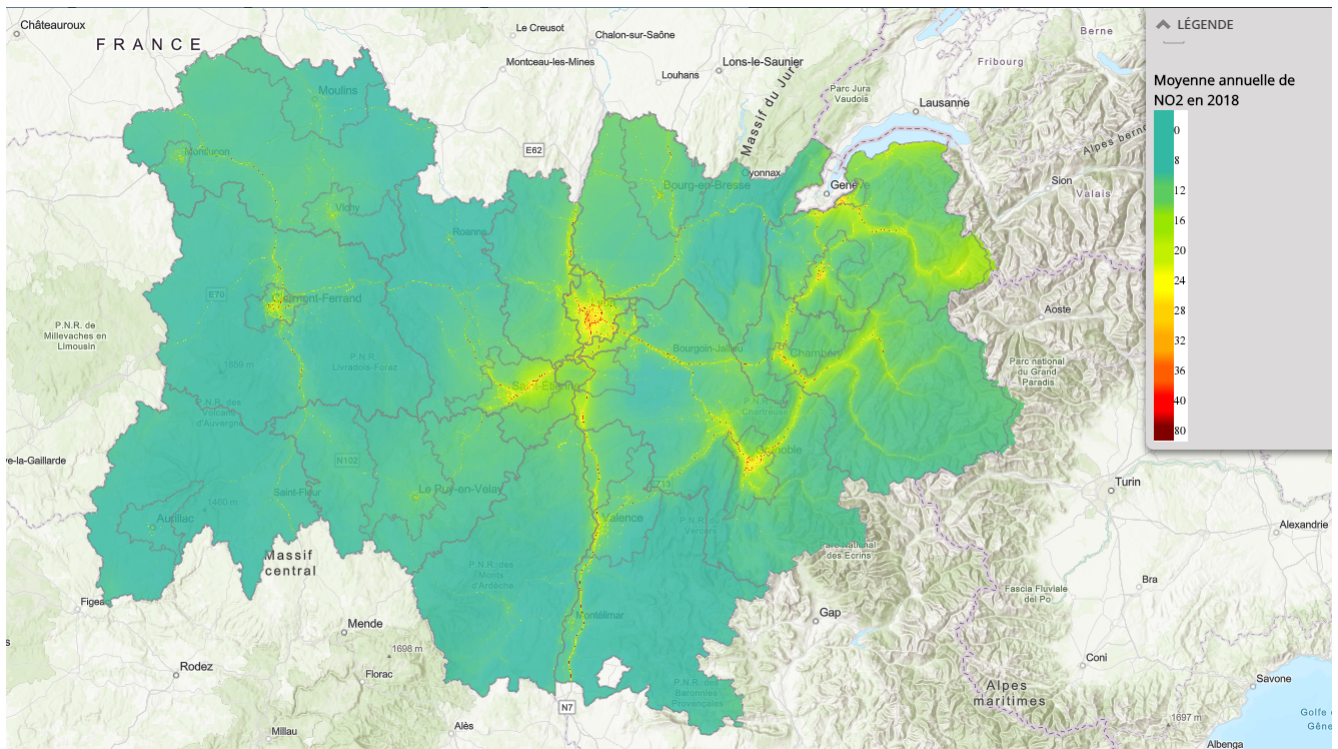


Figure D.12: NO_2 mean annual concentration in Rhone-Alpes [44]

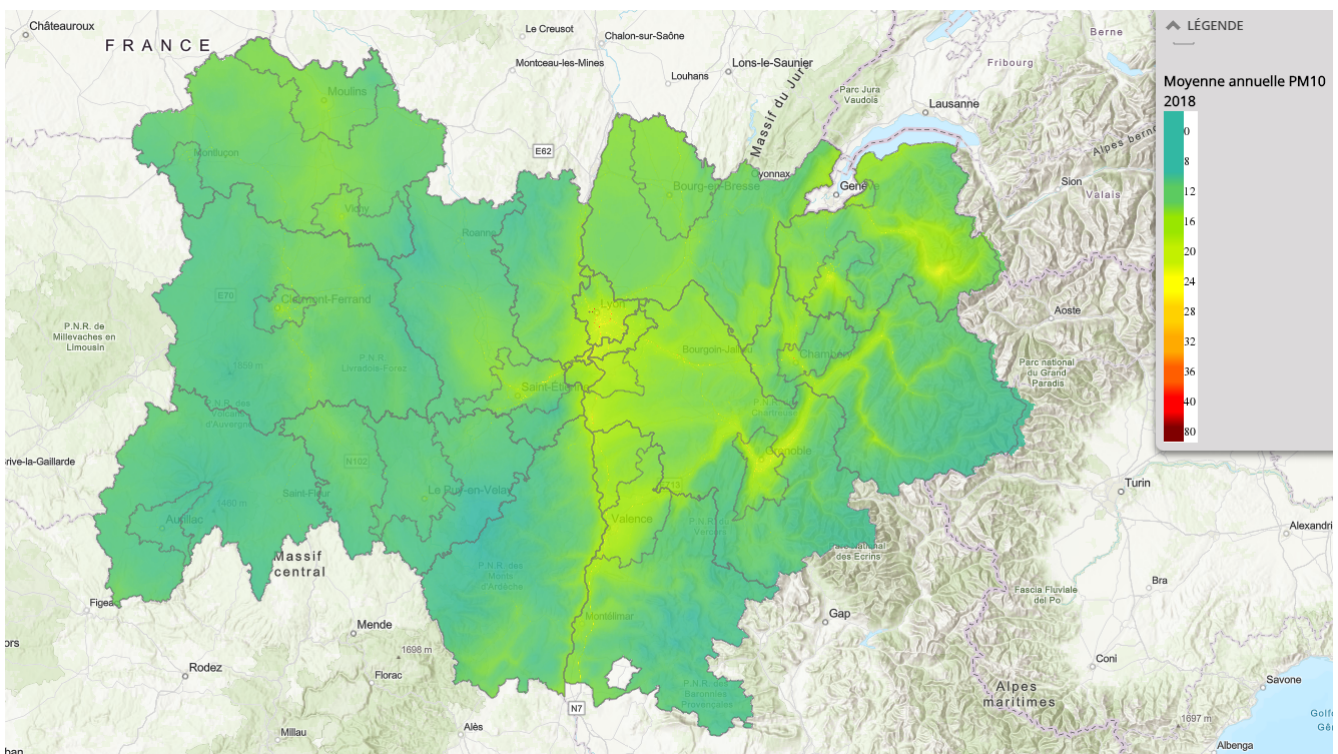


Figure D.13: PM_{10} mean annual concentration in Rhone-Alpes [44]

Bibliography

- [1] <https://www.who.int/airpollution/ambient/en/>, last check May 2019
- [2] World Health Organization, *Ambient air pollution: a global assessment of exposure and burden disease*, 2016.
- [3] European Parliament and Council of May 21, 2008, *Directive 2008/50/EC on Ambient Air Quality and Cleaner Air for Europe*.
- [4] Ministère de la transition écologique et solidaire, *Arrêté du 3 août 2018 relatif aux prescriptions générales applicables aux installations relevant du régime de l'enregistrement au titre de rubrique 2910 de la nomenclature des installations classées pour la protection de l'environnement*, Journal Officiel de la République Française, 2018.
- [5] Ministère de la transition écologique et solidaire, *Arrêté du 3 août 2018 relatif aux installations de combustion d'une puissance thermique nominale totale inférieure à 50 MW soumises à autorisation au titre des rubriques 2910, 2931 ou 3110*, Journal Officiel de la République Française, 2018.
- [6] M. Lateb, R.N. Meroney, M. Yataghene, H. Fellouah, F. Saleh, M.C. Boufadel, *On the use of numerical modelling for near-field pollutant dispersion in urban environments - A review*, 2015.
- [7] N.S. Holmes, L. Morawska, *A review of dispersion modelling and its application to the dispersion of particles: an overview of different dispersion models available*, 2006.
- [8] R. Sokhi, B. Fisher et al., *Modelling of air quality around roads*, 1998.
- [9] R. Britter, M. Schatzmann, *Background and Justification Document to Support the Model Evaluation Guidance and Protocol*, 2007.
- [10] <https://www.shodor.org/os411/courses/411c/module06/unit01/page01.html>, last check June 2019
- [11] R. Stull, *Practical Meteorology: An Algebra-based Survey of Atmospheric Science*, 2017.
- [12] W. L. Lee, A. C. Stern, *The Stack Height Requirements Implicit In the Federal Standards of Performance For New Stationary Sources - Journal of the Air Pollution Control Association*, 1973.
- [13] EPA, *Regulation No. 62.7 - Good Engineering Practice Stack Height*, 1989.

-
- [14] A. A. Abdel-Rahman, *On the atmospheric dispersion and Gaussian plume model, 2nd International Conference on Waste Management, Water Pollution, Air Pollution, Indoor Climate*, 2008.
- [15] A. Bhargava, *Effect of wind speed and stack height on plume rise using different equations*, 2016.
- [16] M. Lateb, C. Masson, T. Stathopoulos, C. Bédard, *Effect of stack height and exhaust velocity on pollutant dispersion in the wake of a building*, 2011.
- [17] P. Wagner, K. Schäfer, *Influence of the mixing layer height on air pollutant concentrations in an urban street canyon*, 2015.
- [18] F. Olofson, *Lidar Studies of Tropospheric Aerosols and Clouds*, 2008.
- [19] R. Istchenko and B. Turner, *Extrapolation of Wind Profiles Using Indirect Measures of Stability, reprinted from Wind Engineering volume 32, no. 5*, 2008.
- [20] S. Hanna, R. E. Britter, *Wind Flow and Vapor Cloud Dispersion at Industrial and Urban Sites*, 2002.
- [21] B. R. Munson, D. F. Young, T. H. Okiishi, W. W. Huebsch, *Fundamentals of Fluid Mechanics – Seventh edition*, Wiley, 2012.
- [22] J.M. Tomas, M.J.B.M. Pourquie, H.J.J. Jonker, *The influence of an obstacle on flow and pollutant dispersion in neutral and stable boundary layers*, 2015.
- [23] Y. Tominaga, T. Stathopoulos, *CFD simulation of near-field pollutant dispersion in the urban environment: A review of current modelling techniques*, 2013.
- [24] Y. Tominaga, T. Stathopoulos, *CFD modeling of pollution dispersion in a street canyon: Comparison between LES and RANS*, 2011.
- [25] F. Toja-Silva, Jia Chen, S. Hachinger, F. Hase, *CFD simulation of CO₂ dispersion from urban thermal power plant: Analysis of turbulent Schmidt number and comparison with Gaussian plume model and measurements*, 2017.
- [26] A. Haq, Q. Nadeem, A. Farooq, N. Irfan, M. Ahmad, M. R. Ali, *Assessment of Lagrangian particle dispersion model “LAPMOD” through short range field tracer test in complex terrain*, 2019.
- [27] J. C. Carvalho, M. T. Vilhena, D. M. Moreira, *Comparison between Eulerian and Lagrangian semi-analytical models to simulate the pollutants dispersion in the PBL*, 2005.
- [28] J. Antony, *Design of Experiments for Engineers and Scientists*, Elsevier, 2003.
- [29] B. Rakkhita, *Physical Modelling of the Atmospheric Boundary Level*, <http://www.engineeringenotes.com/wind-engineering/physical-modelling-of-the-atmospheric-boundary-level-wind-engineering/38810>, last check June 2019.
- [30] A. Venkatram, *Introduction to Aermod*, December 1, 2008.

- [31] P.J. Ross, *Taguchi Techniques for Quality Engineering*, McGraw Hill Professional, 1996.
- [32] Fluidyn-PANACHE <https://www.fluidyn.com/fluidyn/panache>, last check June 2019
- [33] L. Chen, M. Leguellec, *Validation of panache CFD pollution dispersion modelling with dense gas experiments*, 17th International Conference on Harmonisation within Atmospheric Dispersion Modelling for Regulatory Purposes, 9-12 May 2016, Budapest, Hungary.
- [34] J. H. Ferziger, M. Peric, *Computational Methods for Fluid Dynamics – Third edition*, Springer, 2002.
- [35] Fluidyn-PANACHE, *Fluidyn User Manual (Version 5.1.3)*, October 2017.
- [36] N. J. Cook, *The designer's guide to wind loading of building structures: Part 1*. Butterworths, 1985.
- [37] J. Han, S.P. Arya, S. Shen, Y. Lin, *An estimation of turbulent kinetic energy and energy dissipation rate based on atmospheric boundary layer similarity theory*, NASA, June 2000.
- [38] J. Hua, Q. Ying, J. Chen, A. Mahmud, Z. Zhao, S.H. Chen, M. J. Kleeman, *Particulate air quality model predictions using prognostic vs. diagnostic meteorology in central California*, October 2009.
- [39] COMSOL, <https://www.comsol.com/multiphysics/boussinesq-approximation>, last check June 2019
- [40] S. Hanna, G.A. Briggs, R.P. Hosker, *Handbook on Atmospheric Diffusion of Energy*, pag. 3, 1982.
- [41] P. Connolly, https://personalpages.manchester.ac.uk/staff/paul.connolly/teaching/practicals/gaussian_plume_modelling.html, last check August 2019
- [42] Air Pays de la Loire, https://data.airpl.org/dataset/modelisations/MR_PDL_17/N02/99.8th, last check June 2019
- [43] AirParif, <http://www.airparif.asso.fr/etat-air/bilan-annuel-cartes>, last check June 2019
- [44] Atmo Auvergne-Rhône-Alpes, <https://atmoaura.maps.arcgis.com/apps/MapSeries/index.html?appid=758a06eb90fc4b7abee43ca4a3236f3b>, last check June 2019